ENC 2012
EUROPEAN NUCLEAR CONFERENCE

Transactions - Fuel Cycle

Manchester, United Kingdom
9 - 12 December 2012

ENS
EUROPEAN NUCLEAR SOCIETY
ENS CONFERENCE

ENC 2012 Diamond Sponsor:

GE HITACHI

ENC 2012 Gold Sponsors:

AGORIA
Belgoprocess
SCK•CEN
NUCLEAIR FORUM NUCLEAIRE

ENC 2012 Silver Sponsor:

urenco

ENC 2012 Sponsor:

ONET TECHNOLOGIES

organised in collaboration with:

the Nuclear Institute
IAEA International Atomic Energy Agency
NEA Nuclear Energy Agency

European Nuclear Society
Rue Belliard 65
1040 Brussels, Belgium
Phone + 32 2 505 30 54
Fax +32 2 502 39 02
E-mail ens@euronuclear.org
Internet www.euronuclear.org

ISBN 978-92-95064-14-0

These transactions contain all contributions submitted by 7 December 2012.

ENC2012-A0036	Are World Uranium Resources Sufficient to Fuel Global Growth in Nuclear Generating Capacity?	Vance, R. (1); Cameron, R. (1) 1 - OECD Nuclear Energy Agency, France
ENC2012-A0091	The Future Role of Nuclear Fuel Cycle Technology in the UK	Rayment, F. (1) 1 - National Nuclear Laboratory, United Kingdom
ENC2012-A0175	Trends of EDF's fuel core management and consequences on fuel cycle : "Cycle Impact" analyses	Wong, H.-I. (1); Desroches, E. (1); Hansel, L. (1); Gourram, H. (1); Lagrange, M.-H. (1) 1 - EDF, France
ENC2012-A0197	Simulations of CANDU Reactor Core Configurations Utilizing a Thorium Battery Bundle	Golesorkhi, S. (1); Rouben, B. (1); Kaye, M. (1) 1 - Faculty of Energy Systems and Nuclear Science, University of Ontario Institute of Technology, Canada
ENC2012-A0236	Consolidation and advances in technology in the Fuel Cycle to safely address customers' needs and challenges	Teyssier, P. (1) 1 - On behalf of the French industry, France
ENC2012-A0134	SELECTION CONSIDERATIONS FOR GASES USED IN SPENT NUCLEAR FUEL DRY STORAGE	Walters, S. (1); Sims, H. (1); Henshaw, J. (1) 1 - National Nuclear Laboratory, United kingdom
ENC2012-A0168	AUTOMATED PWR FUEL PELLET MANUFACTURE	Mckenzie, B. (1); Livingstone, B. (1) 1 - Springfields Fuels Ltd, Springfields, United Kingdom
ENC2012-A0252	An Investigation on the Contribution of Rod Growth to Assembly Growth in Nuclear Fuel	Jang, Y. K. (1); Kim, J. I. (1); Shin, J. C. (1); Kim, S. D. (1); Kim, M. S. (2); Lee, T. H. (2); Kim, T. W. (2) 1 - KEPCO Nuclear Fuel (KNF), Korea, Republic of 2 - Korea Hydro & Nuclear Power (KHNP), Korea, Republic of
ENC2012-A0054	SAFTEY ASPECTS OF DRY SPENT FUEL STORAGE AND SPENT FUEL MANAGEMENT	Völzke, H. (1); Wolff, D. (1); Botsch, W. (2); Drotleff, H.-W. (2); Hinterding, P. (2); Smalian, S. (2); Kasparek, E.-M. (1) 1 - BAM Federal Institute for Materials Research and Testing, Division 3.4 "Safety of Storage Containers", Germany 2 - TÜV NORD Nuclear c/o TÜV NORD EnSys Hannover GmbH & Co.KG, Germany
ENC2012-A0058	The National Nuclear Laboratory's approach to waste and residues processing	Greenwood, H. (1); Docrat, T. (1); Allinson, S. (1); Coppersthwaite, D. (1) 1 - National Nuclear Laboratory, United Kingdom
ENC2012-A0117	NNL case study: Maximising plant life-time extension of HA evaporators for nuclear fuel waste processing.	Armstrong, M. (1); Whillock, G. (1) 1 - National Nuclear Laboratory, United Kingdom
ENC2012-A0174	Multiple recycling of MOX in LWRs	Bouvier, E. (1); Gain, T. (1); Lelièvre, F. (1); Senentz, G. (1); Bailly, F. (1); Murray, P. (2) 1 - AREVA Back End BG, France 2 - AREVA Federal Services LLC, United States

ENC2012-A0275	Shadow Corrosion Resistant Core design: Cofrentes core design modifications to minimize channel bowing	Galicia Saavedra, A. (1); López Carbonell, M. T. (1); Dey Navarro, J. M. (1); Saiz de Omeñaca Tijero, J. (1) 1 - Iberdrola, Spain
ENC2012-A0041	On composition stabilizing a hypo-stoichiometric uranium dioxide	Alekseev, P. (1); Semchenkov, Y. (1); Shimkevich, A. (1) 1 - NRC "Kurchatov Instittute", Russian Federation
ENC2012-A0064	Thorium option for durable electro-nuclear systems : complementarity of thorium and uranium based cycle in water cooled reactor and advanced plutonium management	Ernoult, M. (1); David, S. (1); Van den Durpel, L. (2) 1 - IPN Orsay, France 2 - AREVA, France
ENC2012-A0081	Framework for the manufacturing development of advanced ceramic nuclear fuels	Shepherd, D. (1) 1 - National Nuclear Laboratory, United kingdom
ENC2012-A0205	Fabrication of (U,Am) mixed-oxide fuels for transmutation	Lebreton, F. (1); Horlait, D. (1); Delahaye, T. (1); Blanchart, P. (2) 1 - CEA, DEN, DTEC/SDTC/LEMA, France 2 - ENSCI/GEMH, France
ENC2012-A0002	The Effect of Temperature and Stress on Hydride Reorientations of High Burnup Claddings under Interim Dry Storage Conditions	Kim, K.-T. (1); Kim, M.-S. (1); Min, S.-J. (1) 1 - Dongguk University, Korea, Republic of
ENC2012-A0040	ON-LINE QUANTITATIVE ANALYSES OF URANIUM IN THE MINING	Sokolov, A. (1); Hasikova, E. (1); Titov, V. (1); Rozite, A. (1) 1 - Baltic Scientific Instruments, Latvia
ENC2012-A0059	NNL Preston Laboratory technologies/processes for the treatment of organic wastes	Greenwood, H. (1); Docrat, T. (1); Allinson, S. (1); Coppersthwaite, D. (1) 1 - National Nuclear Laboratory, United Kingdom
ENC2012-A0076	Novel inspection developments required to underpin the safe operations of Sellafield nuclear fuel reprocessing plant	Armstrong, M. (1) 1 - National Nuclear Laboratory, United Kingdom
ENC2012-A0089	MODELLING OF PROCESSES IN RBMK-1500 FUEL RODS DURING THE OPERATION CYCLE AND SHORT AND INTERMEDIATE TERM STORAGE OF SPENT FUEL ASSEMBLIES	Uspuras, E. (1); Kaliatka, T. (1) 1 - Lithuanian Energy Institute, Lithuania
ENC2012-A0112	Dynamic Analysis of Synergistic Deep Burn High Temperature ReactorScenario with Fast Reactor	Jeong, C. J. (1); Jo, C. K. (1); Noh, J. M. (1) 1 - Korea Atomic Energy Research Institute, Korea, Republic of
ENC2012-A0152	FUEL ANALYSIS IN LBLOCA WITH CODE TRACE/FRAPTRAN	Chen, W. (1); Yang, J. (2); Shih, C. (1); Lin, H.-T. (3); Wang, J.-R. (3) 1 - Institute of Nuclear Engineering and Science National, Tsing-Hua University , Taiwan 2 - Department of Engineering and System Science, National Tsing-Hua University , Taiwan 3 - Institute of Nuclear Energy Research, Taiwan
ENC2012-A0184	THE APPROACH OF USED FUEL INTEGRITY EVALUATION DURING TRANSPORTATION AND STORAGE	Kim, S. (1); Lee, S. (1); Choi, B. (1); Choi, K. (1); Lim, C. (1) 1 - KEPCO Nuclear Feul Co., Korea, Republic of

ENC2012-A0188	HOW RECYCLING CAN HELP RESPOND TO FUKUSHIMA-DRIVEN REQUIREMENTS FOR USED FUEL SAFETY	Chiguer, M. (1) 1 - AREVA, France
ENC2012-A0256	MECHANICAL AND THERMAL CARACTERIZATIONS OF U-MO AND U-NB-ZR ALLOYS	Adorno, D. (1); Restivo, T. (1); Gomide, R. (1) 1 - Centro Tecnológico da Marinha em São Paulo, Brazil
ENC2012-A0268	Development of Quantitative analytical method of U, Pu and fission products in spent fuel by combined chromatographic-mass spectrometric-isotopic dilution technology	Uchiyama, G. (1); Ito, M. (1); Fukaya, Y. (1); Ueno, T. (1); Miyata, S. (1); Sonoda, A. (1); Usami, H. (1); Kawasaki, Y. (1); Sakatsume, K. (1); Kurosawa, T. (1); Suyama, K. (1); Tonoike, K. (1); Inagawa, J. (1); Umeda, T. M. (1); Magara, M. (1); Watanabe , K. (1); Yamamoto , T. (2) 1 - Japan Atomic Energy Agency, Japan 2 - JNES, Japan

FUEL CYCLE

ARE WORLD URANIUM RESOURCES SUFFICIENT TO FUEL GLOBAL GROWTH IN NUCLEAR GENERATING CAPACITY?

R.E VANCE
OECD Nuclear Energy Agency
12, Boulevard des Îes, 92130 – France

R. CAMERON
OECD Nuclear Energy Agency
12, Boulevard des Îes, 92130 – France

ABSTRACT

Increased uranium prices since 2003 have produced more activity in the sector than the previous 20 years. Nuclear reactor construction is proceeding in some countries, ambitious expansion plans have been announced in others and several, particularly in the developing world, are considering introducing nuclear power as a means of meeting rising electricity demand without increasing greenhouse gas emissions. Others have recently decided to either withdraw from the use of nuclear power or not proceed with development plans following the accident at the Fukushima Dai-ichi nuclear power plant in Japan in March 2011. Since the mid-1960s, the OECD Nuclear Energy Agency and the International Atomic Energy Agency have jointly prepared a comprehensive update of global uranium resources, production and demand (commonly known as the “Red Book”). The Red Book is based on government responses to a questionnaire that requests information on uranium exploration and mine development activity, resources and plans for nuclear development to 2035. This presentation provides an overview of the global situation based on the recently published 2011 edition. It features a compilation of global uranium resources, projected mine development and production capability in all the countries currently producing uranium or with plans to do so in the near future. This is compared to updated, post-Fukushima demand projections, reflecting nuclear phase-out plans announced in some countries and ambitious expansion plans of others. The 2011 Red Book shows that currently defined uranium resources are sufficient to meet high case projections of nuclear power development to 2035.

1. Introduction

Uranium 2011: Resources, Production and Demand [1] presents, in addition to updated resource figures, the results of a recent review of world uranium market fundamentals and provides a statistical profile of the world uranium industry as of 1 January 2011. It contains official data provided by 34 countries and 8 national reports prepared by the joint NEA-IAEA Secretariat on uranium exploration, resources, production and reactor-related requirements. Projections of nuclear generating capacity and reactor-related uranium requirements through 2035 are presented as well as a discussion of long-term uranium supply and demand issues.

2. Resources

Total identified uranium resources have increased by over 12% since 2009, adding more than 12 years of global reactor requirements to the existing resource base, but costs of production have also increased.

Total identified resources (reasonably assured and inferred) as of 1 January 2011 declined slightly to 5 327 200 tonnes of uranium metal (tU) in the <USD 130/kgU (<USD 50/lb U_3O_8)

category, a decrease of 1.4% compared to 1 January 2009. However, in the highest cost category (<USD 260/kgU or <USD 100/lb U_3O_8) which was reintroduced in 2009, total identified resources increased to 7 096 600 tU, an increase of 12.5% compared to the total reported in 2009.

Although total identified resources have increased overall, since 2009 there has been a significant reduction in lower cost resources owing principally to increased mining costs (a 14% reduction in the <USD 40/kgU cost category and an 18% reduction in the <USD 80/kgU cost category). Although a portion of the overall increases in the high cost category relate to new discoveries, the majority result from re-evaluations of previously identified resources and conservative Secretariat cost assessments of resources reported by exploration companies active in Africa, particularly in Namibia. At 2010 rates of consumption, identified resources are sufficient for over 100 years of supply for the global nuclear power fleet. An additional 124 100 tU of resources have been identified by the Secretariat as resources reported by companies that are not yet included in national resource totals.

Total undiscovered resources (prognosticated resources and speculative resources) as of 1 January 2011 amounted to 10 429 100 tU, a marginal increase from the 10 400 500 tU reported in 2009. It is important to note however that some countries, including major producing countries with large identified resource inventories (e.g. Australia, Namibia) do not report estimates of undiscovered resources.

The uranium resource figures presented in this volume are a “snapshot” of the situation as of 1 January 2011. Resource figures are dynamic and related to commodity prices. The overall increase in identified resources from 2009 to 2011, including in the high cost category, are equivalent to over 12 years of supply based on 2010 uranium requirements, demonstrating that new resources can be identified with appropriate market signals. Favourable market conditions will stimulate exploration and, as in the past, increased exploration will lead to the identification of additional resources through intensified efforts at existing deposits and the discovery of new deposits of economic interest.

3. Exploration

The increased resource base described above has been identified thanks to a 22% increase in uranium exploration and mine development expenditures between 2008 and 2010.

Worldwide exploration and mine development expenditures in 2010 totalled over USD 2 billion, a 22% increase over updated 2008 figures, as concerted efforts were made to develop deposits for projected future supply requirements. Most producing countries reported increasing expenditures, particularly in Africa, where significant mine development activities are underway. Although the majority of global exploration activities remain concentrated in areas with potential for hosting unconformity-related and ISL (*in situ* leach; sometimes referred to as *in situ* recovery, or ISR) amenable sandstone deposits, primarily in close proximity to known resources and existing production facilities, lower grade, high tonnage deposits became a focus of activity in Africa. Generally higher prices for uranium since 2003, compared to the preceding two decades, have stimulated increased exploration in regions known to have good potential based on past and “grass roots” exploration. Over 85% of exploration and development expenditures in 2010 were devoted to domestic activities. Non-domestic exploration and development expenditures, although reported only by China, France, Japan and the Russian Federation, decreased from USD 371 million in 2009 to USD 274 million in 2010 but remain significantly above the USD 71 million reported in 2004. Domestic exploration and development expenditures are expected to decline somewhat in 2011, amounting to about USD 1.8 billion.

4. Production

Global uranium mine production increased by over 25% between 2008 and 2010 because of significantly increased production in Kazakhstan, currently the world's leading producer.

Uranium production amounted to 54 670 tU in 2010, a 6% increase from the 51 526 tU produced in 2009 and a 25% increase from the updated total of 43 758 tU produced in 2008. In all, 22 countries reported output in 2010, 2 more than in 2008 as production began in Malawi in 2009 and Germany resumed uranium recovery through mine remediation efforts. China reported uranium production figures for the first time and Uzbekistan reported production figures for the first time since 2005. Global production increases between 2008 and 2010 were driven principally by significantly increased output in Kazakhstan (109%). More modest increases were recorded in Canada, China, India, Namibia, Niger, the United States and Uzbekistan. Reduced production was recorded in a number of countries between 2008 and 2010 (including Australia and Brazil) owing to a combination of lower than expected ore grades, technical difficulties and preparations for mine expansions, including regulatory approval processes. ISL mining accounted for 39% of global production in 2010, rising rapidly to become the most important mining method, principally because of significant ISL production increases in Kazakhstan. Underground mining (32%), open-pit mining (23%) and co-product and by-product recovery from copper and gold operations (6%) accounted for the remaining production shares. Global uranium production in 2011 was expected to increase by 5% to over 57 000 tU, with a continuing but less rapid ramp-up in Kazakhstan and expected increases in Australia and Uzbekistan.

5. Environmental aspects of uranium production

With uranium production ready to expand to new countries, efforts are being made to develop transparent and well-regulated operations similar to those used elsewhere in order to minimise local health and environmental impacts.

Although the focus of this publication remains uranium resources, production and demand, environmental aspects of the uranium production cycle are an important part of uranium production and updates on these activities are included in national reports in this edition. With uranium production ready to expand, in some cases to countries hosting uranium production for the first time, the continued development of transparent and well-regulated operations that minimise environmental impacts is crucial. In Botswana, national policies regarding uranium production are under development, since no regulations for uranium mining and milling are in place and resources with potential for extraction have been identified. In Malawi, an atomic energy bill was passed in 2011, the first step towards development of comprehensive legislation on radioactive materials. Zambia and Finland signed co-operation agreements in 2011 to evaluate, update and review regulations regarding the safety of uranium mining. In Tanzania, the Parliamentary Committee for Energy stated that no uranium mining can take place until a policy and legislation on extraction are in place.

In South America, recognising the need to continually improve practices and to inform stakeholders of modern practices, the Argentinian Chamber of Uranium Companies was formed in 1999 to share best practices in uranium exploration and to cooperatively provide information on the industry. In Peru, the Peru-Canada Mineral Resources Reform Project (PERCAN) was established to provide the Ministry of Mines and Energy with input during development of an environmental guide for uranium exploration which was expected to be completed by the end of 2011. Local communities are participating in monitoring the activities of the exploration companies in Peru.

Countries with existing uranium production facilities are also strengthening aspects of health and safety practices at production facilities. In Iran, a comprehensive health, safety and environmental protection programme has been implemented at all production centres (an open-pit mine and mill near Bandar-Abbas, an underground Saghand mine and a uranium mill under construction in Ardakan). In late 2011, AREVA announced the creation of a Health Observatory for the Agadez region of Niger, one year after a similar institution was established in Gabon. These observatories are to monitor the health of former workers in uranium mines as well as the health of the local population. In cases of illness attributable to occupational causes, the cost of corresponding health care is to be covered by AREVA. Other such observatories around mining facilities operated by AREVA are planned.

Uranium mining companies actively contribute to improving social and cultural aspects of communities in the vicinity of operating facilities. For example, in Kazakhstan all contracts for uranium exploration and mining issued by the government require financial contributions (USD 30 000-100 000/yr during exploration and as much as USD 50 000-350 000/yr during mining) to fund health care for employees and local citizens, education, sport, recreation and other facilities in accordance with the national strategy. In 2010, Rössing and others provided financial and/or technical support to the Uranium Institute of Namibia, an organisation established to improve the quality of healthcare, environmental management and radiation safety in the industry, as well as educational and environmental programmes in local communities. Planning and preparing for mine remediation well in advance of mine closure is one of the foundations of modern uranium mining. Along with planning for the life extension of the Rössing mine to 2023, the mine remediation plan was reviewed (including training requirements, demolition, tailings rehabilitation, long-term seepage control and monitoring costs) along with funding requirements to carry out the activities. Funds in the independent Rössing environmental rehabilitation trust fund amounted to USD 24.5 million at the end of 2010 and will be increased in the coming years to provide for the full range of planned closure and remediation activities of the mine and mill. In countries with closed uranium production facilities that operated in the past without strict environmental regulations and where practices that would not be licensed today were used, remediation actions continue. In Brazil, a remediation/restoration study is being carried out on the Poços de Caldas uranium facility that was closed in 1997. In Hungary, after the closure of the mines in 1998, stabilisation and remediation work was finished successfully in 2008. The annual cost of the long-term activities (water treatment, environmental monitoring and maintenance of the remediated sites) amounts to USD 2-3.3 million/yr. Updates on similar activities in Poland, Portugal, the Slovak Republic and Spain are also included in this edition. Additional information on environmental aspects of uranium production may be found in the joint NEA-IAEA Uranium Group publications entitled *Environmental Remediation of Uranium Production Facilities* (OECD, 2002) and *Environmental Activities in Uranium Mining and Milling* (OECD, 1999).

6. Uranium demand

Demand for uranium is expected to continue to rise for the foreseeable future.

At the end of 2010, a total of 440 commercial nuclear reactors were connected to the grid with a net generating capacity of 375 GWe requiring some 63 875 tU, as measured by uranium acquisitions. By the year 2035, world nuclear capacity, taking into account the current understanding of policies announced by some countries (e.g. Belgium, Germany, Italy and Switzerland) following the Fukushima accident, has been projected by the Secretariat to grow to between about 540 GWe net in the low demand case and 746 GWe net in the high demand case, increases of 44% and 99%, respectively. Accordingly, world annual reactor-related uranium requirements are projected to rise to between 97 645 tU and 136 385 tU by 2035. Nuclear capacity projections vary considerably from region to region. The East Asia region is projected to experience the largest increase, which could result by the year 2035 in the installation of between 100 GWe and 150 GWe of new capacity, representing increases of over 125% to more than 185%, respectively. Nuclear capacity in non-European Union countries in Europe is also expected to increase considerably (between 55% and 125%). Other regions with projected growth include the Middle East and Southern Asia, Central and South America, Africa and South-eastern Asia.

In North America, nuclear capacity is projected to grow by between 7% and 28% but in the European Union could either decrease by 11% or increase by 24%, depending principally on the implementation of nuclear phase-out policies. The high case assumes that at least some of these phase-out policies are eased.

There are uncertainties in these projections as debate continues on the role that nuclear energy will play in meeting future energy requirements. Key factors influencing future nuclear energy capacity include projected baseload electricity demand, the economic competitiveness of nuclear power plants as well as funding arrangements for such capital-intensive projects, the cost of fuel for other electricity generating technologies, non-proliferation concerns, proposed waste management strategies and public acceptance of nuclear energy, a particularly important factor following the Fukushima Daiichi accident. Concerns about longer-term security of fossil fuel supply and the extent to which nuclear energy is seen to be beneficial in meeting greenhouse gas reduction targets could contribute to even greater projected growth in uranium demand.

7. Supply and demand relationship

The currently defined resource base is more than adequate to meet high case demand through 2035, but doing so will require timely investments in uranium production facilities given the long lead times required to turn resources into refined uranium ready for nuclear fuel production.

In 2010, world uranium production (54 670 tU) met about 85% of world reactor requirements (63 875 tU), with the remainder of supply coming from uranium already mined (so-called secondary sources) including excess government and commercial inventories, low-enriched uranium (LEU) produced by downblending highly enriched uranium (HEU) from the dismantling of nuclear warheads, re-enrichment of depleted uranium tails and spent fuel reprocessing.

Uranium mine development was responding to the market signal of increased prices and rising demand prior to the Fukushima accident. The drop in market prices following the accident and lingering uncertainty concerning nuclear power development in some countries has slowed the pace of mine development. Nonetheless, as currently projected, primary uranium *production capabilities* including existing, committed, planned and prospective production centres could satisfy projected high case requirements through 2030 and low case requirements through 2035. Meeting high case demand requirements would consume only 35% of the total identified resource base by 2035. Moreover, the entire *conventional resource base* documented in this edition is sufficient to fuel total lifetime requirements for all reactors built by 2035 in the low case scenario projection and over 90% of the requirements for the operational lifetime of all reactors built by 2035 in the high case scenario projection. Nonetheless, significant investment and technical expertise will be required to bring these resources to the market and to identify additional resources. Sufficiently high uranium market prices will be needed to fund these activities, especially in light of the rising costs of production. Secondary sources will continue to be required, complemented to the extent possible by uranium savings achieved by specifying low tails assays at enrichment facilities and developments in fuel cycle technology. Although information on secondary sources is incomplete, their availability is expected to decline somewhat after 2013 when the agreement between the United States and the Russian Federation to downblend HEU to LEU suitable for nuclear fuel comes to an end. There remains however, a significant amount of previously mined uranium (including material held by the military), some of which could feasibly be brought to the market in a controlled fashion. Nonetheless, as secondary supplies continue to be reduced in the coming years, reactor requirements will need to be increasingly met by mine production.

The introduction of alternative fuel cycles, if successfully developed and implemented, could profoundly impact the market balance, but it is too early to say how cost-effective and widely implemented these proposed fuel cycles could be. A strong market for uranium will be needed to bring about the timely development of production capability. Long lead times are required to identify new resources and to bring them into production, typically of the order of ten years or more in most producing countries. The global network of uranium mine facilities is relatively sparse and geopolitical uncertainties increase investment risks in some countries. The market will have to provide sufficient incentives for exploration and mine developments in order to continue to ensure that global nuclear fuel requirements will be met.

8. Conclusions

Despite recent declines in electricity demand stemming from the global financial crisis in some developed countries, demand is expected to continue to grow over the next several decades to meet the needs of a growing population, particularly in developing countries. Nuclear power produces competitively priced, baseload electricity that is essentially free of greenhouse gas emissions, and the deployment of nuclear power enhances security of energy supply. However, the Fukushima Daiichi accident has eroded public confidence in the technology in some countries and prospects for growth in nuclear generating capacity are in turn subject to greater uncertainty. Moreover, the abundance of low-cost natural gas, the risk-averse investment climate and the effects of the global financial crisis have made nuclear capacity growth more challenging, particularly in liberalised electricity markets.

Regardless of the role that nuclear energy ultimately plays in meeting future electricity demand, the uranium resource base described in this publication is more than adequate to meet projected requirements for the foreseeable future. The challenge is to continue developing environmentally sustainable mining operations to bring increasing quantities of uranium to the market in a timely fashion. Strengthened market conditions will be required for resources to be developed to meet projected uranium demand within the time frame required.

9. References

[1] Nuclear Energy Agency (2012), Uranium 2011: Resources, Production and Demand, OECD, Paris.

THE FUTURE ROLE OF NUCLEAR FUEL CYCLE TECHNOLOGY IN THE UK

Dr Fiona RAYMENT
Fuel Cycle Solutions, National Nuclear Laboratory
Chadwick House, Warrington, WA3 6AE - UK

ABSTRACT

As the UK decides on the level of nuclear energy required over the next century it is important to continue to be involved in advanced fuel cycle R&D. This is required to ensure the UK can make informed decisions on future UK energy policy and strategy, and continues to support UK international policy objectives enabling a low carbon economy.

The UK needs to continue to be a credible player in Europe and internationally and maintain technical capability to keep the range of nuclear options open. A further objective is to realise best practice through the opportunity to leverage investment through involvement in International programmes.

The UK's National Nuclear Laboratory (NNL) has a pedigree of underpinning UK fuel cycle decisions and programmes through a combination of its unique skills and facilities.

This paper gives a brief summary of recent NNL R&D work completed to address fuel cycle strategies for the UK.

1. Introduction

As oil and gas prices soar, reflecting the global energy demand from both developed and developing nations, low carbon electricity will become increasingly more important due to its potential to replace fossil fuels. As each low carbon technology has its own advantages and disadvantages there is no silver bullet to meeting future energy needs. Instead an approach of adopting the best energy mix should be employed. This will most probably result in a combination of renewable, nuclear and carbon sequestration technology in addition to adopting an approach to reducing energy consumption per capita.

Nuclear is viewed by many as a mature, reliable low carbon technology with a secure and abundant fuel source and is an essential contributor to the energy mix. Within the UK, the decision has been made to refresh the current nuclear energy plants to at least replacement of the existing nuclear fleet. This will mean the building of new nuclear power plant to ensure energy production of 16 GWe per annum. However it is also recognised that this may not be enough and as such expansion scenarios are being considered beyond the 16 GWe replacement to up to 75 GWe.

A number of parameters will affect fuel cycle options including;

- Economics
- Nuclear energy demand
- Fuel Supply
- Spent fuel storage / recycle
- Geological repository volumetric and radiological capacity
- Sustainability – effective resource utilisation
- Technology viability and readiness level

Advanced fuel cycle research has an important role to play within the UK to ensure the above is realised.

The UK’s National Nuclear Laboratory’s involvement in current and future fuel cycle challenges has been possible through our involvement in a combination of industrial customer driven programmes, investment in our own R&D and leverage of opportunities through involvement in European Framework and other International Programmes.

Key R&D programme areas to ensure energy scenarios are adequately underpinned include;

- Fuel Cycle Stewardship
- Fuel Manufacture and Performance
- Recycle and Storage Technology
- Reactor Systems
- Waste Management and Disposal
- Security and Safeguards

The NNL is actively involved in R&D associated with all the above programme areas. This paper outlines recent work completed in support of the first three of these programme areas.

2. Fuel Cycle Stewardship

NNL has experience in understanding nuclear fuel cycle options within countries, together with practicalities associated with implementing them. To analyse and develop future nuclear fuel cycle options/policy, we own and continually update several fuel cycle modelling computer codes. Our main computer program, ORION, allows modelling of complete and complex nuclear fuel cycle scenarios involving any number of fabrication plants, reactors, processing plants and buffers. The methods used in our program are explicit and accurately represent the physics. These methods in ORION use data from existing neutronics assessments of a reactor which calculate spent fuel composition and make it possible to model any reactor system.

At NNL, we have several neutronics computer codes that can be and have been used to model pressurised water reactors (PWR), boiling water reactors (BWR), legacy reactor systems including the UK's Magnox (using natural unenriched uranium as fuel and magnox alloy as fuel cladding) and Advanced Gas-cooled Reactor (AGR) designs, research reactors and fast reactors (gas, sodium, lead, molten salt). This enables us to assess a multitude of different reactor options and conventional or advanced fuel types in an accurate and informative way. Furthermore, the code allows great flexibility when defining the back end of the fuel cycle including reprocessing and disposal options. ORION together with other NNL computer codes also enables estimation of fuel cycle costs and proliferation risks. This can be used to distinguish between different fuel cycle options and highlight other important limitations.

NNL has extensive experience of the practical application of these codes in an industrial context. ORION has been used extensively in the past to support the US Department of Energy, the Nuclear Decommissioning Authority (NDA), internally funded research programmes and more recently the UK Department of Energy and Climate Change (DECC) programmes of work. For the US Department of Energy, ORION was used to support Energy Solutions to analyse and develop future nuclear strategy involving fully open (once through), modified open (PWR using mixed oxide (MOx) fuel and enriched reprocessed Uranium (RU)) and closed nuclear fuel cycles (fast reactors).

Similar analyses were also done as part of the Energy Research Partnership UK Nuclear Fission Roadmap as well as additional studies for DECC which concentrated more on the impact a closed fast reactor fleet would have on the UK. These analyses concentrated on specific questions relating to the sustainability and long term radiological impact of a particular future fuel cycle scenario. In addition, the code has been used to estimate the practicalities of handling fresh and spent advanced fuel concepts and indefinitely recycling material through a fast reactor fleet.

ORION is being continually developed in house to further its application and to allow even more flexibility when defining future fuel cycle scenarios. A selection of the scenarios currently being considered is shown in Table 1 below.

Capacity	**Options considered**
No new build	N/A
16 GW by 2025	Gen III PWRs open cycle with no recycle Gen III PWRs open cycle with historic Pu and RU recycle
40 GW by 2050	Gen III PWRs open cycle with no recycle Gen III PWRs open cycle with historic Pu and RU recycle Gen III PWRs open cycle with historic Pu & RU & future UO2 spent fuel recycle Gen III PWRs open cycle with limited recycle to 2040 + Fast Reactor closed cycle with Pu & MA & U recycle after 2040
75 GW by 2050	Gen III PWRs open cycle with no recycle Gen III PWRs open cycle with limited recycle to 2040 + Fast Reactor closed cycle with Pu & MA & U recycle after 2040

Table 1: Selection of scenarios considered as part of the UK Nuclear Fission Roadmap

Scenarios to maintain a 40 or 75 GWe PWR fleet are considered however the quantity of Uranium (U) resource required for these reactors, assuming no recycling, could push the U beyond affordable prices. This resource requirement versus price would need to be assessed.

The schematic of a fuel cycle scenario is illustrated in Figure 1. In this illustrative scenario, spent fuel from both PWRs and fast reactors is reprocessed to fully close the cycle.

Figure 1: Illustrative fuel cycle scenario indicating a closed system

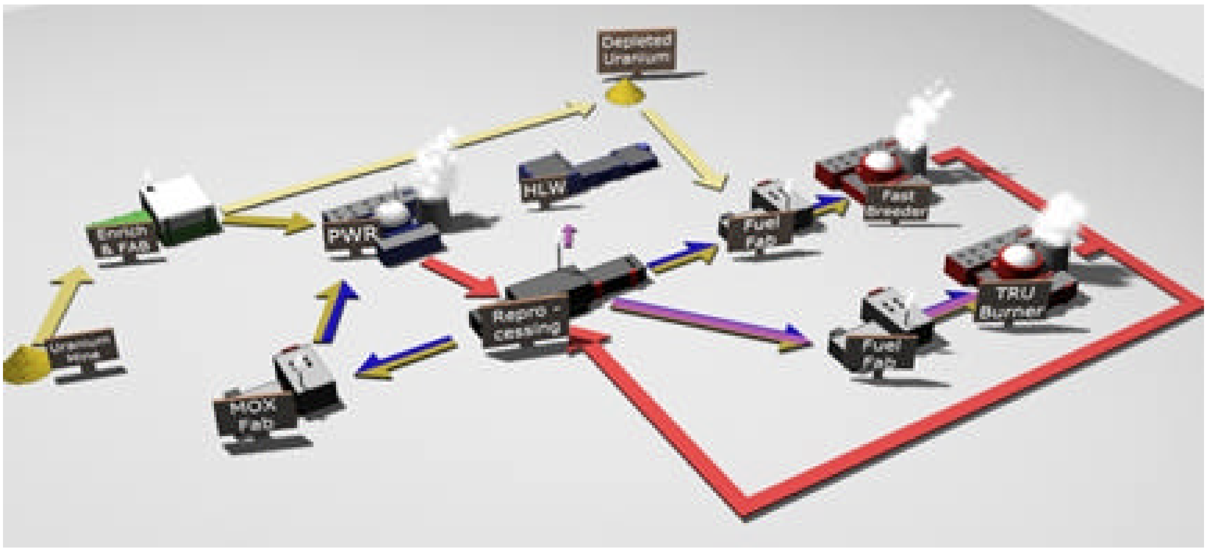

An example scenario illustrated in Figure 2 demonstrates how the 75 GWe by 2050 scenario can be met initially with a fleet of PWRs, before transitioning to a Sodium Fast Reactor (SFR) fleet. By using ORION, NNL can determine whether there is enough Pu available to maintain a 75 GWe fast reactor capacity, whether it would be more efficient to use historic Pu and U as mixed oxide fuel in the fast reactor fleet, how large and for how long a PWR fleet is needed and is PWR recycling needed to sustain a fast reactor programme. In this particular example, the PWR fleet is fuelled partly with mixed oxide (MOx) using plutonium (Pu) from the UK's historic stock and plutonium from reprocessing. The PWR spent fuel is subsequently reprocessed to supply plutonium to the SFRs. There is a period after closure of the PWR fleet where there is only sufficient Pu available to support about 60 GWe of SFR capacity.

Figure 2: Example scenario - meeting 75 GWe by 2050 by loading PWRs with MOx

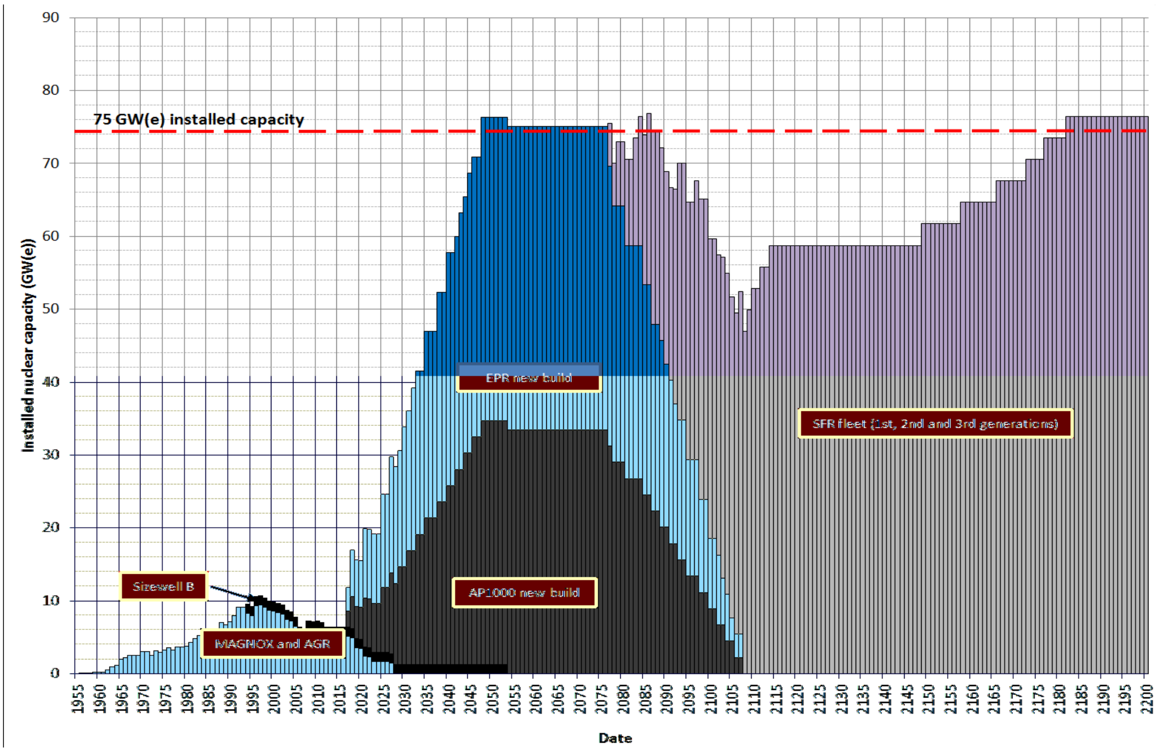

Taking this forward, a future phase of work could consider the optimum combination of PWRs loaded with UO2 fuel and fast reactors to sustain a 75 GWe capacity.

The following factors, amongst others, need to be considered and measured:

- Spent fuel – rate of creation, storage during fuel cycle, and amount at end of fuel cycle
- Sustainability – U and RU requirements / availability, Pu requirements for Fast Reactors
- Repository – decay heat and waste volumes
- Recycle rate – time to recycle is a critical factor
- Waste minimisation – considering the introduction of ‘burner’ fast reactors at end of fuel cycle to minimise remaining waste
- Resource utilisation – should current Pu stocks be used for PWR MOx fuel or saved to kick start the fast reactor programme?
- Proliferation resistance and physical protection measures
- Proposed systems will need to demonstrate compliance with Office for Nuclear Regulation safety requirements.

3. Fuel Manufacture and Performance

Within Europe the Strategic Nuclear Energy Technology Platform (SNETP) has a key goal to develop the technologies needed for GEN IV reactors. A key component of this will require the manufacture of test fuels. The very high costs and long lead times to build skills, experience and new fuel manufacturing facilities continues to represent a significant challenge to the industry.

The development of civil nuclear fuel in the UK has been closely aligned with UK prototype reactor programmes, operation of Magnox and AGR reactor fleets and development of Light Water Reactor (LWR) fuel for the global market. Around 20 UK research reactors have been developed and operated from the 1950s in addition to 26 Magnox reactors, 14 AGRs and 1 LWR. There was a focus on R&D in fuel development and material recycling at Dounreay and Harwell sites while work at Sellafield and Springfields undertook general R&D, developed test fuels and built commercial scale fuel reprocessing and fabrication plants. Over 10 million Magnox fuel elements (natural U metal clad in magnesium alloy), and AGR fuel elements (each consisting of 36 enriched U oxide pellets clad in stainless steel pins arranged in three concentric rings within a graphite sleeve) have been produced at the UK's Springfields site. Novel TRISO fuel for PBMR's has also been researched at the UK's Springfields site using knowledge of particle and graphite technology. Other fuels and associated materials have been produced at both Dounreay and Sellafield including, U metal fuels, mixed oxide, carbide and nitride fuels, fast reactor core fuels, and natural U and thorium (Th) metal breeder blankets. The National Nuclear Laboratory's R&D facilities located on the Sellafield and Springfields sites continue to draw on the knowledge base and skills built up over decades within these local communities.

Advanced fuel R&D is being carried out in NNL R&D facilities for UK industrial, European Framework and International industrial customers. Within the UK technical support is being provided to Springfields Fuels Ltd for UO2 fuel manufacturing. This includes SFL powder quality assurance batch testing by manufacture of sintered test pellets, in addition to plant operational support. Fuel performance support is ongoing with EDF Energy and the NDA for irradiation and dry storage of UO2 fuel in both AGRs and the UK's sole PWR at Sizewell B. This includes development of models for clad bore cracking in AGRs, and calculations of fuel degradation (in particular clad creep) during dry storage for both AGRs and Sizewell B.

Manufacturing and fuel performance support for mixed (U, Pu) dioxide fuel manufacture in the Sellafield MOx Plant, has effectively ceased with the closure of the plant, but the R&D expertise remains and has recently been used to support the NDA in Pu disposition (fuel performance analyses of mixed oxide cores in Sizewell B and potential UK new build units).

Within European Frameworks the use of mixed oxide fuel in gas-cooled fast reactors has also recently been investigated. Safety assessment of mixed oxide fuel designs for the ALLEGRO reactor is being investigated within the GoFastR project. In addition opportunities exist to study mixed oxide fuel in fast reactor systems. Within the ASGARD project (see Figure 3) carbide fuel fabrication is being investigated. The current programme involving initial modelling studies will define design requirements for carbide fuel, and will be followed by fabrication of density gradient pellets.

Figure 3. Fuel cycle phases included in FP7 ASGARD Programme

The fuel performance modelling capability is currently underpinned by the ENIGMA (light water reactor applications), TRAFIC (fast reactor applications), and NEXUS (whole core modelling of rod internal pressure) computer codes (see Figure 4). ENIGMA is being actively developed by the NNL. R&D in both multi-scale modelling and use of high performance computing for improved fuel performance simulation is at an early stage.

Figure 4. Map of rod internal pressure (MPa) in every rod of a 4-loop (51,000 rod) PRESSURISED WATER REACTOR core using NEXUS

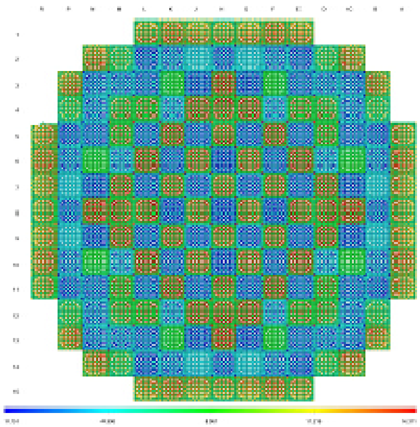

Internationally we are investigating U/Pu nitride and Th/Pu oxide fuel manufacture, initially for test rods, at our fuel manufacturing and qualification facilities (see Figure 5).

Figure 5. Test Fuel Manufacturing Capability

4. Recycle

NNL undertakes a wide range of activities related to spent fuel recycle, from supporting current reprocessing plants at Sellafield to research and development into advanced reprocessing and minor actinide partitioning non-proliferation options for future fuel cycles. Our approach typically combines process modelling, engineering and experimental work.

Experiments range from fundamental studies of actinide kinetics and thermodynamics to lab-scale demonstrations of process flowsheets using realistic concentrations of actinide elements. Our approach is exemplified by work done to develop a new ("Low Acid") flowsheet for Magnox Reprocessing (2000-2009). This programme moved from development of the initial concepts through to testing of flowsheet maloperations to support the new safety case, prior to on-plant introduction of the new flowsheet.

Active experiments are now performed in our Plutonium and Minor Actinides Laboratory at the NNL Central Laboratory site situated at Sellafield, UK (see Figure 7). This laboratory, commissioned in 2010 contains four medium inventory Pu gloveboxes and provides state of the art facilities for experimental studies in dissolution, solvent extraction, conversion and spectroscopy of transuranic actinides. Within this laboratory NNL are currently working on a wide range of projects for UK and European customers as well as internally funded Signature Research into spent fuel and nuclear materials. Specifically, we have long standing interests in the development of an advanced Pu U extraction (PUREX) process with the aim of rationalising the flowsheet to a single cycle.

More recently as part of the 7th Framework Programme funded ACSEPT project we have been engaged in a multi-laboratory effort across Europe to develop a grouped actinide extraction (GANEX) process for homogeneous recycling of actinides in Generation IV fuel cycles. Again, as part of the FP7 funded ACSEPT and ASGARD projects we are studying the dissolution of actinide oxides and carbides into nitric acid, including enhanced dissolution processes.

The design criteria for the GANEX process is to use established chemistry where possible, use existing hot cell configurations and a process compatible with centrifugal contactors,

A robust, operable flowsheet (low pH) is being developed (see Figure 6) to recover neptunium, plutonium, americium and curium in a single solvent extraction cycle, extract actinides in +III,IV,V,VI oxidation states, process 1 to 10's g/L in the feed, avoid plutonium / lanthanide precipitation and avoid reliance on Pu(IV)→(III) reduction.

Figure 6. Development of GANEX Flowsheet

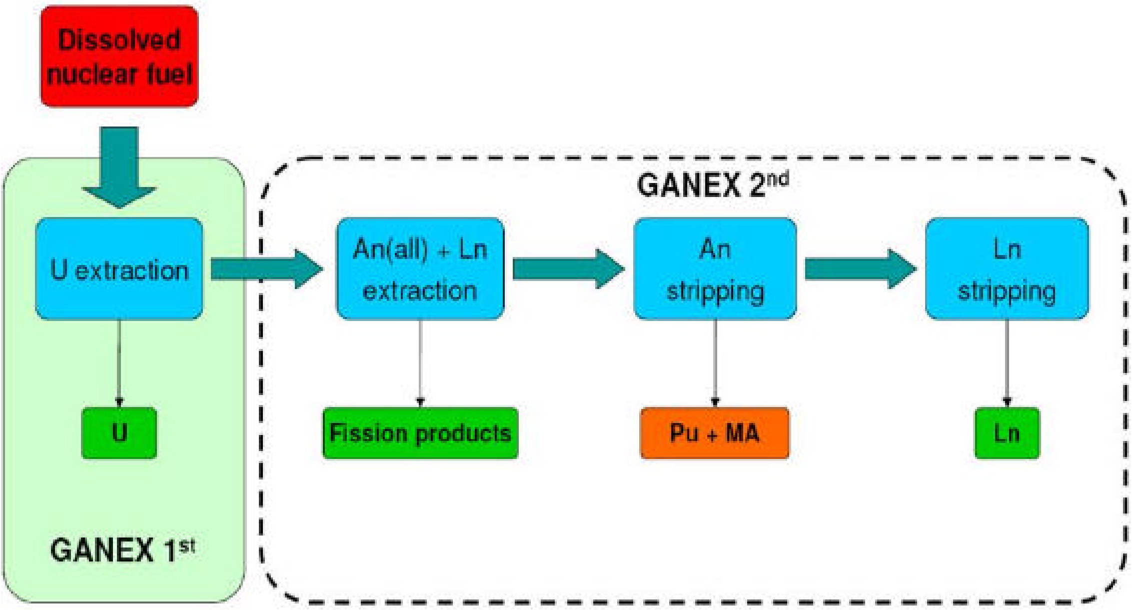

Actinide separations chemistry is also being applied to assess the potential for separation of americium-241 for space battery production and clean up of the Sellafield Pu stockpile ready for recycle as mixed oxide fuel. Support to Thorp and Magnox reprocessing plants is as required by Sellafield but predominantly focuses on supporting continued operations, underpinning reprocessing more challenging fuels remaining in the Thorp baseload, understanding causes of plant blockages and addressing uncertainties in safety cases.

Figure 7. Plutonium and Minor Actinides (PuMA) Laboratory

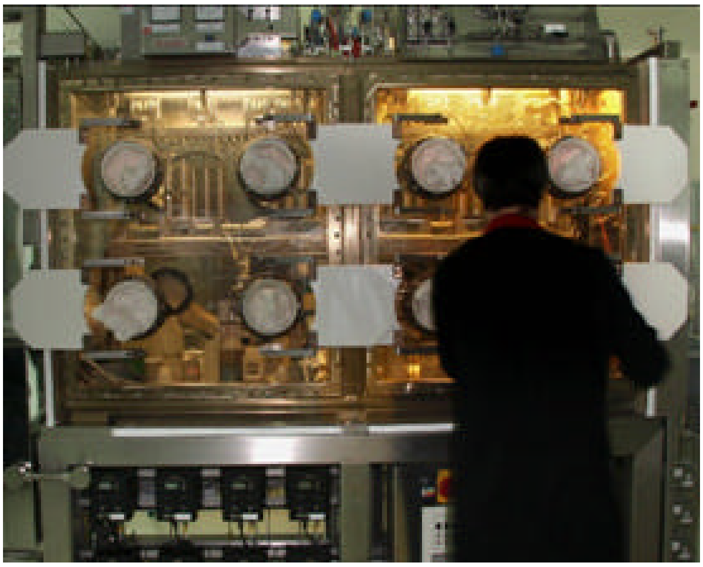

5. Dry Fuel Storage

With the likely cessation of reprocessing in the UK and the long interval before fuel acceptance in a geological repository is available, there is increased focus on the management of spent nuclear fuels over longer timescales than previously experienced and anticipated. This mirrors international agendas, as many other countries are facing similar situations.

NNL is working with a number of customers on the development of suitable dry storage technologies for interim storage of spent nuclear fuels, drawing on it breadth of nuclear expertise. NNL has applied its expertise in fuel performance assessment, both from post-irradiation examination and fuel modelling, to assess relevant behaviours of spent fuels in dry storage environments, with a view to understanding the likely degradation mechanisms and their impact on dry storage system requirements and to assess any knowledge gaps arising from the different timescale and environments associated with dry storage systems.

The thermal performance of dry storage systems is important in determining fuel loading limits, which depend on the decay heat generation, heat transfer paths within the system and the storage materials, which place a variety of temperature limits on the system.

NNL undertakes work supporting option assessment, examining potential storage capacities and safety case assessments, and in examining conservative bounding conditions for both oxide and U fuels. Work by NNL to assess the compliance with fuel cladding failure criteria during fuel storage have shown that much higher fuel and cladding temperatures can be accommodated in Advanced Gas-cooled Reactor fuels than is the case for Light Water Reactor fuels.

NNL expertise in material science and corrosion behaviour is being applied to assess performance of fuel cladding, and to identify suitable environments for extended storage. We have also applied expertise in the analysis of potential fault scenarios associated with storage systems to identify likely behaviours and system responses, as well as conservative analyses to support relevant safety cases.

Its breadth of knowledge and experience with a wide range of fuel types has enabled NNL to assist in the development or refinement of fuel storage systems and safety cases for Magnox fuel, with Sellafield Ltd., Advanced Gas-cooled Reactor fuel, with Sellafield Ltd. and the Nuclear Decommissioning Agency and on Light Water Reactor fuel, with Sellafield Ltd. and EDF Energy. Activities have encompassed initial optioneering and identification of credible options, the identification of knowledge gaps and their significance in relation to the relevant stages of a project life cycle, support to concept design studies and preliminary safety cases and support to detailed design associated safety cases.

NNL is also involved in international activities supporting dry storage of spent Light Water Reactor fuel through which it seeks to apply its expertise and to bring in international experience and knowledge to apply it to UK fuels and technologies. These include:

- IAEA CRP T13014 on demonstrating performance of spent fuel and related storage system components during very long term storage
- EPRI Extended Storage Collaboration Programme member
- IAEA Technical Meeting on Extending Spent Fuel Storage until Reprocessing or Disposal
- Associated Group in the FIRST Nuclides EU FP7 programme (fuel disposal related)

Although NNL is actively involved in R&D associated with reactor systems, waste management and disposal, and security and safeguards technology, these areas have not been covered within this paper.

6. Conclusion

- Nuclear is viewed by many as a mature, reliable low carbon technology with a secure and abundant fuel source and is an essential contributor to the UK energy mix.
- Advanced fuel cycle research has an important role to play within the UK nuclear renaissance.
- NNL continues to play an active role in advanced fuel cycle R&D through a combination of unique facilities, expertise and experience.
- Fuel cycle scenarios require detailed modelling to understand the relationships between reactor type, fuel supply type, fuel recycle and the ability to meet certain energy supply targets by a given date. Other attributes can also be optimised including repository heat loading and repository footprint.

7. Acknowledgements

The author would like to thank the following people from NNL for input into this paper; Robert Gregg, Kevin Hesketh, Robin Taylor, Glyn Rossiter, Paul Glenville, David Hambley, Dan Mathers and Alex Brooke.

TRENDS OF EDF'S FUEL CORE MANAGEMENT AND CONSEQUENCES ON FUEL CYCLE : "CYCLE IMPACT" ANALYSES

HING-IP WONG, ESTELLE DESROCHES
EDF, Nuclear Fuel Division, Spent fuel and radioactive waste management department
1 place Pleyel, Saint-Denis 93 (FRANCE)

LAURENT HANSEL
AREVA NC - BU Recycling -
33 Rue La Fayette 75009 Paris (France)

MARIE-HELENE LAGRANGE, HAKIM GOURRAM
ANDRA, National radioactive waste management agency
1-7, rue Jean Monnet 92298 Châtenay-Malabry Cedex (France)

ABSTRACT

Electricité de France (EDF) has a fleet of 58 PWR and 1 EPR^{TM} under construction. EDF has been continuously fitting fuel core management to nuclear power plants needs. Adapting the nuclear fuel cycle to support fuel core management can be challenging, especially in a closed fuel cycle with plutonium and recovered uranium recycling. EDF's aim is to meet evolutions as needed with a clear commitment to safety and competitiveness. Periodically, the french Nuclear Safety Authority asks EDF to *a)* analyse the coherence of the whole fuel cycle (from natural uranium conversion to radwaste management) for the next decade and *b)* propose evolutions to maintain a high level of safety and robustness. To address this question for the 2007-2017 period, EDF has managed a group made up of main contributors from French nuclear fuel cycle : AREVA and the National radioactive waste management agengy (ANDRA). The presentation will focus on major trends of EDF's fuel core management with the needed evolutions in the nuclear fuel cycle to maintain coherence and guarantee a high level of safety and robustness.

Introduction

EDF is the designer, manufacturer and operator of its own nuclear fleet. EDF divides its PWR reactor model into successive series, incorporating improvements resulting from feedback from operating experience and optimising the electrical power output available:

- series CP0 and CPY comprising 34 plant units of approximately 900 MW;
- series P4 and P'4 comprising 20 plant units of approximately 1,300 MW;
- series N4, the most recent, comprising 4 plant units of approximately 1,500 MW;

or a total of 58 plant units in operation spread over 19 sites representing a total installed output of approximately 63,000 MW. An EPR^{TM} reactor of approximately 1,600 MW is under construction at the Flamanville site.

The performance of a nuclear fleet naturally depends on EDF's ability to operate the power plants as a responsible industrial stakeholder. It is also based on a broad and diverse national and international industrial fabric, enlisted to supply EDF's 58 units with fuel, process and recycle spent fuel as well as to manage and store radioactive waste. Areva and ANDRA (French national radioactive waste management agency) are, naturally, key partners for EDF as part of this industrial fabric.

The average annual reference volume of nuclear fuel consumed by the reactors of the EDF fleet in France is approximately 1,200 tonnes of fuel, of which 1,000 tonnes of UO2 fuels (natural uranium combined with fluorine then enriched), 120 tonnes of MOX fuels (fuel fabricated from recycled plutonium) and 80 tonnes of ERU (enriched reprocessed uranium).

The nuclear fuel cycle includes all the industrial operations undertaken in France and abroad allowing delivery of the fuel to produce reactor-generated power, followed by removal and reprocessing (see Figure 1). The cycle is divided into three parts:

- front end: purchase of natural uranium extracted from the ore material, combination with fluorine (or conversion), enrichment and fuel manufacture;
- service period, which corresponds to use in the reactor: delivery, loading, use and unloading; the fuel spends 4 to 5 years in the reactor;
- back end; for the fleet of reactors in France: interim storage of the spent fuel in a spent fuel pool, transport to the plant in La Hague, reprocessing of the spent fuel, packaging of the radioactive waste and recycling of the recyclable material, interim storage of the packaged waste before deep geological storage as stipulated in the law of 28 June 2006 of the programme for the sustainable management of radioactive materials and waste.

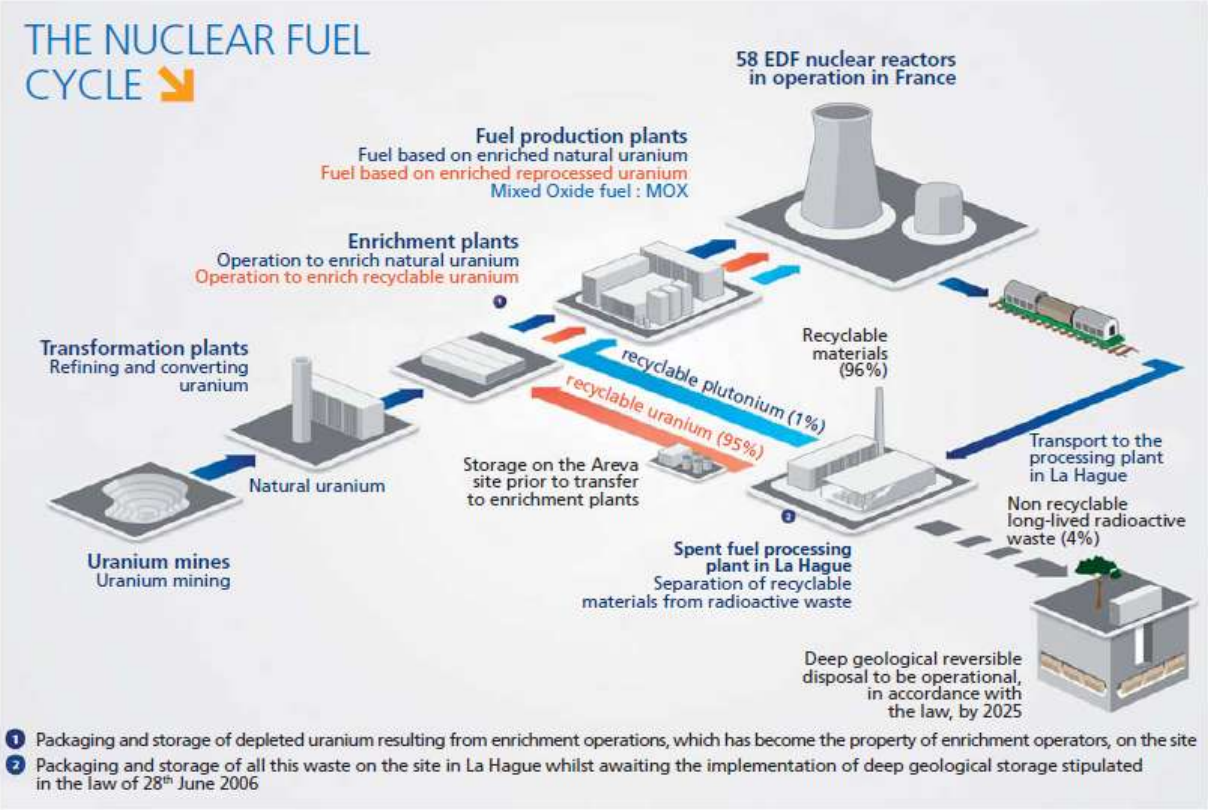

Figure 1: Fuel cycle of French PWRs

The principles of Cycle Coherence for an operator practising reprocessing and recycling

Once the spent fuel has been unloaded from the reactor, EDF remains responsible for its management and must ensure the existence of a safe, regulatory compliant and reliable system capable of managing the spent fuel as well as the final materials and waste of which it is comprised.

Article L542-1-2 of the French Environmental Code states that “the reduction of the amount and toxicity of radioactive waste is sought in particular by the reprocessing of spent fuel”. In agreement with the Government, EDF has chosen to reprocess its spent fuel in order to reduce the volume of its long-lived waste and recycle the recyclable materials contained in the spent fuel.

In this context, ensuring fuel cycle coherence consists of:

- guaranteeing safe interim storage of the spent fuel in the spent fuel pools at the reactors or in the AREVA NC processing plant in La Hague with sufficient operational capacity. Due to their high residual power and the dose rate of the spent fuel, it is vital to have storage available beside the reactor in order to ensure the decay time frame necessary to make the spent fuel assembly compatible with the technical instructions governing transport and delivery to the plant in La Hague. The capacity of the spent fuel pool must, at all times, be sufficient to have the necessary cells available for the complete unloading of the reactor and, prior to shutdown of the plant unit for reloading, sufficient room to receive the replacement load of new fuel. Once the decay period has elapsed, the fuel is transported and stored at the plant in La Hague. The ENU assemblies will be reprocessed, the extracted recyclable materials being recycled to be used in the PWR fleet, whereas the MOX and ERU assemblies are stored for processing for the purposes of supplying a potential future fleet of 4th generation reactors with plutonium. The operator of the plant in La Hague guarantees, in agreement with EDF, sufficient capacity spent fuel pool capacity to accommodate the ENU, MOX and ERU assemblies prior to processing;

- ensuring transport of the spent fuel to the plant in La Hague in compliance with the regulatory requirements in force and shipping cask approvals, while observing the objectives for spent fuel decay times that allow for an acceptable capacity utilisation level at EDF's spent fuel pools; To this end, the shipping cask supplier, a subsidiary of AREVA, is consequently developing new cask models in response to the changing specifications resulting from EDF's management of the fuel cycle;

- guaranteeing the capacity of the plant in La Hague to process the spent fuel over the long term and in compliance with the regulatory requirements concerning nuclear safety. In order to achieve this, it is necessary to ensure that the plant's technical instructions and expected performance are compatible with the characteristics of the spent fuel. This compatibility and performance must be ensured over the long term since the spent fuel is generally processed long after being unloaded from the reactor (as an illustration, the average time between fuel unloading and its processing in the plant in La Hague is around ten years);

- guaranteeing the industrial feasibility of refuelling the reactor with the reprocessed materials (REPU[1] and plutonium) with an identical energy efficiency to that of natural uranium fuel assemblies. Since the characteristics of the materials depend on the irradiation undergone by the fuel, EDF must, in concert with the operators concerned, ensure the technical instructions of the MOX fuel fabrication plant are compatible with those of the REPU recycling division. In order to limit the reduction in power-generating capacity of the plutonium over time, EDF carries out on-load refuelling with the plutonium produced by reprocessing, within the time frames technically feasible. Consequently, in order to balance the flows of plutonium produced from reprocessing and the flows of plutonium loaded into the reactor in MOX fuel, EDF must ensure that the reactor approvals are compatible with the

---

[1] REPU: reprocessed uranium

characteristics of the MOX fuel and that the authorised reactors are in sufficient number to absorb all of the plutonium produced by reprocessing with the required degree of operational flexibility. In order not to penalise the reprocessing/recycling system, EDF expects the same performance in the reactor from fuel assemblies containing recycled materials (REPU and plutonium) as that of natural uranium fuel assemblies. To achieve this objective, the concentration of recycled materials in the fuel must be sufficiently high, which can lead to changes in the reactor or in the fuel cycle plants assigned to the recycling of REPU and plutonium materials. For REPU materials not intended for immediate recycling, the operator guarantees the interim storage capacity and ensures their safety, awaiting their subsequent re-use in accordance with the needs of EDF;

- ensuring the compatibility, existing or planned, of long-term waste management systems. To achieve that, it is necessary, in particular, to ensure that the packaging of the waste results, over the long term, in a volume that complies with the waste volume reduction objective connected with the reprocessing choice. Once packaged, the waste is stored in facilities provided for this purpose, until its sequestration in a permanent repository. EDF must ensure that there is sufficient capacity for ultimate waste storage;

The coherence of the cycle demands appropriate, precise management of each stage of the cycle, avoiding the risk of technical incompatibilities or deterioration in performance of the industrial system. When the fuel loaded into the reactor begins to change, the characteristics of the spent fuel and associated waste can extend beyond the operating range of the existing industrial system. It is then important to ensure that the industrial system will be able to adapt to the needs of the electricity provider without disruption to the overall performance of the system.

Cycle Impact Initiative

Since guaranteeing cycle coherence requires vigilance and forethought, the ASN (French Nuclear Safety Authority) asked EDF, as designer/manufacturer, to evaluate, in concert with the fuel plant operators, transport operator (AREVA) and the storage centres (Andra), the impact of the evolving fuel management needs on their facilities and to draw up an action plan that would allow the coherence of the cycle to be guaranteed over the long term.

This initiative was started by ASN towards the end of the nineties and led to the operators issuing their first “Cycle Impact” study in 2000. The second study, covering a period of 10 years lasting up to 2017, was issued in 2008.

These studies were submitted for expert assessment by the technical bodies that provide support to the ASN (Institute for Radiological Protection and Nuclear Safety [IRSN] and standing committees of experts).

The next “Cycle Impact” study is scheduled for the end of 2016.

Major trends and measures taken by the operators to adapt the fuel cycle

Evolving fuel management needs

Managing a nuclear fleet has to take into account the need to periodically shut each reactor down in order to replenish a part of its fuel and carry out certain maintenance operations. The duration of the shutdown is generally of the order of a few weeks and varies depending on the maintenance work performed. Refuelling adds a stock of energy to the reactor (a few hundred equivalent full power days "EFPD") which must be managed during the subsequent "operating cycle". "Fuel management", i.e. the characteristics of the load added on the occasion of each refuelling outage (amount of fuel, enrichment ratio), determines:

- the potential duration of the operating cycle;
- the cost of the fuel (depending on the amount of fuel and its enrichment).

The choices made by EDF regarding fuel management are in response to objectives relating to:

- fuel safety and reliability which are the overriding priority;
- performance in the reactor and duration of the operating cycle: the fuel must deliver the amount of energy expected by the electricity provider (which is called the burnup fraction and is expressed in MWd/t of fuel). Another important parameter for an electricity provider such as EDF with a large fleet is to be able to achieve the desired length of operating cycle so that the timing of the refuelling outage in relation to the energy balance is optimised;
- securing the fuel supply and performance of the fuel supply: since fuel is an obligatory resource for nuclear production, fuel management choices must allow for diversification of supply sources at competitive rates.

The choices being made now regarding fuel management 10 years from now favour electricity production with the overall discharge burnup fraction of fuel assemblies being maintained in order to increase operating cycle length.

Error! Reference source not found.

Error! Reference source not found.**: Like the majority of other electricity providers around the world, EDF has increased the average burnup fraction of its fuel from approximately 33 GWd/t in the nineties to approximately 45 GWd/t today, while achieving an overall increase in operating cycle lengths by simultaneously increasing enrichment with uranium 235**

Interim storage

The spent fuel discharged from the reactor has to be cooled in spent fuel pools in order to be within the permissible limits for transport packaging, both in terms of removable residual power and dose rates.

Due to the increase in the burnup fraction of the spent fuel assemblies from 33GWd/t to 45GWd/t, the cooling time necessary in the spent fuel pools before transport to the plant in La Hague has become progressively longer. In addition, the introduction of MOX fuel in the eighties further lengthened the cooling time required before transport to the plant in La Hague due to higher levels of decay heat and dose equivalent rate than compared with UOX fuels.

To manage this increase in cooling time, EDF took various steps to free up spent fuel pool cells:

- Removal of spent fuel to the plant in La Hague as soon as possible;

- Installation of waste racks (in operation on series CP0, currently being deployed for series CPY, and planned for series P4 subject to approval);
- Renovation of pools affected by the “Boral” effect. Boral is a neutron absorbing material used in the manufacture of series P'4 spent fuel pool storage racks primarily. Due to a chemical reaction, this material can expand leaving the cell unusable. Since the appearance of this phenomenon in the nineties, pools at risk of being affected are the subject of specific surveillance and there is a pool renovation plan for the worst affected plant units. In 1999, the pool at PENLY 1 was completely renovated and 3 other units are scheduled for the same, subject to approval.

However, EDF believes that these measures have only a limited impact on the problems (renewed increase in plutonium content leading to a lengthening of the cooling time required despite the development of new casks) and difficulties in anticipating transport needs connected with changes in regulatory requirements. Insofar as the interim storage of spent fuel in spent fuel pools is the only link in the chain “ensuring” the robustness of the industrial system in the event of an unforeseen disruption of transport to the plant in La Hague, EDF is planning a structural increase in storage capacity by reracking[2] the plant units. Moreover, boosting capacity by reracking is an opportunity to reduce the radiation dose of the removal operations by making it possible to lengthen the cooling time of spent fuel.

As far as the plant in La Hague is concerned, pool capacity has been optimised by the operator in order to accommodate spent fuel transported to the facility.

Transition to MOX Parity management has seen an increase in the plutonium content and in the burnup fraction. That results in a substantial increase in the neutron source term for spent MOX fuel under MOX Parity management. In order to keep cooling times before removal compatible with the actual capacity of the spent fuel pools, it has proved necessary to develop higher performance casks.

That’s why a new cask called TN®112 was designed and manufactured by AREVA TN International (see Figure 2). The high level of performance has been achieved thanks to very specific materials such as high strength forged austenitic stainless steel, reinforced gamma shielding materials and TN Vyal B™ resin for the neutron absorber. This is a cask with a capacity of 12 MOX or UO2 spent fuel assemblies for PWR power plants for which a B(U) type approval has been granted according to AIEA 96. Thanks to its better performance, the cooling time required to remove the spent MOX fuel under MOX Parity management will be brought down to less than 4 years.

---

[2] Increase in number of cells in the pool by boosting rack density

Figure 2: TN112 Copyright AREVA - J.M. Taillat

The first TN®112 cask was brought into service in 2008 and the second cask will be brought into service in 2012. The objective is to ensure all removal of MOX fuel under MOX Parity management will be done using TN®112 casks by 2014. In anticipation of an impending increase in the plutonium content of MOS fuels (MOX NT2012), an extension of the approval certificate for the TN®112 cask was obtained in 2011.

With regard to the removal of spent UOX fuel, AREVA (TNI) and EDF are currently working on a new cask design (3rd generation) which will be in compliance with the latest AIEA regulatory requirements relating to the transport and containment for future potential EDF fuel management programmes. The objective is to have these enhanced performance casks in operation by 2020.

Reprocessing

In keeping with the objective of controlling waste volume, EDF wishes to keep the production ratio of high-level vitrified waste (HL waste) within the limit of 2 packages (CSD-V) per TWhe. With regard to the increase in burnup fractions of used fuel assemblies, meeting this objective required R&D work in order to draw up a new specification governing the production of vitrified waste.

Recycling

EDF has many years' experience with recycled MOX and ERU products. The use of ERU fuel began in 1994 with fuel assemblies that had an energy performance less than that of natural uranium fuel. Energy equivalence with natural uranium fuel was achieved in 1999. This equivalence requires super-enrichment of the ERU fuel. The amount of ERU loaded depends on the financial appeal of the ERU fuel compared with natural uranium fuel and weighing up of current and future usage against the number of plant units authorised to use this fuel. As of today, four plant units of the French fleet (Cruas site) are authorised to use reprocessed uranium fuel.

The use of MOX fuel began in 1987, with a steady increase in the number of MOX assemblies being loaded into reactors (see Figure 3). Energy equivalence with natural uranium fuel was achieved in 2007. With regard to the amount of MOX fuel loaded into reactors, it is EDF's objective to achieve a “balance of flows”, i.e., to fully recycle the plutonium extracted from the reprocessing of spent fuel at the plant in La Hague within the time frame technically feasible.

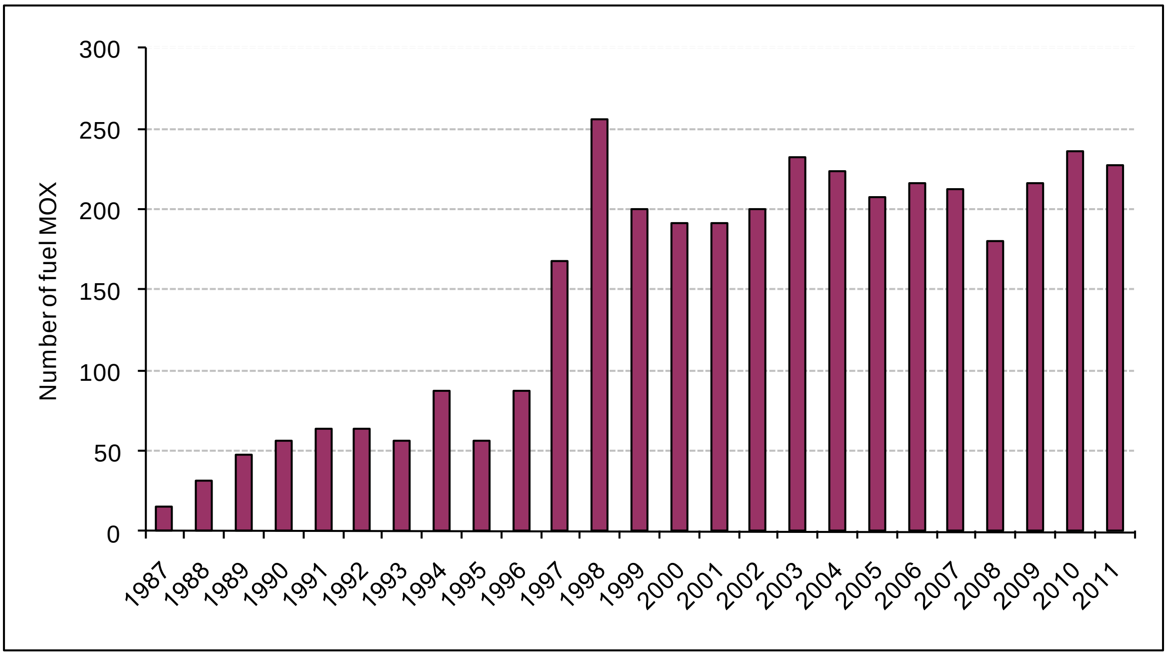

Figure 3: MOX fuel loading in EDF reactors (number of assemblies)

With the increase in the level of recycling from 850tHM (tonnes of heavy metals) per year to 1,050tHM per year from 2012, the amount of plutonium extracted annually from spent fuel has risen by approximately 25%. By virtue of the “balance of flows” principle for plutonium, the tonnage of MOX fuel loaded into reactors has also increased, growing from 100tHM to 120tHM per year (the increase is 20% as opposed to 25% because the plutonium content has increased in parallel). Since the amount of new MOX fuel is set by the fuel management programme, the increase in MOX tonnage meant that authorisation to load MOX fuel into two additional plant units had to be sought, increasing the number of units authorised to use MOX from 20 to 22. This number of plants allows exactly 120tHM of MOX to be loaded per year. In order to have the operational flexibility necessary, EDF wishes to have a slightly higher number of plant units approved to use MOX than is strictly necessary. For that reason, EDF has requested authorisation to be able to load an additional two units with MOX (units 3 and 4 at Blayais).

From a quality perspective, the increase in burnup fractions is leading to deterioration in the materials produced by reprocessing (see Figure 4):

- in the plutonium, the proportion of isotope pairs (Pu238, Pu240 and Pu242) is increasing;
- in the reprocessed uranium, the proportion of isotope pairs (U232, U234 and U236) is also increasing.

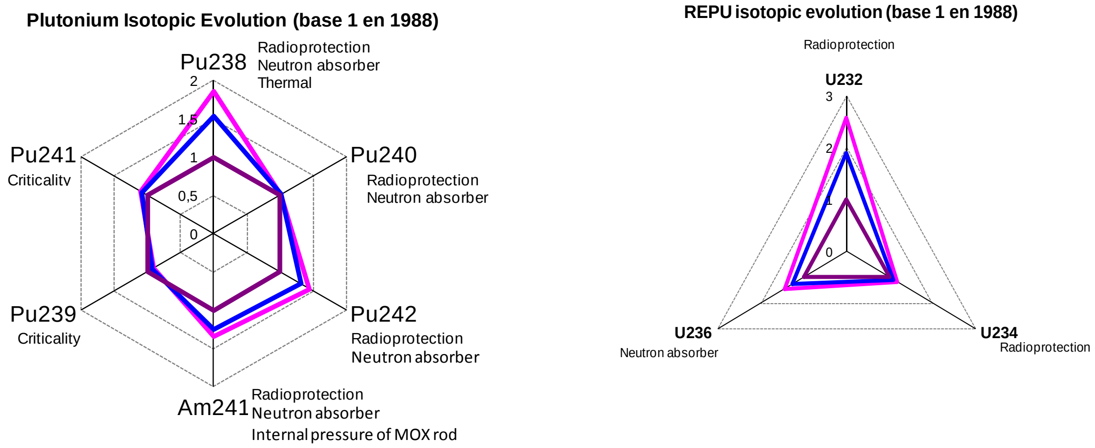

Figure 4: Isotopic quality evolution of materials produced by reprocessing

Since isotope pairs are neutron absorbing in the reactor, the reprocessed uranium or plutonium content must be increased in the fuel assemblies to maintain an energy content identical to that of the natural uranium assemblies. EDF is intending to file a submission with the ASN in 2013 to increase the plutonium content of MOX used in reactors (MOX NT2012). The submission justifying the increase in ERU is currently being drawn up by EDF.

Since both plutonium and reprocessed uranium isotope pairs also emit radiation, the increase in their proportion in recycled material may require modification of radioprotection methods in the fuel cycle plants.

The increase in radiation dose caused by changes in the isotopic compositions of the plutonium and REPU has been limited by certain operational improvements at the MELOX plant and optimisation of the REPU cylinder interim storage fleets at the FBFC fuel manufacturing plant.

Long term management of short-lived waste

Waste from PWR reactors

The Aube Storage Centre (CSA) receives operational waste from PWR reactors; this waste consists of packages of ion-exchanging resins and filter resins used to purify the reactor coolant system. It also receives evaporation concentrates and technical waste from maintenance operations. The main potential impact of any significance identified of a change in the fuel core management programme would be because of a change in the materials used in the cladding or structures. The metallurgical composition of these components can, in effect, affect the particles released into the reactor coolant system through corrosion or abrasion and the nature of the activation products which form in this circuit.

In practice, the only chemical element which shows any significant variation in the zirconium and niobium based alloys is niobium. The activation product in niobium, isotope ^{94}Nb, is subject to two limits at CSA:

- a concentration-based activity limit (CAL) per package,
- a limit connected with overall capacity accommodated (whole of site and all packages).

An attempt to assess the impact on short-lived waste of a potential increase in the release of niobium into the reactor coolant water was attempted by EDF by means of a theoretical approach in combination with feedback from experience. This was based in particular on measurements carried out on the water of the reactor coolant system in a bypass circuit of the Nogent 2 reactor. The measurements show that there is no difference in Nb94/Co60 ratio between plant units using niobium-doped cladding and zircaloy cladding.

Thus, on the basis of analyses made at this stage, Andra considers that the widespread use of fuel assemblies with zirconium and niobium based alloy cladding and structures should not compromise the acceptability of operational waste from EDF power plants as far as the CSA is concerned.

However, in order to back this conclusion up over the long term, EDF is currently continuing with its programme of measurements on the water from the reactor coolant systems of reactors fitted, from 2007 on, with cladding using the new alloys (M5 and Zirlo).

Waste from fuel cycle facilities

Facilities whose waste may be affected by changes in the fuel management programme or fuel products are the plant in La Hague and the MELOX plant.

Waste from the plant in La Hague

The zirconium and niobium based alloys also have to be taken into account in connection with the pool water purification and filtration resins at the plant in La Hague. The release there would appear to be less significant as conditions there are less aggressive. Surveillance of the phenomenon will take account of feedback from experience at the power plant units and shall be included in the programme of periodic adjustment of the ratios used for the evaluation of the long-lived radioactive waste components.

Alpha waste from the MOX fuel assembly manufacturing plant (MELOX plant)

The MELOX plant has taken measures to limit the amount and concentration of alpha emitters in waste products, despite the increase in tonnage and plutonium content of MOX fuel (see recycling paragraph).

With regard to waste, the steps taken by the operator to minimise potential sources, such as the reduction in volume of certain waste, for example, limit the dose impact due to changes in the fuel's composition.

Long term management of long-lived waste

The widespread use of zirconium and niobium based alloy cladding should not have any effect on the production of HL waste (CSD-V) and MLLL (CSD-C), given the relatively insignificant contribution of niobium to the activity of this waste (1% maximum of niobium in the alloy).

Conclusions

For performance reasons, EDF is making changes to its fuel cycle management programme. Guaranteeing the coherence of the fuel cycle in the context of these changes requires forethought in order to verify feasibility at each stage of the cycle, then perform regular monitoring of the changes required for the proper functioning of the fuel cycle.

The Cycle Impact initiative started by ASN makes it possible to unite the stakeholders in the cycle around the common objective of cycle coherence. When examining the last Cycle Impact study, the ASN confirmed the importance of this initiative and asked to receive more regular updates from the operators on their activities.

The last Cycle Impact study issued in 2008 concluded with the measures that should be implemented by operators over the next 10-year period to ensure the coherence of the fuel cycle. In the wake of the Fukushima events in March 2011, additional safety assessments were undertaken by EDF and AREVA on their facilities. After analysis, the ASN released technical instructions, for the attention of the operators, aimed at reinforcing safety measures to deal with extremes of nature. Although it is still too early to learn the full lessons of

Fukushima, the operators have analysed the consequences of this event on the measures established in 2008 in the Cycle Impact study and consider that the solutions envisaged to ensure the coherence of the fuel cycle over the next ten years remain appropriate.

SIMULATIONS OF CANDU REACTOR CORE CONFIGURATIONS UTILIZING A THORIUM BATTERY BUNDLE

S. GOLESORKHI, B. ROUBEN, AND M.H. KAYE*
Faculty of Energy Systems and Nuclear Science, University of Ontario Institute of Technology, 2000 Simcoe Street North, Oshawa, Ontario, CANADA L1H 7K4

Corresponding Author: Matthew.Kaye@uoit.ca

ABSTRACT

Since its inception, the commercial nuclear power industry has relied on uranium as its primary fuel source. Though the supply of uranium available in the earth's crust and in seawater is sufficient to power humanity for centuries, if not millennia, it will not be able to do so economically for very long. As a result, the investigation of alternate fuel cycles stands to be of great benefit. Thorium is a strong contender to supplement uranium in future nuclear fuel cycles due to its fertility and high abundance. Studies have concluded that heavy water reactors are especially well suited to efficiently exploit thorium as a supplemental fuel. The objective of this project was to develop CANDU 6™ reactor core configurations utilizing thorium "battery" bundles. Simulations of various reactor configurations were performed using the DONJON and DRAGON reactor physics codes. The simulated designs were judged based on their ability to extend the length of time the fuel spends in the reactor (i.e., achieve higher burnup and reduce refuelling rate) while maintaining the net power output and criticality.

1. Introduction

Uranium is currently used worldwide at a rate of about 68,000 Tonnes per year [1]. It is estimated that there is 5.3 million Tonnes of easily accessible uranium ore (i.e., approximately 80 years of power production at the current worldwide rate), with an additional 7.6 million Tonnes of supply that would be much more costly to extract. Further, there is estimated to be 4000 billion Tonnes [1] of uranium in seawater, though no commercial process for its extraction currently exists. Based on increasing population, urbanization and energy demand, and the escalating role of nuclear power in meeting that demand, it is very important to use the currently available resources more efficiently.

Due to its relatively high abundance (thorium is three times as abundant as uranium) [2] thorium has been proposed not just as a replacement fuel, but also as a supplemental nuclear fuel. When used in a reactor alongside uranium, the average discharge burnup of uranium fuel can be increased while maintaining criticality and power output. While the fissile content of uranium (natural or enriched) depletes as it spends time in a reactor, thorium will produce new fissile content (^{233}U) with time. Thus the original uranium fuel can be left in the reactor longer, allowing more efficient utilization. This is the idea behind a "battery" bundle, one that can "charge" during the beginning of its life in the reactor and "discharge" towards the end.

Thorium has many advantageous properties for use in nuclear reactors. It has a higher absorption cross section than ^{238}U, leading to an improved thermal utilization factor [3]. When converted to fuel pellets, thorium dioxide (ThO_2) is more chemically stable, has higher thermal conductivity, lower thermal expansion, and higher melting point than UO_2 [4]. ^{233}U also has several advantages when compared to other fissile nuclides. While it has a similar fission cross section, its neutron capture cross section is lower than those of both ^{235}U and

^{239}Pu [3]. This both improves the neutron economy and reduces the amount of minor actinides, allowing for more reprocessing cycles. The presence of ^{232}U in the thorium fuel cycle presents a non-proliferation advantage. The decay chains of both ^{232}U and ^{232}Th contain ^{208}Tl, a high energy gamma (2.6 MeV) [3] emitter. While this prohibits stealthy redirection of spent fuel, it does pose a reprocessing challenge.

Thorium’s high absorption also limits its use in nuclear reactors. It acts as a very severe neutron poison and it is necessary to “prime” it with fissile content. Also, to make effective use of it, a reactor with good neutron efficiency is required. As a result, pressurized heavy-water reactors (PHWR) are most commonly considered ideal for the use of thorium fuel [2]. Many studies have been performed on the use of thorium fuel in CANDU™ (CANada Deuterium Uranium) reactors and AECL (Atomic Energy of Canada Limited) has extensive experience with both fabrication and irradiation of ThO_2 fuel pellets [3].

Work on thorium usage in CANDU™ reactors has previously been performed at UOIT (University of Ontario Institute of Technology) as well. A study of the use of thorium nitrate as a liquid solution in vertical columns in CANDU™ reactors was previously performed and presented at ENC2010 in Barcelona [5]. The concept was found to be sound, but there were concerns with the necessary chemical separation and space requirements inside the reactor vessel.

This study will instead focus on more conventional usage of thorium, using CANDU™ fuel bundles in a standard CANDU 6™ reactor. Natural uranium bundles in the standard 37-element configuration (See Figure 1) shall still be used in the majority of the reactor. Bundles of mixed oxides of thorium and uranium in the annular 28 element configuration (See Figure 2) shall be used in select channels.

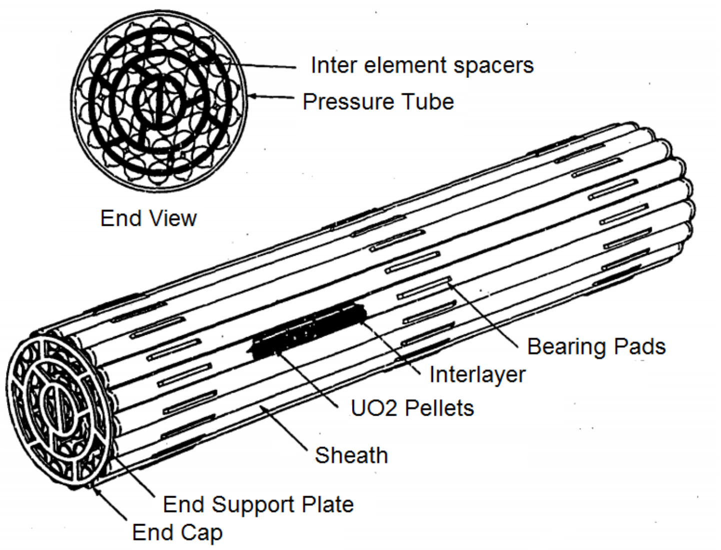

Figure 1 - CANDU™ 37 Element Bundle (Adapted from [10])

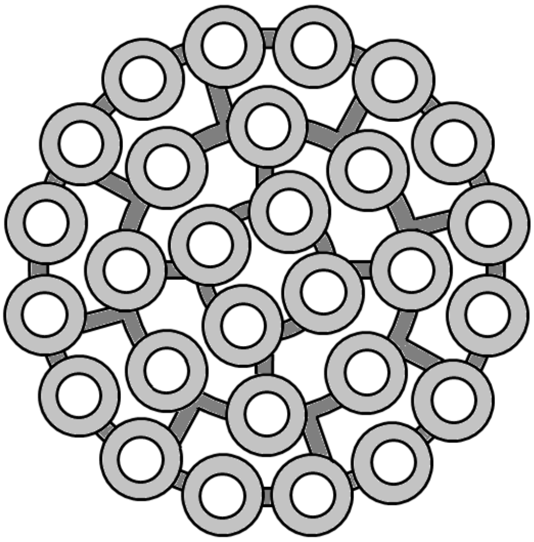

Figure 2 – Not-to-scale diagram of Annular 28 Element Bundle Concept (Front View)

The objective of this research is to develop CANDU 6™ reactor core configurations utilizing thorium bundles which will produce the same amount of overall reactor power, but which will achieve a higher uranium burnup. The goal is to reduce the refuelling rate of CANDU™

reactors in order to decrease fuel usage but also to reduce the workload of the fuelling machines.

The primary methods of calculations for this study have been the DONJON [6] and DRAGON [7] reactor physics codes. Both codes have been developed and maintained by the Groupe D'Analyse Nucléaire at École Polytechnique de Montréal. DRAGON is a cell calculation code that solves the neutron transport equation [8]. It is used to calculate macroscopic cross sections and isotopic densities over a series of burnup increments. DONJON is a finite reactor analysis code that solves the neutron diffusion equation. The cell cross sections calculated in DRAGON are read and used to calculate the reactor's overall multiplication constant, neutron flux shape as well as bundle and channel powers.

2. Experimental Modelling

The natural uranium 37 element CANDU™ bundle and 28 element annular thorium/uranium bundle were both modelled in DRAGON. The burnup of each was calculated using a constant power of 31.9713 MW/Mg (Heavy Element).

Several "enrichments" of ^{233}U in ^{232}Th were attempted in order to find a sustainable fuel cycle. DRAGON calculates isotopic concentrations per burnup step. Each "enrichment" was analyzed so that at an estimated discharge burnup, the sum of the final concentrations of ^{233}U, ^{235}U, and ^{233}Pa were higher than the initial concentration of ^{233}U. The reason for including ^{235}U and ^{233}Pa is explained below.

The process by which ^{233}U is produced in thorium fuel is shown in Equation 1. ^{232}Th absorbs a neutron to become ^{233}Th which beta decays with a half-life of 22 minutes [2] to ^{233}Pa. This radionuclide beta decays to ^{233}U with a half-life of 27 days [2]. ^{235}U is also produced in trace amounts by neutron capture and in high burnup scenarios contributes to neutron multiplication. This is why ^{235}U and ^{233}Pa are also included in the calculation of final fissile content.

Equation 1 - Production of ^{233}U from ^{232}Th

$$^{232}_{90}Th + ^{1}_{0}n \rightarrow ^{233}_{90}Th \xrightarrow{\tau_{1/2}=22\min} ^{233}_{91}Pa + \beta^{-} \xrightarrow{\tau_{1/2}=27days} ^{233}_{92}U + \beta^{-}$$

DRAGON also calculates the cross sections of the fuel lattice model and outputs them in a file (termed the "COMPO" file). These files are utilized as fuel mixture data in a three dimensional DONJON model of the CANDU 6™ core. The core geometry was left unchanged except to designate specific channels as thorium channels. Several configurations were attempted and the output of each was analyzed.

The success of simulations as viable solutions was judged by the shape of the power distribution in the radial and axial directions, the refuelling frequency of the new reactor configuration, the average discharge burnup of the natural uranium fuel and of course, the maintenance of criticality. The uranium channel and uranium bundle thermal powers were judged based on their compliance with the CANDU™ license powers (maxima of 7.3 MW and 935 kW [9], respectively).

Assumptions were made for a number of items. The absolute fuel mixture temperature and average bundle power of the thorium/uranium mixture were assumed to be the same as those of the natural-uranium fuel bundle (approximately 941K and 32 MW/Mg [7] respectively). The H_2O levels in the liquid zone control compartments (LZC) (the “workhorse” reactivity devices in CANDU reactors) are assumed to be at a constant 33%. The adjuster rods are assumed to be 50% inserted into the reactor core.

Table 1 - Inputs and Outputs of DRAGON and DONJON with typical values

	DRAGON	DONJON
Inputs	• Absolute Temperature of Fuel Mixture ○ e.g., 941 K • Mass Density of Mixture ○ e.g., 10.0 g/cm^3 • Relative wt% of isotopes ○ e.g., 86.6% ^{232}Th, 12.1% ^{16}O,1.28% ^{233}U • Bundle Geometry ○ e.g., 28 Element Annular, 37 Element • Average Bundle Thermal Power ○ e.g., 32 MW/Mg • Number of Neutron Energy Groups ○ e.g., 2 Energy Groups • Burnup time limit ○ e.g., 500 days	• Cross sections from DRAGON ○ i.e., COMPO file • Total Fission Power ○ e.g., 2061.4 MW • Number of Neutron Energy Groups ○ e.g., 2 Energy Groups • Fuel Map ○ See Figure 6 • Fuel cell lattice pitch ○ e.g., 28.6 cm • Fuel weight (Heavy Element) ○ e.g., 19.2 kg • Combustion Zones ○ e.g., See Figure 6 • Average Discharge Burnup ○ e.g., 7500 MWd/Mg
Outputs	• Infinite multiplication constant of lattice (k_{inf}) ○ e.g., 1.02 • Isotopic Concentrations ○ See Figure 5 • Macroscopic Cross Sections ○ e.g., COMPO file • Lattice Cell Flux ○ e.g., 4.65E+14 n/cm^{2}s	• Effective multiplication constant (k_{eff}) ○ e.g., 0.996 • Bundle and Channel Powers • Burnup Distribution • Core Flux Distribution • Axial Shape • Refuelling Rate per channel

3. Results and Discussion

Several “enrichments” of ^{233}U in ^{232}Th were simulated in DRAGON in order to find the optimal value which would result in a stable steady state fuel cycle. As mentioned in the previous section, final fissile content was calculated as the sum of the concentrations of ^{233}Pa, ^{233}U and ^{235}U.

Selected results are shown in Figure 3. Although the bundle with the initial ^{233}U content of 1.4% resulted in much higher breeding ratios (and in fact as initial ^{233}U content is decreased, the final fissile content ratio increases significantly), it can be seen from Figure 4 that this bundle also reached subcriticality very quickly, at only about 2500 MWd/Mg (Heavy Elements). Conversely, the 1.6% bundle remained supercritical even over very high burnups, but was not conducive to a stable fuel cycle.

Intermediate “enrichments” of 1.5% and then 1.45% were also attempted and it was found that 1.45% resulted in an acceptable trade-off between fuel cycle requirements and criticality. In this bundle, the amount of fissile content was relatively stable and reached the original value after a burnup of about 4800 MWd/Mg (Heavy Elements). Thus, a thorium bundle with 1.45% initial ^{233}U content was chosen as the working bundle cell for DONJON simulations. The evolution of nuclide concentrations for this bundle is shown in Figure 5.

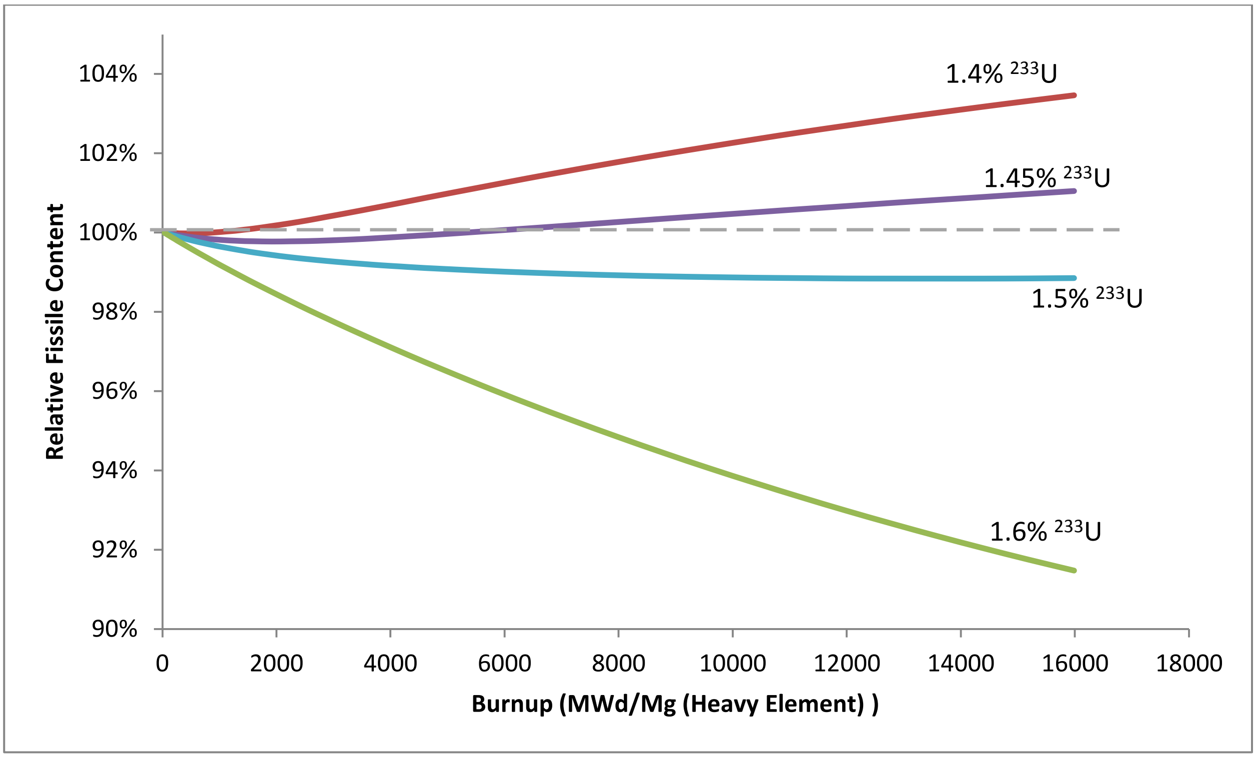

Figure 3 – Relative fissile content over burnup of thorium bundles with various “enrichments” of ^{233}U

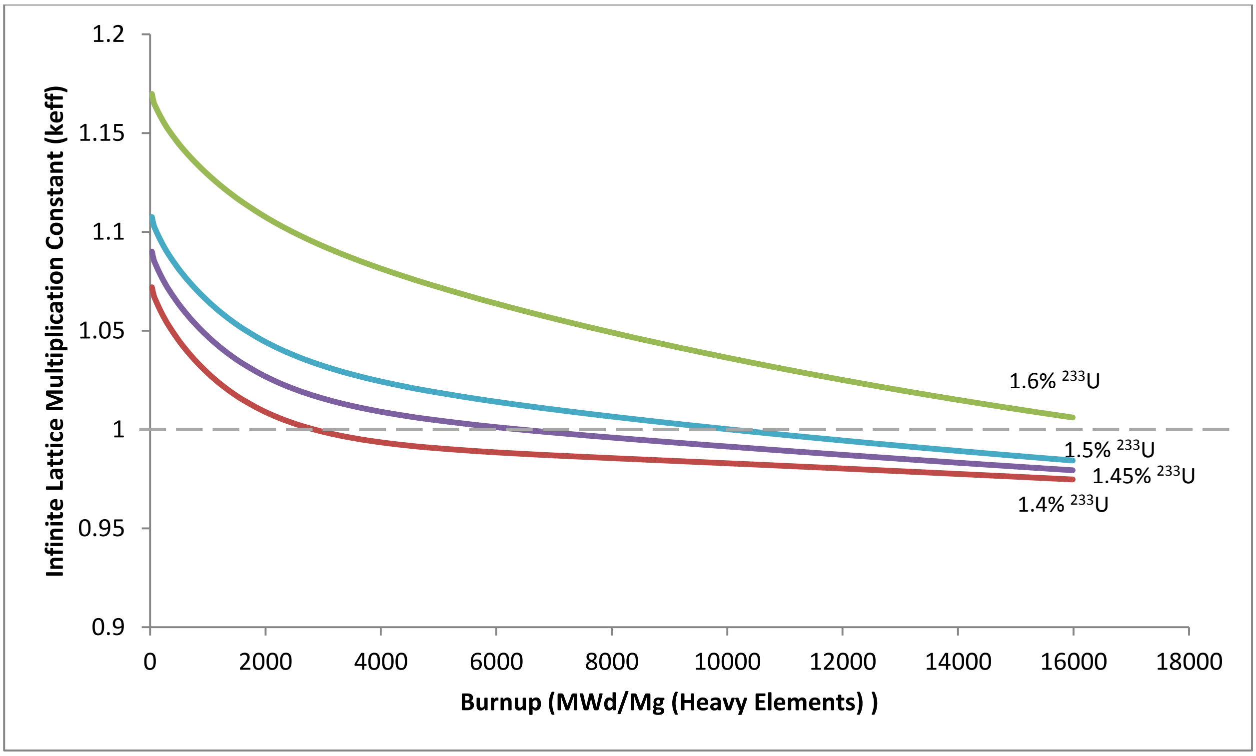

Figure 4 – Infinite lattice multiplication constants of Thorium bundles containing various “enrichments” of ^{233}U

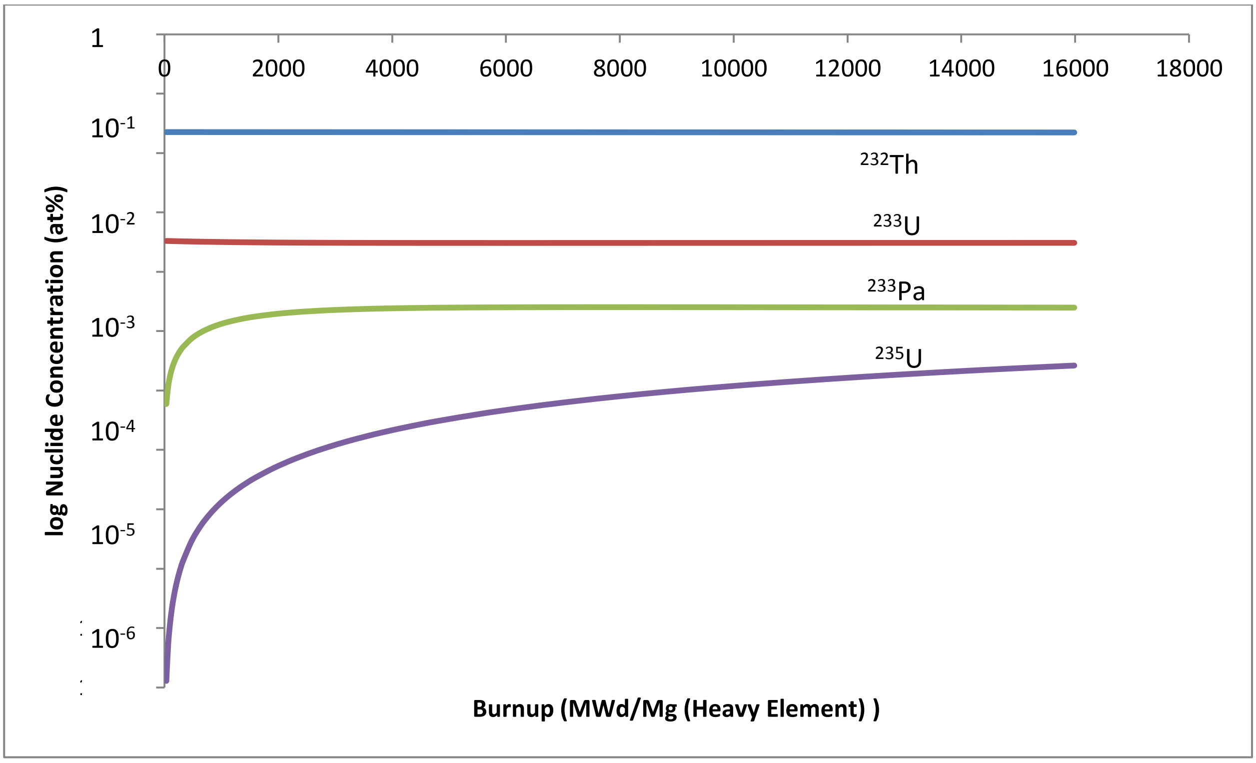

Figure 5 – Concentration of nuclides over burnup values for an annular 28 element CANDU™ thorium bundle with initial ^{233}U content 1.45%

The cross section file for this bundle simulation was used (along with that of the standard 37 element natural-uranium bundle) in several DONJON reactor core configurations. Three variants (labelled A, B, and C) and a standard CANDU 6™ reactor (as a baseline) were analyzed (See Figure 6). Each iteration of the three configurations was compared in key properties against the simulation of the standard CANDU 6™ reactor. The results of the baseline simulation are shown in Table 2. The daily refuelling rate is given in bundles per day. CANDU™ reactors are normally fuelled in a bundle-shift scheme. Each "channel visit", 8 bundles (of 12 total per channel) [10] are refuelled and the remaining four are shifted from the front to the end of the channel.

Table 2 – Results of a DONJON simulation of a standard CANDU 6™

Property	Standard CANDU 6™
Average Discharge Burnup (MWd/Mg (Heavy Elements))	7500
Effective Multiplication Constant (k_{eff})	0.99625
Maximum Bundle Power (kW)	835.4
Maximum Channel Power (kW)	7003.6
Daily Mass Discharge Rate (kg/d)	274.9
Daily Refuelling Rate (bundles/d)	14.4
Refuelling Scheme	8 bundle-shift
Reactor Fission Power (MW)	2061.4
Number of Fuel Channels	380

Configuration C does not seem to be viable, although criticality levels approximating the baseline could be reached while holding power output constant. A wide range of burnup patterns and values were attempted with this configuration, but it consistently resulted in maximum uranium channel and uranium bundle powers far beyond the limits dictated by the CANDU™ operating license. Furthermore, it resulted in an overall increase in refuelling rate.

Several iterations of configuration B resulted in a working solution. A higher uranium burnup zone around the thorium fuelled channels was designated. A particular solution involved average discharge burnups of 7,300 and 9,000 MWd/Mg(U) for the uranium fuel and 10,500 MWd/Mg (Heavy Elements) for the thorium fuel. Subcriticality approximating the baseline case was achieved with maximum bundle and channel powers well below the limits (902.5 kW and 7,096.5 MW, respectively.) Channel power distribution for this solution is shown in Figure 8. Refuelling rate did drop, though very slightly (14.1 bundles/d).

Configuration A yielded the best result. Again, a region of high burnup was designated at the center of the core. This configuration allowed the average discharge burnup of uranium to be pushed as high as 10,500 MWd/Mg(U) at the center and 6,900 MWd/Mg(U) at the surrounding region. The average discharge burnup was set to 11,500 MWd/Mg (Heavy Elements) for the thorium channels. In this case, the effective multiplication constant (k_{eff} = 0.996083) was very slightly lower than the baseline case. Refuelling rate dropped (again to 14.1 bundles/d), though still not very significantly. Channel and bundle powers were higher than Configuration B, but remained below license limits. Channel power distribution for this solution is shown in Figure 7. Further iterations shall be carried out in the future to reduce these values so they are more in line with the baseline CANDU 6™.

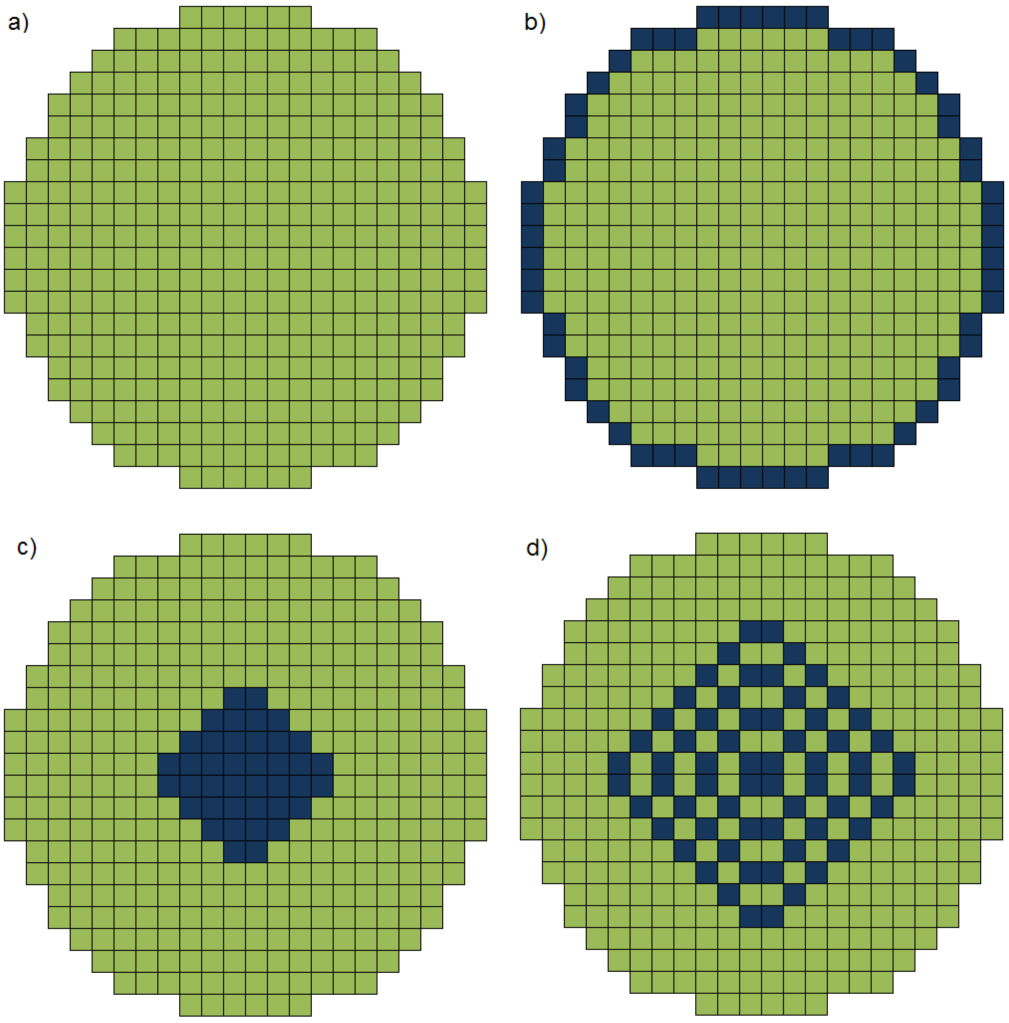

Figure 6 - Reactor configurations mapped in DONJON. Natural uranium channels are coloured light green, thorium channels are coloured dark blue. Configurations: a) Standard CANDU™ Reactor b) Configuration A c) Configuration B d) Configuration C

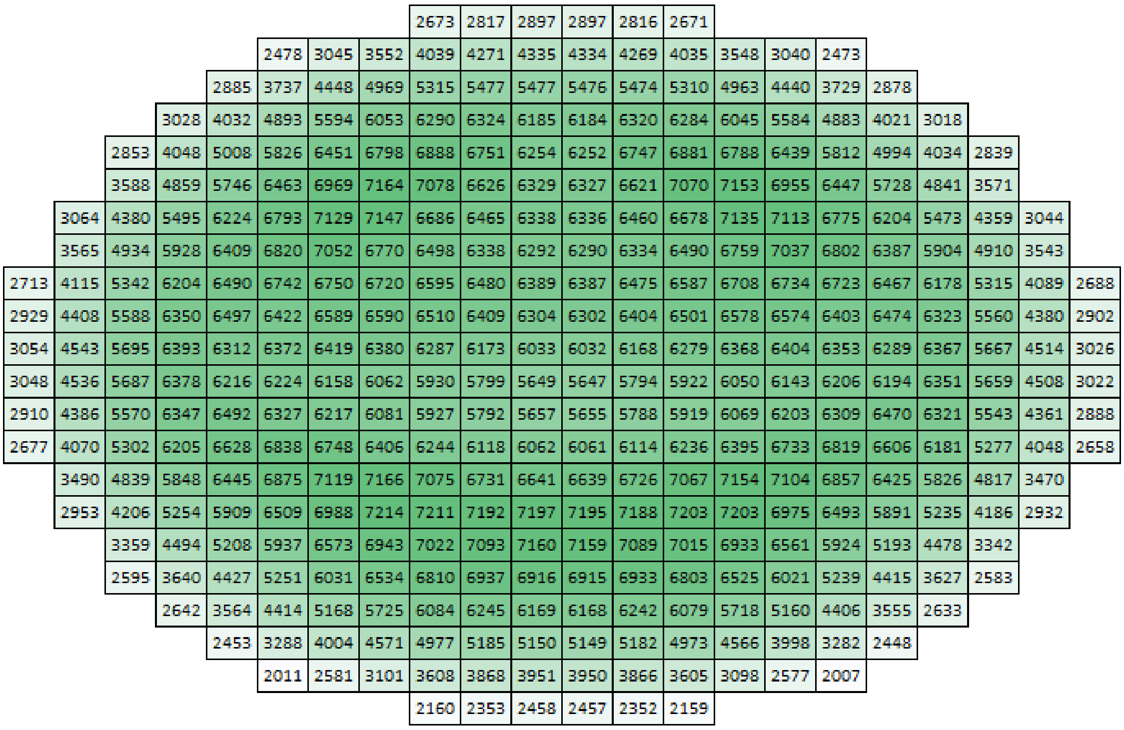

								2673	2817	2897	2897	2816	2671								
					2478	3045	3552	4039	4271	4335	4334	4269	4035	3548	3040	2473					
				2885	3737	4448	4969	5315	5477	5477	5476	5474	5310	4963	4440	3729	2878				
			3028	4032	4893	5594	6053	6290	6324	6185	6184	6320	6284	6045	5584	4883	4021	3018			
		2853	4048	5008	5826	6451	6798	6888	6751	6254	6252	6747	6881	6788	6439	5812	4994	4034	2839		
		3588	4859	5746	6463	6969	7164	7078	6626	6329	6327	6621	7070	7153	6955	6447	5728	4841	3571		
	3064	4380	5495	6224	6793	7129	7147	6686	6465	6338	6336	6460	6678	7135	7113	6775	6204	5473	4359	3044	
	3565	4934	5928	6409	6820	7052	6770	6498	6338	6292	6290	6334	6490	6759	7037	6802	6387	5904	4910	3543	
2713	4115	5342	6204	6490	6742	6750	6720	6595	6480	6389	6387	6475	6587	6708	6734	6723	6467	6178	5315	4089	2688
2929	4408	5588	6350	6497	6422	6589	6590	6510	6409	6304	6302	6404	6501	6578	6574	6403	6474	6323	5560	4380	2902
3054	4543	5695	6393	6312	6372	6419	6380	6287	6173	6033	6032	6168	6279	6368	6404	6353	6289	6367	5667	4514	3026
3048	4536	5687	6378	6216	6224	6158	6062	5930	5799	5649	5647	5794	5922	6050	6143	6206	6194	6351	5659	4508	3022
2910	4386	5570	6347	6492	6327	6217	6081	5927	5792	5657	5655	5788	5919	6069	6203	6309	6470	6321	5543	4361	2888
2677	4070	5302	6205	6628	6838	6748	6406	6244	6118	6062	6061	6114	6236	6395	6733	6819	6606	6181	5277	4048	2658
	3490	4839	5848	6445	6875	7119	7166	7075	6731	6641	6639	6726	7067	7154	7104	6857	6425	5826	4817	3470	
	2953	4206	5254	5909	6509	6988	7214	7211	7192	7197	7195	7188	7203	7203	6975	6493	5891	5235	4186	2932	
		3359	4494	5208	5937	6573	6943	7022	7093	7160	7159	7089	7015	6933	6561	5924	5193	4478	3342		
		2595	3640	4427	5251	6031	6534	6810	6937	6916	6915	6933	6803	6525	6021	5239	4415	3627	2583		
			2642	3564	4414	5168	5725	6084	6245	6169	6168	6242	6079	5718	5160	4406	3555	2633			
				2453	3288	4004	4571	4977	5185	5150	5149	5182	4973	4566	3998	3282	2448				
					2011	2581	3101	3608	3868	3951	3950	3866	3605	3098	2577	2007					
								2160	2353	2458	2457	2352	2159								

Figure 7 - Channel power distribution in the solution using Configuration A

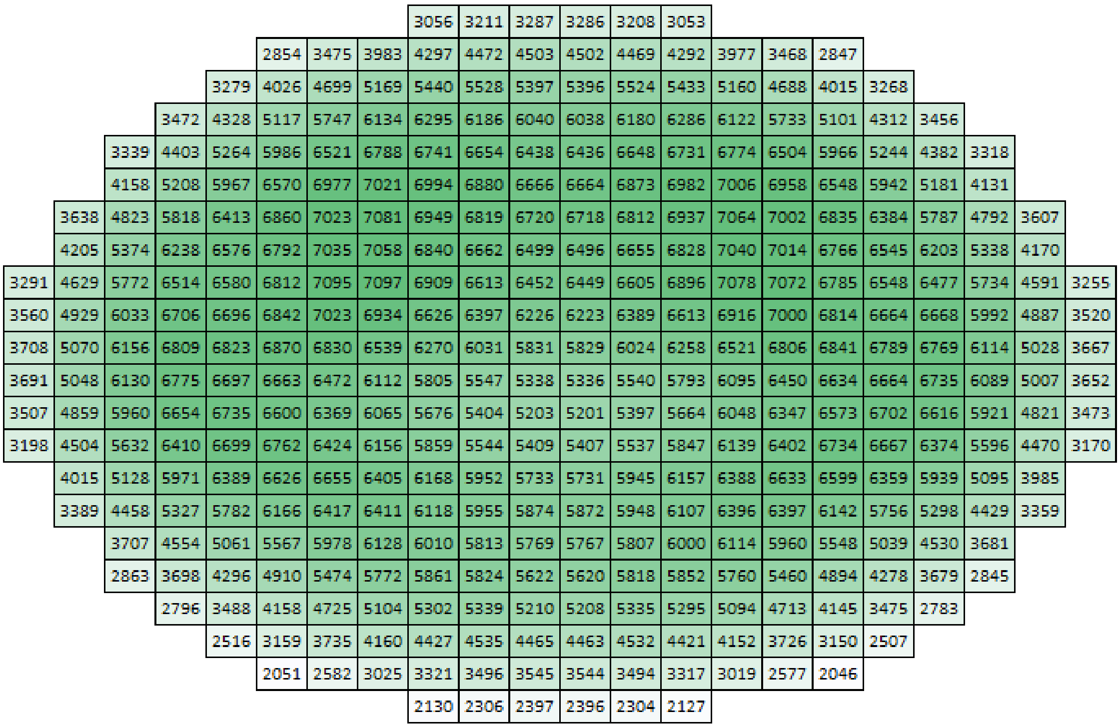

								3056	3211	3287	3286	3208	3053								
					2854	3475	3983	4297	4472	4503	4502	4469	4292	3977	3468	2847					
				3279	4026	4699	5169	5440	5528	5397	5396	5524	5433	5160	4688	4015	3268				
			3472	4328	5117	5747	6134	6295	6186	6040	6038	6180	6286	6122	5733	5101	4312	3456			
		3339	4403	5264	5986	6521	6788	6741	6654	6438	6436	6648	6731	6774	6504	5966	5244	4382	3318		
		4158	5208	5967	6570	6977	7021	6994	6880	6666	6664	6873	6982	7006	6958	6548	5942	5181	4131		
	3638	4823	5818	6413	6860	7023	7081	6949	6819	6720	6718	6812	6937	7064	7002	6835	6384	5787	4792	3607	
	4205	5374	6238	6576	6792	7035	7058	6840	6662	6499	6496	6655	6828	7040	7014	6766	6545	6203	5338	4170	
3291	4629	5772	6514	6580	6812	7095	7097	6909	6613	6452	6449	6605	6896	7078	7072	6785	6548	6477	5734	4591	3255
3560	4929	6033	6706	6696	6842	7023	6934	6626	6397	6226	6223	6389	6613	6916	7000	6814	6664	6668	5992	4887	3520
3708	5070	6156	6809	6823	6870	6830	6539	6270	6031	5831	5829	6024	6258	6521	6806	6841	6789	6769	6114	5028	3667
3691	5048	6130	6775	6697	6663	6472	6112	5805	5547	5338	5336	5540	5793	6095	6450	6634	6664	6735	6089	5007	3652
3507	4859	5960	6654	6735	6600	6369	6065	5676	5404	5203	5201	5397	5664	6048	6347	6573	6702	6616	5921	4821	3473
3198	4504	5632	6410	6699	6762	6424	6156	5859	5544	5409	5407	5537	5847	6139	6402	6734	6667	6374	5596	4470	3170
	4015	5128	5971	6389	6626	6655	6405	6168	5952	5733	5731	5945	6157	6388	6633	6599	6359	5939	5095	3985	
	3389	4458	5327	5782	6166	6417	6411	6118	5955	5874	5872	5948	6107	6396	6397	6142	5756	5298	4429	3359	
		3707	4554	5061	5567	5978	6128	6010	5813	5769	5767	5807	6000	6114	5960	5548	5039	4530	3681		
		2863	3698	4296	4910	5474	5772	5861	5824	5622	5620	5818	5852	5760	5460	4894	4278	3679	2845		
			2796	3488	4158	4725	5104	5302	5339	5210	5208	5335	5295	5094	4713	4145	3475	2783			
				2516	3159	3735	4160	4427	4535	4465	4463	4532	4421	4152	3726	3150	2507				
					2051	2582	3025	3321	3496	3545	3544	3494	3317	3019	2577	2046					
								2130	2306	2397	2396	2304	2127								

Figure 8 - Channel power distribution in the solution using Configuration B

4. Conclusions and Future Work

Although there is currently no shortage of cheaply available uranium, the increasing population of the world and the escalation of nuclear power's role in meeting the world's energy needs necessitate more efficient resource usage. Thorium has been studied as a supplemental fuel that can be used to increase the burnup of uranium. Heavy-water reactors are particularly suited to this concept.

The DONJON and DRAGON reactor physics codes were used to simulate CANDU™ reactor core configurations that utilized thorium fuel in select channels. Using DRAGON, it was determined that a bundle utilizing a mixed oxide of thorium and 1.45% ^{233}U resulted in a steady fuel cycle. Using DONJON, three particular reactor core configurations using both standard natural-uranium fuel and thorium/uranium fuel were analyzed. While one configuration was deemed not viable the other two resulted in working solutions. In both cases, power output and criticality were maintained, and refuelling rate dropped very slightly. Configuration A seemed to provide the most optimal properties, having the lowest refuelling rate and highest multiplication constant while still meeting license limits on channel and bundle power.

The focus of this project thus far has been the reactor physics challenges associated with the incorporation of thorium fuel into a CANDU 6™ reactor. Additional inquiry is required into fuel reprocessing methods. Liquid extraction and pyroprocessing methods have been developed worldwide but have not yet been studied during the preparation of this report. The results contained in this report pertain only to a steady state solution (i.e. once a self-sustaining fuel cycle has been established.) Calculations for start-up of the reactor using Pu239 or U235 as the primer in Thorium bundles shall be carried out in the future. Further analysis and validation of the results already obtained is necessary. Although DONJON and DRAGON have been used extensively in industry and academia, the results of this particular project require verification. It may be prudent to benchmark the results against another reactor physics code.

Several assumptions were made for input constants in each of the codes. It would be ideal to find realistic values for these assumptions in order to decrease the margin of error in the results. The calculations in this report were performed with two neutron-energy groups in order to decrease computation time. In order to achieve greater accuracy, a calculation with 69 neutron groups will be performed. Lastly, more detailed permutations of the reactor core configurations will be attempted in order to optimize results.

5. Acknowledgements

The authors would like to thank Dr. Bronwyn Hyland and Dr. Jeremy Pencer of AECL for their help and support with this project. They would also like to thank Dr. Glenn Harvel of UOIT for his advice and input on design decisions.

6. References

[1] World Nuclear Association, "Supply of Uranium," August 2012. [Online]. Available: http://www.world-nuclear.org/info/inf75.html. [Accessed October 2012].

[2] World Nuclear Association, "Thorium," August 2012. [Online]. Available: http://www.world-nuclear.org/info/inf62.html. [Accessed October 2012].

[3] International Project on Innovative Nuclear Reactors and Fuel Cycles (INPRO), "Role of Thorium to Supplement Fuel Cycles of Future Nuclear Energy Systems," International Atomic Energy Agency (IAEA), Vienna, 2012.

[4] International Atomic Energy Agency, "Thorium Fuel Cycle - Potential Benefits and Challenges," International Atomic Energy Agency (IAEA-TECDOC-1450), Vienna, 2005.

[5] B. Holmes, M. Geweida, M. Simon, B. Rouben and M. H. Kaye, "Neutronic Analysis of an Incorporated Thorium-Uranium Breeder Booster in a CANDU-6," Oshawa, 2010.

[6] A. Hébert, D. Sekki and R. Chambon, "A User Guide for DONJON Version4 (Technical Report IGE-300)," École Polytechnique de Montréal, Montréal, 2012.

[7] G. Marleau, A. Hébert and R. Roy, "A User Guide for DRAGON Version4 (Technical Report IGE-294)," École Polytechnique de Montréal, Montréal, 2012.

[8] Groupe d'Analyse Nucléaire, "The Groupe d'Analyse Nucléaire," 2012. [Online]. Available: http://www.polymtl.ca/nucleaire/en/GAN/GAN.php.

[9] B. Rouben, "Fuel Management in CANDU," Presented at Chulalongkorn University, Bangkok, 1997.

[10] G. Bereznai, Nuclear Powerplant Systems and Operation, Oshawa: University of Ontario Institute of Technology, 1998.

ENC 2012 - Abstract for Fuel Cycle presentation on behalf of the French Nuclear Industry

“Consolidation and advances in technology in the Fuel Cycle to safely address customers’ needs and challenges”

The current decade gathers several key milestones for the global nuclear industry. As a prominent part of this global industry, the French nuclear industry is also setting the stage through major investments in France and abroad in addition to continuing improvement of processes as well as exploring, developing and implementing new and innovative solutions.

Front-end of the fuel cycle:

In the field of the nuclear fuel cycle, by the end of the decade, most of the essential steps of the front-end cycle will be based upon brand new facilities able to supply the reactor fleet in the very long run:

- In uranium production, most of AREVA’s concentrate production will come from new large projects in Niger, Canada and Kazakhstan, all based upon large and quality resources ensuring deliveries well into the coming decades. A wide and geographically diversified portfolio of resources and a continuous exploration effort will allow launching other mining projects when required by the market.

The currently prevailing market conditions reflect the fact that supply and demand balance has been disrupted in the aftermath of Fukushima and that the increase in demand is slower than originally expected. However, mines already under development are still needed around 2014-2015 to cover the growing demand, compensate for the decrease in secondary resources and replace exhausted deposits.

A supply deficit is looming post-2020 justifying for new mines to be developed. Such mines need to be identified and characterized much in advance (typically 15 years are required before production start). They will only be developed & commissioned if rate of return is sufficiently attractive. Despite shaky market conditions, AREVA remains committed to be a first-class uranium producer, through a wide exploration program (~ 55 M€ per year), with a target to keep 20 years of reserves and resources and an intensive R&D program.

Development of projects at different maturity stages: AREVA has for now rationalized its projects portfolio while focusing on two projects to be launched in the 2013-15 timeframe: Imouraren in Niger, along with Cigar Lake in Canada, are currently the two AREVA flagship projects under development, contributing to serve world growing demand in this decade. Some additional projects may further come on line depending future market conditions: AREVA keeps a diversified portfolio strategy, from exploration to production. Their development will be launched once uranium price in long-term contracts secures a sufficient level.

- For uranium refining and UF6 conversion, the brand new COMURHEX 2 project already in an advanced construction stage will replace the ageing COMURHEX 1. In this segment, AREVA is still the sole supplier on the way to totally renew its production tool, thus betting that the other will follow in order to safely cover the customer needs in the long run.

The UF6 conversion market currently experiences a dichotomy between spot and long-term prices. Spot indicators are rather low, but do the long-tem ones indicate that operators of nuclear power plants are getting worried about security of supply? Whatever the answer, there is a market consensus that investments are needed for a sustainable long-term for the main following reasons:

  - Updated safety standard levels
  - Increasingly stringent environmental standards
  - Decommissioning cost to be aligned with up to date regulations.

AREVA is the first to invest in a new conversion facility that is confirmed as part of AREVA’s priority strategic investments. Comurhex 2 will be based on the same basic process as Comurhex 1, with a few technological innovations. Important to mention is that the new facility is already fulfilling post-Fukushima safety and operating requirements. In terms of market supply, it will maintain UF6 production close to

European enrichment needs. Comurhex 2 will have a capacity of 15,000 tons uranium per year, expandable to 21,000 tons uranium only with market support.

According to prevailing market conditions and following a review of required design and operation conditions for fuel cycle facilities, Comurhex 1 is slated to be shutdown in 2015, and the Comurhex 2 business plan is being updated accordingly. If required, existing commitments will be fulfilled by stockpile buildup before Comurhex 1 shutdown. The renewal of France's conversion footprint is confirmed as part of AREVA's priority projects.

- For uranium isotopic enrichment, the incredibly safe, flexible and reliable Eurodif gaseous diffusion plant has been shut down in May this year. Despite the above mentioned advantages and track record and the fact it was maintained in a very good shape, this technology is too much energy hungry to be further extended in our environmentally conscious new world and had to be replaced. The brand new Georges Besse 2 project consisting in two separate and independent units is now smoothly ramping-up its operable capacity along with its commercial production. Based upon the outmost advanced centrifuge technology, it will consume 50 times less electricity than Eurodif.

The main features of the Georges Besse 2 project are as follows:

  - The project is composed of two independent units: North & South units. They are both located on the Tricastin site in the South of France
  - Nominal capacity of 7.5 million SWU/y (Separative Work Units per year), and an extension possible if market conditions request
  - Commercial production began in April 2011
  - In February 2012, two modules were operational (for a combined capacity of 1.4 million SWUs)
  - An installed capacity of 2.5 million SWUs should be reached by year-end
  - The nominal capacity is targeted by 2016

The project is a fruitful partnership, as customers have taken minority stakes in the SET Holding operating Georges Besse 2 and discussions are on-going with other utilities. One figure showing the strong customer support the project enjoys: 80% of the capacity is sold through 2030.

Again on the enrichment segment, notwithstanding current market conditions, but without ignoring them, AREVA is committed to serving the market and ensuring security of supply.

- In the domain of fuel fabrication, while less capital consuming than the above mentioned facilities, significant investments were recently devoted to facility upgrades, especially in compliance with updated safety schemes and regulations at a moment when capacity optimization and modernization was needed to better adapt to market needs. Besides enriched uranium re-conversion and fuel elements fabrication, a lot has been achieved in zirconium material and zirconium cladding production.

A specificity of this segment extremely focused on quality, is the paramount importance of fuel engineering and codes & methods. In France, in the US and in Germany, many specialists are working at improving the current designs and preparing future fuels in permanent dialogue with reactor design specialist, fleet operators and regulators.

Back-end of the fuel cycle

With over 28,000 tHM of used fuel reprocessed at La Hague and over 14,000 recycled fuels assemblies, MOX as well as ERU fuels, fabricated at AREVA plants, MELOX and FBFC respectively, AREVA is operating strategic and outstanding facilities for the safe and optimized used fuel management starting at its very first stage, namely the unloading of used fuel at reactor pools up to the disposal of the final waste.
The operational feedback of more than 14,000 recycled fuels (MOX and ERU) highlights outstanding in-core behaviour. This coupled with portfolio benefits, notably security of supply; uranium savings, price

predictability and competitiveness explain the lasting and widespread use by utilities over the past few decades.

Moreover, AREVA, in collaboration with the CEA and other industrial partners, is dedicated to continuous improvement of the reprocessing and recycling process and has committed R&D teams, working not only on optimizing existing processes, but also exploring, developing and implementing new and innovative solutions in order to meet customer needs for today and for tomorrow.

- Increased Reprocessing capacity and capabilities: La Hague reached production levels higher than 1700tHM/yr in 1997 and since, has continued to reprocess an average of 1200tHM per year. Furthermore, since January 2003, La Hague obtained new administrative limits allowing acceptance of used fuel with an initial ^{235}U enrichment of 5% and maximum burnup of 60GWd/tHM, to best meet needs of future reactors.

The La Hague is a major economic player and one of the largest employers in the Nord-Cotentin area with 3,000 AREVA la Hague employees, 1,000 other AREVA employees and 1,000 subcontractors' staff. The total investment in the facilities was € 80 Million in 2011 and the duties and taxes paid amounted to € 81 Million (also in 2011).

- The MELOX plant in the south of France for MOX fuel fabrication with a current throughput of 145 tHM/y. The plant has been granted a new license capacity up to 195tHM/yr. The performance and integrity of MOX fuel has had a perfect track record since its development. No quality failure due to MOX fabrication or design has ever occurred in a reactor as of today, nearly 40 years after first commercial MOX use (1972). Furthermore, as production levels increase, burn up rates and performance have been steadily increased as well. Since 2006, EDF has achieved MOX "parity", such that their MOX fuel performs at the same fuel characteristics as the UO2 fuel. For German and Swiss clients, MOX fuel has successfully reached burn up rates of up to 62.5 GWd/tHM.

- The European platform for RepU recycling, with the FBFC plant in France and the Lingen plant in Germany, for ERU fuel fabrication with a capacity of 150 tHM/yr and 50 tHM/yr respectively, where more than 4,000 ERU fuels, PWR and BWR type, have been already fabricated.
- Used MOX Fuel Reprocessing: Since 2004 an unprecedented scale of approximately 70 tHM of used MOX fuel was successfully reprocessed and recycled at AREVA plants in France. The scale of the campaigns as well as the large range of characteristics (burnup ranging from 30-55 GWd/t, Pu content ranging from 4%-7.2%) demonstrate the feasibility of MOX reprocessing at an industrial scale. AREVA continues to research optimization of MOX fuel recycling and plutonium multi-recycling.

- Reprocessing of Research and Test Reactor (RTR) Fuel. In 2005, La Hague obtained necessary authorizations to treat RTR fuel. Since then, 4 tonnes of U-Al type fuel have been processed and approximately 17 tonnes of used fuel are stored in the pools awaiting treatment. AREVA and CEA's R&D teams are currently researching treatment of advanced new fuel types including USi and UMo fuels.

Operating those facilities contribute to maintaining France's international leadership in the businesses of the back end of the fuel cycle. One specific mission is to reduce the environmental footprint of nuclear power which will be achieved through substantial investment in nuclear safety and maintenance over the 2012-2016 period, and sustained R&D spending over the period.

Although the reliability of AREVA's reprocessing processes and recycled fuel assemblies is excellent, AREVA has never stopped improving them:

- MOX for present and future: In generation III+ reactors, such as EPR, opportunity is given to the utilities to operate with a full MOX core. A 100 % MOX reactor core provides total homogeneity with a single Pu content. 100 % MOX core opens up new possibilities of highly increased performances, equivalent to 4.95 % enriched natural uranium, together with highly simplified and thus less costly design. Furthermore, The 100 % MOX core benefits from high homogeneity and stability, providing margins during operation and safe behaviour in accidental situations.

- HLW Vitrification: The Cold Crucible Induction Melter implemented at La Hague is a recent (first industrial operation took place on April 2010) and major milestone in technical advancement of the vitrification process to optimize HLW management. The project is the successful result of 25 years of R&D by the CEA in collaboration with AREVA. The cold crucible works by induction and can reach temperatures higher than 1200°C thanks to the glass protection layer. Increase in production capacity and acceptance of wider range of waste type are among the major improvements.

Concluding remarks:

Despite the currently prevailing situation and the legitimate questions raised about nuclear energy, nuclear utilities' needs still must be addressed in a sustainable and responsible way, ensuring security of supply of nuclear fuel and safe used fuel management, while keeping public confidence. To earn it and keep it, we can not make any compromise on safety.

Today's investment in fuel cycle facilities ensures the safety and the renewal of industrial capacities, while maintaining industrial solutions alive for our customers: it is tomorrow's "Security of supply" for the power plant operators.

Contacts : on behalf the French Nuclear Industry, Patrick Teyssier
G.I.I.N.
39-41 rue Louis Blanc
92400 Courbevoie. France
Tél : (+33) 1 47 17 62 78
E-mail : marie-jose.guillon@giin.fr

SELECTION CONSIDERATIONS FOR GASES USED IN SPENT NUCLEAR FUEL DRY STORAGE

W.S. WALTERS*, H.E. SIMS and J HENSHAW
National Nuclear Laboratory (NNL), Reactor Materials & Chemistry Dept.,
B168 Harwell Science Campus, OX11 0QT, Didcot, Oxfordshire, U.K.

Introduction

If dry storage is to be pursued, then the choice of cover gas and its radiation chemistry needs to be compatible with the fuel, which is one of the main considerations of this paper.

A proportion of the SNF from AGR stations becomes sensitised whilst irradiated in core, leaving the fuel susceptible to intergranular stress corrosion cracking (IGSCC). The presence of sufficient water vapour and corrosive species to propagate IGSCC is a concern as there have been failures in fuel stored in PIE caves (i.e. air and reasonably high humidity) [1]. In dry storage the fuel will consist of dismantled pins located in a slotted can (SC) and the SC would be considered the “unit of fuel” to go into dry storage, as repacking is not considered credible. The SC will have some moisture adhering to it as it will have been in a storage pond. The degree of self-drying of the fuel (and the SC around it) will depend on the cooling time and residual decay heat. Generally there is a large degree of uncertainty regarding the atmosphere likely to be present at the start of the dry storage period.

The National Nuclear Laboratory (NNL) has considered a range of possible fill gases for SNF containers and evaluated their likely performance on the basis of their radiation chemistry. In particular NNL has examined the formation of gaseous species by radiolysis of a fill gas mixture that may cause corrosion of the fuel clad and storage container. If air and moisture are present they radiolyse to form NOx, HNO_2 and HNO_3 all of which may be corrosively aggressive. Irradiation of air in the presence of argon is known to increase the production of nitrate ion [2]; this may be due to energy transfer from the irradiated inert gas to other constituents such as air and water vapour. This paper considers the gas-phase radiation chemistry occurring in these systems by modelling the chemical kinetics taking place. Illustrative calculations are provided indicating the rate of production and final yields of corrosive species likely to be present. Some comparisons of the model with experimental data are shown and discussed.

General principles of gas selection and gas radiolysis

Drying of fuel is usually performed by applying a vacuum / dry gas cycle which is repeated as needed and the fuel is then placed in a storage can and the space filled with a nominally inert gas such as helium [3]. This paper will consider some alternative fill gas options and what constraints there may be on their selection. The choice of the fill gas will be influenced by a number of factors such as:

- Provision of an environment in which the system components, particularly the container and the fuel, do not corrode and provide a containment barrier for as long as possible;
- Avoidance of a flammable gas composition, via radiolytic hydrogen production;

Air is not considered as a viable fill gas option because the radiolytic production of nitric acid would be large if significant moisture was present. The viable options for the fill gas are considered to be Ar, He, CO_2 and N_2 and these are discussed below.

When gases are irradiated, radiation energy is absorbed by each component, the amount depending on their relative concentrations and associated radiation cross-sections. The primary products are ion pairs and excited states, which then interact with each other or with ground-state molecules to form product species which may include both re-formed reactant molecules and new molecular species. Continued irradiation in an idealised system would result in steady state concentrations of all stable species. The presence of water molecules in the gas phase means both hydrogen atoms and hydroxyl radical species may be formed, as ions or as free radicals, and these will then react with all the species derived from N_2 and O_2. If an inert gas is present, then that can excite or ionise to give energetic species which may subsequently transfer their energy to other species present. For example,

(1) $He \rightarrow He^*$ (formation of excited state He)
(2) $He^* + N_2 \rightarrow He + 2\,N$ (energy transfer from He to N_2 with N_2 dissociation / ionisation).

The rate of production of ion pairs or excited states depends on both the radiation dose rate and the yield of each product per unit of absorbed radiation energy. The yield is characterised by a G-value, and is the number of species (molecules, atoms, ions etc.) produced per 100 electron Volts absorbed energy. Table 1 [4, 5, 6] gives the ionisation energies and ion pair formation energies (or work function) for He, Ar, N_2, O_2, H_2O and CO_2. For CO_2 this is around 33eV, so G (ion pair) for CO_2 is approximately 3 molecules $100eV^{-1}$. For gas phase radiolysis the mean energy absorbed per ion pair formed (W) is very nearly the same regardless of the nature of the radiation.

Gas	Ion Pair formation (W)	Ionisation (I)
He	41.3 eV/ ip [4] or 46.0 [5]	24.5 eV [6] or 24.6 [5]
Ar	26.4 eV/ ip[5]	15.8 eV [4]&[5]
CO_2	33.0 eV/ ip [4] or 34.3 [5]	13.8 eV [5]
N_2	36.4 eV/ip [5]	15.6 eV [6] or 15.6 [5]
O_2	32.2 eV/ip [5]	13.8 eV [6] or 12.1 [5]
H_2O (gas phase)	30.5 eV/ip [5]	12.6 eV [5]

Table 1: Energy terms for the irradiation of possible storage gases.

It can be seen from Table 1 that He has the highest ionisation potential and oxygen the lowest so it is possible for He ions to ionise any of the other gases present in the table, while Ar ions can ionise all except He. The net result of irradiating a gas mixture is that energy can transfer from one constituent to another, giving higher yields of ionised N_2 and O_2 than would be expected from the initial partitioning of energy. This aspect of radiation chemistry needs consideration when considering cover gases when impurities such as air and water may be present.

Energy transfer will influence the rate at which molecules such as N_2 and O_2 are dissociated. However in a system considered over a very long timescale, the impact of this effect may be lessened if the N_2 and O_2 experience direct radiolysis anyway. The rate of removal of the reactants can in such circumstances be approximated to a half-life relationship. For example, assuming a dose rate of 1 kGy/hr and $G(HNO_3) = 2$ then the effective half-life of N_2 (to form HNO_3) is 27 years. Thus over a 100 year period, the process would have anyway attained almost full conversion. Over shorter timescales, energy transfer would be more significant in accelerating the rate of radiolytic production of HNO_3.

Detailed consideration of the gas systems

A detailed model of all the possible gas phase radiolytic reactions has been constructed and used to perform a series of calculations reported here. The model is based on that described in reference [7] and numerically solves the chemical rate equations associated with the problem. The reaction sets only consider gas phase processes and not any interactions with surfaces, although the model does consider partitioning of nitric acid into any liquid water present. Calculations have been performed for different possible fill gases for two possible cases, given in Table 2.

	CASE 1	CASE 2
Temperature °C	100	50

Water carry-over (g/teHM)	~ 90	~ 4900
Fill gas	99%	99%
Adventitious air	1%	1%
Radiation dose rate (kGy/h)	0.4	0.04

Table 2: Parameters for radiolysis calculations in storage environments.

The two cases relate to (1) fresh warm AGR fuel with self-drying attributes, and (2) older (non-self-drying) AGR fuel containing the maximum credible proportion of failed fuel.

1. Nitrogen.

The radiation chemistry of N_2 has been studied experimentally and its use as a fill gas for SNF storage was once considered [8]. However, that regime would need to have tight controls on residual air and water. The formation of HNO_3 from irradiation of water vapour / air and ammonia from irradiation of N_2 / H_2 is well documented The reaction set for this mechanism has been used to calculate the evolution of gas chemistry in a SNF disposal container context [7] and is now used to calculate this in an interim storage context.

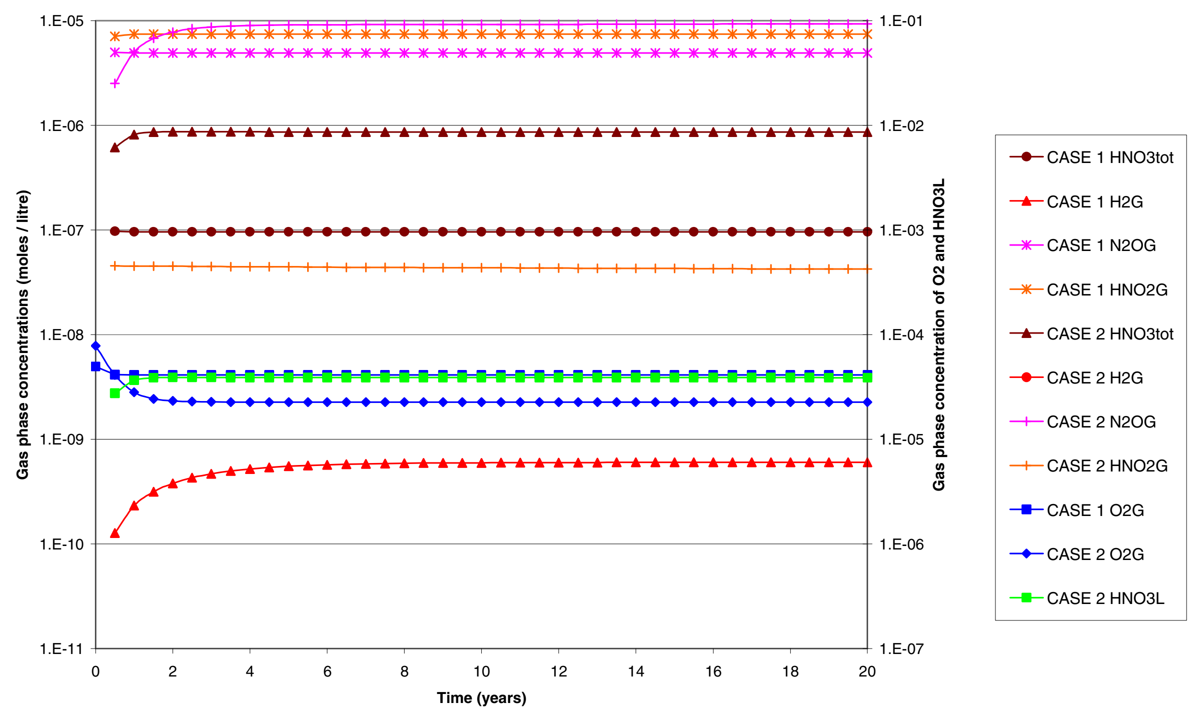

Figure 1 Model output for nitrogen fill gas.

In Figure 1, it can be seen that for Case 1 the radiolysis products come to steady state within approximately two years. The most abundant species are HNO_2 and N_2O. For Case 2 the situation is different in that there is liquid water present. In this case the model allows the HNO_3 vapour to partition into the liquid phase. The concentration of liquid-phase nitric acid then builds up (it is essentially trapped) and becomes the dominant product, denoted by HNO_3L. An important point is that there is slightly less HNO_3 formed, in total, when there is liquid water present; this is because some of the HNO3 precursors are also water-soluble and their removal from the system influences subsequent HNO3 production in the gas phase. The system takes up to three years to equilibrate. Note that O_2 and HNO_3(liquid) are plotted against the right hand axis. In both cases oxygen decreases and hydrogen increases, but the concentrations are orders of magnitude below flammable proportions.

2. Argon

Argon was previously considered for interim dry storage of AGR fuel [9] and there is a good amount of information available concerning the radiation chemistry of Ar / air / water vapour systems. The reaction scheme for irradiation of moist air has been added to with reactions for the ionisation and excitation of Ar [7] and the interaction of these Ar species with those deriving from air radiolysis. This has been used to simulate experimental data [2] as a benchmark for the model. The same cases (Table 2) have been calculated with Ar fill gas.

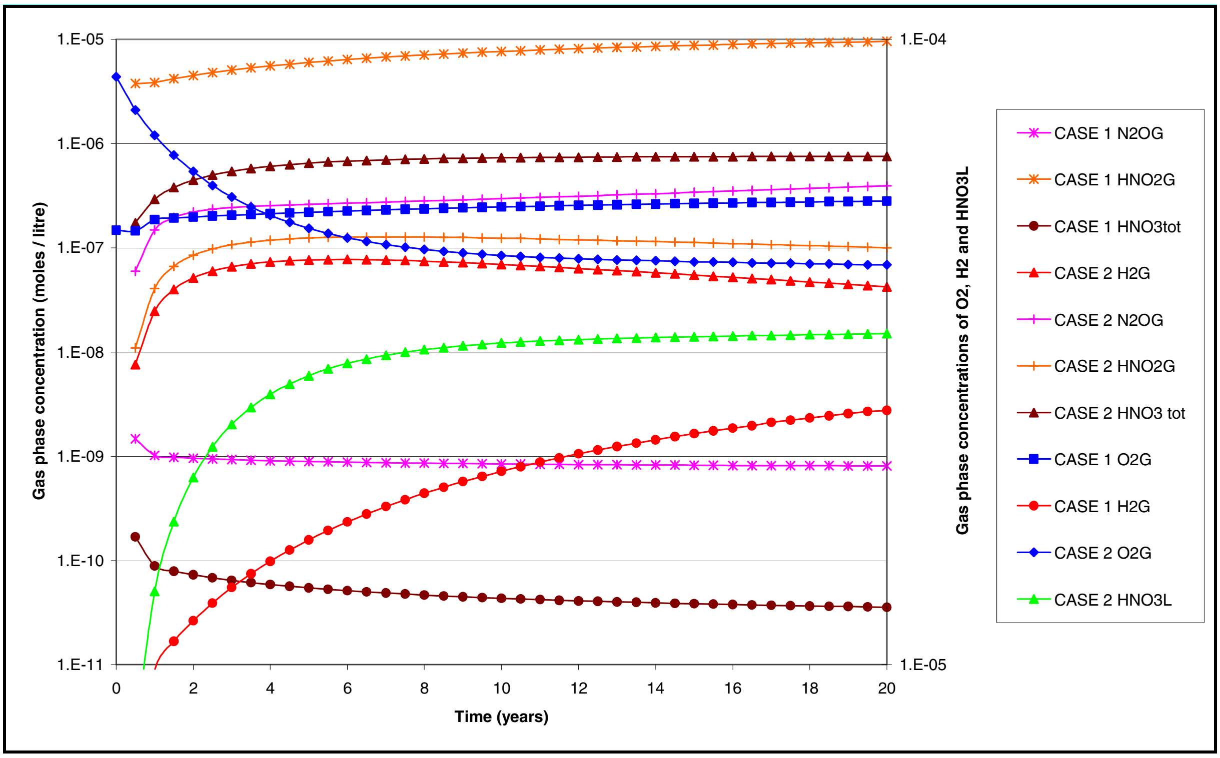

Figure 2. Model output for argon fill gas.

From Figure 2 it can be seen that in Case 1 the most abundant NOx products are again HNO_2 and N_2O (as for N2 fill gas). In Case 2 the most abundant species is again HNO_3 trapped in the liquid phase.

3. Helium

Helium is widely used as the fill gas of choice and is the industry standard [3] particularly for LWR fuel. There is also a body of information on the radiation chemistry of He. Utilities are increasingly looking to store fuel on-site at the power plant in an Independent Spent Fuel Storage Installation (ISFSI) and He is the most widely used gas in terms of SNF dry stores already in operation. Like Ar, He both ionises and excites under gamma radiation. However, the higher energy of excited state He means that it is more readily able to transfer that energy to other gases via ionisation processes. Under irradiation [10] He (with a trace of air impurity and controlled water content) produces some nitric acid as a radiolytic product, as did Ar in a similar experiment. Calculation results are as follows.

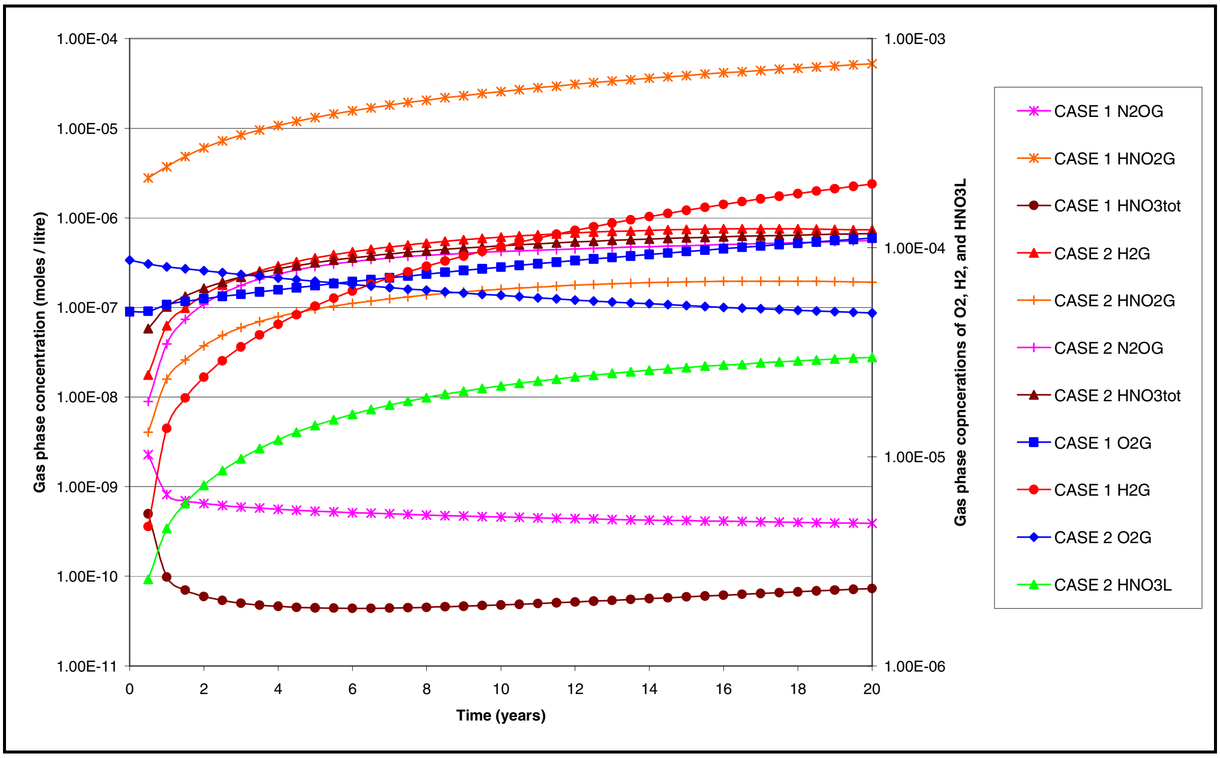

Figure 3. Model output for helium fill gas.

These calculations show that the He system does not arrive at steady state within 20 years, and that the inventory of nitric acid is still increasing at that time. Ultimately it will be limited by the available amounts of O_2 (Case 1) and N_2 (Case 2).

4. Carbon Dioxide

AGR fuel was designed and intended to be compatible with CO_2 which is the primary coolant in the AGR. Again there is a large body of information on the radiation chemistry of CO_2 with various impurities; this has probably been the most intensely studied gas radiolysis system of interest to the UK nuclear industry [11]. However the models intended for reactor operation are quite complex and more detailed than required for this purpose.

As a first consideration, the mass of gas in the system (and consequently the amount of energy absorbed by the gas) would be considerably greater than in the case of a helium gas fill, and similar to an argon gas fill. The primary products of CO_2 radiolysis [4] are CO_2^+, CO^+, C^+ and O^+ ions, O atoms and CO. But excited state CO_2^* is not important as it has too low an energy to cause further dissociation of N_2 or O_2. Consequently the effect on radiolysis of trace N_2 and O_2 would be expected to be considerably less than for argon. In addition, from the energies noted in Table 1, the reaction

(3) $CO_2^+ + N_2 \rightarrow CO_2 + N_2^+$

is not favoured as the required ionisation potential energy for nitrogen is greater than the available energy from ionised CO_2. The same applies to other ions produced in the radiolysis of CO_2. However there are other possible ion reactions such as

(4) $O^+ + N_2 \rightarrow NO^+ + N$

which might ultimately lead to the production of oxidised nitrogen. Although a number of qualitative factors suggest that the irradiation of a CO_2 / trace air mixture will produce less net radiolysis of nitrogen and oxygen than in an equivalent argon or helium / trace air gas mixture, the overall reaction set is very complex so it is not possible to draw any firm conclusion. The adaptation of the full reactor core model to this application has not yet been carried out, and at this point is a “work in progress”.

In summary, there does not appear to be any fundamental reason why CO_2 would not be an acceptable dry storage medium.

Summary and Conclusions

- It must be stressed that the calculations presented here are for idealised systems with no surfaces. For real systems, reactions with surfaces should be taken into consideration. The numerical outputs from these studies therefore provide only a qualitative ranking of which fill gas produces the most nitric acid.
- For the simplest conditions, with a system at 100 °C and no liquid water present, the greatest production of HNO_3 occurs from a N_2 atmosphere, although HNO_2 and N_2O are always present in greater abundance. The water vapour present is radiolytically dissociated and for both He and Ar fills, the gas phase concentrations of H_2 and O_2 both increase. This may be due to the higher radiation dose rate tied to the higher temperature.
- For the more complicated conditions where liquid phase water is also present, the nitric acid preferentially partitions into the liquid phase and is essentially trapped there; consequently it builds up. In Ar, this eventually equilibrates but for He and N_2 it appears to continue to increase linearly over the 20 year period modelled and will exceed the concentration obtained in Ar. In the gas phase, N_2O remains the most abundant NOx product, whilst O_2 decreases and H_2 goes through a transient then decreases.
- This work demonstrates a method to calculate, at least comparatively, the relative merits of the candidate fill gases. With addition of surface-specific processes it may be possible to get a more quantitative model for plant-specific applications.

Acknowledgement

This work was supported in part by The UK Nuclear Decommissioning Authority.

References

1. G Knowles "Corrosion of sensitised AGR fuel cladding in moist air environments at 35 and 50 °C", Proceedings of U.K. Corrosion '93, Volume 3 (1993). Institute of Corrosion.
2. R May, D Stinchcombe and H P White, "The radiolytic formation of nitric acid in argon / air / water systems" UKAEA report AERE-R-8176 (Revision 1) (1992).
3. ASTM Standard C-1553-08 "Standard guide for drying behaviour of Spent Nuclear Fuel". ASTM International 2008
4. J W T Spinks and R J Woods "Introduction to radiation chemistry" 3rd edition, Wiley Interscience, 1990.
5. A Mozumder, "Fundamentals of Radiation Chemistry", Academic Press, 1999.
6. CRC Handbook of Chemistry and Physics, 58th Edition, 1978.
7. J Henshaw "Modelling of nitric acid production in the Advanced Cold Process Canister due to irradiation of moist air", SKB report TR-94-15 (1994).
8. J P Roberts Nuclear Regulatory Commission (NRC) March 22 1988. Letter to H C Pickering Jr. (NRC Accession No. 8803290114-880323).
9. C.J. Baglin, R.V. Killingley, D. Anderson and S.R. Donald, Paper 18 in "Fuel Management and Handling", BNES conference proceedings, 1995.
10. W S Walters, "Review of the dry storage environment" NNL report 10062 (2009).
11. A R Anderson and D R Dominey "Radiolysis of carbon dioxide" Radiation Research Reviews, Vol 1, pp 269-300 (1968).

AUTOMATED PWR FUEL PELLET MANUFACTURE AT SPRINGFIELDS FUELS LTD.

R A McKENZIE, B J LIVINGSTONE
Product Design Group, Springfields Fuels Ltd.
Springfields, Preston – United Kingdom

Westinghouse has recently completed a multi-million pound investment to reinstate PWR fuel manufacturing capability at its Springfields site near Preston in Lancashire. The project has maintained the strategy operated within the Oxide Fuels Complex since the mid 1990's to utilise a considerable amount of automation, particularly in the manufacture of high quality uranium dioxide fuel pellets.

In March 2012 PWR fuel pellet manufacture recommenced at Springfields Fuels Ltd (SFL) following a 12-year break. The main enabler was the installation of a new automated pellet grinding line that was coupled to the existing pressing/sintering facility, which also provides pellets to the Advanced Gas-cooled Reactor (AGR) grinding line. The design philosophy of the reinstatement remained consistent with SFL's strong safety culture that aims to minimise radiation dose rates through the avoidance of operator/product contact. A high level of automation also aligns pellet manufacture with Westinghouse's 'zero-leaker' operating strategy and the drive to eliminate leaking fuel rods caused by chipped/cracked pellets.

AN INTEGRATED FACILITY

The Oxide Fuels Complex (OFC) is a relatively modern integrated facility that was brought on-line in the mid 1990's to replace existing plants that were spread across the Springfields site. Current capacity is approximately 750 tonnes of powder and 400 tonnes of pellets. Cylinders of UF_6 and components are received into the building and finished fuel or intermediate products are shipped out to customers.

The ability to manufacture large quantities of uranium dioxide (UO_2) fuel pellets with very few defects, with or without automation, is reliant on good powder quality. Since its initial development approximately 40 years ago SFL has used integrated dry route (IDR) technology to produce a high-purity/low fluoride content UO_2 powder capable of yielding very high density pellets (>99% TD). Production rates exceeding 90kg/hr UF_6 are achievable.

IDR powder is transferred directly to one of several blending vessels to facilitate consumption and homogenisation of recycled/recovered material. Blended powder is discharged to drums that are either stored or positioned at one of a series of vacuum transfer cell by means of linear transfer units (LTU's). These LTU robots start the use of automation within


Image 1 – Oxide Fuels Complex

OFC and interface directly with the central control system to place drums in any of 600 different locations using barcode identification and traceability.

Operators are required to remove drum lids at vacuum transfer cells but powder is removed and transported to the granulation tower using an automated wand that descends into the drum at a controlled rate to avoid blockages and the need for manual intervention.

SFL use 16-toolset Courtoy presses for both granulation and pellet pressing with solid lubrication of granules by means of a vibro-energy mixer.

Soft handling of pellets begins at the press where two independent mechanisms operate in synchronous. The first of these devices picks up pellets 23 at a time as they exit the press on a moving belt and places them on a molybdenum tray. Pellets are handled by air suction to avoid the use of mechanical grippers that could damage the relatively fragile un-sintered or 'green' pellets. The lifting device contacts the pellet OD which allows the pellets to be placed onto trays sitting on their end faces. To maximise throughput rate two pick-up arms are used such that when one is transferring pellets to a tray the other is collecting the next row.

Image 2 – Pellet loading on to sintering trays

A robot is then used to move full or part-full trays to the collection point. Trays are placed on top of each other to create vertically stacked 'charges' ready for placing in the sintering furnaces. The robot also handles empty trays returned from the stack break-down area.

The pelleting and stack make-up are contained within a transparent-plastic cubicle to avoid the spread of uranic contamination. When a stack has been built an Automatic Guided Vehicle (AGV) docks at the collection point, makes a seal with the cubicle, opens both doors and pulls the stack into a containment chamber. The cubicle is resealed and the AGV takes a pre-programmed route to the destination sintering furnace. A similar transfer operation takes place to again ensure pellets are not exposed to the operators working environment.

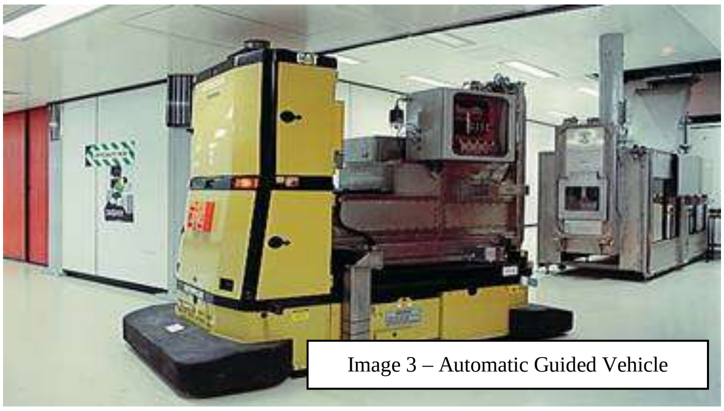

Image 3 – Automatic Guided Vehicle

Pellets are sintered in a BTU walking-beam furnace at temperatures in the range 1700C to 1800C depending on the customers pellet specification requirements.

Following sintering, each charge is collected by an AGV and transferred to either the PWR or AGR stack break-down cell. These cells use robots similar to those in the charge make-up areas, where the charge is dismantled one tray at a time. Pellets are gently pushed off each tray by means of an actuator rod and then the tray is assesses for flatness before being returned by an AGV to the charge make-up cell or the workshop where distorted trays can be rectified or scrapped.

Cushion transfer of pellets has been used at SFL since OFC was first brought on-line and this technology has again been adopted for the new PWR grinding line. The term cushion transfer was adopted to describe the relatively simple principle whereby vibration of specifically selected carpet tiles will cause pellets sat on the carpet to move in the direction of the 'nap' (i.e. the as-made orientation of the bristles). Carpet is precision cut into a series of shapes that, when fitted to buffering stations or trackways, cause pellets to circulate in a gentle controlled manner between individual pieces of equipment such that impact collisions are avoided and pellet damage minimised. All equipment surfaces are carpeted to ensure that no part of a pellet abrades against metal. Qualification of vibration frequencies and carpet wear rate has demonstrated that pellets are at low risk from hydrogen pick-up. Maintenance of the carpet is relatively low, only requiring vacuum cleaning to remove uranic dust that may impair bristle vibration. Individual pieces of worn carpet can be replaced but it is the norm for whole areas to be replaced at the same time. Vibrating tables and trackways require more traditional maintenance to ensure that mechanical components remain tuned to the correct harmonic frequency.

Image 4 – Pellet buffer

Pellets are transported by cushion transfer on the PWR line from the point the exit the stack break-down cell to the location where they are placed on the trays used to feed the rod loader. This route encompasses the auto-density check, grinding, drying, auto-diameter check, metrology and visual inspection. All pellets from a charge are held in a buffer before being sent to the diameter grinder until in-process pellet density checks have been performed and 'accepted'.

Image 5 – Pellet buffer

Pellet density checks must be performed on a sample taken from every tray in every stack. This task is also automated and involves the use of a miniature multi-jointed Movemaster robot that picks up individual pellets from the trackway at a location upstream of the centreless grinding machine. The robot performs a repetitive series of tasks that entails each sample pellet is correctly weighed in air and water and the apparent density calculated. Test data is uploaded to the central control system and pellets will remain in the buffer until instructed to proceed by the central control system. Manual intervention is required should an unsatisfactory density result be recorded.

Image 6 – Auto density check robot

Diameter checks must be performed on all pellets exiting the grinder. This task is carried out automatically but simply entails the pellets passing through a laser micrometer.

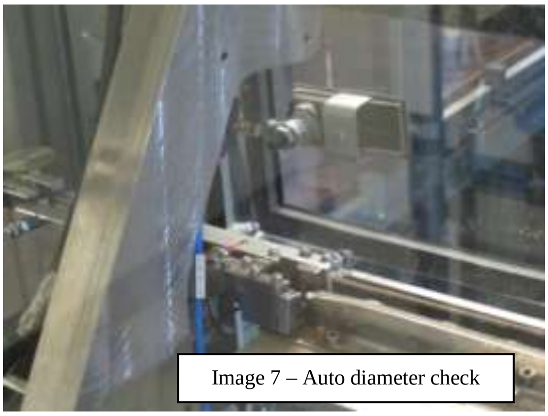
Image 7 – Auto diameter check

However, due to the sensitivity of the measuring apparatus the equipment has to be insulated from all vibrations emanating from the cushion transfer system, hence are fed passed the laser on a stainless steel guideway.

Visual inspection requires an operator to examine all surfaces of the pellet. This task is again facilitated through the use of the cushion transfer system, which can also transport pellets that are laid on their OD. The trackways are required to have a 'v-shaped' cross-section but, through angling the nap of the carpet to the direction of travel, pellets can be made to move along the trackways and rotate at the same time as they pass by the inspector allowing the full circumference to be checked. Pellets are guided towards one of two trackways so that as one stack is being checked the next stack is being loaded. Automatic visual inspection equipment is currently under development, which will result it the grinding line becoming fully automated.

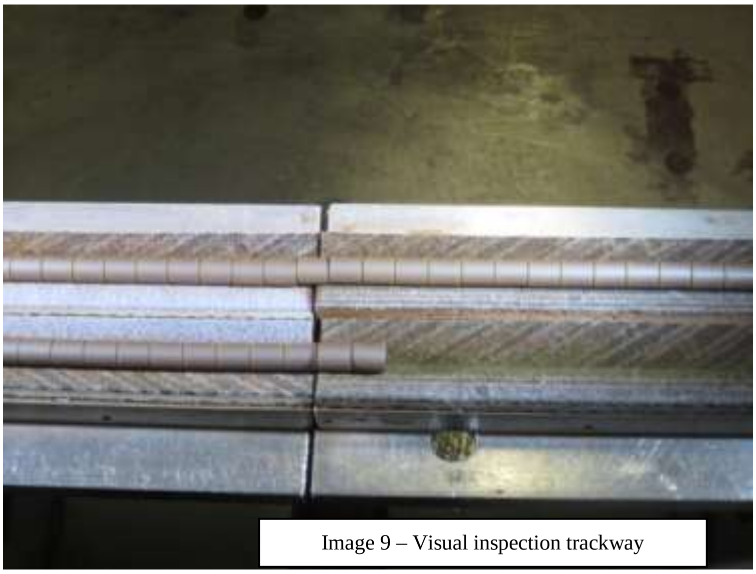
Image 9 – Visual inspection trackway

A conveyor system is used to transfer pellets to the rod loader, temporary buffer storage leg of the conveyor or to the long-term pellet storage area. Pellets leaving the inspection station are channelled into a single file and then pushed on to grooved trays, a fixed quantity at a time. Multiple rods are loaded with pellets at the same time; hence the trays contain the same number of grooves as there are rod loading positions. This set up simplifies the equipment configuration at the loader but it also minimises the risk of post-inspection pellet chipping.

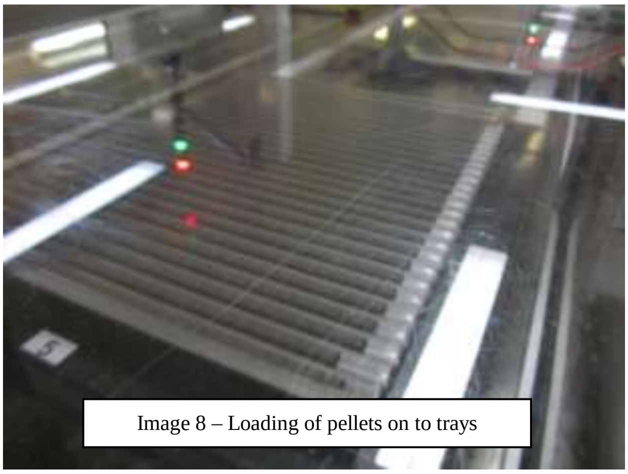
Image 8 – Loading of pellets on to trays

Rod loading also involves the use of cushion transfer, with each of the narrow lanes clad with strips of carpet. During loading, the equipment vibrates causing the entire stack of pellets in each of the multi-lane loading beds to march into the pre-plugged fuel tubes at the same time. Automatic plenum length measurement takes place followed by automatic spring and end plug insertion.

LOW OPERATOR DOSE

The Ionising Radiations Regulations 1999, Schedule 4 stipulates the limit on effective dose for any employee of 18 years of age or above shall be 20 milli Sieverts (mSv) in any calendar year.

SFL's safety strategy is to maintain operator dose rates below regulation limits by implementing ALARP principles. Maximising the use of automation and by carrying out all pelleting and grinding line activities within the confines of enclosed cubicles have been major contributors towards this goal.

Figure 1 – Operator annual dose

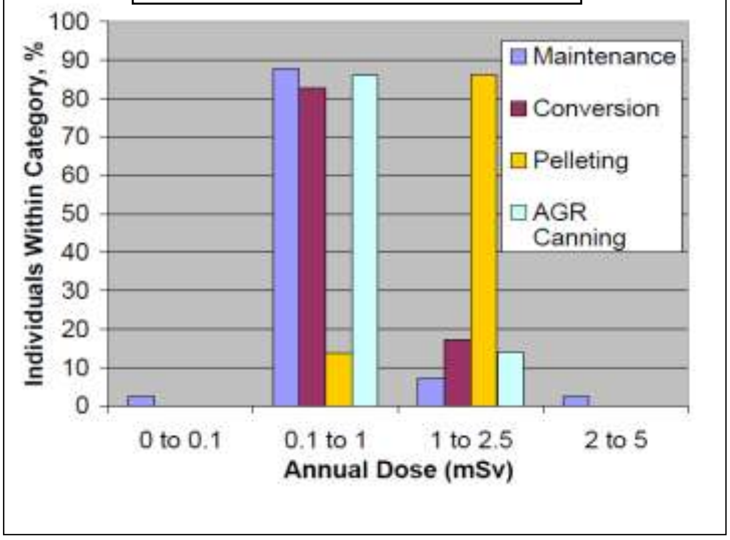

The data in Figure 1 relates to OFC for calendar year 2011. The highest individual dose was acquired by a maintenance operator. The dose of 2.66 mSv was made up of 2.40 mSv external, 0.26 mSv internal.

LOW PELLET REJECT RATES

Fuel pellets can be prone to damage in both the 'green' and 'sintered' condition. This damage usually takes the form of chipping or cracking, which if undetected at inspection could lead to fuel failure. A very low defect rate is advantageous for several business reasons but it is an important defence from a quality perspective as it lessens reliance on inspectors to screen out defective product.

SFL's newly reinstated PWR pellet line has manufactured around four million pellets to date. Plant trending records show the current reject rate at visual inspection is less than 0.1%.

A further benefit from automation is the reduced risk from foreign material contamination that results from keeping operators away from the product as much as possible. Carrying out operations within cubicles also keeps out airborne dust and from a safety perspective prevents operators from coming into contact with moving machinery.

SFL considers that its strategy to maintain a high reliance on automated technology within the PWR pelleting plant is a positive business investment that will result in customer confidence that fuel manufactured at Springfields will possess high mechanical integrity.

In the 15 years since OFC first commenced manufacture of AGR fuel assemblies approximately six million rods have been produced. To date none of these rods has failed in service due to manufacturing related issues such as chipped pellets. This level of quality is considered to be directly related to the use of automation and SFL are confident that all future fuel manufactured in the various areas of the Oxide Fuels Complex will continue to exhibit similar levels of in-reactor integrity.

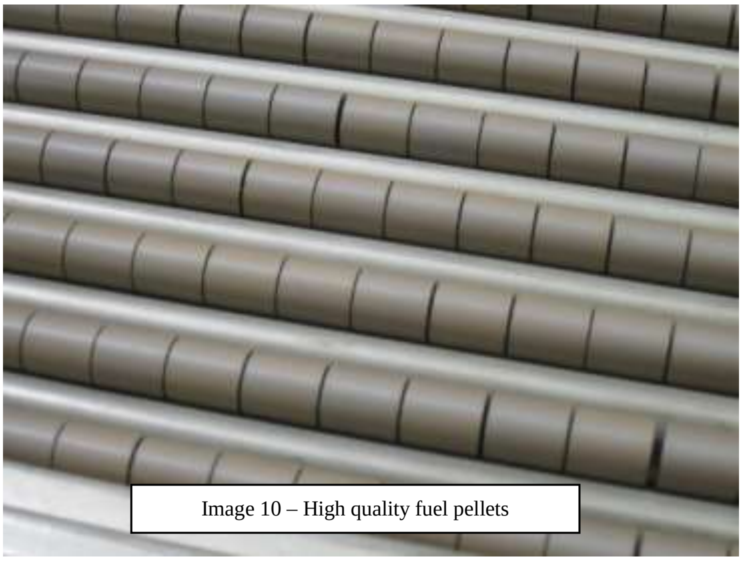

Image 10 – High quality fuel pellets

AN INVESTIGATION ON THE CONTRIBUTION OF ROD GROWTH TO ASSEMBLY GROWTH IN NUCLEAR FUEL

Y. K. JANG, J. I. KIM, J. C. SHIN, S. D. KIM
KEPCO Nuclear Fuel (KNF)
1047 Daedukdaero, Yuseong-gu, Daejeon, 305-353, Republic of Korea

M. S. KIM, T. H. LEE, T. W. KIM
Korea Hydro & Nuclear Power (KHNP)
411 Yeongdongdaero, Kangnam-gu, Seoul, 135-791, Republic of Korea

ABSTRACT

An advanced nuclear fuel of PLUS7 developed to improve the performances from economy and safety points of view was tested using 4 lead test assemblies (LTAs) in Ulchin unit 3 in Korea. Based on the successful irradiation test, this fuel is being supplied to all currently operating eleven (11) optimized power reactors of 1000 MWe (OPR1000s) in Korea. For neutron economy during the commercial supply, this fuel adopted axial blankets on the top and bottom of fuel rod even though there was no axial blanket during the irradiation test. In addition, another commercially verified material was tried to this advanced fuel for fuel rod cladding diversification.

Three kinds of poolside examinations (PSEs) were performed to examine the influences due to design differences: irradiation test using LTAs, surveillance during region implementation and additional surveillance during the other cladding material. The different assembly growth behaviours were witnessed during 3 types of irradiations even though these fuel assemblies used the same skeletons. The excessive fuel assembly and rod growths resulting in the fuel rod and assembly bows should be prevented.

On this paper, the evaluation results as well as the devices and methods to measure axial growths of irradiated fuel assembly and rods in poolside are described. The visual-dimensional measurement device installed on the elevator was used to measure each elevation of the assembly including top/bottom nozzles, grids and rod positions. The assembly growth was obtained by comparing with the as-built data measured during the fuel assembly fabrication. The rod growths were not measured directly by using this measurement device but obtained by evaluating the recorded videotapes of top nozzle-to-rod gap.

The evaluation results show that top nozzle-to-rod gaps have nothing to do with rod growth differences, and larger rod growth plays a role on larger fuel assembly growth. This means that the rod growth can contribute to assembly growth by reducing guide thimble compressive creep due to grid-to-rod friction forces which is dependent on assembly design feature. Particularly, in case of different materials between guide tube and fuel rod in growth point of view, larger rod growth reduces guide tube compressive creep.

1. Introduction

The advanced nuclear fuel of PLUS7^{TM} was jointly developed with Westinghouse for the following objectives : the batch average burnup of 55 GWD/MTU, over 10% thermal margin increase, neutron economy, improvement of seismic resistance, improvement of grid-rod fretting and debris-induced fretting wear performances, and manufacturability improvement, etc.

PLUS7^{TM} for Optimized Power Reactor of 1,000 MWe class in Korea (OPR1000) and Advanced Power Reactor of 1,400 MWe class in Korea (APR1400) shown in Figure 1 has the following performances: easily reconstitutable top nozzle, top grid to reduce rod bow, mid grid for high strength, high thermal margin, and excellent grid-to-rod fretting wear performance, bottom grid for high burnup, multiple debris filtering devices to prevent debris-induced fretting wear, fuel rod for neutron economy and high burnup, and grid-to-thimble joint for manufacturability [1,2]. Table 1 shows the key parameters for this fuel.

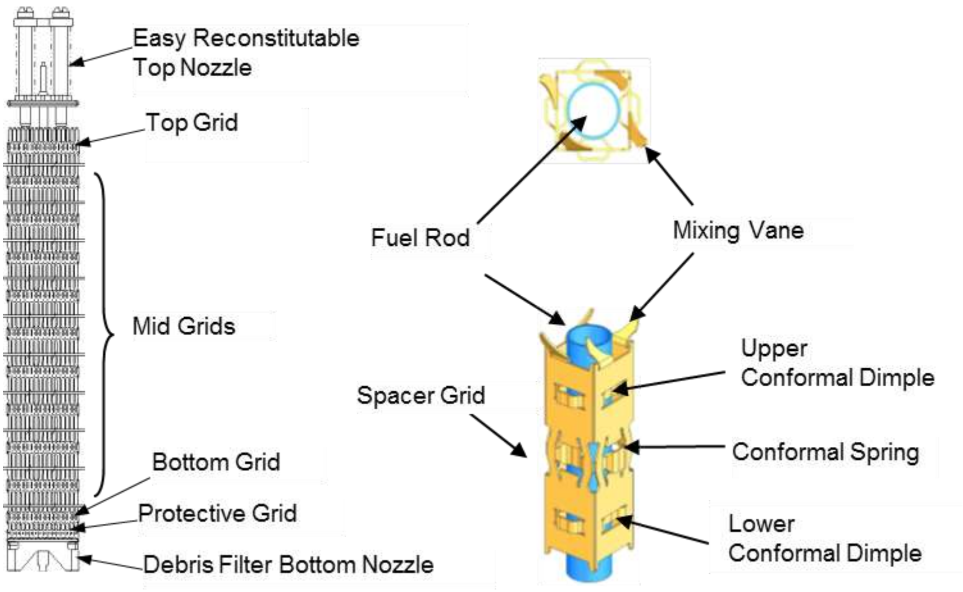

Fig 1. PLUS7^{TM} nuclear fuel

Design Features	Parameters
Rod Array	16x16
Rod Pitch (nominal), mm	12.85
Rod Outer Diameter (nominal), mm	9.5
Assembly Overall Length, mm	4527.55
Assembly Pitch (nominal), mm	207.78
Type of Top Nozzle Spring	Coil
No. of Guide Thimbles (GTs) No. of Instrumentation Tube (IT)	4 1
Outer Diameter of GTs & IT (nominal), mm	24.89
No. of Grids - Top (Inconel) - Mid (Zr-Nb Alloy) - Bottom (Inconel) - P-Grid (Inconel)	 1 9 1 1

Tab 1: Key parameters of the advanced fuel of PLUS7^{TM}

Four(4) LTAs were manufactured and loaded symmetrically in Ulchin unit 3 for in-reactor verification before the full batch implementation. These LTAs were successfully irradiated during 3 cycles. Three times of PSEs (Poolside Examinations) without disassembling during each refuelling outage after each cycle were performed by assembly-wise and one LTA was disassembled after discharge and examined by rod-wise. In addition, the detail examinations for one LTA are being performed in the hotcell test facility. After the irradiation test using LTAs, the region implementation was introduced in all operating OPR1000s successively. Axial blankets were adopted on top and bottom positions of fuel rods for neutron economy. Fig. 2

compares two fuel rods for LTA and region implementation. The surveillance program was launched to evaluate the influences of axial blankets as well as re-confirmation of LTA data.

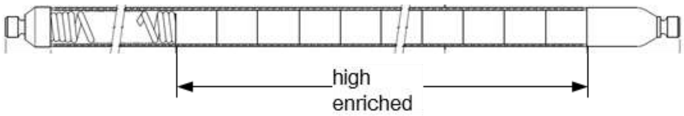

(a) Fuel rod design for PLUS7 LTA

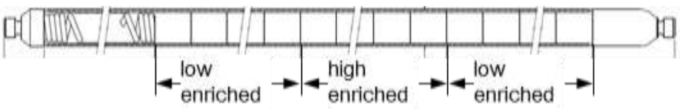

(b) Fuel rod design for PLUS7 region implementation

Fig 2. Comparison of fuel rods between LTA and surveillance fuel

In the meanwhile, another cladding material was adopted for material diversification. So, additional surveillance program had been launched and is being performed. Currently, PLUS7 assemblies using this cladding material are being irradiated for the 3rd cycle. PLUS7 fuel assemblies with the same skeleton showed different rod and assembly growth behaviours. The purpose of this paper is to investigate the contribution of rod growth to assembly growth.

2. Poolside Examinations

Visual examinations and more accurate measurements on surveillance fuels as well as four LTAs during refuelling outage after each cycle were performed using the same high density camera and four measurement equipment: equipment for dimensional measurement, linear variable differential transducer (LVDT) equipment for grid width measurement, another LVDT for rod outer diameter measurement and eddy current test (ECT) equipment for rod oxide thickness measurement. Measurement items for the assembly-wise inspection were assembly length, assembly bow and twist, top nozzle-to-rod gap, rod-to-rod gap, spacer grid width, rod outer diameter, and cladding oxide thickness, etc.

Fuel assembly elevations are measured by the calibrated encoder. Fuel assembly length change is calculated from the difference between the post-irradiation and pre-irradiation fuel assembly length. Fuel assembly bow and twist can cause an effect on fuel loading and unloading, control rod insertion performance and the compatibility with reactor internals. The excessively closer gap between rods due to rod bow results in Departure from Nuclear Boiling (DNB) penalty which generally occurs when the rods cannot grow axially due to excessive force by the grid springs. Assembly bow, twist and rod-rod gap are evaluated by analyzing videotapes. The excessive growth of grid width can cause an effect on loading and unloading fuel assemblies into the reactor as well as the compatibility with the reactor core shroud. The spacer grid width is directly measured by using LVDT equipment. The rod outside diameter to evaluate cladding creepdown or pellet swelling is measured using LVDT equipment, too. The cladding oxide thickness to evaluate thermal performance is measured using ECT equipment.

The assembly growth and rod growth among the 8 irradiation performance parameters during two surveillance programs were the interesting items although the other 6 parameters confirm the LTA data well. Visual-Dimensional measurement device is installed on the elevator and the calibrated ruler is installed vertically as shown in Figure 3(a). The encoder binded on the device is calibrated at intervals using the ruler by moving the device on the elevator up and down. For the next step, a fuel assembly hanged on the grapple shown in Figure 3(b) is installed on the same distance apart as the ruler’s position. The elevations of the assembly including top/bottom nozzles, grids and top positions of rod, etc. are measured using the encoder and then compensated for temperature. To evaluate the assembly growth, the elevation measurements are compared with the as-built data measured during the fuel assembly fabrication.

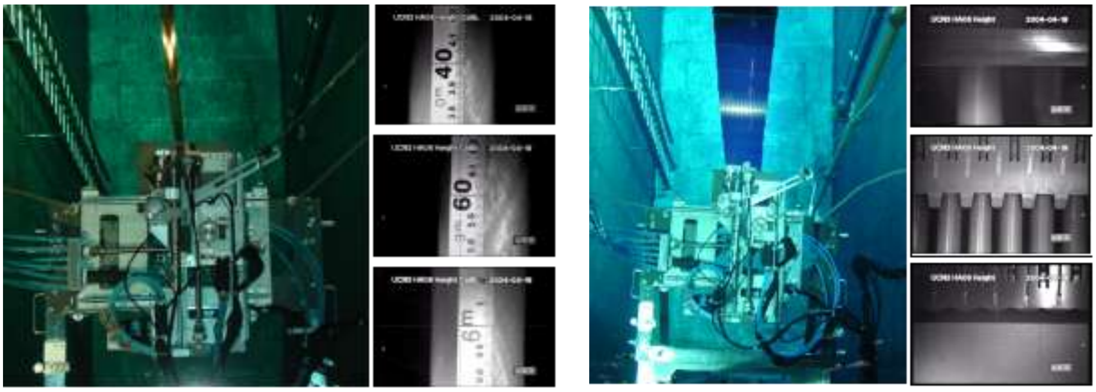

(a) Calibration of encoder using calibrated rule (b) Measurement of assembly elevation

Fig 3. Calibration of encoder and assembly growth measurement

Fuel rod growths cannot be measured using the visual-dimensional measurement device directly because the bottom positions of fuel rods are invisible. At the first step, the configuration containing top nozzle and top of fuel rods is recorded as shown in Figure 4. The top nozzle-to-rod gap on the rod at the center of the assembly face is measured by encoder. The top nozzle-to-rod gaps on the other rods are evaluated by analyzing the videotapes and by using the known value at the center rod. Rod growth which is obtained by subtracting as-built rod length from irradiated rod length is calculated by adding top nozzle-to-rod gap change to assembly growth.

Fig 4. A Picture showing top nozzle-to-fuel rods

3. Evaluation Results and Consideration

The irradiation growth is the change in shape of solid at constant volume that occurs during irradiation in the absence of stress and depends on the chemical composition, manufacturing processes and operating condition. It was known that assembly growth depends on the guide tube stress-free axial growth, hydriding and compressive creep, etc. Although a lot of researches to investigate this mechanism had been tried and are being tried, most fuel vendors are using empirical models based on the measured data [3,4]. The excessive fuel assembly length increase can cause an adverse effect on the compatibility with reactor internals.

As per SRP 4.2 [5], excessive fuel assembly or rod growth is restricted to prevent their bows resulted in fuel failure. Assembly growth is dependent on stress-free axial growth, hydriding and compressive creep [6]. By considering the same stress-free axial growth and hydriding due to the same material and operating conditions, the different assembly growth results from the different compressive creep due to the design difference between two assemblies. The only one different thing between LTAs and assemblies for surveillance is that the surveillance fuel rods have axial blankets on both ends to improve neutron economy while LTA fuel rods do not.

Figure 5(a) compares the remaining top nozzle-to-rod gaps between rods with axial blankets and rods without axial blankets. The remaining top nozzle-to-rod gaps on LTAs without axial blankets decreased about 2~3 mm after each cycle while those on surveillance fuels with axial blankets remained nearly unchanged. The top nozzle-to-rod gap decrease means that the continuous friction forces between grid springs and fuel rods occur as a function of burnup. These friction forces by rod growths contribute to reduce compressive guide thimble creep occurred due to the compressive force caused by holddown spring and uplift force caused by pressure drop. This contributes on the larger assembly growth shown in Figure 5(b).

In the meanwhile, another cladding material which shows larger rod growth behaviours was adopted in this fuel. Assemblies with another cladding material had larger assembly growth comparing to one using the same material as shown in Figure 6. This is due to that the friction force between grid and rod is contributing to reduce guide thimble compressive creep. This phenomenon might be dependent on grid design feature.

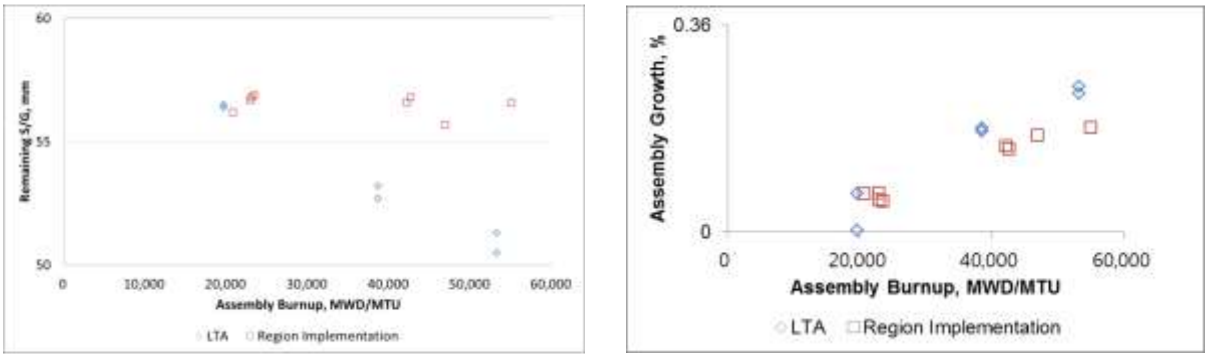

(a) Remaining top nozzle-to-rod gap

(b) Assembly growth

Fig 5. Top nozzle-to-rod gap and assembly growth by axial blankets in fuel rods

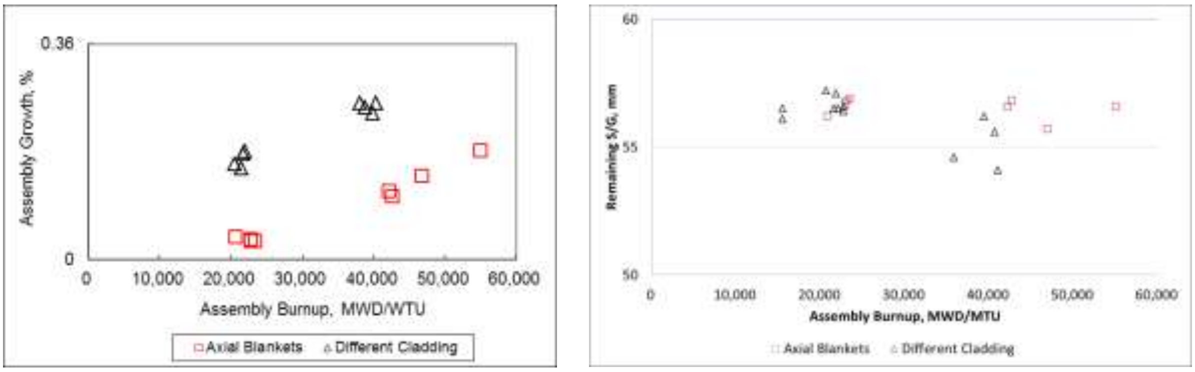

(a) Assembly growth

(b) Remaining top nozzle-to-rod gap

Fig 6. Comparison of same cladding and different cladding on assembly growth and remaining top nozzle-to-rod gap

4. Conclusion

Three cycle in-reactor verification tests of the advanced fuel of PLUS7^{TM} were completed in Korean nuclear power plants. All burnup-dependent fuel performance parameters such as fuel assembly growth, top nozzle-to-rod gap, rod-to-rod gap, fuel assembly bow and twist, fuel rod diameter, cladding oxide thickness after three cycles were met their design criteria. It is, therefore, concluded that the advanced fuel were successfully irradiated. As a result, the current fuels in all 11 Korean PWRs were replaced with PLUS7^{TM}. Additional examinations such as post-irradiation examination (PIE) using hotcell test facilities are being performed continuously.

Another interesting point is that PLUS7 rod growth difference contributes to the assembly growth due to grid-to-rod friction force differences which is dependent on assembly design feature. Larger rod growth reduces guide thimble compressive creep and contributes to larger assembly growth.

5. References

[1] K. T. Kim, Y. H. Kim, Y. K. Jang, D. L. Stucker, "PLUS7^{TM} Advanced Fuel Development for the CE 16x16 Type Nuclear Power Plants," The 13th Pacific Basin Nuclear Conference (2002).
[2] Young Ki JANG, Kyeong Lak JEON, Kyu Tae KIM, Jae Ik KIM and Jong Ryul PARK, "Irradiation Performances of Korean Advanced Fuels for Nuclear Power Plants," The 16th Pacific Basin Nuclear Conference, (2008).
[3] S.N. Buckley, "Properties of Reactor Materials and the Effects of Irradiation Damage, Butterworths," London (1979).
[4] R.B. Adamson, "Zirconium in the Nuclear Industry, " Third Conference, STP 633, ASTM, (1977).
[5] U.S. Nuclear Regulatory Commission, "Standard Review Plan - 4.2 Fuel System Design," NUREG-0800.
[6] P. Rudling, T. Ingemansson, "Fuel Vendor – PWR Fuel Failure Management Handbook," ANT International, Sweden (2004).

SAFETY ASPECTS OF DRY SPENT FUEL STORAGE AND SPENT FUEL MANAGEMENT

H. VÖLZKE, D. WOLFF, E.-M. KASPAREK
Division 3.4 Safety of Storage Containers
BAM Federal Institute for Materials Research and Testing
Unter den Eichen 44-46, 12203 Berlin, Germany

W. BOTSCH, H.-W. DROTLEFF, P. HINTERDING, S. SMALIAN
Radiation Protection and Waste Disposal
TÜV NORD Nuclear c/o TÜV NORD EnSys Hannover GmbH & Co.KG
Am TÜV 1, 30519 Hannover, Germany

ABSTRACT

Dry storage systems are characterized by passive and inherent safety systems ensuring safety even in case of severe incidents or accidents. After the events of Fukushima, the advantages of such passive and inherently safe dry storage systems have become more and more obvious. In Germany dry storage of spent nuclear fuel (SNF) and high level wastes (HLW) in dual purpose casks fulfills both transport and storage requirements. Basic safety requirements consider safe enclosure of the radioactive materials under normal operation and accident conditions, safe decay heat removal, subcriticality and shielding. Mostly, storage facilities are designed as concrete buildings above the ground, but due to regional constraints, one storage facility has also been built as a rock tunnel. The decay heat is always removed by natural air flow; further technical equipment is not needed. Safe enclosure, subcriticality and shielding are mainly guaranteed by massive thick-walled metal casks.

TÜV NORD Nuclear and BAM present their long experience concerning the licensing process for sites and casks and inform about spent fuel management and issues concerning dry storage of spent fuel and high level waste.

1. Introduction

From the production of electricity by nuclear power plants spent nuclear fuel (SNF) and from reprocessing of this nuclear fuel, high level wastes (HLW) accrue, both of which have to be stored in a safe way until their final disposal. For their long-term interim storage different technical concepts have been established from wet storage in pools to dry storage in transport and storage casks. The events of Fukushima in March 2011 have shown different effects on both options with specific advantages and disadvantages and that dry cask storage is a concept with inherent safety margins to prevent activity release.

Currently the dry storage of SNF and HLW gains more and more importance, because dry storage features advantages in safety and logistics. This paper describes different systems for dry storage of SNF and HLW and explains their specific advantages in comparison to other storage systems based on BAM and TÜV experience.

2. Safety regulations and requirements

As with the storage of all radioactive materials, the storage of SNF and HLW must conform to safety requirements. Following safety aspects must be achieved throughout the storage period:

- All unnecessary radiation exposure and contamination of man and nature must be avoided and
- All radiation exposure or contamination of man or nature must be kept as low as reasonably achievable (ALARA)

These goals are achieved by

- Secure encapsulation of the activity
- Safe discharge of the decay heat
- Subcriticality
- Shielding of gamma and neutron radiation

Basic requirements are defined in “Guidelines for dry interim storage of irradiated fuel assemblies and heat-generating radioactive waste in casks” edited by the German Waste Management Commission /1/. Furthermore the ability to ship the casks for their further treatment after interim storage must be ensured, so additional requirements may arise from the transport regulations. Therefore dual purpose casks which are suited and approved for transportation and storage similarly are utilized in many countries.

The implementation of the safety requirements is achieved through different storage systems in different ways. In case of wet storage the SNF is stored in spent fuel pools with active cooling systems. The water in the pools has the function of heat dissipation and shielding; the activity is encapsulated as long as the fuel rods remain intact. Where necessary, additional filtration of the outgoing air must ensure that no activity is released into the environment. This concept of wet storage is used for spent fuel pools inside nuclear power plants and e.g. at the reprocessing facilities in Sellafield and La Hague. These systems are cheaper in installation but more expensive during operation compared to dry storage in casks. This aspect becomes more and more relevant with increasing storage periods.

For the dry storage of SNF and HLW different concepts are in use worldwide. These include HLW storage in concrete vaults with natural air-cooling, e g. at Cogema, La Hague, or SNF stainless steel canisters being stored in concrete over-packs. Other storage casks consist of various materials like concrete, forged steel or ductile cast iron.

3. Spent fuel storage in Germany

In Germany, SNF and HLW from SNF reprocessing are stored in thick-walled metal dual purpose casks with a double lid system which are approved for transportation and storage. With this concept SNF can be removed from nuclear power plants flexibly during operation or later decommissioning and can be stored on-site or elsewhere, e.g. in centralized storage facilities.

Initially, the dry storage of SNF in Germany was performed in two central storage facilities in Ahaus and Gorleben starting in the 1980’s. This concept was executed for BWR/PWR-SNF and THTR (thorium high temperature)-SNF from commercial nuclear power plants. High active vitrified radioactive waste from reprocessing of SNF in France is already stored in Gorleben. Public discussion about transportation of SNF and HLW in Germany and possible contamination of casks during transportation lead to the construction of on-site storage facilities, which are located adjacent to the power plants. For these on-site storage facilities three different designs were chosen: two different storage building-types and a tunnel-design. In a few cases SNF dual purpose casks were stored in small concrete shelters (short term interim storage limited to 5 years) prior to completion of licensing and construction of the main interim storage facility.

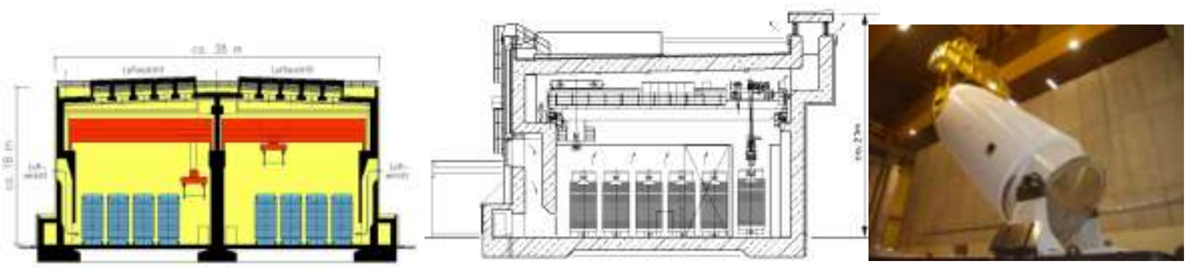

Figure 1: Storage buildings and dual purpose casks for SNF and HLW interim storage

Together, the cask and building assure the compliance with the safety requirements. The building protects casks additionally from harmful weather conditions, external effects or man-made hazards. Safe and secure enclosure of the radioactive material as well as the subcriticality is ensured by the cask design. The secure heat removal and shielding is conducted by interaction of cask and building structure. Therefore it is possible to apply only passive systems on the basis of natural convection, which are nearly maintenance free and can ensure their function for a long time without intervention.

Meanwhile, besides the two central storage facilities, many other on-site storage facilities for dry cask storage are in operation at each nuclear power plant but also at shut-down reactors like Interim Storage North (ZLN). TÜV NORD Nuclear and BAM were assigned as independent experts by the competent authorities in the licensing procedure for their safety expertise about the application, erection and the operation of the storage facilities on all of these sites. TÜV NORD Nuclear and BAM have checked and reviewed all safety assessments and documentations in the fields of cask designs, location, building structures and technical equipment, heat removal, shielding, subcriticality and safety under operational and accident conditions. For some of these sites the TÜV NORD Nuclear and BAM are still in charge on behalf of the competent authorities for supervision of the sites during operation. New cask designs and changes in operation procedures, the building structures or the technical equipment are checked and reviewed by BAM and TÜV NORD Nuclear continuously. Furthermore TÜV NORD Nuclear and BAM lead a German-wide interchange-platform of experience concerning all loadings of SNF into casks, so all relevant information is available to all involved experts organizations, competent authorities, and utilities.

Based on this long-standing and fruitful common work, BAM and TÜV NORD Nuclear have gained huge and unique knowledge and experience that can be used beneficially for similar studies or projects in other countries, especially where dry storage concepts may be considered for the safe long-term management of SNF and HLW at present or in the future (http://www.tuev-nord.de/de/storage.htm).

4. Site specific safety assessment

Any application for SNF and HLW interim storage has to assess safety under consideration of the above mentioned safety requirements, taking into account all site-specific aspects including cask handling and possible severe incidents or accident scenarios like fire or cask drop from a crane. All safety assessments have to be reviewed and evaluated by the competent authority and their experts. Because of similar or identical technical solutions like buildings, casks, operational procedures, many aspects are equally relevant for several sites and safety demonstrations can be easily transferred from one site to another to reduce effort. Some common aspects are explained in the following:

Heat removal: All storage facilities are designed in such a way that the cooling of the casks is performed passively by natural convection of air. The cooling air enters the building at the sides, flows around the casks and is released at the roof, so the decay heat removal is ensured by natural convection without active systems, even under accident conditions and without the need of intervention by working personnel.

Shielding: The thick concrete walls of the storage buildings and the chosen thick-walled cask design reduce the dose rate outside the storage buildings effectively to acceptable levels where no further measures for the protection of the workers on the site or the public outside need to be established. The casks themselves reduce the dose rate within the storage building to a level where handling, emplacement and displacement of casks as well as service operation can take place whenever necessary.

Subcriticality: In order to secure nuclear criticality safety, possible effects of accidents are taken into consideration. In case of dry storage, e.g. re-positioning of fissile material inside the cask is excluded by the cask design including spent fuel basket.

Apart from the storage hall design, rock tunnels can also be used for dry storage of SNF, and at the Neckarwestheim nuclear power plant this concept is used due to the specific geography of the site location. In this case decay heat removal is ensured by natural convection from the rock tunnel to the surface by additional shafts and the surrounding rock effectively reduces the dose rate on site.

Safe enclosure: The German concept of dry storage of SNF and HLW gives a maximum level of safety for design base accidents and even beyond design base accidents. This includes on one hand external hazards such as fire, earthquakes, flooding, landslip, shockwave, lightning strike or airplane crash and on the other hand internal effects such as handling failures or casks drop. The casks and the storage building provide effective protection of the encapsulated activity and guarantee the compliance with the safety requirements. Even after a collapse of the storage building, caused by a beyond design base accidents (e.g. aircraft crash), the casks remain intact and no activity will be released. This high level of safety is established by using passive safety systems and a matching combination of cask and storage building. Even in the Fukushima event, storage casks with SNF were not affected significantly by the earthquake or the tsunami /2/. But the storage pools inside the nuclear power plants, depending on active cooling systems, caused massive problems and release of activity after their cooling failed. By using thick dual purpose casks with double lid sealing systems, the activity stays encapsulated under normal operation and even under severe accident conditions without active measures.

If casks have to be repaired, for example in the case one barrier of the double lid sealing system failed, different concepts exist. The casks can be unloaded in the nuclear power plant or – if this option is no longer available – the double lid system can be reestablished by adding an additional third lid above the secondary lid that e.g. is welded to the cask body.

5. Cask design testing and approval

As mentioned above thick-walled dual purpose casks are the main safety component of dry interim SNF and HLW storage in Germany. These casks have to demonstrate safety with regard to all relevant objectives as mentioned before. The concept implies a monolithic cask body with integrated neutron shielding components and closed by a monitored double lid barrier system with metal gaskets. Further details are described in the recent ESK guideline /1/.

BAM is the competent authority in design testing and evaluation of all quality assurance measures within the transport license approval procedure and BAM is also involved in the storage licensing procedures by the competent authority for the same cask related aspects. This enables high efficiency and comparative evaluation methods for the same technical and scientific aspects. A major aspect of BAM design testing for interim storage are safety demonstrations for a cask drop onto the ground of the storage building without shock absorbers and in the most severe drop orientation. This requires a systematic study of handling procedures to determine from which positions a cask drop has to be considered and which the most severe scenarios with regard to drop orientation, drop height and target are. Subsequently, safety demonstration for selected most severe drop scenarios can be performed by experiments and/or numerical calculations. BAM operates state of the art equipment in both fields with a large drop test facility for cask gross masses up to 200 metric tons and a 2.400 metric tons unyielding concrete foundation in compliance with IAEA requirements and with capable computer systems and different finite element codes such as ABAQUS®, LS-DYNA® and ANSYS®. The analysis of hard cask drop scenarios needs demanding dynamic measurements and/or calculations including specific material data and sophisticated stress and strain evaluation procedures. Verification of numerical models and calculation results by full-scale, model or component tests is usually necessary and also adequate modeling of the foundation or impact limiting structures is essential. BAM has broad experience and competence in these experimental as well as numerical test methods.

Other major issues for the interim storage safety evaluation consider the long-term performance of cask systems and components under operational conditions during the entire storage period which is 40 years in Germany so far. Because dual purpose casks are equipped with a double lid system the proper function of the metallic barrier seals is essential. Not only for that reason quality assurance measures for fabrication, assembling and loading procedures and cask operation are of particular importance as well. Each cask has to be fabricated in accordance with approved manufacturing and testing plans. Finally, certificates of compliance are issued for transport as well as storage purpose and with these documents the cask can be loaded and assembled for transport and storage use. Cask loading under wet conditions in a spent fuel pool requires very accurate dewatering and drying procedures afterwards to prevent any relevant corrosion effect during the subsequent storage decades.

BAM safety evaluation reports on cask safety under normal operation and accident conditions in combination with TÜV NORD Nuclear safety evaluation reports on inventory and site specific safety aspects are the major basis for any storage license issued by the Federal Office for Radiation Protection (BfS) as the competent authority in Germany. Licenses have been issued for all applied storage facilities so far and on that basis all storage facilities have been operated safely without any major problems.

For the future, extended storage periods are an upcoming issue due to delays of establishing a deep geological repository in Germany. With regard to that aspect and further international and European developments guidance documents for periodic safety inspections and ageing management have been improved recently and are currently tested with selected storage sites. Furthermore, additional research and development is essential to gain required data on the long-term performance of materials and components like metal seals and polymer components for neutron radiation shielding. BAM has already started such investigations by experimental and analytical methods and an additional test facility with heating and cooling chambers and specific measurement equipment is nearly finished on the BAM Test Site Technical Safety (BAM TTS, see http://www.bam.de/en).

6. Conclusions

Dry and wet storage of SNF are established throughout the world in a safe and reliable manner. While wet storage is used in Germany at all nuclear power plants during plant operation, dry storage in dual purpose casks is the established concept for long-term interim storage of SNF and HLW whether on-site or in centralized interim storage facilities. Dry storage systems are usually characterized by passive and inherent safety functions ensuring safety even in case of severe incidents or accidents. After the events of Fukushima, the advantages of such passive and inherent safe dry cask storage systems have become more obvious. Safety assessment and evaluation procedures are sometimes challenging but have been performed successfully for many interim storage facilities throughout Germany. Additional licenses are required for various new or modified cask designs and additional spent fuel configurations in the future and under consideration of the German phase out decision. Further delays in the national site selection for a deep geological repository will lead to extended interim storage periods with significant consequences for additional long-term safety demonstrations for storage as well as subsequent transportation. BAM and TÜV NORD Nuclear have broad experience and knowledge in safety evaluation of dry SNF and HLW storage systems under all relevant safety aspects defined by international and national regulations. BAM supports also national and international organizations like IAEA with its expertise and cooperates with several international institutes. Both, TÜV NORD Nuclear and BAM, are willing to offer their expertise and support also to international organizations and projects in nuclear waste management if requested.

7. References

/1/ ESK-Recommendation of 21.06.2012: Guidelines for dry interim storage of irradiated fuel assemblies and heat-generating radioactive waste in casks (in German). http://www.entsorgungskommission.de/englisch/default.htm

/2/ http://www.brattle.com/NewsEvents/NewsDetail.asp?RecordID=1177

THE NATIONAL NUCLEAR LABORATORY'S APPROACH TO WASTE AND RESIDUES PROCESSING

H. GREENWOOD, T.I. DOCRAT, S.J. ALLINSON, D.P. COPPERSTHWAITE
Waste Management and Decommissioning Directorate, National Nuclear Laboratory
Preston Laboratory, Springfields, PR4 0XJ - UK

ABSTRACT

The National Nuclear Laboratory (NNL) treats a wide variety of materials produced as by-products of the nuclear fuel cycle, mostly from uranium purification and fuel manufacture but also including materials from uranium enrichment and from the decommissioning of obsolete plants. In the context of this paper, treatment is defined as recovery of uranium from residues, its recycle to the fuel cycle or preparation for long term storage and the final disposal or discharge to the environment of the remainder of the residue.

NNL's systematic but flexible approach to residue assessment and treatment is described in this paper. The approach typically comprises up to five main phases.

- Phase 1: For any unknown, or poorly or vaguely understood residue, the first step in its treatment is a study of available historic data.
- Phase 1A: A characterisation programme usually involving inspection and sampling of the residue stock, instrumental analysis and small scale chemical testing.
- Phase 2: Testing the suitability of the residue for existing plant e.g. on the Customer's premises or the suitability of a previously developed process.
- Phase 3: Where Phase 1, 1A and/or 2 work has shown that a residue is not suitable for treatment via existing processes, a process specifically tailored to treatment of the residue in question is developed. Typically, processes which are unsuited for existing plant are implemented in the NNL Preston Laboratory Residue Treatment Plant.
- Phase 4: The development of the selected process to a point where it can be implemented at full scale. Typically Phase 4 is only required for very complex multi-step processes.

Each phase of work is described in detail with examples used to illustrate the benefits of a systematic approach to waste and residue assessments and processing.

1. Introduction

The National Nuclear Laboratory (NNL) works with a variety of customers in the uranic waste and residue treatment area. Traditionally, treatment of materials has encompassed the recovery of uranium from relevant wastes or residues, its recycle to the fuel cycle or preparation for long term storage, and the final disposal or discharge to the environment of the remainder of the residue. The bulk of the wastes and residues assessed and/or treated to date have been produced as by-products of front end of nuclear fuel cycle operations and from decommissioning of associated plants. In the main they have arisen from the manufacture of nuclear fuels and intermediate products, uranium purification operations and enrichment operations.

In the context of this paper, a uranic waste is a material that cannot be disposed of without treatment, but which has no intrinsic value whereas a uranic residue is a material that has some intrinsic value owing to its uranium content.

Over the years, many similar residues from other parts of the nuclear fuel cycle and from other uses of uranium have been found to be treatable by similar methods to front end fuel cycle residues. This has allowed the experience gained by NNL to be applied over an ever widening range of materials. This paper describes the challenges that need to be addressed when dealing with uncharacterised and often unknown legacy materials and the future challenges posed by the wide range of materials which reside on the UK's nuclear sites.

2. Historical Perspective

NNL has its roots in British Nuclear Fuels Limited (BNFL) and maintains close working relationships with the former BNFL companies, all of which are now separately managed under contract or under relatively new ownership. An extremely successful working partnership was initiated in the mid 1980's between the now NNL Preston Laboratory and SFL Waste Management; the aim of this partnership was to characterise and process the entire backlog of residues stored on the Springfields site.

At their peak, around 1998 to 1999, uranic residue stocks at Springfields totalled c. 40,000 drums (generally 205 dm^3 capacity plastic or metal drums), c. 150 ISO containers and a range of other items. The stocks comprised many diverse materials which were grouped together in a number of different categories; these were dependent on the nature (or suspected nature) of the materials, potential or defined processing routes, and the enrichment (i.e. isotopic abundance, or IA) of the uranic component of the residue. Much of this residue backlog has been or is currently being processed and by the end of 2011 drum numbers had been reduced to about one third of their peak. As historic residues are processed, process residues continue to arise and, as decommissioning and demolition of old plant accelerates, new types of residue are arising both at the Springfields site and from elsewhere in the UK.

Many of the remaining and arising residues are being processed, or are expected to be processed, via existing SFL residue treatment plants. Some residues, however, currently have no proven treatment method or are unsuitable for treatment in such plants. A similar situation exists with respect to many off-site residues. For such residues, NNL has developed a systematic methodology which has facilitated the assessment of over 40,000 drums and similar items. The benefits of such an approach to waste and residue assessments have been shown to include the early identification of processing routes or processing issues and the avoidance of capital investment.

As experience has been gained during the SFL programme and as the issue of uranic residues in the UK has risen in prominence, it has become clear that many residues exist which could be processed via existing or planned NNL and SFL facilities. Accordingly, support work by NNL on behalf of SFL and other customers has expanded to cover such off-site residues, using similar methodologies to those developed for SFL residues.

3. A phased approach

Investigations into residues deemed unsuitable, or at least not obviously suitable, for processing in existing or planned plant have been carried out using the methodology outlined in Fig 1 and described in detail in the following sections.

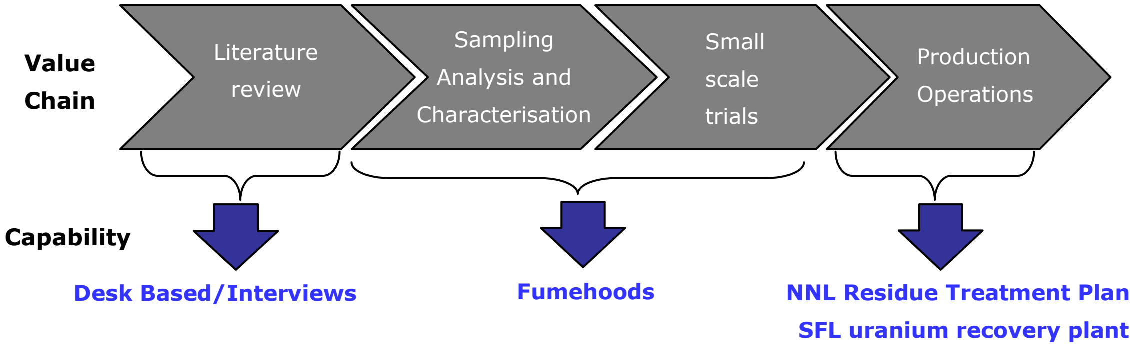

Fig 1. NNL Residues Phased Methodology

3.1 Phase 1

The initial stage in an investigation comprises the gathering of historic information in an attempt to discern the chemical and physical characteristics of any given residue, how it arose, what problems might be associated with its processing and whether any fraction of the material has previously been processed by any currently viable method.

Although the questions posed at this stage of an assessment can seem somewhat mundane, their importance cannot be overstated since the outcome of a detailed Phase 1 investigation could negate the need for further development work and may result in the direct processing of the material in existing or planned NNL or SFL plants. Historically, lines of investigation have targeted uranic wastes and residues but many of the questions are equally applicable to other materials containing a wider variety of radioisotopes. The questions are grouped into a number of categories as described below.

3.1.1 General description

It is important to understand the material in terms of its general composition, its history, its level of characterisation and its uranium content (if relevant). It is essential to understand whether more than one type of material is present since minor fractions can prove to be the most problematic when it comes to processing. For example, materials such as tissues, gloves, wipes, filter media, tape, vacuum bags, etc. can be processed but segregation from the bulk material is typically required (Fig 2).

Fig 2. A fairly typical decommissioning residue

The presence of reprocessed uranium or isotopes not normally associated with uranium processing and fuels manufacture can be problematic for certain processing routes and effluent/solids discharges. As such, characterisation data is an extremely important factor in understanding what is known about the material and what still needs to be discovered.

While assessing any available characterisation data, it often useful to concurrently assess the softer or more anecdotal data relating to the waste or residue. Such data may include when, where, how the material arose and how long it has been in its current form.

Experience has shown that the older the material, the less well characterised it is likely to be. It is similarly useful to know whether the material has always been in the possession of the customer, whether they actually produced it themselves and has any processing been attempted by any method, be it at laboratory or full scale. If processing had been attempted, what was the outcome and why was such processing nor pursued?

3.1.2 Storage

How a material is stored, particularly in terms of its storage container(s), is much more important than it might seem. Many plant processes require feedstocks to be fed from a specific container and modifications to feed from different containers is expensive in terms of plant modification and impact on ongoing operations. Re-drumming of materials can also be considered at this stage.

The presence of secondary containers such as bags or bottles will have a major impact on material processing as these will probably need to be removed and would rule out direct processing in some plants.

3.1.3 Physical Properties

The physical nature of the material impacts on how it might be processed, in particular how the material is handled in terms dust hazards, flammability, the tipping of drums, the removal of organics or pre-processing requirements such as sorting and crushing.

Key factors which affect pre-processing requirements include whether the material is physically homogeneous i.e. are there distinct differences between drums of ostensibly the same material or within individual drums; whether the bulk material comprises fine powder, coarse powder, lumps or a mixture of all three; whether the material is mixed with tramp objects such as hard agglomerates of the main constituent material or extraneous materials such as wire, plastic, metal, paper, etc; whether the material is dry, damp or contains free standing liquor; whether the material contains macroscopic quantities of organic materials such as oils, solvents or solid organics and; whether the material is free flowing, sticky or adhesive.

3.1.4 Chemical Properties

The chemical properties of the material are paramount in determining its processiblitiy. They affect the process by which the residue may be treated, the processing rate and how effluent liquors and solid residues may be disposed of. As with physical properties, homogeneity both within drums and across the stock is important since much reported data on chemical composition is based on sampling and analysis. It is vital that any chemical analysis is based on representative sampling of the material to avoid processing issues down the line. In many cases, fully representative sampling is impossible and a degree of judgement is required.

Many factors will affect the process selection but the main considerations usually include; how the material would behave on contact with acid e.g. gas evolution, foaming, heat evolution and the generation of flammable gases; the properties of the leach slurry e.g. corrosivity (particular in relation to 304L stainless steel) and; the presence of any species which would impact on discharge authorisations or could adversely affect uranium purification. For uranium targeted for reintroduction into the fuel cycle, a range of additional factors which might affect product specifications would also need to be considered.

3.1.5 Radioisotope content

The radioisotope content of the material is very important in terms of the specification of any final product. Uranium isotopes such as ^{232}U, ^{234}U and ^{236}U are of particular interest since they cannot be removed during residue processing, though blending opportunities can often be considered. For material which has undergone enrichment blending involving highly enriched uranium (HEU), unusual ^{234}U concentrations are often encountered whereas ^{232}U and ^{236}U are often encountered when reprocessed uranium has been processed in the same plant as non-irradiated uranium. All minor uranium isotopes are tightly controlled in fuel and intermediate product specifications.

Isotopes not normally encountered in nuclear fuel processing are of increasing interest as the range of wastes and residues amenable to treatment expands. NNL works closely with SFL, the Springfields Site License holder, and the Environment Agency (EA) to develop pragmatic strategies for dealing with any discharge issues arising from such isotopes. Early identification of potential discharge issues is paramount in developing appropriate processing and effluent treatment options.

3.1.6 Radiological Properties

This section refers to dose rates associated with the material. Owing to the nature of many of the materials historically treated on the Springfields Site, many of the processes tend to be somewhat “hands-on” when compared with other nuclear sites. This is highly advantageous in terms of ease of implementation but means particular cognisance of operator doses must be taken into account. Dose rates in excess of those normally encountered during processing of low enriched uranium (typically up to 5 g ^{235}U/100 g U) are of interest. Additionally, those materials for which working times exist would require further consideration.

3.1.7 Other factors

While the preceding lines of investigation have been found to be reasonably comprehensive in terms of initial material assessments, the nature of many wastes and residues dictates that something unexpected is likely to be found. As such, it is important that any additional information relating to the material is shared.

A further consideration relating to processed materials is whether the customer is expecting to take back process wastes or separated uranium and what constraints this might impose on processing routes. If there is a requirement to return materials, it is important to understand whether there is a specification for the materials generated.

3.2 Phase 1A

Many materials cannot be sentenced as a result of Phase 1 assessment due to a lack of prior characterisation or a low level of confidence in the precise nature of the material, its origin or its storage conditions. In these cases, inspection and sampling of the residue stocks is required. This phase is routinely supplemented by instrumental analysis of feedstocks, particularly where poorly understood materials are involved. The instrumental analysis of materials was introduced as an additional phase of work to allow some characterisation prior to specifying the next phase of work. Samples of the dried material are typically subjected to X-ray diffraction (XRD) analysis and scanning electron microscopy-energy dispersive X-ray (SEM-EDX) analysis and the results used to assess the composition of the residue. Other techniques, such as thermogravimetric analysis (TGA) and infra-red spectroscopy (IR) are utilised as required.

A typical inspection programme will involve opening drums or other containers and visually examining the contents. The selection of drums is guided by the findings of Phase 1, particularly where groupings of items was apparent. The grouping of drums or other items is normally based on the apparent source of the material and sequences of batch numbers or other identifying marks but experience has shown that mislabelling or misidentification of drums can occur. As such, it is crucially important that the proportion of drums inspected and sampled is sufficient to provide reliable data on the entire stock. For certain poorly characterised and highly variable materials, 100 % sampling can be required. These types of materials normally require the development of specific processing routes and are discussed in more detail under Phase 3. Inspection and sampling can be undertaken in the field by NNL or Customers’ staff or within purpose built facilities within the Preston Laboratory.

Characterisation work typically involves the identification of major phases within the residue, often with identification of the main acid soluble species and the quantification of any organic content. This initial characterisation work, coupled with the inspection programme, allows those materials which are obviously unsuitable for processing in SFL uranium recovery plants to be identified at an early stage in the programme, avoiding unnecessary process testing. Those materials identified as potentially suitable for SFL plants, either directly or following pre-treatment, are subjected to Phase 2 process testing. Targeting processing via SFL plants is often the most cost effective route where large volumes of residues requiring reasonably standardised processing conditions exist.

Many materials have been sentenced directly to established residue processing routes following Phase 1A characterisation. This tends to occur when only confirmation of a material type is required.

3.3 Phase 2

SFL operates a uranium recovery plant for the treatment of depleted to c. natural enrichment residues and a separate plant for enriched residues. Laboratory investigations and detailed analysis of materials aimed at determining if materials are processible via these SFL plants are termed “Phase 2” investigations. These generally involve leaching in nitric acid under typical plant conditions and analysis of leachates and residual undissolved solids.

A “standard” leach apparatus (Fig 3), with a typical capacity of 2 dm^3, is used in the majority of this work, though smaller equipment sizes can be utilised as considered necessary. The reaction vessel is fitted with a multi-necked and flanged lid, and located on a halogen hotplate. The central lid neck is fitted with a stirrer which is connected to an overhead stirrer motor. One neck of the lid is fitted with a condenser, and a second with a temperature probe (typically a PTFE coated thermocouple connected to a digital thermometer). Spare necks are fitted with stoppers.

Fig 3. The “standard” Phase 2 leach apparatus.

For each experiment, the apparatus is assembled and the acid heated to the target temperature. Any required materials such as alumina are then added (alumina is normally added where fluoride is present at notable levels, to ensure complexation for the purposes of dissolution and minimisation of corrosion), followed by the feedstock residue.

Residue additions are initially made in small aliquots to determine if any vigorous reaction occurs, and then in bulk if this is indicated as safe by the initial additions. The slurry is then heated (if necessary) to a desired temperature and held there for the desired time.

Following leaching and cooling, the apparatus is inspected and the appearance of the contents noted; the apparatus is then dismantled and the slurry subjected to solid-liquid separation. Recovered solids are washed with deionised water with the bulk of the wash water being collected separately from the leachate.

Recovered solids are weighed, dried and reweighed before being crushed and mixed prior to sampling and subjected to quantitative uranium analysis. In addition, samples of dried residual undissolved solids are (where considered necessary) subjected to analysis by XRD and SEM-EDX techniques.

Leachates are analysed for uranium, uranium enrichment, heavy metals, and a range of chemical species and radioisotopes of importance to onward uranium processing and site discharges.

Using the Phase 2 experimental data, the processibility of the materials via SFL plants has generally been assessed in terms of the chemical and physical form of the residues, likely ease of feeding to dissolution equipment, reactivity on contact with nitric acid, solid-liquid separation of leach slurries, residual solids uranium concentrations, and onward processing of recovered liquors in terms of chemical compatibility with the residue plants, environmental discharges and the presence of materials which might cause out of specification pure uranic product post purification.

The outcome of Phase 2 investigations has historically been to recommend processing in SFL plant, sometimes with a specific non-standard process regime stipulated, or to recommend the development of a residue specific process (this latter generally being termed "Phase 3" – see later)

Often, parts of existing plants can be adapted to permit the implementation of a non-standard process. The processing of Casting Shop Graphite which historically made up a large fraction of the Springfields residue stock is an example of such an adaptation. The graphite residue from the vacuum casting of uranium metal into rods had been accumulating since 1966 when the previous method of treating the material ceased. The residue comprised relatively large pieces of graphite, occasionally with pieces of uranium adhering to the surface, and free uranium metal (Fig 4).

Fig 4. Casting Shop graphite.

The requirements for the graphite treatment process were that it should utilise existing Springfields facilities as far as practically achievable in order to recover the uranium for recycle and render the graphite suitable for disposal. While direct leaching could clearly recover the bulk of the uranium, the leached graphite contained too much residual uranium to allow direct disposal to landfill. Disposal of leached graphite to LLWR was not considered feasible due to the high volume of material (> 10,000 drums) that would need to be disposed of and the substantial residual alpha activity associated with the leached graphite. The unsuccessful leaching of bulk graphite was believed to be due to be presence of uranium metal in the pours of the graphite and size reduction prior to leaching was considered necessary.

NNL undertook Phase 2 leaching trials using, as a basis, leach conditions that could be realistically achieved in the Springfields magnesium fluoride treatment line. This line involved a wet milling process followed by leaching in dilute nitric acid at ambient temperature. It was demonstrated that near quantitative removal of uranium from graphite could be achieved if graphite was milled to the size likely to be achieved in the magnesium fluoride treatment line.

Following demonstration of the process feasibility, SFL undertook to segregate the bulk of the uranium from the graphite by hand sorting and worked with NNL and equipment suppliers to identify a suitable pre-crusher for use in reducing the size of the graphite pieces prior to milling. Selection of crushing equipment was complicated by the presence of residual uranium metal (post sorting) which could present a pyrophoricity hazard or might damage the crushing equipment. Owing to these concerns, high speed crushers were considered to be unsuitable.

Following the identification and successful testing (using new graphite components) of suitable low speed crushing equipment, a unit was installed at Springfields in 2006. Extended plant trials were undertaken in order to optimise the residue feed rate to the milling stage of magnesium fluoride treatment line and the acid and water feeds to the process. The resulting process was successfully implemented in 2007 with the bulk of the residue stock being processed over a period of c. 4 years. About 40 te of extracted uranium has been returned to the fuel cycle (Fig 5) via this process.

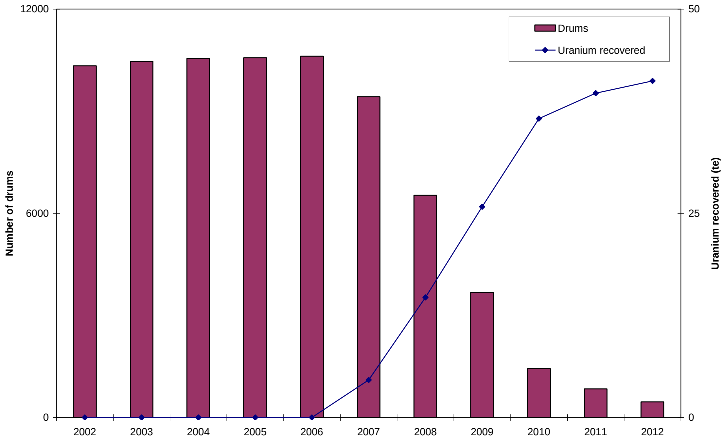

Fig 5. Casting Shop graphite processing.

The graphite slurry was filtered using standard plant filtration equipment with a modified wash procedure to ensure adequate removal of dissolved uranium and nitric acid from the free draining graphitic filter cake.

The success of the adapted graphite process has allowed the plant and process to be further flexed to allow the processing of several other previously intractable resides such as building rubble and incinerator ashes.

3.4 Phase 3

As previously mentioned, where the outcome of phase 2 investigations has been to recommend the development of a residue specific process, this work has generally been termed “Phase 3”. Much current waste and residue treatment work within the NNL Preston Laboratory is concentrated on those residues, identified in prior investigations or experimental work, as unsuitable for treatment in SFL residue plants. These targeted development programmes involve detailed technical investigations designed to produce viable processing methods allowing particular residues to be sentenced with confidence.

A huge variety of materials has been assessed for treatment via Phase 3 process development, a few examples are presented as part of this paper.

- Filter cakes containing high concentrations of uranium from previous chemical leaching operations (typically containing uranium encapsulated within nitric acid insoluble materials).

- “Oily residues”; typically cutting or lubricating oils containing pyrophoric uranium swarf or degraded uranium fines.
- Contaminated oils and solvents containing dissolved uranium (including oils and solvents absorbed on filter aid, sawdust or similar.
- “Copper based” residues (copper hydroxides, fluoride-sulphates, bicarbonates) containing uranium.
- Sludges from solvent extraction operations (some are > 50 years old; high in ^{231}Pa).
- Resinous floor polish containing high concentrations of enriched uranium.
- Highly pyrophoric “uranium-zirconium” metal residues stored under kerosene.
- Various uranium metal and alloy items.
- Ventilation filters of many kinds.
- Contaminated paper, plastic, clothing, gloves etc.
- Decommissioning residues (concrete, bricks, blocks, timber, metals, etc).

Phase 3 experiments are carried out in similar fashion to the Phase 2 leaches, with ad hoc modifications as necessary, such modifications being specifically tailored to the individual residue. Typically, experimental work is carried out at a scale of several hundred grams but pilot scale processes of several tens of kilograms can also be employed.

The outcome of the Phase 3 experiments is generally a fully defined process, specified for particular residue type or group of residues. The developed methods are generally, but not exclusively, targeted for full scale implementation via the NNL Preston Laboratory Residue Treatment Plant which is far more flexible than the conventional uranium plants.

3.5 Phase 4 processing

The NNL Preston Laboratory Residue Treatment Plant contains a wide variety of modular plant items which can be quickly configured to differing roles. The plant area was constructed with a view to being used both for development work in chemical engineering and for specialist processing tasks requiring unusual equipment and/or close technical control by professional staff.

The plant area (Fig 6) comprises 10 large “Bays”, each Bay having a series of “risers” supplying services such as power, process and cooling water, off gas extraction, compressed gases, steam etc. Modular plant available currently includes a variety of stirred vessels, some lined for corrosion resistance and with capacities from 100 dm^3 to 10 m^3, these can be used for a wide variety of tasks such as dissolution, leaching, precipitation, settling, decantation and oil and solvent clean up; a variety of solid-liquid separation equipment; a flammable solvent treatment rig; oil/water centrifuge; nitric acid capable industrial washing machine and; solvent extraction equipment.

Fig 6. The NNL Preston Laboratory Residue Treatment Plant

Although constrained in terms of processing capacity, there are many advantages of Preston Laboratory equipment for low to medium volume materials requiring particularly complex multistage processes. Specifically designed stirrers and vessels have been incorporated for improved solids suspension, resulting in improved dissolution/leaching. In addition, corrosion resistant plant allows processing of high fluoride/sulphate/chloride residues to be undertaken and materials other than nitric acid to be used.

The manual nature of many of the Preston Laboratory operations means that wet, sticky and/or reactive materials can be fed safely and with relative ease. A typical material loading operation by a member of the NNL production team is shown in Fig 7. Ongoing processing is supported by integral laboratory facilities and professional staff who are available for immediate trouble shooting.

Fig 7. Loading a corrosive residue into a leach vessel.

Hundreds of drums of residues, intractable to processing in conventional recovery plants, have been processed to date and processing programmes extend out for some years into the future. Processing of residues has ranged from single drums of material to many tens of similar drums; some future work is likely to involve hundreds of drums of essentially similar materials using processes not applicable to normal processing plant operations.

4. Conclusions

Historically, at Springfields, waste and residue treatment work for “no route” or “orphan” residues tended to concentrate on one particular residue at a time. It was recognised in the mid 1990s that the broader picture needed to be assessed. In 1997, BNFL Springfields (now Springfields Fuels Ltd) embarked on a major programme of residue characterisation and method testing/development; most of the technical aspects of this work are being carried out by NNL. This programme, known within NNL as the Uranium Residues Management Support (URMS) Programme, has now been running for 15 years and has some years at least to run. Similar programmes have been carried out at other NDA sites over the same time period and more recently NNL has started to forge partnerships with a range of new customers.

These ongoing waste and residue characterisation and treatment programs developed between NNL and its partner organisations demonstrate that wide ranging legacy uranic materials can be successfully treated with recovered uranium being returned to the fuel cycle or rendered stable for long term storage. Success in discharging historic liabilities has been achieved through the maintenance of a long term and co-ordinated approach to residues and a clear and structured technical strategy.

NNL CASE STUDY OVERVIEW: MAXIMISING PLANT LIFE-TIME EXTENSION OF HA EVAPORATORS FOR NUCLEAR FUEL WASTE PROCESSING

M.G. ARMSTRONG
Plant Inspection and Materials Group
National Nuclear Laboratory
Central Laboratory, Sellafield, Cumbria, CA20 1PG, United Kingdom

PROF. G. WHILLOCK
Corrosion
National Nuclear Laboratory
Central Laboratory, Sellafield, Cumbria, CA20 1PG, United Kingdom

R. FIELD
Engineering Modelling
National Nuclear Laboratory
Chadwick House, Birchwood Park, Warrington, WA3 6AE, United Kingdom

DR. B. GEDDES
Thermo Modelling
National Nuclear Laboratory
Chadwick House, Birchwood Park, Warrington, WA3 6AE, United Kingdom

A. FELLERMAN
Statistical Analysis
National Nuclear Laboratory
Central Laboratory, Sellafield, Cumbria, CA20 1PG, United Kingdom

DR. S. SHACKLEFORD
Asset Care
National Nuclear Laboratory
Central Laboratory, Sellafield, Cumbria, CA20 1PG, United Kingdom

Acknowledgement: *This work was funded by Sellafield Limited (SL) and the Nuclear Decommissioning Authority. We thank members of both SL and NNL technical teams who supported the various aspects of this work.*

ABSTRACT

The Highly Active (HA) evaporators at Sellafield Nuclear Fuel Reprocessing plant are critical plant items in the management of the HA waste streams. These need to support current Magnox and Oxide fuel reprocessing, HA liquor stock reduction and deliver post operational clean out. The kettle type reduced pressure evaporators use steam heated coils and jacket to provide the evaporation in the semi-batch process. It was known that the combination of steam temperatures and high concentrations of nitric acid, metal nitrates, fission and activation products would produce highly corrosive environments. Sellafield Ltd Site Licence Company (SLC) had initially undertaken condition assessments, based on laboratory corrosion rate data, simple heated surfaces temperature models and inspection data from other nitric acid plant to satisfy continued operational requirements.

To satisfy the increased design longevity of the system, risk based assessment processes were established requiring increased quantitative measurements. The first series of results taken from the steam heated components found that the corrosion rates were significantly higher than previously considered. This instigated a new remanent life methodology that included continuous In-Service-Inspection and

developments to cover all the steam heated corroding surfaces, and the development of thermal and structural assessment models which were underpinned by significant laboratory experimentation. The latter work was performed by NNL utilising its specialist knowledge and resources and at the request of SLC HA evaporator technical support team.

This paper presents a case study of the work required to support the remnant life assessment methodology of the current operational HA evaporators including inspection equipment development, corrosivity of process liquors, high temperature/radiation environments, thermal and structural model development, and the use of this information to forecast future degradation. This has culminated in direct feedback to plant and change of operational conditions, and the requirement for new evaporator capacity to fulfil the future site HA liquor processing requirements.

1. Introduction

Sellafield, in West Cumbria UK, contains two reprocessing plants, one designed to process nuclear fuel from Magnox reactors (CO_2 cooled with Uranium bar fuel) and the other to process nuclear fuel from light water or Advanced Gas cooled Reactors[1]. (enriched UO_2). These processes generate products that can be used to power future nuclear reactors, but also radioactive solid and liquid effluents. The safe management of these effluents is critical to the continuation of operations at Sellafield.

The primary solvent extraction stage of each reprocessing plant segregates >99% of the fission products and some activation products into nitric acid based raffinates (HA liquors). The remaining fission/activation products from the other separation process are eventually recombined with these via concentrated medium active liquor waste streams. The fission/activation products are then incorporated into glass in the Waste Vitrification Plant (WVP) prior to being returned to the customers or sentenced, in due course, to a repository (should that be the outcome of UK policy decisions). The intermediate steps between the chemical separation and vitrification are to concentrate the HA raffinate by evaporation and temporarily store this reduced volume, self heating, HA liquor in a number of water cooled tanks (HASTs). This process is schematically shown in Figure 1. The critical HA raffinate concentration is performed by a suit of ageing HA evaporators pending completion of a replacement evaporator (D). A risked based longevity assessment of these HA facilities instigated by Sellafield Ltd Site Licence Company (SLC) has provided sufficient confidence that continued nuclear fuel reprocessing will meet the current UK nuclear fleet energy needs until their final closure, in ~2020.

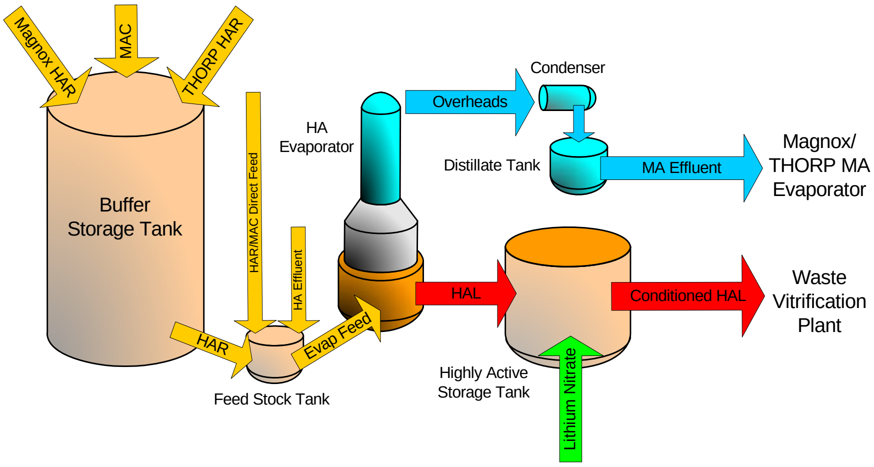

Figure 1. HA evaporator link with other processes

---

[1] Light water reactors e.g. Pressurised Water Reactor (PWR), Boiling Water Reactor (BWR), and Advanced Gas-Cooled Reactor (AGR) are collectively termed “oxide” herein

There are three HA Evaporators on Sellafield site, denoted HA evaporators A, B and C. HA evaporators A and B were built in the early 1960's and were designed to be used to concentrate raffinates arising from the Magnox reprocessing plant. HA Evaporator C was built in the mid 1980's and can be used to concentrate HA liquors from both the Magnox and Oxide reprocessing plants. These kettle type evaporators are of a similar design and all operate under reduced pressure and with bulk liquor temperature of ~ 60°C in order to control corrosion. The evaporation is promoted by steam heated internal helical coils and a steam jacket round the vessel.

Through routine programmed inspections and condition assessments it was identified that the operational throughput of HA evaporators A and B would be limited by failures associated with the evaporators heating/cooling coils The cause of the failures was established to be a combination of chloride pitting of the inner surface of the stainless steel coil pipework[2] allowing actual penetration when the ongoing process-side thinning, attributed to general intergranular corrosion, intersects the cavity. As a consequence the continued safe operation of the HA evaporator C is critical to the continued operations of both Magnox and Oxide reprocessing plant. Also the safe operations of these plants are governed by the Site Licence under which all nuclear establishments operate. Site Licence Condition 28 states that "the licensee shall make and implement regular and systematic Examination, Maintenance, Inspection and Testing (EMIT) of all plant which may affect safety". Compliance with this condition ensures that all plant that may affect safety remains capable of performing the function required by the safety case[3] assumptions to the required level of reliability.

No access facilities for inspection had been designed into the HA evaporator vessels to aid the condition monitoring of the plant. It was expected that high nitric acid/metal nitrate/fission and activation product concentrations would produce highly corrosive environments on steam heated surfaces and would be depth dependent due to increased surface temperature with pressure. The early condition assessments had been based on a combination of laboratory corrosion rate data, simple heated surfaces temperature models, and the use of inspection and operational data from other Magnox plants at Sellafield[4]. The limitations of these assessments to underpin the future safe reprocessing operations at Sellafield highlighted the requirement to measure actual degradation of the vulnerable evaporator components, the steam heated coils and vessel base.

After reviewing the design of each evaporator, it was considered that an inspection system for the steam heated coils was feasible to provide thickness data over the full depth of any evaporator coil. This was developed over a short period with a similar development for the HA evaporator base occurring later. It was understood that the use of the base device would only occur when necessary, due to the greater risk to plant operations if vehicle failure occurred. The first quantitative measurements from the steam heated components were undertaken in 2006 in HA evaporators A and C, covering both Magnox and Oxide HA liquor corrosive conditions. This found that the thickness loss (corrosion rates) were significantly

---

[2] Cooling water was left stagnant within coils for prolonged off-duty periods. The radiolytic degradation of the soft water containing low ppm levels of Cl^- ions resulted in increased potential for the initiation of crevice corrosion most likely near welds [1]. Once this localised corrosion has initiated it propagates to form pit cavities within the wall of the steam heated coils.

[3] Safety case: Is the totality of documented information and arguments developed by the licensee to substantiate the safety of a facility, activity, operation or modification.

[4] Early corrosion assessments for the HA Evaporators were based on: (a) laboratory corrosion rate data obtained in the most part from non-active simulants; (b) corrosion rate data obtained from test coupons exposed to dissolved fuel in the ullage space of one of the Magnox dissolvers; (c) relatively simple temperature models predicting maximum surface temperatures for heating components; (d) operating experience of other (Magnox) plants on the Sellafield site. The corrosion simulants contained dissolved iron as the dominant corrosion accelerator since other potential corrosion accelerators were considered to be radiolytically reduced to benign valency states. Hence, it was considered that corrosion of submerged components was likely to proceed at low rates. It is now known that, owing to the conditions that exist, powerful corrosion accelerators (see later) form and corrosion rates are consequently very high in the HA Evaporators.

higher than previously predicted, but within the safety case for safe continued operations. Furthermore it was identified that Oxide liquors were much more corrosive than Magnox liquors. The generation of increasingly comprehensive thickness surveys of the coils from subsequent inspections permitted the development of a new remanent life assessment methodology that has allowed the condition of uninspected components, notably the vessel bases, to be predicted with confidence. This includes continued In Service Inspections (ISI) of the coils and continued inspection equipment development, experimentation to underpin the heat transfer models, the development of corrosion stimulants, and the development of structural models to justify minimum acceptable component thicknesses, thus allowing remanent lives to be calculated against various future operating assumptions. The methodology and science that underpins the predictions has been independently verified by UK experts and accepted by the Office of Nuclear Regulation (ONR) (formerly the Nuclear Installations Inspectorate).

This paper presents an overview of the unique combination of ingenuity and expertise that has underpinned the safety case for future operations of the HA evaporators on Sellafield site.

2. HA Evaporator design and operational conditions

HA Evaporators within Sellafield are of a very similar design. HA evaporator C is a kettle-type evaporator heated by a steam jacket and six coils arranged in a top and bottom bundle, each bundle containing three concentric coils. Evaporators A and B have four heating cooling coils, two bundles of two coils, and a similar steam jacket. Each evaporator has a height of ~ 11 m high, with an internal diameter of 3.05 m and holds a volume of 13.7 m^3 of liquor. Figure 2 shows the general layout of HA Evaporator C and Figure 3 presents a 3-D representation of the lower half of the vessel.

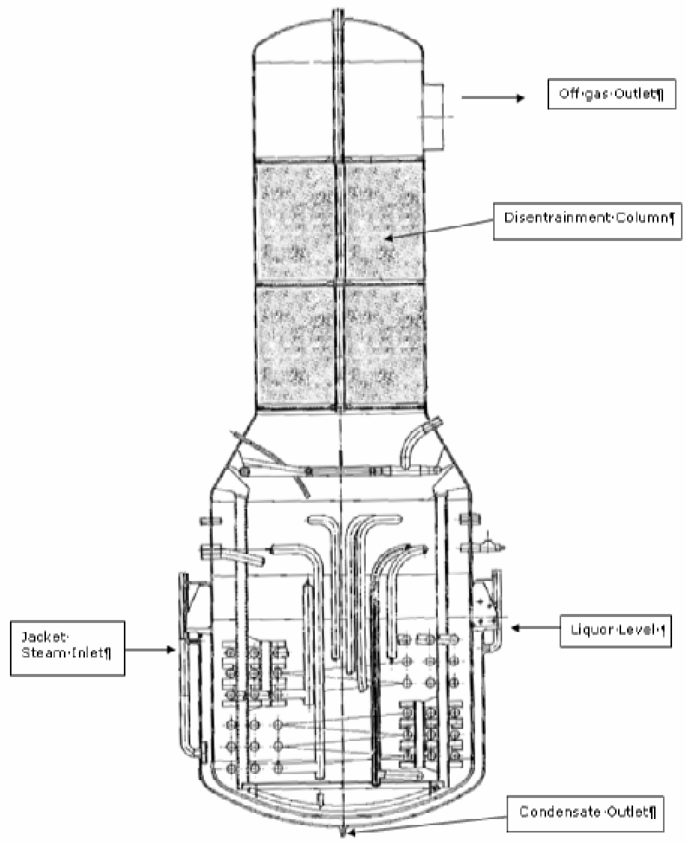

Figure 2 General arrangement of HA Evaporator C.

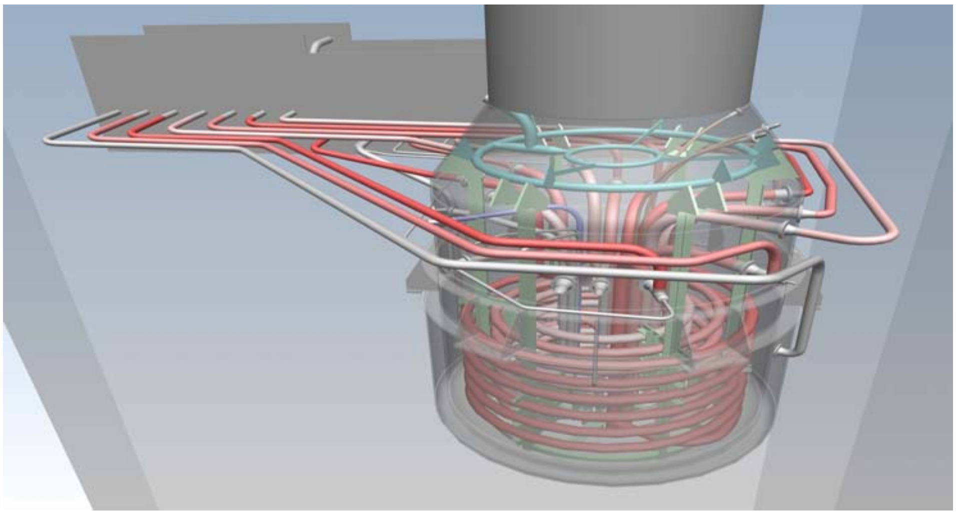

Figure 3. 3D CAD model of HA Evaporator C steam heated coils and jacket

Each HA evaporator vessel and all internal components are manufactured from fully austenitic 18/13/Nb stainless steel (niobium stabilised) produced in general accordance with the specifications in force at the time of design (early 1960s to early 1980's). The modern low carbon stainless steel grades, which were used in e.g. Thorp, were not available at the time of the evaporator construction [2].

The length of the helical sections of the coils range from 12.0 m (inner) to 24.5 m (outer). The maximum submerged depth of the top coils is ~ 0.86 m and the bottom coils are ~1.68 m. The lowest point of the base is at 2.215 m submergence. Four different casts of 4½" OD 18/13/Nb stainless steel pipe were used to fabricate the coil turns in HA Evaporator C. Information relating to the relative corrosion resistance of these casts (for example, ASTM A262 Practice C Huey test [3]) was found either not to have been measured or not preserved. Additionally, previous experience of 18/13/Nb stainless steel indicates that it is not possible to infer the corrosion resistance from knowledge of the compositional analysis alone. Also, cast utilisation during manufacture for each coil segment was not been recorded. Therefore information on the relative corrosion resistance of coil sections was not known. The 18/13/Nb stainless steel was also used for the construction of the base. Slight sensitisation in the heat affected zone (HAZ) of welded base plates has been considered and may be present despite the niobium stabilisation.

3. Operational conditions

The HA Evaporators operate under reduced pressure, ~ 90 mbar absolute, in order to control corrosion and increase throughput rates. The bulk liquor temperature is reasonably uniform at ~ 60°C at all heights due to liquor recirculation. The HA evaporators are unique in that they are kettle evaporators operating under very low pressure. This means that the liquor depth has a significant effect on the temperature at which the liquor boils increasing from 60°C at the liquor surface to around 90°C at the base. Occasionally temperature rises have occurred at the bottom of the evaporator vessel and are attributed to temporary solids build-up, an artefact of reprocessing. These are removed during washout at the end of each batch. The coils and jacket are heated by steam at 127°C. Liquor temperature within the HA evaporators is measured at three discrete heights; near the vessel bottom, middle and upper liquor regions. The measurement occurs by contact of a stainless steel sheathed resistance thermometer residing within a sealed stainless steel tube. The steam coils and jacket are also used to cool the evaporator at the end of each batch using recirculating cooling water.

HA evaporator operations are carried out in discrete batches during which vapour is driven off and the concentration of fission/activation product nitrates rises. The volume of the evaporator contents is maintained by balancing the raffinate feed. The raffinate concentration factor is usually between 30 and 90 depending on the raffinate type. The nitric acid concentration increases relatively quickly from ~ 3 M to the range 9 - 11 M, then decreases slowly as the metal nitrate concentration rises. Towards the end of each batch, raffinate feed is discontinued and replaced with water reducing the nitric acid concentration to ~ 2 M whilst maintaining the fission/activation product concentration constant. The resulting liquor is then suitable for storage and vitrification.

4. Corrosion rate variables

There are a number of variables that would contribute to the corrosivity in the HA evaporators. These are outlined below:

Fuel burn-up: This dictates the concentration of fission and activation product corrosion accelerators in the liquor. Figure 4 presents the significant variation in the fuel burn-up, and therefore trends in corrosivity, over the operating history of HA evaporator C.

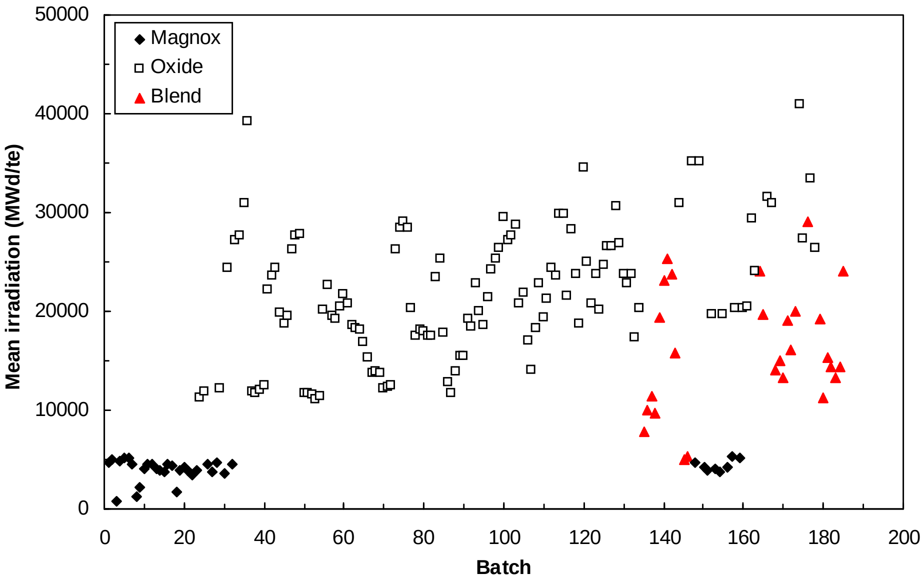

Figure 4. Burn-up history of fuel giving rise to liquors processed by HA Evaporator C

Corrosion accelerators: High corrosion rates identified from the evaporator heated components indicate the presence of powerful corrosion accelerators such as Np (VI) and Ce(IV) [4]. However none of these species is present in their highest oxidation state in the feed raffinate direct from reprocessing and it is known that corrosion rates in the downstream HASTS are very low. This indicates that the most potent corrosion accelerators must form under evaporator operational conditions.

- Neptunium. Corrosion tests with plant liquors containing Np have shown it to be a potent corrosion accelerator and is considered to contribute to the high liquor corrosivities evident from the Evaporator inspections. In oxide fuel raffinates, the concentration increases with burn-up and can be at levels of 2.3 g/l.
- Cerium. When present as Ce(IV), is considered to be the most potent corrosion accelerator in the HA evaporator with typical concentrations of up to 9 g/l in oxide fuels.
- Iron. Both from fuel assembly dissolution and plant corrosion was considered to be a strong corrosion accelerator but is now known to be a weak corrosion accelerator in the HA evaporator operational environment. Concentrations can reach 20 g/l.

Temperature: The external temperature of the steam heated components are significantly greater than the bulk temperature and will increase with depth within the liquor and with increased thinning of the coil wall due to operational corrosion. Accurate prediction of component surface temperature when heated by steam is achieved through extensive laboratory experimentation and mathematical modelling, discussed below. The lower regions of under-liquor coil surfaces and the base have been predicted to be at ~ 90^{o}C and ~ 96^{o}C respectively. Thickness surveys of the temperature measurement tubes have demonstrated that the non-heated surface corrosion rate within the bulk liquor is low and essentially uniform throughout the depth of liquor.

Stainless steel corrosion variability: Each cast and batch of the 18/13/Nb stainless steel would have a different corrosion rate in similar evaporator conditions, varying by up to ± 20% on the basis of other evidence.

Component original thickness: The original coil thickness can vary circumferentially by ± 5% during manufacture. This in turn affects the remanent life of the steam heated components.

The number of variables affecting corrosivity create significant uncertainty in the potential to predict corrosion rates for the steam heated stainless steel components throughout the HA evaporator system. The combination of the changing acidity, metal ion nitrate concentrations, potential corrosive ion valence state change, effects of radiation, and the effect of corrosion accelerators on other potential accelerators cannot, at present, be confidently replicated or simulated in laboratory conditions. Thickness loss data through the depth of liquor and for many different HA raffinate feeds would provide the base line information to develop thermal and corrosion models to predict losses at locations that have not been inspected. These predictions were validated by comparison with measured thickness loss along certain coils that were not used in derivation of the predictive models. It was therefore essential to develop remote inspection equipment that would provide such data.

5. Inspection systems development

The potential life limiting components of the HA evaporators at Sellafield are the surfaces that contact the product liquor at elevated temperatures i.e. the steam heated surfaces of the coils within the evaporator vessel and the vessel base and wall surrounded by the steam jacket. A comprehensive programme of work was instigated to develop invasive methods to quantify the corrosion of these key components. In 2003 NNL (in partnership with SLC) led an inspection vehicle development programme, using a combination of in-house, national and international expertise. By 2006 the first generation of coil inspection vehicles was used to inspect HA evaporator coils. The success of this inspection vehicle development has led to further challenges resulting in an extended programme of development to include new areas of inspection, such as the evaporator wall and base.

The fundamental understanding of the corrosion mechanisms occurring on the process liquor side of the 18/13/Nb stabilised stainless steel was explored to ensure the vehicle development program would provide the required degradation information. Mechanistic corrosion knowledge had been built up over many years through examination and condition assessments of similar corroded components across the Sellafield processing plants. From this it is considered that general intergranular corrosion would be occurring in the conditions found within the HA evaporators and would have resulted in a surface containing attack penetrating a short distance ahead of the surface, which continuously strips away as grains fall out [5]. Additionally, this stainless steel can be susceptible to localised corrosion, endgrain[5], in exposed surfaces, where the parent material has corroded faster than the rest of the pipe, such as adjacent to welds. The corrosion locations, surface topography and grade of stainless steel, were considered together with the access constraints to identify a tool package that could be deployed and retrieved safely from the coil pipework. The specific locations within the coil pipework where data was needed were coil forgings, splash zone/liquor level regions, all submerge coil regions, and HAZ regions of the pipework.
However, it should also be noted that the steam heating components are crucial to the long term operations of the HA evaporators. Any inspection system that was to be deployed into

---

[5] Endgrain corrosion: Localised tunnels with widths of many grain diameters aligned longitudinally through plate and pipe [6]. Can be many millimetres in length.

these components had to demonstrate low risk to retrieval and to damaging plant. The loss of one coil heating component significantly reduces the operational flexibility and remnant life of this critical plant.

The following outlines the methodology used to develop a suit of inspection vehicles that demonstrate reliable functionality, robust construction, and the ability to be retrieved from any location within the heating components.

5.1 Inspection constraints and requirements

The main consideration from the plant owners was that any heating component was not lost to operations due to the inability to retrieve an inspection vehicle and that no damage would occur from the deployment of the inspection vehicle. This was a significant challenge since the heated components of the HA evaporators were not designed for invasive inspections. Therefore the inspection system had to demonstrate the capacity for very low risk to retrieval and damage through continued routine deployments. The inspection tool package operations had also to meet these requirements.

Two types of inspection vehicle were developed, one for the coils for all HA evaporators and the other for the base of the HA evaporator C.

The generic plant owner specification included the following main features:

- Inspection system that can be demonstrated to be very low risk to retrieval and not damage plant components
- Robust design, able to withstand an applied retrieval load of 1 te without plastic deformation.
- High quality assembly procedure
- All materials tolerant to evaporator conditions and of zero halide content.
- Inspection vehicle to be resistant to plant conditions for up to 40 hrs total and 12 hrs for one continuous inspection.
- Inspection vehicle designs and testing passed through the rigorous Sellafield Ltd design review process.
- Deployment system would be manual. Motorised systems were not preferred due to minimal feed back on the deployment/retrieval characteristics during an inspection i.e. perceived higher risk than manual deployment.

The general conditions within the HA evaporators would be:

- Radiation levels estimated up to 1000 Gy/h gamma.
- Temperature <60°C
- Heating components filled with water up to a depth of 5 m.

The HA evaporator steam heated coil pipework inspection routes were interrogated for each coil in each evaporator. Figure 3 provides a 3D model view of some HA evaporator C pipework inspection routes from out-cell to bottom of HA evaporator coils. The many coil inspection routes contained:

- Variable pipe sizes. The pipe sizes were not standard due to the increased wall thickness requirements within the steam heated coil pipework. This resulted in an internal bore variation from 82-90 mm (90 mm within the helical coil). The potential weld penetration was additional to this with extremes of 3 mm at two circumferential locations allowable.
- The bend radius of the in-cell general pipework was as low as x3 Outer Diameter (OD). However some in-cell pipework routes contained elbows with x1.5 OD radius (133 mm).
- Inspection route pipework lengths were as long as 39.5 m.

A full height degradation survey for the HA evaporator C base was only available through one access route. This was into the steam jacket via the 80 mm Nominal Bore cooling water outlet line. The consequence of an inspection vehicle not being retrieved from the jacket would be total lose of the operational jacket and serious limitations to any future operations of the evaporator. This inspection route is more onerous than that for the coils due to the access geometry into the jacket. This is via an x1.5 OD elbow and then over a knife edge and into a vertical jacket interspace. The jacket interspace opposite the access nozzle is 124 ± 10 mm by design. This interspace changes width down through the jacket with a minimum width of 83 mm at the bottom. A schematic representation of the access route is shown in Figure 5. The main development challenge, therefore, was to create an inspection system that would be sufficiently small and flexible to negotiate the access route with very low risk to retrieval and still provide the quantification of degradation required

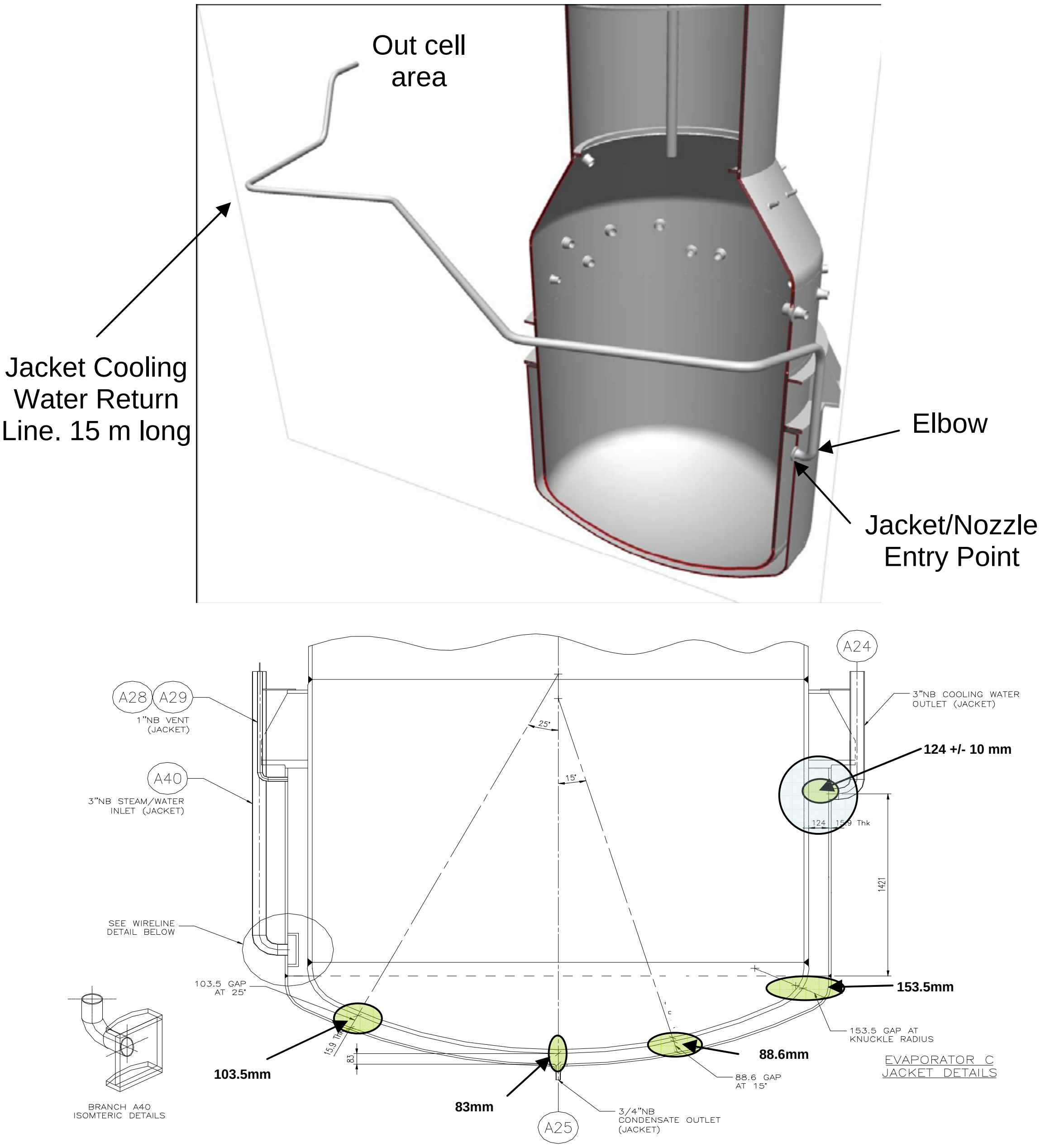

Figure 5. HA evaporator C base inspection access route

5.2 Inspection vehicle development

Due to the non magnetic nature of the austenitic 18/13/Nb stainless steel and the expected far wall corrosion morphology, an ultrasonic thickness measurement technique was the preferred NDT method to provide the data required to determine the corrosion rates from the operational conditions of the evaporator and support the predicted remnant life assessment. The design of the inspection vehicles used 3D CAD modelling to be assured that each vehicle section would easily deploy through the most restrictive section of the inspection access route. A modular approach to vehicle design was applied. The outer diameter of each module was <70 mm. Flexibility between modules was facilitated by the use of captive stainless steel springs which also protected the signal cables. Components that contacted the coil inner stainless steel surface were of a low friction coefficient and were malleable to eliminate any potential damage through scratching. Also these inspection vehicles were designed and manufactured to be partially dissolvable to aid recovery from fault conditions.

Full scale rigs were an essential aid to inspection vehicle development and to demonstrate low risk of retrieval to plant owners, see Figure 6.

Figure 6. Full scale inactive mock-up rigs of HA Evaporator C steam heating coil and vessel base at NNL Laboratory, UK.

Using as built drawing and the output from the routine statutory in-cell remote CCTV inspections it was possible to identify key pipework bends that were tighter than originally specified. These tighter bends were replicated and added to the full scale rigs. Replication of internal features within the inspection access pipework was critical to the development of low risk inspection vehicles. At each weld location the potential penetration on plant was replicated in the rig by introducing a very onerous 4 mm concentric (total 8 mm reduction in bore) flat faced insert resulting in a minimum bore of 74 mm within the in-cell section of the inspection routes. The bore changes due to reducers and forging thickness were also replicated. The addition of rippling due to pipe bending on the inner bore surface of the inner coils was added to ensure the inspection vehicle would easily deploy over such features, if present in a coil. The combination of all these features contributed to the test rig being considered to be a worst case deployment/retrieval route and any inspection vehicle that can readily be deployed and retrieved through this rig would be considered to be a low risk to plant components.

5.2.1 HA evaporator coil inspection vehicle

The coil inspection vehicle had the requirement for a forward CCTV system to ensure any obstructions to safe deployment could be assessed and evaluated prior to deployment. This was required to be resistant or tolerant to the high ambient gamma radiation levels present within the HA evaporator. The first generation of the coil inspection devices employed a shortened radiation resistant tube camera. The later devices employed a radiation tolerant CCD system that could be easily replaced at the inspection face and reduced the overall costs of the device. The agreed thickness measurement package was an array of x8 uniformly spaced circumferential arranged ultrasonic transducers (5MHz, 0° incident, compression). These were held in a carousel that in turn was held in a central location within a coil by adjacent spring-loaded units. The calibration of the thickness measurement system used an NDT test block manufactured from 18/13Nb stainless steel. During the early coil inspections the thickness was measured at defined locations. Latterly the encoded “A” scan response was captured and interrogated off-line with thicknesses measured every 2 mm along the coil. An example of the thickness data obtained from one inspection using this system is shown in Figure 7. Early in the vehicle development an inclinometer was added to relate thickness measured to circumferential location within the pipe.

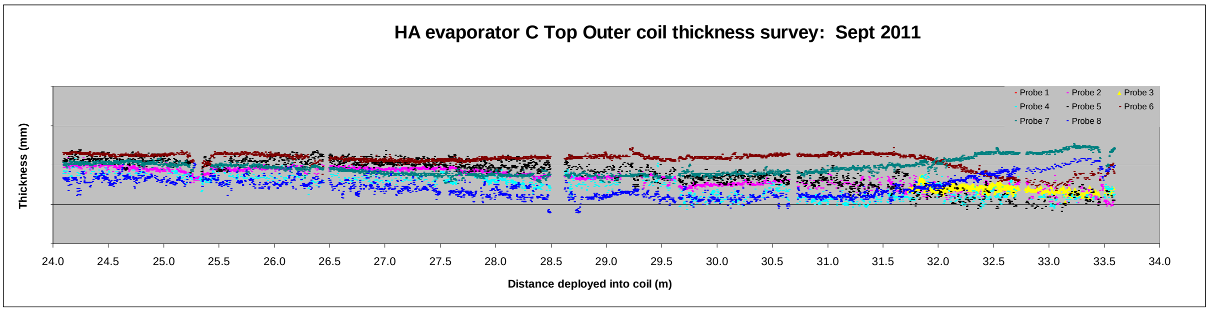

Figure 7. Thickness profile of the lower 10 m of HA evaporator C top outer steam heating coil (as a function of deployed length)

The inspection vehicle head was attached to a NNL designed umbilical that was critical to the smooth and easy deployment and retrieval of the inspection vehicle through the HA evaporator coils. The maximum load required to remove the vehicle from the furthest deployment point at 39 m within the full scale rig while full of water was <25 kg, including retrieval round elbows within the mock-up in-cell pipework route. The latter load requirement was mainly due to the weight of the inspection vehicle and displacement of water. A close-up and schematic of the inspection vehicle can be seen in Figure 8. To date more than x30 inspections have been performed on the steam heated coils within the HA evaporator suit at Sellafield and have provided the invaluable chronology of thickness change data from which corrosion rates with depth has been generated.

Figure 8. Variation in the HA evaporator steam coil inspection vehicle

5.2.2 HA evaporator base inspection vehicle

The requirements for the evaporator base inspection vehicle are very similar to that of the coil inspection device. Figure 9 provides a schematic representation of the access route into the steam jacket. The route is more onerous that the coil inspection route due to the elbow to nozzle and knife edge drop into the jacket interspace. The weld between the elbow and nozzle is a critical feature with respect to deployment and retrieval of the base inspection vehicle through this region. From specification the inner bore of the elbow is smaller than that of the nozzle. The simulation of weld penetration was required to be the same as for the coil inspection route. Therefore this weld insert has a 4 mm step on deployment through the nozzle and a 6 mm step on retrieval, a very challenging obstacle.

The shape and size of the inspection tool was a balance between the functionality required to perform the vessel base survey and the ability to demonstrate reliable retrieval from the steam jacket. The scheme design of the vehicle defined the outer surface envelope of the tool and the connection to the umbilical. A dummy system was created for deployment trails to confirm the minimum interspace gap that permitted reliable retrieval from the jacket. This was shown to be 90 mm. This was ~25% less than the design specified gap and therefore considered to be beyond the potential as-built variation in this gap.

The specification for the HA evaporator C base inspection required a line of evaporator wall thickness data from the access location into the jacket interspace, down the vertical section of the wall and round the bottom head to the lowest location of the vessel.

The inspection tool contained a front facing CCTV system to ensure any obstructions to safe deployment could be assessed and evaluated prior to deployment over the feature. The CCTV system comprised a radiation tested C-mos camera with led illumination, the latter housed in a bespoke waterproof chamber. The inspection tool was designed so that no component could protrude out of the outer surface envelope thereby assuring retrieval characteristics of the inspection tool were maintained during an inspection. A water coupled ultrasonic thickness measurement system using a 5MHz, 0° incident, compression transducer was designed to provide the thickness survey. Since the orientation of the inspection tool could not be predetermined after the deployment into the steam jacket, articulation of the transducer was required. The inspection tool permitted the transducer to be rotated circumferentially 360° and tilted ± 40° longitudinally. This articulation has been shown by calculation and trials on the full scale rig to be more than sufficient to provide the required perpendicular alignment of the transducer to the outer surface of the evaporator base to affect the thickness measurement at any location within the jacket. Figure 9 provides a visual appreciation of the required articulation.

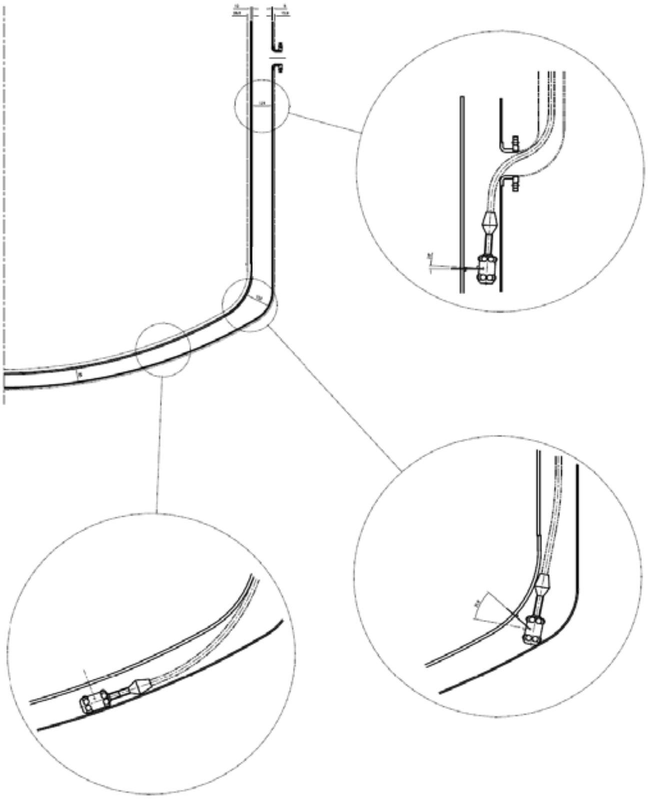

Figure 9. Schematic representation of transducer articulation requirement within the HA evaporator C steam jacket.

This inspection vehicle has been manufactured and successfully trialled, with respect to deployment/retrieval and functionality, in the full scale rig of HA evaporator C. Figure 10 shows the base inspection vehicle head. The data from the regular HA evaporator coil inspections have been used to demonstrate, with sufficient confidence, that the coils are the HA evaporator C life limiting components. Hence, the HA evaporator base inspection on the active plant has not yet been required.

Figure 10. HA evaporator C base inspection vehicle tool package

Recent CCTV inspections of HA evaporator C base inspection access route, using other NNL bespoke inspection systems, have proven the full scale rig to be the more onerous deployment route, thereby providing confidence that the deployment of the base device would be of low risk to plant.

Current inspection vehicle developments are concentrated on the application of phased arrays to improve the resolution of the corrosion profile adjacent to welds in coils. Inspection vehicles containing these are likely to be deployed within evaporator coils in 2013.

6. Use of Coil thickness data to predict HA evaporator remnant life

The successful series of coil inspections since 2006 have provided data on the change in thickness with each operational condition between inspections. This opened the possibility of estimating future coil thinning and that of HA evaporator wall and base, as-yet uninspected components, by extrapolation of the measured data and thereby circumventing the need to risk an invasive inspection into the steam jacket. These thickness data obtained from the inspections also provides the ability to validate the experimental estimates of corrosion rates based on data from corrosion test obtained using simulants.

The coil inspections showed clearly that corrosion losses increased with submerged depth. The only credible cause of this is depth-dependent temperature, with exposure time being the same over the entire length of a given coil. For stainless steel corroding in nitric acid, the functional relationship between the corrosion rate and temperature is well understood; in all cases Arrhenius behaviour is observed [6] i.e.

$$\text{corrosion rate} = Ae^{-E/RT} \quad = \exp\left(\ln A - \frac{E}{RT}\right) \tag{1}$$

where A is a constant (usually termed the pre-exponential factor), E is the activation energy of the rate-controlling step, R is the molar gas constant (8.314 J/mol/K) and T is the absolute temperature of the metal.

The corrosion rate at each measurement point can be determined from the thickness loss as shown in the expression below since:

$$\text{loss} = \text{corrosion rate x time} \tag{2}$$

Since the age and operational history of a given coil is known, the application of thermal models that correctly predict the temperature profile along the coil allows determination of the constants A and E in Equation (1). Non-linear models [7, 8] are required that take account of operations carried out on the different liquor types (i.e. Magnox, oxide or blends) since these have different corrosive and thermal properties (see below). The thermal models[6], which predict how the metal temperatures vary as walls thin due to corrosion, were generated and validated using data from a boiling rig that was developed to mimic HA evaporation processes and operated with a range of inactive simulants under evaporator operating conditions, see Figure 11. Following derivation of the corrosion rate expressions (i.e. Equation (1) derived for each of Magnox, oxide and blended liquors), the application of temperature models for the base allowed prediction of losses to that component [9, 10].

---

[6] Thermal data are available for Magnox liquors in HA Evaporators A and B, and for both oxide and Magnox liquors in HA Evaporator C. For each liquor type, data are available for simulant liquors representative of conditions at six stages throughout a batch. Eighteen temperature models consequently result.

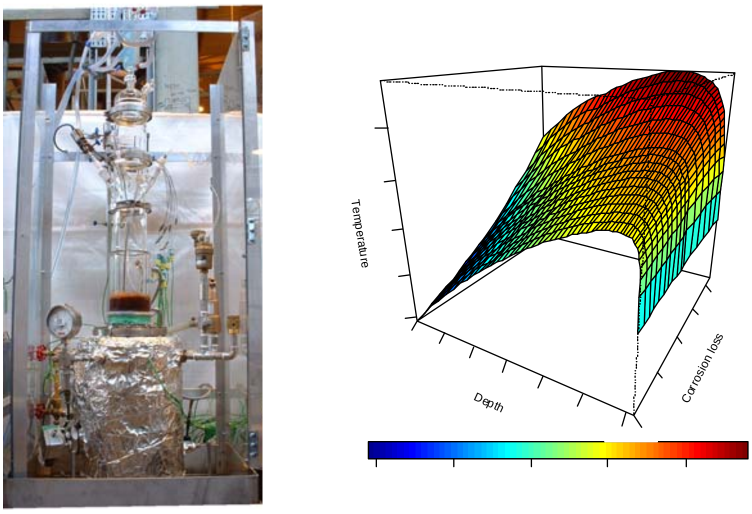

Figure 11. HA Evaporator C base boiling rig and plot of predicted temperatures for oxide liquor.

There are, however, a number of factors which considerably complicate the above process:

- HA Evaporator C has processed singular batches of Magnox, oxide and percentage blend combinations of both, all of which have different corrosivities owing to their different compositions.
- The thermal models depend on the liquor type and the batch stage.
- The heating components have different wall thicknesses and hence, require different thermal models. In addition, the surface temperature increases as the wall thickness at a given point decreases due to corrosion [9, 10].
- The steam supply pipework to each heating component promotes varying pressure drops, leading to a unique temperature model for each component.
- Thickening of the condensate layer underneath the vessel base reduces the heat flux through the metal at this point and hence the temperature of the metal in contact with the process liquor.
- All coils are never used simultaneously, hence individual coils experience varying times when they are not energised but are exposed to hot liquor. This is considered to promote low, but not insignificant, corrosion losses.

Significant development of Equation 1 has occurred to reflect the above factors and solving the equation simultaneously for all inspected coils has generated the constants A and E for all liquor types. This permits the thickness loss to be predicted for any future operations of the evaporator.

The five principal stages in the computational process, using the data provided by plant inspections/experimental and modelling as discussed above, to predict the thickness of HA evaporator C base along with confidence ranges are outlined below:

- ***data input.*** Supplied as a series of Excel spreadsheets, covering the thermal model predictions, the inspection data and the operating time data.
- ***corrosion rate determination.*** Initially the measurement locations with respect to depth at the surface of the pipe are defined. Thickness loss is calculated from the estimated original thickness. Given the assigned depth, the surface temperature of the metal component is predicted for each fuel type in the batch. Operating and non-operating times are assigned. Blended liquors are assumed to corrode at a rate equal

to a weighted average of the equivalent Magnox and Oxide rates at the weighted average of the temperatures for each fuel at the appropriate depth and corrosion loss. Corrosion rates are estimated from previously discussed equations. The inspection data indicates that there are differences in the corrosion behaviour of different sections of pipe, due potentially to varying initial thickness, corrosion resistance variation, bending effects and flow regimes. Hence a statistical model using a mixed-effects model is used to describe this variation. Re-sampling using a bootstrap method is used to evaluate corrosion rate parameter uncertainty.

- ***corrosion rate application.*** The inclusion of the predicted jacket condensate layer in the temperature models means that the deepest point of the base, at the centre of the HA Evaporator, is no longer the worst case. The Monte Carlo simulation predicts the likely range of thickness of components at a range of depths. In addition to the parameter uncertainty described above, uncertainty in initial base plate thickness, batch to batch variability of the corrosion resistance of the steel, corrosion associated with welds, through thickness corrosion resistance variations and possible effects of solids are also taken into account.
- ***remanent life calculation.*** Minimum acceptable working thicknesses have been derived for the coils and the base, using structural analyses to establish the feasible failure modes, see Figure 12, and appropriate design codes to give an acceptable margin of safety. Future operational conditions assume that the three separate fuel types continue to be processed. Current thickness for the three top coils is taken as the minimum thickness found by inspection. The distribution of predictions provided by the Monte Carlo simulations is used for the base thickness.
- ***model validation.*** In order to test the model predictions and judge their suitability the predicted thickness of two of the bottom coils in HA Evaporator C was compared with the actual inspection findings. Using the mixed effect model it was found that a good match could be obtained if the mean random effects obtained from the bottom outer coil segments were used to take account of an apparently depth–related bias considered likely to originate from the toroidal liquor circulation pattern deduced to exist in the HA Evaporators; the close proximity of the bottom outer coil to the base suggesting that these heating components are likely to experience similar thermal and flow conditions.

Other mechanisms of failure such as fatigue are also being considered in the structural modelling work programme and these involve identification of the high stress locations, the latter dependent on notch sensitivity of the heating component surface topography.

Figure 12. HA Evaporator C structural model and examples of stress concentration locations.

7. Summary

This multi-discipline team and extended work programme has provided the baseline data and methodology to confidently predict thickness loss throughout the heating components of the HA evaporator for future operational programmes. This has shown that the life limiting components of the HA evaporator are the steam heated coils and not the base. There is no longer a strong requirement to deploy an inspection vehicle into the steam jacket thereby removing the risk to the plant operability in the scenario where such a vehicle cannot be retrieved. This work has also generated additional benefits, with significant improvements identified to the evaporator operations to reduce corrosion, such as acidity reduction and blending of batches. Coil heating/cooling management has reduced the stress loadings during batch shutdown and improved the fatigue life of the coils.

Future work is concentrating on the development of inspection vehicles to resolve the degradation that may be occurring in localised regions of coils, and using the boiling rigs to improve the understanding of temperature variations due to fluid flow within the HA evaporators. Also the corrosivity of future new feed liquor is being addressed by corrosion simulant development studies.

A continual peer review process is applied to this remanent thickness prediction methodology using UK experts in their field.

This work has demonstrated that HA evaporator C has a finite operational life that should be able to service reprocessing operational requirements until the HA evaporator D (currently under construction) is completed and commissioned. Input into the design of the new HA evaporator D has ensured inspection access is less onerous.

8. References

[1] Whillock G O H 2010 Corrosion in Radiolysis Induced Environments. In: Richardson J A et al. (eds.) Shreir's Corrosion, volume 2, pp. 1330-1339, Amsterdam: Elsevier.

[2] R D Shaw and D Elliott: "Stainless steels in UK nuclear fuel reprocessing plants", Proc. conf. Stainless Steel '84, Gothenburg, pp 395-402.

[3] A262-Practice C; Standard Practice for Detecting Susceptibility to Intergranular Attack in Austenitic Stainless Steels. In *Annual Book of ASTM Standards*; ASTM International: West Conshohocken, PA, 1985; pp 7-10.

[4] McIntosh, A. B.; Evans, T. E. In *Peaceful Uses of Atomic Energy*, Proceedings of the 2nd International Conference, Geneva, Switzerland, September, 1958; pp 206-225; UN: Geneva, Switzerland, 1958.

[5] B F Dunnett and G O H Whillock: "Intergranular corrosion of stainless steels: A method to determine the long-term corrosion rate of plate surfaces from short-term coupon tests", Corrosion, 59, 274 - 283 (2003).

[6] Whillock G O H and Worthington S E 2010 Corrosion in Nitric Acid. In: Richardson J A et al. (eds.) Shreir's Corrosion, volume 2, pp. 1250-1269, Amsterdam: Elsevier.

[7] Pinheiro, J. C. and D. M. Bates (2000). Mixed-effects models in S and S-plus. New York, Springer Science + Business media.

[8] Vonesh, E. F. and V. M. Chinchilli (1997). Linear and nonlinear models for the analysis of repeated measurements. New York, Marcel Dekker/CRC Press.

[9] Boiling Heat Transfer in Highly Active Liquors. Paper 076 11th UK Heat Transfer Conference 6-8 September, 2009. Queen Mary College, University of London, W R Geddes, B Perry, M J Wakem and C L Wylie.

[10] Heat transfer in a Highly Active Evaporator. Paper 077 11th UK Heat Transfer Conference 6-8 September, 2009. Queen Mary College, University of London, M J Wakem, C L Wylie, J Spencer, T S Graham, G Whillock, and T Ward.

MULTIPLE RECYCLING OF MOX IN LWRS

E. BOUVIER, T. GAIN, G.H. SENENTZ, F. LELIEVRE, F. BAILLY
AREVA Recycling Business Unit
1 place J. Millier, 92084 Paris la Défense, France.

P. MURRAY
AREVA Federal Services LLC
7207 IBM Drive, Charlotte, NC 28262, US

ABSTRACT:

Plutonium from used MOX fuel still contains a significant quantity of fissile materials. This plutonium could hence be used to produce more energy and further decrease the total Pu inventory.

This opportunity has already been investigated by AREVA through the reprocessing of several used MOX fuels in the La Hague plant and the subsequent manufacturing of new MOX fuels in the MELOX plant. AREVA has hence gained experience in the recycling of used MOX fuel and is now able to define different strategies to better manage the Pu isotopy of one used fuel inventory and foster the recyclability of the Pu present in MOX fuels through a multiple recycling of this fuel in LWRs. This Pu management offers interesting solutions to deal with current Pu inventory (whether in used fuel or in an oxide powder form). It also leads to new opportunities to ease used fuel management in interim storage and nuclear waste management in disposals.

1. Context

Due to its low fissile content after irradiation, Pu from used MOX fuel is considered by some as not recyclable in LWR. The point of this paper is hence to go back to those statements and provide a new analysis based on AREVA extended experience in the fields of fissile and fertile material management and optimized waste management. This is done using the current US fuel inventory as a case study.

2. Current fuel cycles

Used fuel management scheme practiced in the US is done through a direct disposal of used fuel in a final geological disposal.

In the US-context, given the size of the LWR park and the history of storing used fuels next to reactors due to absence of any recycling policy, volumes and masses of used fuel are important (US inventory at the end of 2009 represents 64,000 tons of UO_2 used fuels).

Apart from the important interim storage capacity needed in such a scenario, several issues need to be addressed carefully:

- The applicability of safeguards over very long time horizons with an improving Pu-vector in disposal which becomes significantly less self-protected over time
- The Pu toxicity in the storage.

- The disposal footprint of a direct disposal option compared to a recycling options
- The loss of valuable uranium and plutonium resources.

Recycling U and Pu contained in used UO_2 fuels in LWR through ERU and MOX fuels as implemented by AREVA adresses most of those issues. In addition, the recycling of used UO_2 fuels in LWR brings a significant reduction of used fuels to be stored.

Assuming a comparable U/Pu-recycling strategy in the US as applied in France, the 64,000 tons of US inventory could be reprocessed to recycle its Pu into fresh MOX fuel. This strategy leads to a significant reduction of the used spent fuel while producing MOX fuels and vitrified waste. An often perceived impediment for such a strategy refers to the future management of the used MOX fuels. In fact, two typical options are most often proposed in order to deal with used MOX fuel: either the storage of MOX used fuels in a final disposal or what is refered as the reference scenario in terms of resource management, a recycling of Pu from MOX fuels in SFRs.

This paper will focus on another option for extended Pu-management by further recycling Pu from MOX into LWRs through a MOX multi-recycling in LWRs. In order to assess the outcome of this new strategy, two types of scenarios will be compared:

- Two MOX multirecycling scenarios where US inventory in 2009 is entirely reprocessed and Pu is recycled in LWRs MOX. When the entire initial inventory is reprocessed, both scenarios are arbitrarily ended. This arbitrary choice leads to a fairly good view of what would be a continuous scenario while avoiding to make assumptions on the future of the US power plant fleet and its resulting used fuel. At the end of those scenarios, some used MOX fuels are waiting to be reprocessed.
    - Scenario A illustrates a situation when used fuels are no longer reprocessed. As a consequence, resulting disposal will consist of the vitrified and compacted waste as well as all the non-reprocessed used MOX.
    - In scenario B, remaining used MOX fuel is reprocessed and its Pu is recycled in LWRs or SFRs.
- An open cycle scenario that will serve as a reference scenario for comparison purposes. The open cycle strategy considers US inventory of used fuel in 2009 with an additional number of UO_2 assemblies equals to the number of MOX assemblies produced in the MOX multirecycling scenarios. A burnup similar to the MOX produced in scenario A and B is taken for UO_2 assemblies.

3. Main challenges for Multirecycling

Several challenges are to be looked at in order to multirecycle MOX in LWRs. The main challenges stem from the degradation of the Pu fissile content. And since the point is also to propose a scenario that is compatible with existing technologies and facilities, a second challenge is to mitigate the doses and thermal decay heat of the recylcled Pu.
Given those two challenges, ^{238}Pu management appears of prime interest. ^{238}Pu is a neutron absorber and is also responsible for most of the decay heat of the Pu powder and most of neutron doses in a MOX fabrication unit.

LWR MOX Multirecycling scheme aims at addressing these challenges by a comprehensive look at the main mechanisms behind ^{238}Pu production in LWRs.

4. Main mechanisms behind MOX Multirecycling in LWRs

First let's analyze the actinides chain in the reactor, and particularly the mechanisms of ^{238}Pu production in a LWR fuel.

We consider a Plutonium that comes from a UO_2 used fuel with a 7-year cooling time before reprocessing and a 45GWd/t burnup. This Pu is characterized by a high amount of ^{241}Pu (half life of 14 years). If used in a MOX fuel (with standard depleted uranium medium), this Pu isotopy will evolve as follows after an irradiation of 45GWd/t:

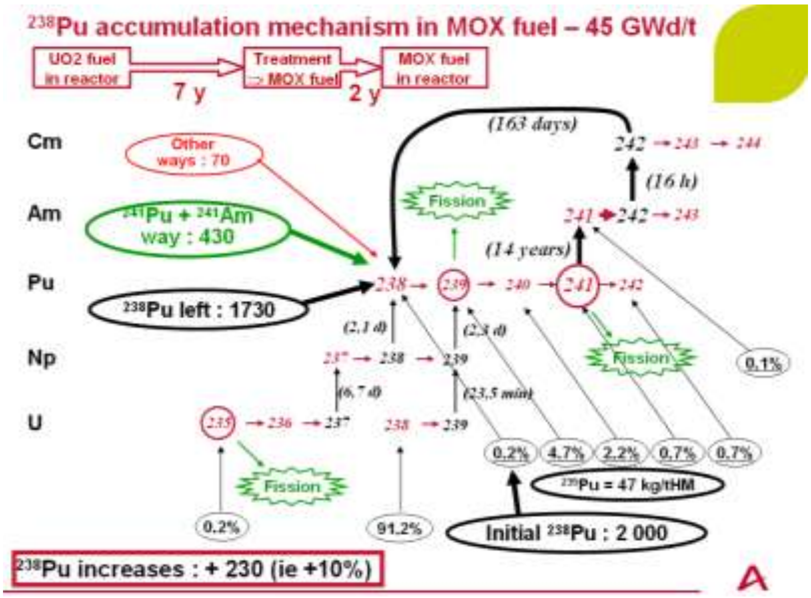

Fig 1: ^{238}Pu accumulation mechanism in MOX Fuel [7yr cooling time for UO_2 fuel]

One can observe that after a 45GWd/t irradiation most of the initial ^{238}Pu remains and more ^{238}Pu is produced from ^{241}Pu and ^{241}Am. Reducing ^{241}Pu and ^{241}Am initial content in fresh MOX fuel would hence reduce the final inventory of ^{238}Pu.

The average cooling time of US inventory is large enough to have a low ^{241}Pu content thanks to its radioactive decay (half life 14years) into ^{241}Am. ^{241}Am initial content is driven by the duration between reprocessing and MOX fabrication. ^{241}Am is indeed cleaned out from Pu at reprocessing while ^{241}Pu fuels back the ^{241}Am through decay after the reprocessing step. ^{241}Am content can therefore be limited via supply chain optimization by minimizing the time between reprocessing and MOX manufacturing.

The scheme below, representative of the US inventory situation, shows the MOX fuel isotopy evolution with an initial Pu isotopy coming from used UOX with 28-year cooling time before reprocessing.

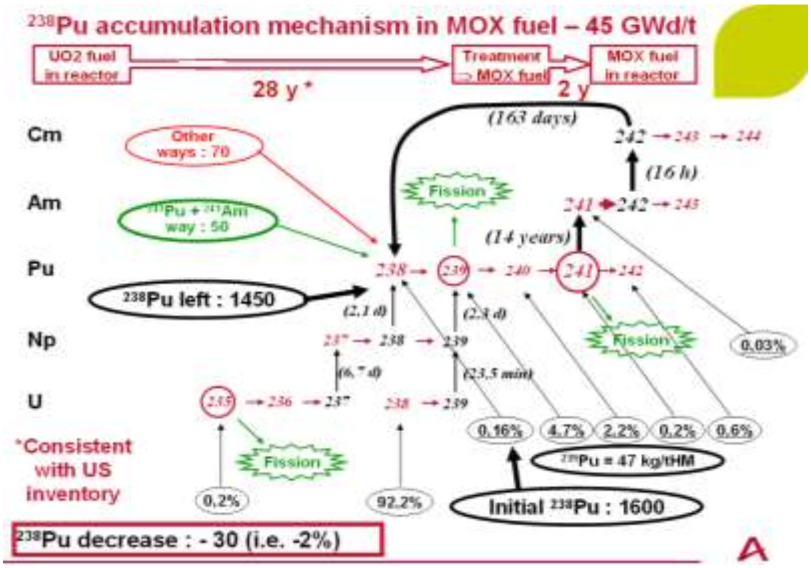

Fig 2: ^{238}Pu accumulation mechanism in MOX Fuel [28yr cooling time for UO_2 fuel]

The main contributor to the final ^{238}Pu is still the initial ^{238}Pu but this time the initial ^{238}Pu is lower than in the previous case (28yr cooling time compared to a 88yr half life) and the ^{241}Pu contribution has strongly decreased. It results a final mass of ^{238}Pu slightly below its initial level and significantly lower than the ^{238}Pu content observed in used MOX fuel from the previous case. This statement illustrates an opportunity for country that have not taken the way towards a strategy that recycles fresh used fuel in order to avoid the build-up of ^{241}Am and keep this Pu for SFRs. Old inventory of used fuels offers indeed a set of fuels that can limit ^{238}Pu build-up and improve the recyclability of the Pu used in a MOX fuel. Based on this statement, the following paper illustrates a MOX-multirecycling scheme applied to US fuel inventory.

5. LWR MOX-Multirecycling applied to a US context

5.1. Scenarios description

The study was carried out on 64,000 tons of UO_2 fuel representing the US inventory at the end of 2009. All this inventory is recycled in a PWR at a burnup of 45GWd/t. For each MOX fuel, Pu content has been calculated to reach the same reactivity than a UO_2 fuel irradiated at 45GWd/t. MOX fuel medium is depleted uranium

The recycling of used UO_2 fuel from the initial inventory starts in 2030 and MOX manufacturing is arbitrary ended when no more used UO_2 fuel is available in the initial inventory. As mentioned before, this arbitrary end avoids a new set of assumptions on the future of the US power plant fleet. Hence used UO_2 fuel produced after 2009 is not taken into account in the study.

In addition to those assumptions, the LWR MOX multirecycling scenarios have been optimized along two main constraints: Pu content and ^{238}Pu content.

In the core, Pu content must be lower than 12.5%. This limit is due to the void effect simultaneously to a harder neutron flux in MOX reactor. An operational limit of 11.5% is used in MELOX plant and MOX multirecycling scenarios have been optimized in order to comply with this limit.

Furthermore to take into account ^{238}Pu impact on decay heat and radioprotection during MOX manufacturing, ^{238}Pu content has been kept below current operational limit in.MELOX.

The workflow of this study can be summed up as follows:

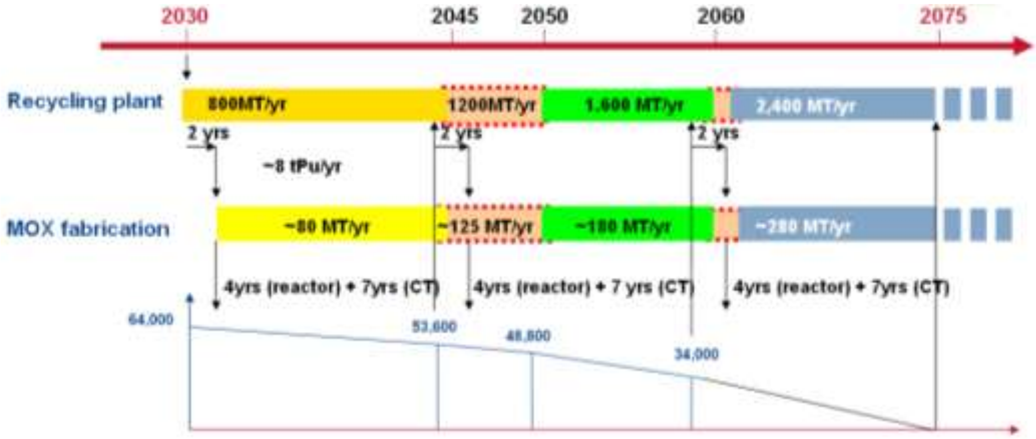

Fig 3: Scenario description : Reprocessing and MOX fabrication capacities with time

Reprocessing capacities go progressively from 800Mt/yr up to 2,400Mt/yr through the addition of 800t/yr recycling plant modules in 2045 and 2060. MOX fuel fabrication capacities increase accordingly. The duration of a MOX fuel cycle is about 14 years: 4 to 5 years in reactor, 7 years minimum of cooling time and 2 years for all recycling operations including Pu extraction, MOX manufacturing and introduction in the core.

All along the scenario, calculations were made to assess the vitrified high level waste and compacted metallic waste inventory that resulted from the reprocessing of used fuels.

5.2. Results

Under these assumptions and after the reprocessing of the entire initial inventory of 64,000 tons, 7,000 tons of MOX fuels were manufactured among which 2,800 tons were recycled. Therefore 4,200 tons of used MOX fuels remain not treated when the optimization ends. As mentioned above, those 4,200 tons of remaining used MOX fuels will be considered in two different ways.

- In scenario A, the Pu contained in the remaining 4,200 tons of used MOX is chose not to be recycled anymore, Therefore the final disposal inventory of scenario A consists of the Vitrified and Compacted Universal Canisters produced while reprocessing the 64,000 t of used UO_2 and 2,800 tons of used MOX. The 4,200 tons of non reprocessed MOX is added to this inventory.
- In scenario B, contrary to scenario A, the 4,200 ton remaining used MOX is assumed to be reprocessed and its Pu is recycled either in LWR reactors or in SFR reactors. It comes that the final disposal inventory of scenario B consists of the vitrified and compacted universal canisters produced while reprocessing the 64,000t of UO_2 fuels as well as the 7000t of used MOX fuel.

Both scenarios A and B are compared to the UO_2 inventory that consists of the 64,000 tons of initial UO_2 fuels plus 7,000 tons UO_2 fuels equivalent to the MOX fuels irradiated during the multirecycling scenarios..

For each scenario, the total radioactive inventory has been assessed in order to calculate the evolution with time of different quantities. The Pu mass and heat load evolutions are described hereafter.

5.2.1. Pu mass results

Results can be first set out for the plutonium mass in the final disposal.

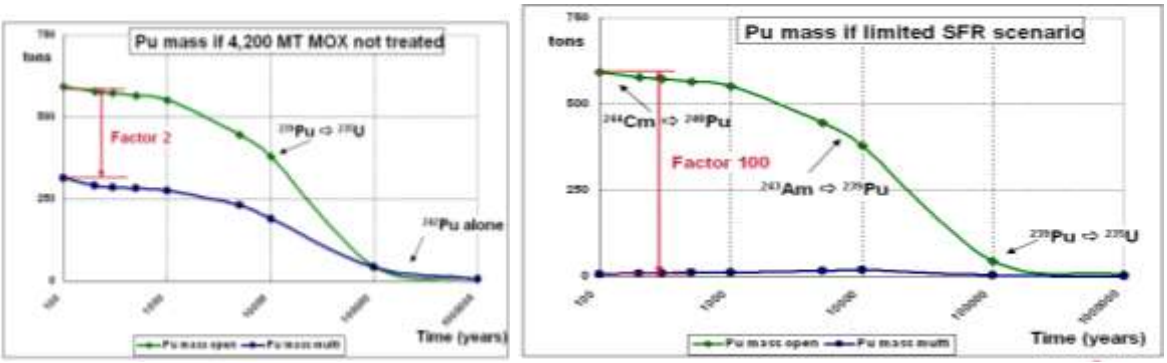

Fig 4: Pu mass evolution with time (Open cycle (green); Optimised scenario (blue))

For scenario A, we notice a reduction of a factor 2 of the total Pu mass after 100 years. Moreover we also notice a significant reduction of fissionable isotopes by a factor of 6. This effect comes from the reduction of fissionable Pu isotopes (^{239}Pu becomes ^{235}U with time). This fact is important in terms of criticality for the final disposal.

This very strong reduction of the total Pu mass allows for the definition of scenarios where a limited number of SFRs is enough to improve a lot fuel cycle management. A limited fleet of SFRs would indeed burn the Pu in excess, possibly feeding in return LWR with good Pu.

5.2.2. Heat load results

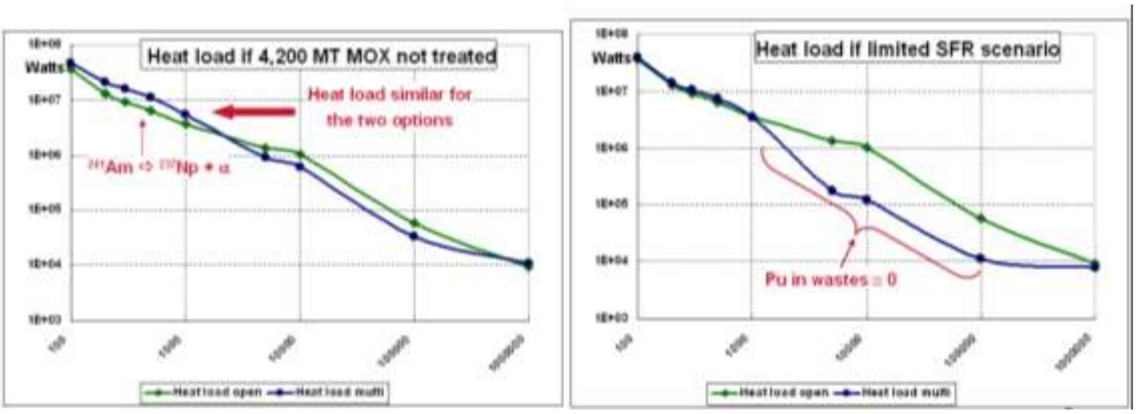

Fig 5: Pu mass evolution with time (Open cycle (green); Optimised scenario (blue))

In scenario A, the heat load is similar to the Open cycle, while in scenario B, one can observe a very similar initial level and a strong reduction after a thousand years. This outcome is explained by the fact that in scenario A, the ^{241}Am comes from the disintegration of ^{241}Pu in non-treated used MOX while in Scenario B, Pu (and hence ^{241}Pu) from non-treated used MOX is recycled and kept apart from the inventory put in final disposal.

6. MOX-Multirecycling in LWR, a solution that keeps all options opened

MOX Multirecycling in LWRs is a closed cycle scenario where U and Pu management through reprocessing and recycling leads to a significant reduction of the used assemblies to be stored. The recycling of Pu in MOX fuel is moreover a way to maintain the self-protection of the Pu-bearing assemblies. With this scenario, Pu content is also reduced repetitively via a multirecycling of MOX in LWRs. Simultaneously, ^{238}Pu content decreases.

All along this scenario, HLW vitrified canisters are produced and planned for deep geological disposal. Contrary to used fuel, HLW vitrified canisters do not contain proliferation materials. This waste management alleviates concerns about safeguard issue and Pu toxicity. Glass canister storage duration is hence not constrained by proliferation concerns (proliferation materials and access to them). If one adds the fact that the reprocessing of used fuel limits the space needed on current interim storage, it can be underlined that this overall strategy contributes to giving more time for a final disposal to be defined safely. And it achieves this while being neutral or having a significant positive impact on waste disposal (Pu mass, heat load constraints) when compared to an open cycle strategy.

At the end of this multirecycling scenario, several options are available for the 4,200 tons of used MOX fuels resulting from the recycling of 64,000 tons of UOX and part of the MOX produced.
- Either an end is put to recycling (scenario A), in such a case used MOX fuels go to the final disposal with a total decay heat and radioactivity similar to a once through scheme, while the volume is significantly reduced
- Or it is decided to continue using Pu from used MOX fuel in LWR reactors, or in a few SFR reactors while keeping a LWR fleet (Scenario B). If so we can imagine a symbiotic scenario linking LWR and SFR, which number would depend on economic performances. A LWR MOX fleet is set up to produce electricity and is able to recycle most of the plutonium it produces, while a few SFRs improve degraded Pu isotopy to allow its return into LWRs, thus using the full energy potential of the uranium resources without the need for a 100% FBR fleet.

With MOX-multirecycling in LWR, Pu isotopy needs to be managed carefully all along the scenario. The early introduction of a limited number of SFRs can therefore be a real asset for the overall system. A few SFRs would be enough to improve the Pu isotopy from used LWR MOX fuel and provide a Pu-isotopy that could be mixed back with multirecycled Pu from LWRs, hence increasing the Pu multi-recycling potential in LWRs.

MOX-Multirecycling in LWRs is hence a strategy that addresses waste management issues from material accessibility to Pu toxicity or disposal availability. At the same time, it offers flexibility for Pu management depending on the choice that could be made in the future on nuclear energy generation technology

Shadow Corrosion Resistant Core design:
Cofrentes core design modifications to minimize channel bowing

ANDRÉS GALICIA SAAVEDRA, Mª TERESA LÓPEZ CARBONELL,
Core Design of Cofrentes, Iberdrola Generación S.A.
Tomás Redondo, 1. 28033 MADRID

JOSÉ MANUEL DEY NAVARRO,
Core Design of Cofrentes, Iberdrola Ingeniería y Construcción SAU.
Tomás Redondo, 1. 28033 MADRID

JESÚS SAIZ DE OMEÑACA TIJERO.
Internship at Core Design of Cofrentes, Fundación Iberdrola S.A.
Tomás Redondo, 1. 28033 MADRID

ABSTRACT

Channel bowing has recently become important due to the numerous problems it has caused on BWR long cycles. This effect can cause friction between channels and control rods and it can even prevent them from entry to the core. [5]

One of the most influential factors which contribute to channel bowing is Shadow Corrosion. It has been demonstrated that it affects controlled cells which are loaded with fresh elements. [5]

To minimize shadow corrosion, a core design in which the number of fresh elements in controlled zones is reduced has been proposed and studied, in contrast to the normal strategy of fresh elements in grid layout. Therefore, most A2 sequence cells are not loaded with fresh elements and only A2 and B2 sequences are used in the cycle management.

In this paper the Shadow Corrosion Resistant Core Design (SCORE) alternative is described, the results are assessed and some important conclusions are presented, being impact on bowing channel and extracted energy the most relevant matters. –More energy can be obtained with this strategy, contrary to first possible thoughts.

SCORE was proved to be feasible for the twentieth cycle of Cofrentes Nuclear Power Plant (in Valencia, Spain) with a specific flow and control rod management during the cycle.

Overview:

In recent years, BWR assembly channels have suffered the effects of differential neutronic irradiation, being “Shadow Corrosion” one of the most important concerns. [5]

BWR assemblies are covered by a channel which avoids transversal flux in the core. The inside and outside faces of these channels are exposed to a different level of neutronic irradiation, thus an important deformation of these elements is expected to occur. This deformation consists on a considerable bowing which may even prevent control rods from entering in the core, among other related matters. [3]

Besides, when fresh assemblies are controlled, the channel oxidation is increased due to a electrical potential difference between the zirconium of channels and the steel present in control rods. As a result, the increase of oxide thickness produces a higher absorption of hydrogen in the channel side which lies juxtaposed to the control rod. Once the hydrogen solubility limit in zirconium is exceeded, it precipitates in form of hydride which causes a crystal structure distortion thus an increase of the channel outside face length. [3], [5]

Due to the fact that this effect is principally noticed when a control rod is inserted -as it is the moment in which neutronic irradiation is negligible on the outside face of the channel, which faces a control rod, and it has a maximum on the inside part, which faces the clads of the assembly; and because the hydrogen absorption rate is higher too,- it has given the name of: "Shadow Corrosion", giving the idea that control rod neutron-irradiation shadow is the responsible of the undesired consequences. [4], [5]

Shadow Corrosion is therefore mainly noticed in long fuel cycle BWR assemblies, which have to be re-canalized -i.e.: replace the assembly channels- and therefore being a time consuming task in which the reactor has to be stopped [5]. It has to be noticed that this kind of reactors utilize control rods more frequently than they do PWR, as there is not boron in the primary circuit and reactivity is mainly controlled with pressure of water and control rods. [3]

One of the possible procedures to reduce the so-called Shadow Corrosion in BWRs is to avoid the introduction of control rods next to fresh fuel assemblies -which are the ones which posses the highest activity and thus the ones in which differential neutronic irradiation on channels is more important. Therefore, aspects in loading the core have to be taken into account in order to avoid certain loading patterns which may induce fresh elements to be shadowed by control rods. This new core loading pattern has been called “SCORE”, short for “Shadow Corrosion Resistant Core Design”.

The present paper consist on the exposition of the study and its results, concerning the core loading of one fuel cycle at the Nuclear Power Plant of Cofrentes (Valencia, Spain). This study was made for Iberdrola Generación S.A.U. (owner of the Nuclear Power Plant of Cofrentes) under a professional training program in the company, along with employees of Iberdrola which supervised the performance of the work, elaborated different related tasks and shared their knowledge among other important parts of the study.

Details of the execution and results

Control rods of BWRs are classified under four sequences based on its position in the core, as shown in the figure 1. Sequences are called A1, A2, B1 and B2. This means that not all control rods are used at the same time along the fuel cycle of the plant, being the mos usual a fuel cycle being controlled by the A2 sequence at Beginning Of Cycle -which uses the central control rod- and subsequently, sequence changes are programmed at a certain level of fuel burnt -e.g.: each 2000 Mw·day/st- so as to avoid excessive control rod burnt. [4], [5]

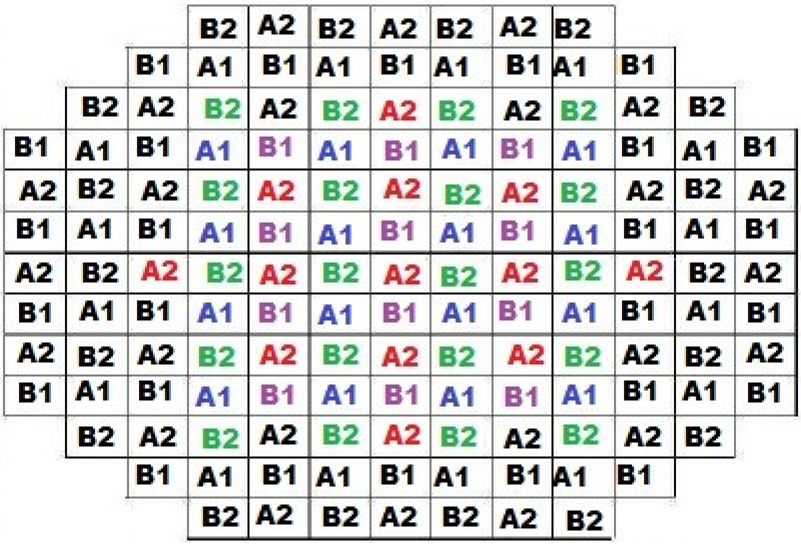

			B2	A2	B2	A2	B2	A2	B2			
		B1	A1	B1	A1	B1	A1	B1	A1	B1		
	B2	A2	B2	A2	B2	A2	B2	A2	B2	A2	B2	
B1	A1	B1	A1	B1	A1	B1	A1	B1	A1	B1	A1	B1
A2	B2	A2	B2	A2	B2	A2	B2	A2	B2	A2	B2	A2
B1	A1	B1	A1	B1	A1	B1	A1	B1	A1	B1	A1	B1
A2	B2	A2	B2	A2	B2	A2	B2	A2	B2	A2	B2	A2
B1	A1	B1	A1	B1	A1	B1	A1	B1	A1	B1	A1	B1
A2	B2	A2	B2	A2	B2	A2	B2	A2	B2	A2	B2	A2
B1	A1	B1	A1	B1	A1	B1	A1	B1	A1	B1	A1	B1
	B2	A2	B2	A2	B2	A2	B2	A2	B2	A2	B2	
		B1	A1	B1	A1	B1	A1	B1	A1	B1		
			B2	A2	B2	A2	B2	A2	B2			

Figure 1: Sequences of Cofrentes Control Rods. The coloured control rods correspond to the principal rods, whereas the black ones are barely used control rods -as being peripheral control rods. [4], [5]

In order to execute the SCORE strategy, not only the loading pattern has to be altered, but the control rod sequence and the overall reactor management too, in order to comply with the exigences of the CSN (Consejo de Seguridad Nuclear, the Spanish Authority dedicated to Nuclear Safety) as well as the physic limitations of control rod sequences, among other important aspects such as pressure and temperature conditions, maximum fuel burn-up reached, shut-down margin, Departure from Nuclear Boiling, thermal and power limits, etc.

As a consequence: for this study, the A2 sequence was chosen to start the cycle to control the reactor during the first half of the two year cycle period. Then, the core is controlled with the B2 control rod sequence until the End Of Cycle. This fact allows to place a certain number of cells (see Figure 2) whose control rod will not be used during the first half of the fuel cycle, therefore being the ideal place for fresh fuel assemblies in order to avoid Shadow Corrosion.

Figure 2: BWR fuel assembly cell. Each cell consist on four adjacent elements with a cruciform control rod in the centre.

This implies that the usual loading pattern of fresh elements following a chequerboard structure will be no longer used as three of the four elements of non-controlled cells will be fresh assemblies -instead of two- and no fresh fuel is to be placed at controlled cells.

It must be specially noted that core symmetry -in terms of assembly type, enrichment, fuel burnt, etc.- has to be respected in order to avoid unbalanced power production and/or thermohidraulic misbehaviour in the core.

Special attention has to be paid to the requirements of shut-down margin as well as thermal and power limits among other important demands which come to be the most limiting factors of the study.

All of these demands, limitations and regulations require the fourth element of the non-controlled cells to be sufficiently burnt so as to avoid a high excess of power and temperature ratio and ensure a safety Shut Down Margin, but it also has to be sufficiently capable to withstand the high neutronic irradiation, coming from its three fresh adjacent assemblies, within the fuel burn-up limit, which ensures the fuel integrity, i.e.: it should be fresh enough to resist the irradiation of its three adjacent fresh elements without being excessively burnt. Besides, the burn-up value of this fourth element depends not only on the cell position inside the core, but it is also contingent on the activity and loading of neighbour cells.

This problematic was finally solved after several calculations and optimizations carried out with SIMULATE (Studsvik) [1] and FINELOAD (Tepsys) [2] nuclear codes. The result was:

- A load pattern with 40 non-controlled cells in which three fresh fuel assemblies were placed;
- Controlled cells were loaded with fuel from previous cycles; and
- All physical conditions and safety requirements were satisfied without modifications of the assembly type, enrichment and/or gadolinium content. -i.e.: only relative assembly position in the core was altered.

All the thirteen A2 control rods coloured in red on the Figure 1 of precedent page were free of fresh fuel assemblies.

Beneath, Figure 3 shows the core as loaded following the SCORE strategy. Yellow squares correspond to fresh fuel, whilst blue denotes the presence of assemblies from previous cycle -difference from light and dark blue indicates the burnt level of the element. Finally, brown coloured elements are the ones with up to two cycles old.

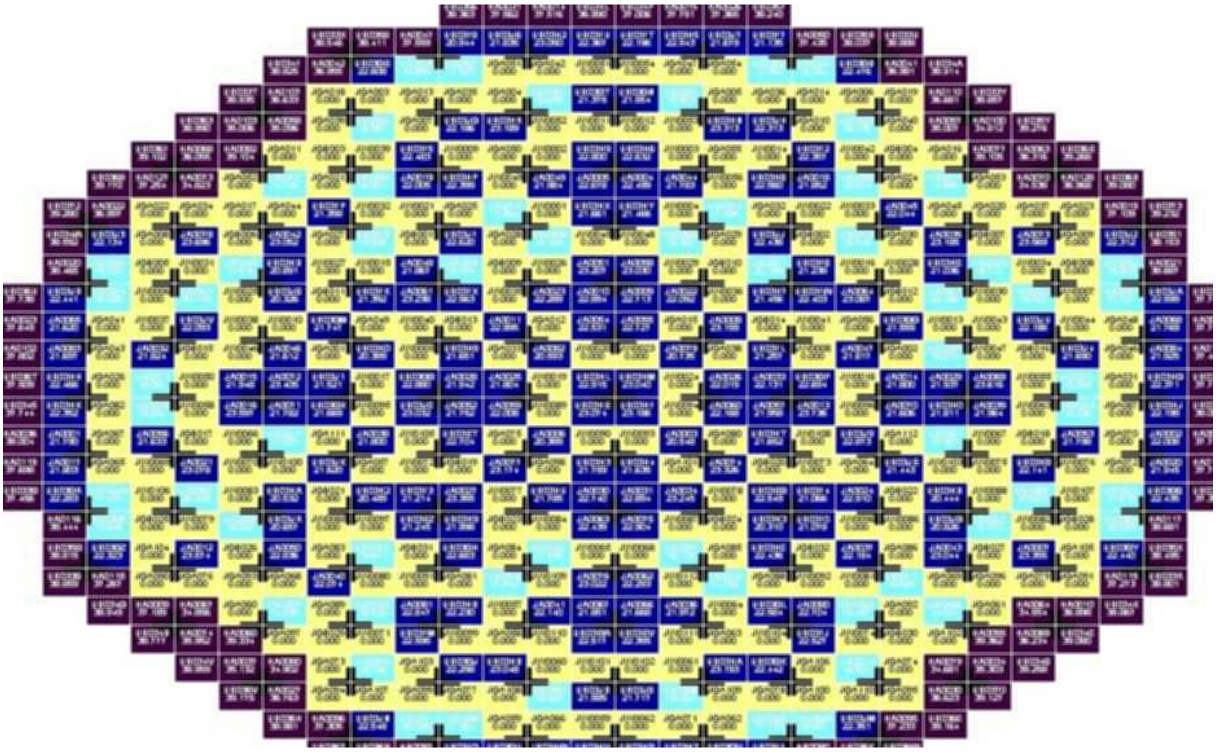

Figure 3: SCORE loaded core map.

Conclusions

Finally, not only good results were withdrawn in terms of shadow corrosion -thus decreasing channel bowing effect- but also a better performance of the fuel was perceived, meaning that: in comparison to the usual loading pattern of the same core, the SCORE strategy allowed to obtain more energy from the same kind of nuclear fuel and same number of fresh elements at the same enrichment level.

Hence the length of the cycle was demonstrated to be longer than usual by using this loading technique with the given advantages of reduced shadow corrosion effects on channel assemblies.

Bibliography and references:

[1] SIMULATE-3 User's Manual (Studsvik.)
[2] FINELOAD-3 System User's Manual (Tepsys.)
[3] Station Nuclear Engineering Manual – Principles of Nuclear Engineering. (General Electric) J.C. Barchler, C.D. Hendricks, J.S. Marks, B.U.B. Sarma, C.W. Smith.
[4] Technical report: Summary of SVEA-96 OPTIMA2 Bundles MN0741617GZ Nuclear design for Cofrentes reload. (Internal document of Iberdrola.)
[5] Informe técnico de Gestión del Núcleo. (Internal document of Iberdrola.)

On composition stabilizing a hypo-stoichiometric uranium dioxide

P.N. Alekseev, Yu.M. Semchenkov, A.L. Shimkevich
NRC "Kurchatov Instittute"
1, Kurchatov Sq., Moscow, 123182, Russia
Phone: +79859241638, E-mail: shall@dhtp.kiae.ru

Abstract

For modifying a nuclear fuel, it is offered choosing such the composition of uranium dioxide that it would became stable in hypo-stoichiometric state, UO_{2-z}, and have dense tetrahedral fractal clusters in the solid matrix as a ramified vacancy structure of an effective trap for fission products.

In this connection, a search of multi-component system, UX (X is a mixture of different metalloids including glassy-forming ones), can provide the stability of such the state in solid solution in terms of uranium dioxide and become a new direction for designing perspective nuclear fuel. This solid solution can have high density, low coefficient of fuel swelling and improved physical, chemical, and thermal properties in comparison with the oxide fuel.

Studying (in frame of the band theory) an electron structure of such the solid solutions as well as the investigation of influence of alloying additives on their physical and chemical properties will allow to obtain a material with the needed characteristics.

A concept for designing the modified oxide fuel can be useful for developing nuclear reactors of new generation. In order to provide the needed characteristics of the hypo-stoichiometric uranium dioxide, it is necessary to stabilize its crystalline lattice, replacing oxygen atoms with lesser number of another-metalloid ones with the greater valence than oxygen, for example, carbon.

Key words: hypo-stoichiometric state, stabilizing components, oxygen vacancies, and properties.

1. Introduction

Uranium dioxide is the high-temperature fuel material with the density at the level of 11 g/cm^3. It is essentially less than the metal fuel density and another lack of oxide fuel is very low heat conductivity [1]. Therefore it is very important improving these properties by studying ways for specifying and managing such the parameters [2].

In comparison of heat-conductivity temperature plots for some material [1], it is obvious these characteristics for uranium (and plutonium) dioxide are essentially lower than the same parameter for monoxide, carbide, metal fuel, and cermets (MO_2+M). This is most likely caused by electronic conductivity of metals and composites [2].

However in comparing their temperature dependences for the same materials, there are doubts concerning correctness of this conclusion. Indeed, electronic-conductivity levels of metals and oxides differ in five orders but their heat-conductivity levels are no more than in the order [1].

In this paper, we consider these problems in the frame of band theory for variable-composition compounds.

2. Band structure of non-stoichiometric uranium dioxide

A striking example of non-stoichiometric materials is uranium and zirconium dioxides, $UO_{2\pm z}$ and $ZrO_{2\pm z}$, which alloy phase diagram from [3] is shown in Fig. 1. One can see that the liquidus and solidus of this binary system are closely related and the first can be described by hypotenuses of congruous triangles (red lines). It means that the systems, $UO_{2\pm z}$ and $ZrO_{2\pm z}$, are similar in liquid and solid state, and the band structure of them is general. Then we can present thermodynamic characteristics of $UO_{2\pm z}$ as the partial oxygen pressure in the function of temperature and electron-energy states in the band model of $ZrO_{2\pm z}$ [4] shown in Fig. 2.

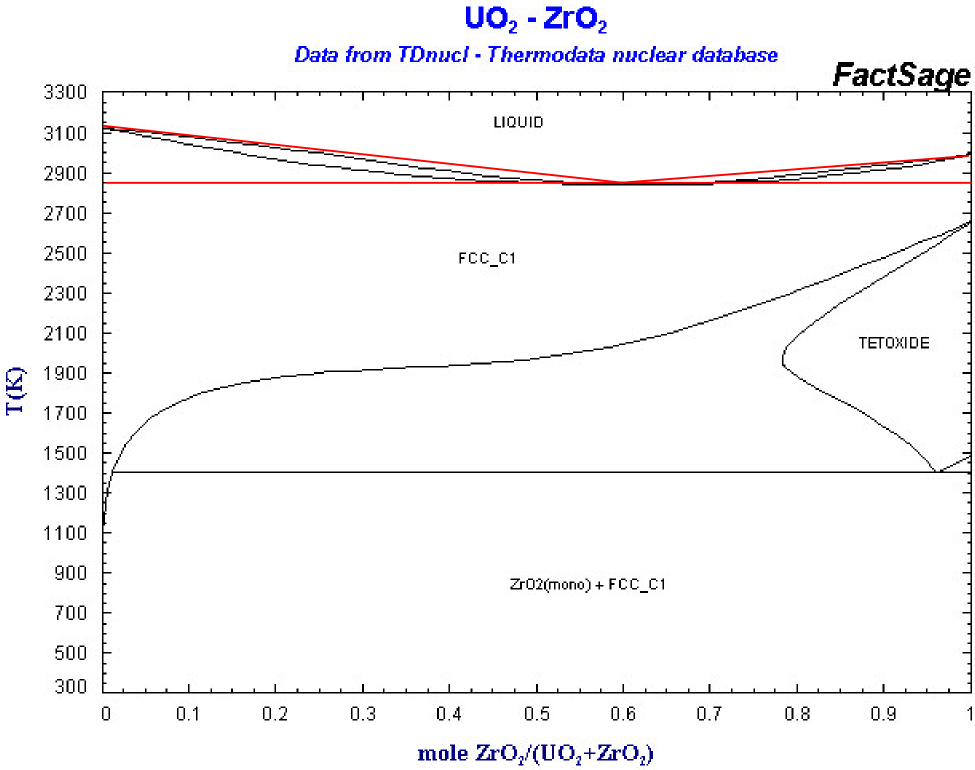

Figure 1 Phase diagram of binary system, UO_2–ZrO_2, with congruous triangles (red lines) of system liquidus

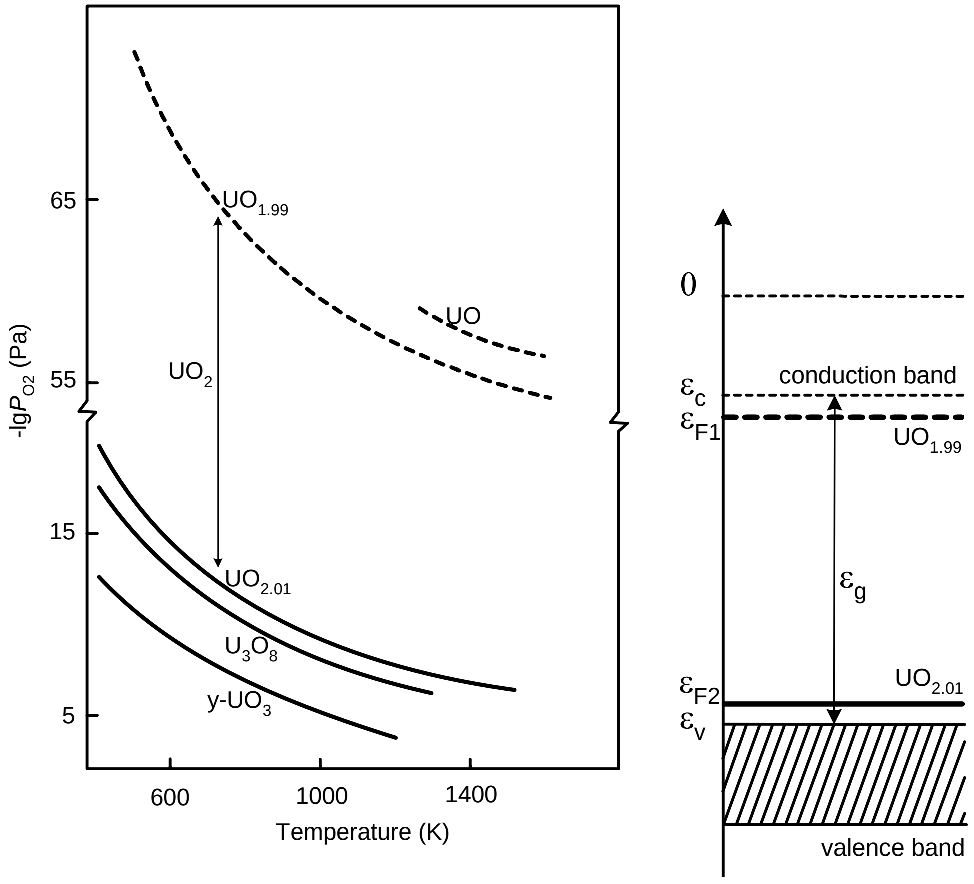

a) b)

Figure 2 Graphs of $-\lg P_{O2}$ (atm) as temperature functions for uranium oxides (a) and the band diagram of electron-energy levels (b) with two different Fermi levels for hypo- (ε_{F1}) and hyper- (ε_{F2}) stoichiometric uranium dioxide, $UO_{2\pm0.01}$

One can see in Fig. 2b that the hypo-stoichiometric uranium dioxide, $UO_{1.99}$, being stable at the low oxygen pressure, $P_{O2} > 10^{-65}$ Pa, conforms to the shifting of Fermi level, ε_F, up to value of ε_{F1} in the band gap, ε_g, near the bottom, ε_c, of conduction band.

For the hyper-stoichiometric uranium dioxide, $UO_{2.01}$, stable at $P_{O2} < 10^{-15}$ Pa, Fermi level comes to ε_{F2} near the top of valence band, ε_v, according to the equation [4, 5]

$$\varepsilon_F = \varepsilon_0(T) - (1/6)k_B T \cdot \ln P_{O2}, \qquad (1)$$

where $\varepsilon_0(T)$ is the standard chemical potential of uranium dioxide, k_B is Boltzmann constant, T is the absolute temperature, and the coefficient (1/6) is caused by arising 4 electrons and 2 vacancies per lost oxygen molecule. At the same time, the dioxide composition practically does not vary ($z < 0.01$) though the pressure of oxygen varies over a wide range (forty orders, see Fig. 2a).

Uranium dioxide is a semiconductor material with band gap, ε_g, is about 1.3 eV. The non-stoichiometry of the material dramatically influences its electrical properties. For example, the electrical conductivity of $UO_{1.99}$ is orders of magnitude lower at higher temperatures than the conductivity of $UO_{2.01}$ [6]. It may be caused by decay of hypo-stoichiometric uranium dioxide, $UO_{1.99}$, to dispersed metal in quasi-stoichiometric $UO_{2.00}$.

In other words, the hypo-stoichiometric state of uranium dioxide is absolutely unstable at high temperatures in contrast to the hyper-stoichiometric one. Therefore the stable state of UO_{2-z} is possible only in multi component system, M–U–O–X, where M is the metal with the valance less than the one of uranium and X is the metalloid with the valance more than the one of oxygen [2].

3. Composition stabilization of UO_{2-z}

The effective decision of this problem is noticeable increasing the solubility of oxygen vacancies in the regular lattice of uranium dioxide. In nominal raising the equilibrium concentration of oxygen vacancies in the oxide fuel, we, first, increase its density and stabilize its face-centered cubic structure on the analogy of zirconium dioxide [7]. Secondly, we bring an element of the chemical disorder of the regular lattice that is equivalent to make the solid as quasi-equilibrium amorphous. Thirdly, we reduce the influence of irradiation-induced vacancies on the decomposition reaction of oxide fuel and increase the rate of their relaxation in the equilibrium state.

The increase of vacancy solubility in the uranium dioxide, UO_{2-z}, is based on well-known technology for stabilizing the structure of zirconium dioxide by dissolving in it a metal impurity of lesser valence, for example, Y, Pu. It is caused by forming a solid solution stable in the wide interval of temperatures [7, 8]. Then, there are equilibrium vacancies with the atomic portion of $z/2$ in oxygen sublattice of $(UO_2)_{1-z}(M_2O_3)_z$ with structure of fluorite, CaF_2, where z is ~0.1. As a result, we have the ~5% portion of the vacancies in the nuclear fuel with the volume density of ~10^{20} v/cм^3 that essentially exceeds the concentration of irradiation-induced vacancies [5]. Fig. 3 illustrates the formation of such the solid solution by the composition triangle for MOX fuel in stoichiometric state (blue line) and its hypo-stoichiometric state (red line).

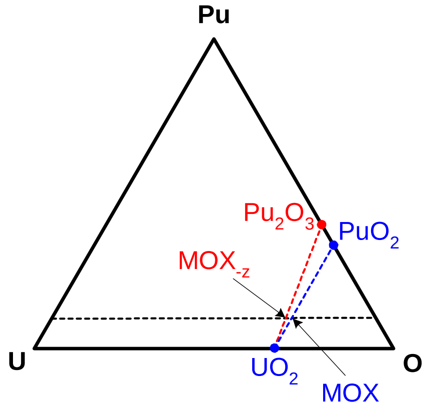

Figure 3 The composition triangle for MOX fuel in stoichiometric state (blue line) and its hypo-stoichiometric state (red line); the black arrows indicate these states at 9% of Pu in uranium dioxide

One can see that the stable MOX$_{-z}$ at the composition of MO$_{1.95}$ can be the result of solving Pu$_2$O$_3$ in the face-centered cubic lattice of uranium dioxide. The phase diagram of the system, Pu–O, shown in Fig. 4 [3] confirms the thermodynamic stability of Pu$_2$O$_3$ in the wide range of temperatures and what is more, PuO$_2$ is reducing by water to Pu$_2$O$_3$ in this temperature range [9].

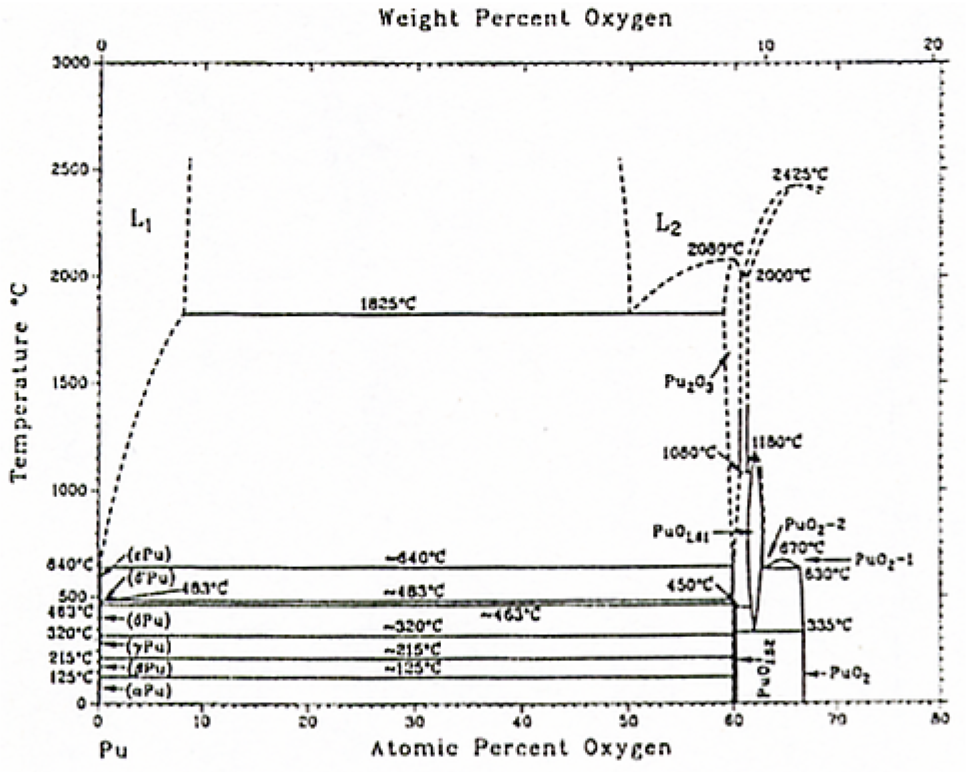

Figure 4 The phase diagram of system, Pu–O

Thus, the hypo-stoichiometric state of uranium dioxide is possible only for multi-component systems. It is clear that the additive of glass-forming elements (C, Si) in the fission materials can provide the further stabilization of the hypo-stoichiometric MOX$_{-z}$ (with $z > 0.05$) in the ramified chains of micro defects with oxygen vacancies [10]. Opposite to Eq. (1), Fermi level, ε_F, in this case is more sensitive to oxygen pressure according to the following equation [4]

$$\varepsilon_F = \varepsilon_0(T) - (1/4)k_B T \cdot \ln P_{O2}. \qquad (2)$$

4. Discussion

Vacancy doping the oxygen sub-lattice of uranium dioxide is necessary for getting hypo-stoichiomentric UO$_{2-z}$. However the realization of such the condition for $z \geq 0.05$ in MOX fuel of PWR is impossible.

Opposite uranium dioxide with the gap-band of ~2 eV, uranium monocarbide have a wide valence zone crossed with their conductivity zone. It indicates to strong covalent bonds between atoms of uranium and carbon in UC whereas for uranium dioxide the contribution of these bonds does not exceed 20%. Due to strong covalent bonds, phonons in uranium monocarbide have the long run that provides its high heat conductivity [17].

On the other hand, replacement of oxygen with carbon in the hypo-stoichiometric MOX$_{-z}$ does not only increase its heat conductivity and density but also creates conditions for amorphous transforming the fuel matrix. Hence, carbon carries out double mission: 1) rigidly connects atoms of uranium together by covalent bonds and 2) provides high-frequency phonons in a molecular crystal of uranium carbide. Therefore, one can expect that strengthening the molecular bonds in MOX-carbide due to an additive glass-forming element with covalent bonds will increase its heat conductivity.

Basic configuration for modifying the nuclear fuel is uranium dioxide. The concept of fuel modification consists, step-by-step, in changing UO_2 to the hypo-stoichiomentric MOX$_{-z}$ and then, stabilizing it by carbon to MOX$_{-z}$C shown in Fig. 5.

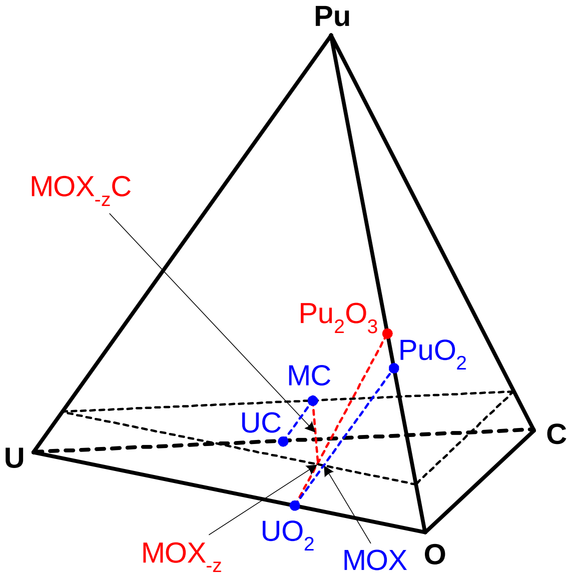

Figure 5 The composition tetrahedron of four-component system, Pu–U–O–C: stoichiometric reference states (blue points and lines) and its set of hypo-stoichiometric states (red lines); the black arrows indicate these states at 9% of Pu in uranium dioxide

Transformation of UO_2 to MOX$_{-z}$C can be carried out by different ways. In this case, the accent is made to the hypo-stoichiomentric MOX$_{-z}$ as an intermediate state of oxide fuel of solid solution $(UO_2)_{1-z}(Pu_2O_3)_z$ in the face-centered cubic lattice of CaF_2. Then, the process follows along the direction MOX$_{-z}$ ⇒ MC by annealing the first in graphite powder at high temperatures.

The theoretical density of MOX$_{-z}$C fuel composition, $Pu_{0.09}U_{0.91}O_{0.96}C_{0.5}$, in the hypo-stoichiomentric state, $MX_{1.46}$, of CaF_2 crystalline lattice is estimated as 12.5 g/cm^3. 27% of oxygen vacancies in the sublattice of MOX$_{-z}$C are the good way for effective relaxing the irradiation defects in fuel matrix and decreasing its swelling.

5. Conclusions

For solving the problem of the vacancy swelling of crystal fuel, it is necessary to increase the solubility of vacancies in its regular lattice. The structure of UO_2 unloaded by oxygen vacancies is susceptible to accumulate the fission products and has the high density of the recombination centers for radiation point defects.

The search of threefold compound in the system, UO_{2-z}–Pu_2O_3–UC, with the face-centered cubic structure can appear the perspective direction for designing the fuel with the low swelling factor, high density, and heat conductivity.

The hypo-stoichiomentric state, $MX_{1.46}$, of MOX$_{-z}$C fuel can have high metal density, reduce the fuel-swelling factor, and improve physical, chemical, and thermal properties.

References

[1] High-temperature nuclear fuel / Moscow: Atomizdat, V. 2, 1978.
[2] A.S. Kolokol and A.L. Shimkevich. On Advanced Fuel with Improved Properties // In Proceedings of "16th International Conference on Nuclear Engineering"(ICONE16), Orlando, Florida, USA, May 11-15, 2008, Paper ICONE16-48090.
[3] http://www.crct.polymtl.ca/fact/Documentation/TDNucl/TDNucl_List.htm
[4] V.V. Osiko, A.L. Shimkevich and B.A. Shmatko. Electronic Model for FIANIT // Transactions of Russian Academy of Sciences (Doklady Akademii Nauk), 1982, V. 267, pp. 351-354.

[5] P.N. Alekseev, et al. On Designing Nuclear Fuel with Low Factor of Swelling," Preprint IAE-6259/11, RRC KI, Moscow, 2003.
[6] http://english.turkcebilgi.com/uranium+dioxide
[7] F. A. Kröger. The Chemistry of Imperfect Crystals. 2nd ed., Vol. 1: Preparation, Purification, Crystal Growth And Phase Theory / New York: American Elsevier Publishing Company, Inc., 1973.
[8] Yu.Ya. Gurevich. The Solid Electrolytes / Moscow: Science, 1986.
[9] Water and its Ambiguous Role in Nuclear Waste Storage http://www.avssymposium.org/Open/SearchPapers.aspx
[10] K. Niwase et al. J. Nucl. Mater, 1988, V. 155-157, P. 303
[11] High-temperature nuclear fuel. Ed. 2. M.: Atomizdat, 1978.

THORIUM OPTION FOR DURABLE ELECTRO-NUCLEAR SYSTEMS : COMPLEMENTARITY OF THORIUM AND URANIUM BASED CYCLE IN WATER COOLED REACTORS AND ADVANCED PLUTONIUM MANAGEMENT

M. ERNOULT, S. DAVID
IPN Orsay
15 rue Georges Clémenceau, 91400 Orsay – France

L. VAN DEN DURPEL
AREVA
Tour AREVA 1, place Jean Millier, 92400 Courbevoie - France

ABSTRACT

The possible delay of decades for the deployment of fourth generation reactors bring up new issues. First, the possibility of higher tension on uranium mining motivates the research of a better use of resources in PWR. Second, countries like France which are storing Plutonium for years in prediction of starting FBR could have to adapt their plutonium management strategy.

Different options and different types of uranium and/or thorium based fuels in PWR have been studied using the MURE core. The equilibrium state of all considered strategies are calculated taking into account the whole nuclear cycle, allowing a precise description of the fuel composition and behavior at each step.

The study is made in the most similar strategy of fuel reprocessing and allows a real comparison of U and Th cycles. It will confirm or refute some beliefs and show that no strategy offers a enhancement in all fields considered.

1. Introduction

1.1 Thorium and Uranium based cycles in PWR

The goal of this study is to compare and to understand the differences between different fuel cycles in water cooled reactors and to see how thorium can improve them. This focus on the fuel cycle has driven us to choose the most common water cooled reactor : PWR. Indeed more than 2/3 of the power produced in the world by nuclear reactors are produced by PWR and all the reactors in France are PWR [1].

To explore all the possible fuel cycles usable in PWR to recycle plutonium, we have to use all the possible elements, that are, if we want to stay within PWR utilisation, the 235 and 238 isotopes of uranium and 232 thorium. The ^{235}U is the only fissile isotope and will keep an important role in any strategy since uranium and thorium cycle cannot be breeding in PWR. However it represents only 0.7% of the natural uranium so a sustainable use of the nuclear would require to use the other two. ^{238}U and ^{232}Th are fertile nucleus, which means that they can produce fissile nuclei after neutron capture, respectively ^{239}Pu and ^{233}U. This new fissile material can fission directly in the assembly in which it has been created, allowing the increase of the total burn-up, or be used to created a new type of fuel. Today only the uranium isotopes are used in an industrial way, but thorium shows some very promising properties.

The most important of These promising properties is the positive number of available neutrons in thermal energy as shown on the figure 1. The number of available neutrons is the difference between the number of neutrons produced by one fission and the number of neutrons necessary to maintain the chain reaction and produce a new fissile nucleus by capture on a fertile one. The fact that U/Pu cycle has a negative number of available neutrons in a PWR spectrum means that it will never be possible to achieve breeding in thermal spectrum with this cycle. The number of available neutron with Th/U cycle is positive in PWR spectrum. Theoretically the breeding is therefore possible. Practically it is very hard to achieve[2] but this property generates a better conversion ratio for thorium cycle than uranium cycle which should allow good economy of resources

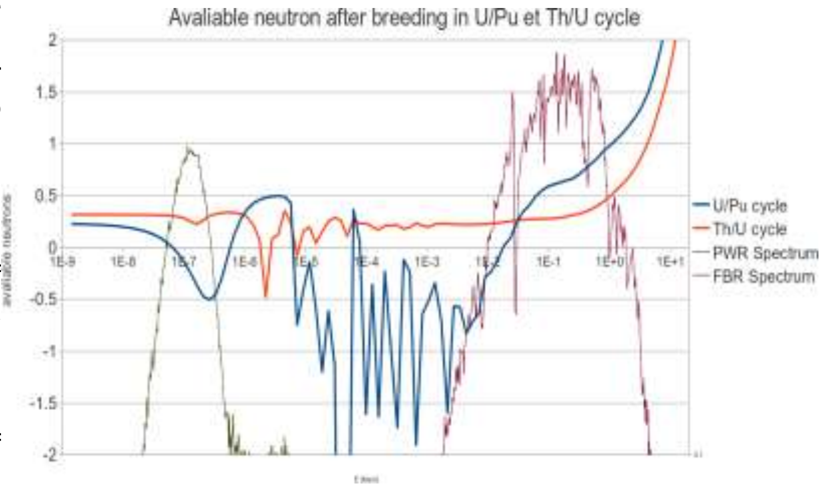

Fig. 1. Available neutrons in U/Pu and Th/U cycles

1.2 Equilibrium scenarios

A scenario has to define entirely the reactor fleet at each time: which reactors are in the fleet, which kind of assembly with which kind of fuel inside, how much fresh fuel needs to be produced and transported and with which isotopic composition, how much used fuel is produced and have to be transport, how much time each step take and how much time is needed between two steps.

The initial conditions of a scenario are the composition of the fleet, in terms of reactor type, at the beginning of the study and the isotopic composition for all the inventories. If the composition of the fleet is quite easy to know it's not the same for the isotopic composition of the inventories.

To be released from the necessity of knowing these initial stocks, the solution is the equilibrium scenario. In an equilibrium scenario all parameters are at steady state. It doesn't mean that all isotopic vectors are always exactly constant but it impose that all the flux before and after a whole cycle are constant. The reactors present in fleet are constant, in number and in type, and all the resultes will be normalized per GWe.y. They use the same kind of assemblies with the same initial composition and the same fuel reloading scheme in each successive cycle. The flux from mine, fresh fuel, used fuel and waste are constant. To sum it up, each cycle is exactly similar to the previous and the following cycle; each cycle starts and ends in the same way as the previous did and the next will.

2. Different scenarios of plutonium management in PWR

In this study, all reactors are standard PWR, a fresh fuel element always waits exactly two years after its fabrication before it goes in the reactor, all assemblies are irradiated up to a burn-up of 50 GWd/t_{HM} and a used fuel element always remains exactly five years for cooling before it is reprocessed.

In the fabrication of enriched uranium fuel, the depleted uranium final enrichement is 0.2% of ^{235}U. The irradiation is simulated with fuel reloading scheme by quarter of the core. And the efficiency of all the chemical separation process is considered as 99.9%. In this study minor actinides are not reprocessed and sent into ultimate waste withi fission products

2.1 Homogeneous recycling of plutonium in PWR

The easiest way to conceive scenario for recycling plutonium in PWR is the homogeneous multirecyling of plutonium.

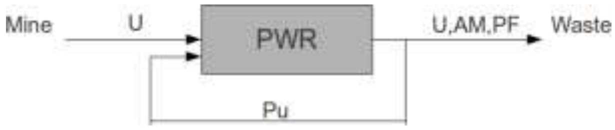

Fig. 2 : Scheme of multiUePu scenario

In this scenario, there are only one kind of assembly. The plutonium produced during the cycle is added to enriched uranium to produce the new fuel which is irradiated in the core. This fuel will produce plutonium during irradiation which will be recycled.

This scenario will be thereafter named multiUePu, for a scenario using multi-recycling of a mixed oxide fuel with enriched uranium and plutonium inside.

2.2 Separation between Plutonium production and Plutonium burning

In scenarios so-called “multiUePu”, all the fuel assemblies contains plutonium. A big part of what is relevant for the fuel behavior is simply ^{235}U fission and ^{239}Pu production through capture on ^{238}U, exactly what happens in our well-known standard UOX fuel. To take advantage of this knowledge of the UOX, one option is to separate the plutonium production, in UOX fuel, and the plutonium burning. It leads to parallel utilisation of two kind of assemblies, as what is done today in France with the mono-recycling of Pu.

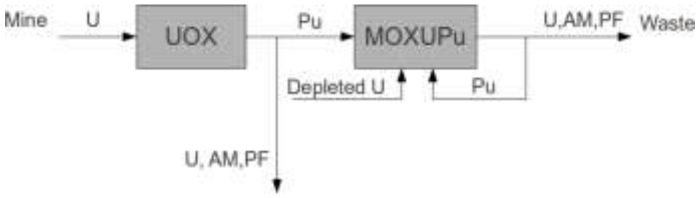

Fig. 3 : Scheme of multiUPu scenario

In this scenario, there are two kind of assemblies. The first kind is the standard UOX assembly made of enriched uranium, and produces plutonium. The second kind is made by mixing the plutonium produced by the UOX assemblies and the multiUPu with depleted uranium, and this limit the fabrication of Pu loaded assemblies. In this second kind of assembly the plutonium is multi-recycled, no plutonium goes to waste (or only the 0.1% for chemical loss). If the U/Pu cycle could breed in PWR, the UOX assemblies would not have been necessary, the plutonium coming from these assemblies is just here to compensate the under-breeding. The uranium isn't recycled.

This scenario will be thereafter named multiUPu, for a scenario using multi-recycling of a mixed oxide fuel in U/Pu cycle.

2.3 Thorium option

Once the production and the burning of plutonium have been separated in two different kind of assembly, there is room for thorium utilisation. We have seen that in the precedent scenario, multiUPu, the UOX assemblies are needed to compensate the under-breeding of U/Pu cycle in PWR, as explicited in 1.1 the thorium should allow a better conversion ratio

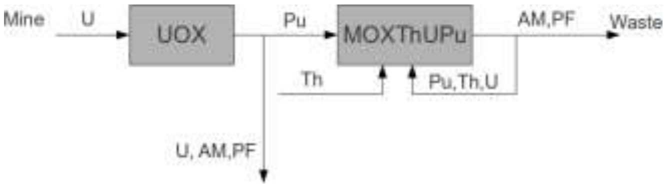

Fig. 4 : Scheme of multiThUPu scenario

and therefore a smaller need of plutonium from UOX assemblies.

As before, there are two kind of assemblies. The first kind is, as in multiUPu, the standard UOX assembly. The second kind is made by mixing the plutonium produced in the UOX and the ThUPu assemblies, the uranium, mostly ^{233}U, produced by the multiThUPu assemblies with thorium. The uranium and plutonium produced in the multiThUPu assemblies are multi-recycled in the same kind of assembly.

This scenario will be thereafter named multiThUPu, for a scenario using multi-recycling of a mixed oxide fuel in Th/U cycle with addition of plutonium coming from UOX assemblies.

2.4 Separation between Uranium233 production and Uranium burning

In the same way, we can separate the production and the burning of 233 uranium. In this context we have conceived two different scenarios, named multiThU and multiThU2. In both of them, the plutonium produced by UOX assemblies is burned in thoriated assemblies and the uranium produced in plutonium charged thoriated assemblies is burned in other thoriated assemblies which are plutonium free. The difference between these scenarios is the multi-recycling or not of the plutonium in the second kind of assemblies.

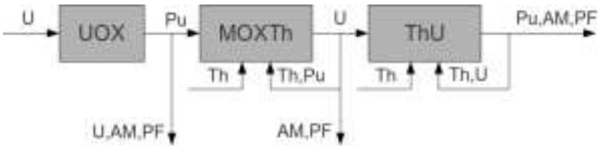

Fig. 5 : Scheme of multiThU scenario

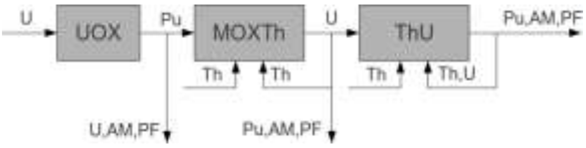

Fig. 6 : Scheme of multiThU2 scenario

In the scenario multiThU there are three kind of assemblies. The first is the standard UOX, it provides plutonium to the second kind. The second is mixed thorium plutonium fuel, it provide fissile uranium to the third kind and multi-recycles its own plutonium in assemblies named multiThPu. In the third kind of assemblies , the uranium coming from second and third kind of assemblies is multi-recycled mixed with thorium. This allows to concentrate the difficulty of fabrication of Th/U fuel (due for example to the presence of ^{232}U) on a small amount of assemblies.

The scenario multiThU2 is very similar to the multiThU. The only difference is in the second kind of assemblies. In the multiThU2, the plutonium is not multi-recycled. The second kind of assemblies is therefore monoThPu

2.5 Open cycles used as reference

In order to be able to understand precisely the scenarios presented above, it is necessary to consider also their open counter parts: the total UOX open cycle, the monoUPu and the monoThPu. The UOX open cycle is the very standard cycle, very simple and very well known. The monoUPu consists on utilising the plutonium coming from UOX assemblies to make MOX assemblies without recycling the plutonium coming from these MOX assemblies; this is the actual French scenario. The monoThPu is the pendant of the monoUPu using thorium.

3. Tools

3.1 MURE

To study all these scenarios we simulate irradiation of about ten very innovative fuel in reactor. For these simulations the MURE package is used[3]. MURE is a depletion code which determines time-dependent fuel composition and reaction rates. It is based on solving the Boltzmann equation using Monte-Carlo method for neutron transport and the Bateman equation for depletion. The Monte-Carlo part is implemented by using the widely-used particle transport code MCNP.

In MURE, due to the Object-oriented programming, any user can define his own way to interact with evolution. Moreover, MURE provides a simple graphical interface to visualize the results.

The MURE package is continuously improved and for this study some development have been made to be able to easily simulate numerous cycle following the fuel from fabrication to irradiation to the reprocessing and the new irradiation.

3.2 Khi definition

In order to simulate easily all the considered scenarios, a standardized representation has been created. In fact an assembly in an equilibrium scenario is completely defined by a small number of parameters.

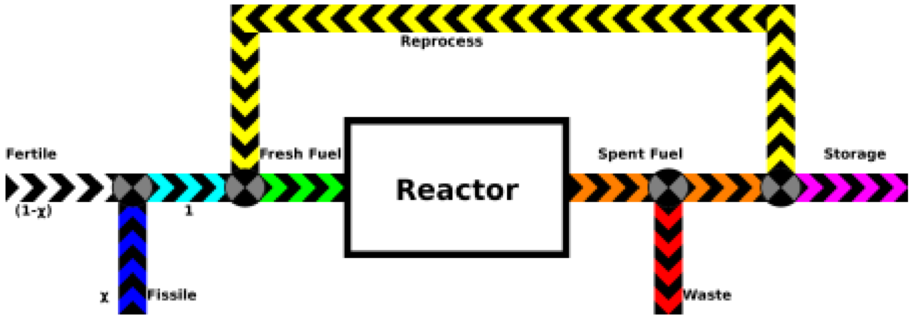

Fig. 7 : Life cycle of an assembly and his material

As shown on the figure 7, the fresh fuel of one assembly is made by adding to the reprocessed isotopes, some fissile and some fertile elements. The fresh fuel is therefore completely defined by the elements which are reprocessed, the added fissile and the added fertile, three parameters which are clearly defined in the presentation of each scenario, and by the proportion between fissile and fertile added to the reprocessed elements. The proportion between reprocessed elements and fresh elements is fixed because of the steady state hypothesis which implies that each assembly has to consume the same quantity of reprocessed elements that it produces. This proportion named χ is the last parameter needed to define each scenario. We want assemblies that remain critical in core and can achieve a fixed burn-up. These constraints impose χ and we have to calculate it to have an equilibrium we can analyse.

3.3 Khi calculation

The first way to calculate χ is to come back to the physics. The initial composition of the fuel is directly dependant of χ so we can express the initial multiplication factor k as a function of χ and physical parameters, such as the cross sections or the flux. Through some easy numerical manipulation we obtain the expression of χ shown in figure 8

$$\chi=\frac{k_{\infty}^{BOC}\left(\sum_{reproc} N_i\sigma_i^a\varphi+\sum_{fertile} N_i\sigma_i^a\varphi\right)-\sum_{reproc} N_i\nu\sigma_i^{fiss}\varphi-\sum_{fissile} N_i\nu\sigma_i^{fiss}\varphi}{\sum_{fissile} N_i\nu\sigma_i^{fiss}\varphi-\sum_{fertile} N_i\nu\sigma_i^{fiss}\varphi-k_{\infty}^{BOC}\left(\sum_{fissile} N_i\sigma_i^a\varphi-\sum_{fertile} N_i\sigma_i^a\varphi\right)}$$

fig. 8 : χ as a function of k and XS

But there are some issues with this formula. First the spectrum, and therefore the average cross sections, depend on the isotopic composition and the equation isn't a simple linear equation. But the evolution of k, and therefore the k needed at the beginning of the cycle in order to achieve the expeted burn-up, also depends on this composition and on χ. The prediction of the evolution of k is something very complex that need a entire simulation. The calculation of χ even with this exact, physical formula could therefore not be direct and would need numerical resolution without any insurance that a solution will be reached.

Thus, we developed a numerical method (see figure 9), which insure to reach a solution and minimize the calculation time.

First the definition of the scenario imposes the isotopic vector which will be used for fertile and fissile elements. Afterwards the χ_0 is fixed arbitrarily and the iteration begin.

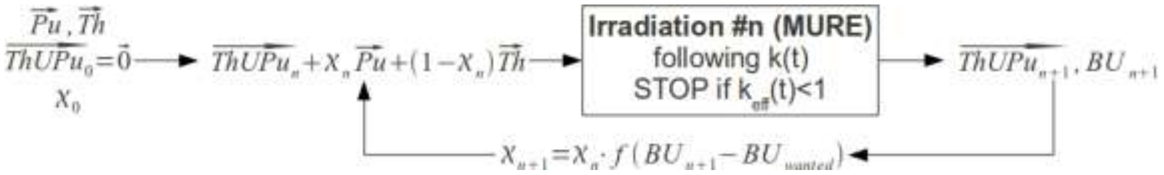

Fig. 9 : numerical calculation scheme for χ

At each iteration, a new fresh fuel composition is created by adding to the reprocessed elements, χ% of the mass missing in fissile element and (1- χ)% in mass of fertile element. Then the irradiation of the assembly with this new fuel is simulated. At each time step, the value of k_{eff} is checked. If the global k_{eff} goes below 1, the irradiation is stopped. In our simulation, we consider a loading of the core quarter by quarter, and we consider that all the assemblies will have a similar behavior so that the average k_{eff} is the average between four k_{eff} shifted in time by one quarter of the irradiation time. Once the irradiation has stopped we extract the final isotopic vectors for recycled elements after reprocessing and fabrication times ,and the burn-up which have been finally reached. We calculate χ for the next iteration by multiplying the last χ by a function depending on the difference between the actually achieved burn-up and the targeted burn-up. If the burn-up is too low, we increase χ in order to have a chance to increase the burn-up on next iteration. If the burn-up is too high we decrease χ. So the f function presented in figure 10 has to respect some simple conditions. To follow the logic explained before f has to be below 1 if the reached burn-up higher than the wanted burn-up and has to be greater than 1 if the reached burn-up is smaller than the targeted burn-up.

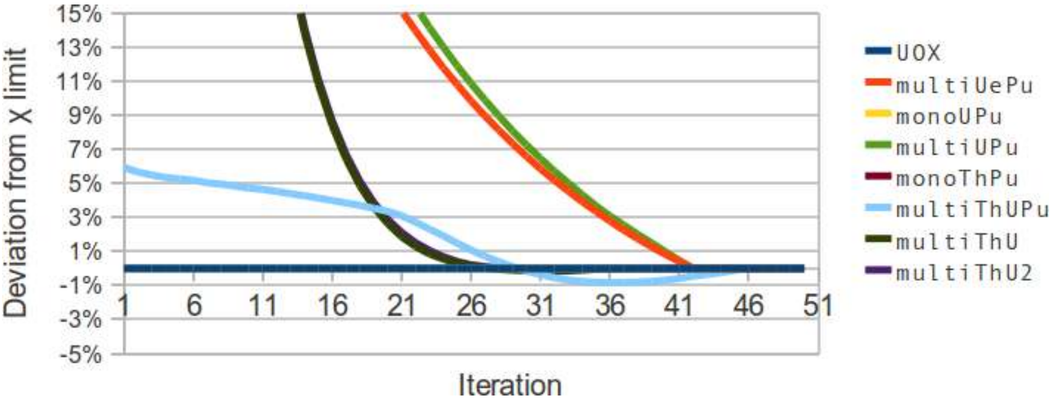

Fig.10 : Evolution of χ through iteration

As shown on the figure 10, through the successive iteration the reached burn-up approaches the wanted burn-up and χ reached a limit value. Even if a stabilisation of χ isn't equivalent directly to be in an equilibrium scenario, the fact that for the same addition of fresh fissile and fertile the reached burn-up doesn't change suggests that the recycled elements are the same and therefore that the composition in the core is periodic : the equilibrium has been reached.

This method allows to simulate only realistic times of irradiation (during the iteration the burn-up varies from 40 to 60 GWd/t) and is relatively low in computational needs (only about fifty irradiations simulated for each scenario) but the intermediate iteration has no real meaning because it's unrealistic that similar irradiation would have been done in an industrial management. Thereover for each scenario the first cycle simulated is similar to the open cycle.

4. Comparison of the scenarios

4.1 Criteria

In order to explicit advantages and drawbacks of each scenario and to see which are reasonably implementable in real operation, the studied scenario have been compared in many points of the cycle: mining, front-end path, irradiation in the core and waste production.

The results are sumed up in the table of the figure 13.

4.2 Mining

About the need in natural actinides, uranium and thorium, the plutonium homogeneous multi-recycling leads to an augmentation of the natural uranium consumption. This overconsumption has two main reasons. The first is that the plutonium vector in the fuel has a very low quality, around 50% of fissile isotopes and a lot of 240 and 242 isotopes. To achieve a correct reactivity at the beginning of cycle the quantity of ^{235}U needed is equivalent to the one needed in UOX fuel. This high amount of ^{235}U prevents to have a spectrum too much directed by plutonium which leads to a high capture cross-section on these isotopes. These captures lead to the second point: at the end of the cycle the quantity of minor actinides is far higher than in UOX fuel and they have a stronger effect on the reactivity. In order to be able to achieve a high burn-up, a greater initial fissile mass is therefore needed.

These two reasons are no longer relevant when the production and the burning of the plutonium are separated. In the multiUPu scenario the plutonium imposes the spectrum in the second kind of assemblies. The spectrum is harder and the self-shielding is therefore important. The capture rate on ^{240}Pu and ^{242}Pu are lower and this allows the plutonium to assume its fissile role. This leads to a 23% less need of natural uranium than multiUePu and 18% less than UOX.

The results also show a relative lack of effects of the use of thorium. Indeed the replacement of uranium by the thorium (multiThUPu compared to multiUPu scenario) brings only a relative economy of 5%, which is not relevant. The separation of the production and burning of ^{233}U doesn't correct this fact and even leads to an increase of natural uranium consumption.

4.3 Front-End Path

In the considered scenarios there are two very different kinds of front-end path: those with uranium enrichment and those only with chemical processes.

To compare the effort needed in uranium enrichment, we can compare their needs in working separation unit[4]. The multiUePu scenario needs 168k of WSU to produce fuel for 1GWe.y against 153k for the UOX scenario, representing an increase of almost 20%. This augmentation has the same origin as the ones expressed in the mining part. For the other scenarios there is a reduction of the needed working separation unit, thanks of the diminution of the UOX assemblies quantity.

For the re-fabrication of fresh fuel using the reprocessed actinides the main problem is radio-protection during the fabrication process. As of now, the main issue is the gamma emission from the ^{241}Am. The figure 13 shows that only multiUePu has a higher ^{241}Am concentration in their plutonium vector than the monoUPu scenario,the actual French scenario. And even for the multiUePu it is below the threshold for acceptance in the MELOX facility (French facility for MOX fabrication) which is 5%. But in the thoriated assemblies the presence of ^{232}U in the reprocessed fuel, which leads to a 2.6 MeV gamma ray emission, is certainly a big issue but the very low quantity of this isotope, less than 0.35% of the uranium vector, allows to envisage it nevertheless.

For neutron emissions, the main contributor is 238 plutonium by (n,alpha) reaction on the oxygen. The figure 13 shows that the proportion of 238Pu in the plutonium vector can be more than three time the proportion in the monoUPu scenario. For multiThUPu, and in all scenarios with multi-reprocessing of plutonium this proportion goes higher than 4%. Neutron radio-protection will certainly be an issue with this kind of multi-recycling scenario but the neutron flux during fabrication stays very low incomparison to those from fuels for minors actinides transmutation and the developments made for these fuels could solve the problem.

4.4 Core properties

To determine if it can be realistic to use these new fuels in reactors, the first point to check is if the control of the core will be possible. In figure 13 we see that the delayed neutron fraction, named βeff, is very low in all assemblies, almost a half of the βeff of the UOX assemblies. It could seem an issue but as it is never significantly smaller than in the monoUPu scenario, which is the actual French scenario and therefore a realistic one, it seems to be manageable.

On the topic of accidental situations, further inquiry would require complete safety studies but requires time consuming process. For a first step this point is limited to a few basic parameters.

The firsts are the temperature coefficient s: the effect on the reactivity of an increase of the temperature of the fuel or the moderator. The fuel temperature coefficient varies between the scenarios but as it remains always significantly negative, all of the same order of magnitude, there are no problems on this side. For the moderator temperature coefficient it is quite the same exept for the multiThU and multiThU2 scenarios. In these two cases, the moderator temperature coefficient is positive but their fuel temperature coefficient is very negative, and the sum is negative. This means that further studies are needed ti conclude on the issue for both scenarios

The second is the void coefficient : the effect a lack in moderator has on reactivity. In most of the scenarios the void coefficient stay significantly negative, sometimes even more than for UOX. MultiThUPu assemblies have a small void coefficent but it is really close to the one of monoUPu, our reference. The problem appears in multiUPu and multiThPu assemblies which have a big positive void coefficient, more than forty time the value of their respective βeff. Those are therefore impossible to be used alone in a reactor and a priori simply impossible to be used alone. A optimized core management icould perhaps make it acceptable. This result is the main reason we have studied the multiThU2 scenario in complementarity of the multiThU, a scenario which avoid the use of degraded plutonium to avoid this positive void coefficient.

4.5 Back-End Path

As expected, the multirecycling of plutonium increases the production of minor actinides and decreases the quantity of fissile material which are not used in the cycle. The separation between the production and the burning of the plutonium have a negative effect on the minor actinides production because of the hardening of the spectrum leading to an increase of the equilibrium inventory of Pu. The use of thorium almost offsets this increase in the multiThUPu scenario but the separation of production and burning for ^{233}U leads to a significant decrease of the minor actinides production. In the multiThU2 scenario, the production of minor actinides added to the production of plutonium in the second kind of assemblies is even the same as the production of minor actinides in the multiUPu scenario.

Figures 12 and 13 show high amount of uranium 235 in the non reprocessed material in all scenario. It encourages to make further studies about the possibility and the effect of multirecycling of the uranium, specially in the UOX assemblies. We also see that the total production of minor actinides stay below 103 kg per GWe.y, i.e. 11.8 kg per TWhe, in average over the fleet, and the production of americium is limited to a maximum of 9.3 kg per TWhe, 7.3 with thoriated fuel. which is not significantly higher that the production of americium in FBR, which is 4.9 kg per TWhe[5].

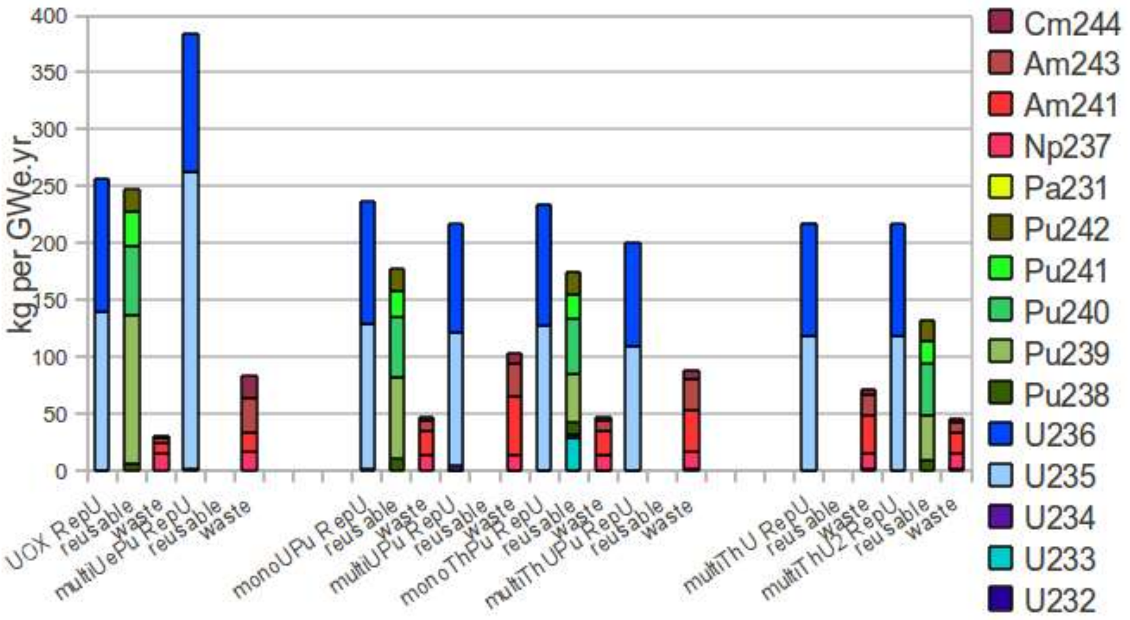

Fig. 12 : Actinides at the Back end of the scenario

5. Conclusions

This study is based on detailed neutronic calculation coupled with the simulation of the entire cycle. It allows a précised comparison of several strategies of Pu multirecycling in PWR.

The study of all these scenarios has shown that, even combined with the thorium cycle, the multirecycling of the plutonium in standard PWR cannot lead to a significant economy of resources as compared to the standard UOX cycle : no more than 22%.

Two scenarios among those which multirecycle the plutonium seem to be realisable, multiUePu and multiThUPu. Their productions of minor actinides, and specifically of ^{241}Am are higher than in FBR but remain within acceptable range. But the total amout of Pu stored inside the cycle at equilibrium is widely reduced as compared to a FBR strategy.

In all the cases and regardless of the chosen scenario, thoriated or not, the reprocessing is an issue that needs futher studies. This methodology allows now to consider innovative water reactors (as Candu, High-conversion reactors, ...) to improve the conversion of thorium fuels in thermal spectrum and try to reduce significantly the consumption of uranium.

6. References

[1] IAEA PRIS - Power Reactor Information System.

[2] Perrine GUILLEMIN, (2009) *Recherche de la haute conversion en cycle thorium dans les réacteurs CANDU et REP*, PHD thesis, Institut polytechnique de Grenoble

Scenario		UOX	multiUePu	monoUPu		multiUPu		monoThPu		multiThUPu		multiThU			multiThU2		
Assembly				UOX	UPu	UOX	UPu	UOX	ThPu	UOX	ThUPu	UOX	ThPu	ThU	UOX	ThPu	ThU
Fleet composition		100%	100%	91%	9%	81%	19%	91%	9%	78%	22%	85%	8%	7%	84%	8%	8%
Mining	U (t per Gwe.yr)	175.96	188.06	159,79	1.78	141.84	3.28	160.61	0	137.14	0	149.17	0	0	148.64	0	0
	Th (t per Gwe.yr)	0	0	0	0	0	0	0	1.67	0	0.48	0	0.04	0.06	0	0.13	0.06
Front-End	U enrichment (kWSU)	153	168	141	0	126	0	140	0	119	0	130	0	0	129	0	0
	Am241 (% Pu vector)	0.00%	3.55%	0.00%	3.48%	0.00%	2.76%	0.00%	3.48%	0.00%	3.08%	0.00%	2.62%	0.00%	0.00%	3.48%	0.00%
	U232 (% U vector)	0.00%	0.00%	0.00%	0.00%	0.00%	0.00%	0.00%	0.00%	0.00%	0.18%	0.00%	0.00%	0.26%	0.00%	0.00%	0.34%
	Pu238 (% Pu vector)	0.00%	4.44%	0.00%	2.54%	0.00%	5.38%	0.00%	2.54%	0.00%	8.19%	0.00%	5.08%	0.00%	0.00%	2.54%	0.00%
In Core	β_{eff} (pcm)	723	576	723	370	723	378	723	314	723	349	723	404	340	723	314	352
	T. coef. Fuel (pcm/K)	-1.69	-2.58	-1.69	-2.41	-1.69	-2.37	-1.69	-3.29	-1.69	-3.49	-1.69	-2.72	-2.54	-1.69	-3.49	-2.47
	T. coef. Mod. (pcm/K)	-0.99	-2.34	-0.99	-2.5	-0.99	-1.5	-0.99	-2.08	-0.99	-0.88	-0.99	-0.99	0.82	-0.99	-0.88	0.79
	Void coeff. ($)	-115	-83	-115	-17	-115	41	-115	-60	-115	-13	-115	45	-260	-115	-60	-260
Back-End	A.M. (kg per Gwe.yr)	30	83	28	19	25	78	28	19	24	64	26	43	1.8	26	17	1.6
	Am (kg per Twhe)	1.61	5.5	1.47	1.92	1.3	7.98	1.47	1.9	1.26	6.08	1.37	4.37	0.05	1.35	0.69	1.08
	Fissile (kg per Gwe.yr)	298	262	126	98	112	4.6	127	93	108	0	118	0	0.1	118	59	0.1

Fig. 13 : summary table

[3] Méplan O., Nuttin A., Laulan O., David S., Michel-Sendis F. et al., (2005) *MURE : MCNP Utility for Reactor Evolution - Description of the methods, first applications and results,* European Nuclear Conference

[4] Ivan Oelrich, Federation of American Scientist, www.fas.org

[5] Stéphanie SALA, (1995) *Réduction de la radiotoxicité des déchets nucléaires à vie longue : études théoriques et stratégiques de la transmutation des actinides mineurs et des produits de fission dans les réacteurs électronucléaire*, PHD thesis, Université Aix-Marseille I

FRAMEWORK FOR THE MANUFACTURING DEVELOPMENT OF ADVANCED CERAMIC NUCLEAR FUELS

D.J. SHEPHERD M Eng (Hons) ProfGrad IMMM
NNL Fuel Technology, National Nuclear Laboratory Ltd.
NNL Preston Laboratory, Springfields, Salwick, Preston, Lancs. PR4 0XJ – UK

ABSTRACT

The manufacture of ceramic nuclear fuel is achieved by the conversion of source powders to densified pellets through a series of process steps: milling, granulating, pressing of 'green' pellets, high temperature sintering. The development of advanced high quality ceramic nuclear fuels requires the important properties of the fuel materials to be measured before and after each process stage in addition to logging key data from the equipment during processing.

Measured powder properties include chemical composition, morphology, particle size, flow behaviour and pour-tap densities. The strength, dimension, density and composition of green and sintered pellets should also be measured. Ceramographic cross-sections of sintered pellets should also be prepared in order to assess grain size and morphology, residual porosity and the presence of any inclusions or compositional segregation.

By gathering this data, the quality of the source material, the product and the processing can be carefully evaluated and compared. This information can then be utilised in order to continuously improve future processing to ensure an optimised product. Statistical design of experiments can be employed for process improvement trials. These may include investigating the effects of varying the process parameters including milling speed, pressing force and sintering atmosphere as well as the effect of any process additives such as milling lubricant, sintering pore formers or pressing binder.

This paper draws on the manufacturing experience of the National Nuclear Laboratory to discuss methodologies and best practice for the development of advanced ceramic nuclear fuels such as advanced UO2, MOX, carbides and thorium-containing fuels.

1. The Manufacture of High Quality Nuclear Fuel

The principle of manufacturing high quality ceramic nuclear fuel is a simple one and one which applies to all other forms of quality materials manufacture. That principle is to measure the relevant properties of the material before and after each production stage as well as measuring all the relevant process data during production. Is this manner, the production engineers will have all the information that they need in order to either control or to improve the process.

However, applying this principle in practice may be far from straightforward for a number of reasons. Measurement is time consuming and costly and there are an extraordinarily large number of material properties and process data that can be measured and therefore it is not practical to measure them all. Selecting the relevant measurements to make is crucial as is the frequency at which are they made. This is where both a statistical approach and production experience must be applied in order to achieve the right balance between scientific and commercial considerations.

In addition, over and beyond the production difficulties of high quality materials manufacture, the fabrication of nuclear fuel is hampered by the uniquely hazardous nature of the materials involved and the accompanying safety restrictions.

2. Example Ceramic Fuel Process Sheet

Figure 1 shows an example powder process flow sheet for the production of conventional ceramic nuclear fuel (uranium dioxide – UO_2 based e.g. MOX) alongside some example parameters, process data, additives and measurable material properties.

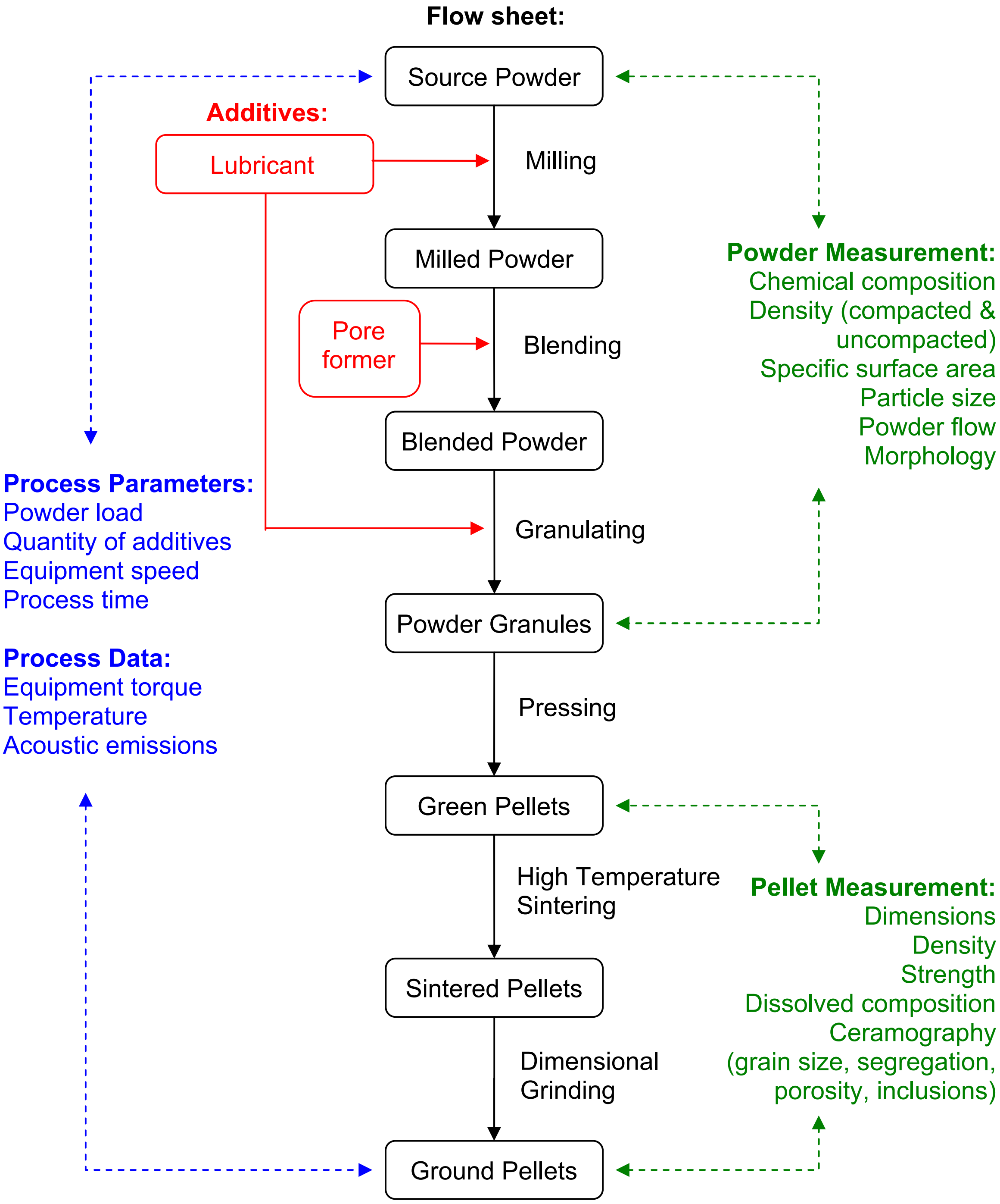

Figure 1: Example ceramic nuclear fuel powder process flow sheet

2.1 Properties of Source Powders

The powder properties of the source powders can be assessed by measuring the un-compacted (pour) and compacted (tap) densities as well as by shear cell testing and the measurement of other powder flow properties as necessary using a rheometer. The powder morphology can be examined using Scanning Electron Microscopy (SEM). The particle size and Specific Surface Area (SSA) should also be measured. The chemical composition of the source powder will be measured such as Mass Spectroscopy (MS).

2.2 Milling/Blending

If source material is not of the correct powder particle size, then milling is necessary in order to reduce the powder particle size to the necessary degree. The addition of a solid state milling lubricant is usually required. Milling also has the benefit of heating the powder and driving off moisture, which allows for better flow. In addition milling may be necessary in order to allow the incorporation into the process of any recycled material (sintered or otherwise) that may also need particle size reduction. The addition of appropriately treated recycled material (residues or out-of-specification product) allows the process to minimise waste and reduce the associated environmental footprint. The presence of recycled material may also help to improve the flow of powders.

An incorporated or separated blending stage may also be necessary in order to ensure a homogeneous mixture for fuels that incorporate recycled material and/or utilise more than one different specification of source fissile/fertile nuclear material. This could be different isotopic enrichments of U or additional plutonium in the case of mixed U, Pu oxide (MOX) fuel. A pore-forming additive may also be added at this stage to control density in sintering.

There are a number of different parameters that can be optimised for milling and blending such as equipment speed and process time. In addition, there are various process data items that can be logged such as equipment torque, temperature and acoustic emissions. The same powder properties for milled and blended powders should be measured as for the source powders in order to allow comparison.

2.3 Granulating

Milled, blended powders with a small particle size have a very high specific surface area and tend not to flow very well due to the predominance of interparticle forces and adhesion to the process equipment over gravitational forces. Powders need to flow well in order to allow for good pressing and therefore an additional granulation stage is needed that allows for the selective compaction of groups of individual powder particles into agglomerates. Solid state lubricant is also used for this stage. These granules are able to flow to much better and will allow for successful pressing. Similar parameters can be optimised for granulating as for milling and blending and similar process data logged. Again the same powder properties should be measured for the granules.

2.4 Pressing

The granules are formed into pre-densified ‘green’ pellets using a pelleting press. The correct pressing parameters such as pressing speed, force and ‘hold-down’ time must be used in order prevent defects such as ‘end-capping’ where one pellet end is weak and may fracture upon press release or subsequently during sintering. This weakness can be detected in un-fractured pellets by immersing in methanol and observing for bubbles. Pellets are weighed and the dimensions are measured in order to calculate the green density. Sample green pellets can also be tested for strength.

2.5 Sintering

The green pellets are then sintered in a furnace at very high temperature (e.g. 1750°C) with a carefully controlled atmosphere and time-temperature profile. This ensures that the pellets are densified to the correct degree with the burning out of the pore-former ensuring that pores are small, evenly distributed and not interconnected (i.e. closed). Sintered pellet density can then be measured accurately by immersion along with sintered pellet strength for sample pellets. Sintered pellets will inevitably have a variation in diameter along their length and the degree of ‘wheatsheaf-ing’ or ‘bowing’ can be assessed (this will be removed by a final grinding stage which is not discussed in this paper). Sintered pellets can be dissolved in order to assess the chemical composition against the Quality Assurance (QA) specification for the fuel. Ceramography can be performed to produce ground, polished cross-sections of pellets which can by analysed using optical microscopy for pore and grain size distribution as well as the presence of any inclusions. Energy Dispersive X-ray Spectroscopy (EDX/EDS) can be used to qualitatively map any compositional segregation and to examine the composition of any inclusions in order to determine their source.

3. Development of Advanced Ceramic Fuels

Advanced ceramic fuels will be required for Generation III/III+ and IV reactors. The development of these materials will present a number of challenges for nuclear laboratories.

3.1 Advanced UO_2

Advanced UO_2 fuels will aim to be able to achieve higher burn-up in reactors for the same volume of fuel compared with current fuels [1], which could be achieved in a number of ways. Doped fuels have been experimented with for a number of years and these will either necessitate separate fuel production lines or present significant challenges in terms of clean-out of equipment and impurity control. The use of burnable neutron ‘poisons’ such as gadolinia may be particularly problematic as currently considerable effort is expended in the exclusion of these chemicals from the fuel cycle. Other options for enhanced burnup are ‘duplex’ fuels where pellets may have an inner core at a different enrichment but again this will either require separate lines or a time-consuming clean out process and will also complicate uranic accountancy. The pressing of such pellets would require multiple stages. By contrast annular pellets with a hollow core have been proposed in order to allow for so-called ‘dual-cooled fuels’ with additional cooling via a central cladding tube. This is not anticipated to present as great an issue for development, particularly in the UK, as annular pellets have been produced for many years for the British Advanced Gas-cooled Reactors (AGRs).

3.2 Carbide/Nitride Fuels

The development of carbide and nitride fuels is desirable as MOX fuels have high breeding gains (less proliferation resistant) and also because carbide/nitrides have greater thermal conductivity than oxides [1]. The production of these fuels requires additional chemical processing stages. Also both materials (especially nitrides) are much harder than oxides and this makes them more difficult to mill. Development is significantly hampered by pyrophoricity (carbide more than nitride) and the need to use an inert atmosphere. This provides a number of challenges for process stages such as pressing, sintering and ceramography.

3.3 Thorium (Th)-containing Fuels

Th has been increasing proposed in recent years as an alternative to the U-base fuel cycle for which various potential advantages and disadvantages have been cited [2]. From a practical point of view in a development laboratory, Th may have more significant dose implications than U and this presents a number of challenges for the development of Th-containing fuels in laboratories that have primarily focused on the U-based fuel cycle. Contamination controls may be stricter and may include a greater shielding requirement. In addition, nuclear material accountancy will be more complicated and new recycle or disposal routes will need to be proven.

3.4 Inert Matrix Fuels (IMFs) or Dispersion Fuels

The use of IMFs or dispersion fuels has been considered for a number of years as a means of utilising and disposing of Pu or minor actinides in a once-through cycle with no Pu breeding [1]. Yttria-stabilized zirconia (YSZ), zirconium carbide (ZrC) and silicon carbide (SiC) have been suggested as ceramic inert matrices. Dispersion fuels such as pelletized particle or prismatic fuels have been suggested where coated fuel particles, such as the TRISO particles developed for High Temperature Reactors (HTRs), are pressed into pellets which can then be utilised in standard fuel pins rather than ‘pebble beds’. One of the benefits of pelletized particle fuels would be greater fission product retention. The primary challenge for the development of IMFs and dispersion fuels is limited experience of the radically different production flow sheets that will be needed for the production of these novel fuels.

3.5 Advanced Pu or Minor Actinide (MA)-containing Fuels

Pu-containing fuels (MOX, mixed carbides) can only be developed in highly specialised glovebox laboratories such as NNL’s Central Laboratory at Sellafield. There is a limited number of such facilities worldwide. Development work with Pu should be minimised as much as possible for reasons of operator dose and work within a Pu-glovebox environment is significantly physically impaired even compared with U-gloveboxes due to the additional shielding requirements. The situation will be even worse for fuels containing MAs such as Americium (Am) as these may have even more significant dose implications than Pu.

For this reason Pu/MA fuel development may be increasingly performed using simulant materials in uranic laboratories (such as NNL Preston Laboratory) or non-active laboratories with Pu and MAs only used in the very final stages of development. Non-radioactive substitutes with similar crystal structures may be used such as a Cerium Oxide (CeO_2) instead of PuO_2 or Neodymium Oxide (Nd_2O_3) instead of Am_2O_3. In addition fuels will only ever contain a small proportion of Pu or MAs (maximum 20%) and so in line with current practice, it will be acceptable to initially perform most of the development using the majority component only (U-based, Th-based, IM) or the majority component with a substitute before proceeding to final Pu/MA trials.

4. Conclusions

The development of advanced ceramic nuclear fuels is a considerable challenge and significant effort will be required to successfully develop these fuels on a laboratory scale in order to underpin any larger scale production activities. Any development must always consider the end goal and laboratory processes must ensure that they are scalable to meet larger production requirements.

5. References

[1] Development status of metallic, dispersion and non-oxide advanced and alternative fuels for power and research reactors; IAEA-TECDOC-1374; 2003
[2] The Thorium Fuel Cycle: An independent assessment by the UK National Nuclear Laboratory; NNL Position Paper; 2010

FABRICATION OF (U,Am) MIXED-OXIDE FUELS FOR TRANSMUTATION

F. LEBRETON, D. HORLAIT, T. DELAHAYE
CEA, DEN, DTEC/SDTC/LEMA, CEA Marcoule
30217 Bagnols-sur-Cèze cedex – France

P. BLANCHART
GEMH/ENSCI, Université de Limoges
12, rue Atlantis, 87065 Limoges – France

ABSTRACT

In the framework of minor actinide transmutation in heterogeneous mode, its application to americium through $U_{1-x}Am_xO_{2\pm\delta}$ MABB (Minor Actinide-Bearing Blanket) fuels represents a major research focus. Recently, two experimental irradiations of $U_{1-x}Am_xO_{2\pm\delta}$ fuels were programmed: *MARIOS* and *DIAMINO*, for which dense fuels were fabricated using two different processes, hence discrepancies in their characteristics. Here, we use dilatometric measurements to explain the differences observed. Notably, we describe the reasons for the limitations in terms of density of the process used for MARIOS, and how these limitations were overcome for *DIAMINO* with the development of the *UMACS* process.

1. Introduction

Minor actinides (MA: neptunium, americium and curium) produced in nuclear reactors during irradiation of UOX (uranium dioxide) or MOX (mixed uranium plutonium dioxide) fuels represent a large part of the radiotoxicity of nuclear waste. After 100 years of storage, they are the second-largest (after plutonium) contributor to radiotoxicity and heat generation [1]. Application of P&T (partitioning and transmutation) to these elements is thus of great interest in order to reduce the radiotoxicity of spent fuels, especially in countries where plutonium is already, or will be, recycled (e.g. France). Several scenarios of P&T are proposed, including the use of FNR (fast neutron reactors) or ADS (accelerator-driven systems), and taking into account the possibilities for recycling all minor actinides together, or separated from each other using a dedicated process. Considering transmutation in FNR, two modes are envisaged: homogeneous and heterogeneous. For the former, a low amount of minor actinides, inferior to 5 wt.%, would be added to MOX fuels [2] to be irradiated in assemblies in the whole core of the reactor. For the latter, a higher amount of minor actinides (between 10 and 20 wt.%) would be diluted in depleted UO_2, and the obtained fuels destined for specific assemblies located along the periphery of the core (known as the blanket region), hence their name: MABB (minor actinide bearing blanket).

Over the past few years, research has been focused on transmutation of americium in heterogeneous mode, considering the predominant impact of its isotopes on the radiotoxicity and heat generation of the MA. Thus, data on $U_{1-x}Am_xO_{2\pm\delta}$ MABB fuel behaviour during irradiation are required. To this purpose, two experimental irradiations were planned to acquire data describing the fuel behaviour during irradiation. The first one, *MARIOS* [3,4], was performed in *HFR* (Petten, Netherlands) from March 2011 to May 2012 (for a total of 305 equivalent full-power days), and was dedicated to the assessment of the influence of irradiation temperature, 1000 or 1200°C, on $U_{0.85}Am_{0.15}O_{2\pm\delta}$ fuels. The second, *DIAMINO* [5], should begin in 2013 in *Osiris* (CEA Saclay, France) and is complementary to *MARIOS* as two additional temperatures will be studied, 600 and 800°C, as well as two compositions, $U_{0.925}Am_{0.075}O_{2\pm\delta}$ and $U_{0.85}Am_{0.15}O_{2\pm\delta}$.

In addition to temperature and composition, the influence of the fuel microstructure is also considered in both experiments, through the comparison of two microstructures. The first one is the current standard microstructure of oxide fuels, i.e. dense fuels with a density above 93% TD (theoretical density) and less than 3 vol.% of open porosity. The second, referred to as “tailored open porosity”, consists of fuels exhibiting lower densities, below 88%TD, and more than 9 vol.% of open porosity. The purpose of these porous fuels is to take into account the considerable gas release (He and fission products) from fuels containing a significant amount of americium, and to try to reduce the swelling of these pellets during irradiation. In this paper, we focus on the fabrication of dense fuels of composition $U_{0.85}Am_{0.15}O_{2\pm\delta}$.

2. Fuels fabricated for MARIOS and DIAMINO

For these two experiments, the R&D on fabrication processes and the fuel fabrications were performed in dedicated hot cells and glove-boxes in the *Atalante* facility (CEA Marcoule, France). Several processes were thus developed in order to obtain fuels complying with the specifications.

For *MARIOS*, a *MIMAS*-like process was used, consisting, as presented in Fig 1 (left), of a reactive sintering of pellets prepared from a mixture of AmO_2 and UO_2 powders. In such a process, solid solution formation and densification thus have to occur during a single heat treatment, i.e. at the same time. This process produced fuels with a density close to 92%TD (theoretical density), which is just under the requirement of 93%TD; consequently, the open porosity ratio was too high [3]. Moreover, heterogeneous microstructure and distribution of porosity were obtained, as seen in Fig 2 (left). These fuels were however used for *MARIOS*, as they were considered to be close enough to its requirements.

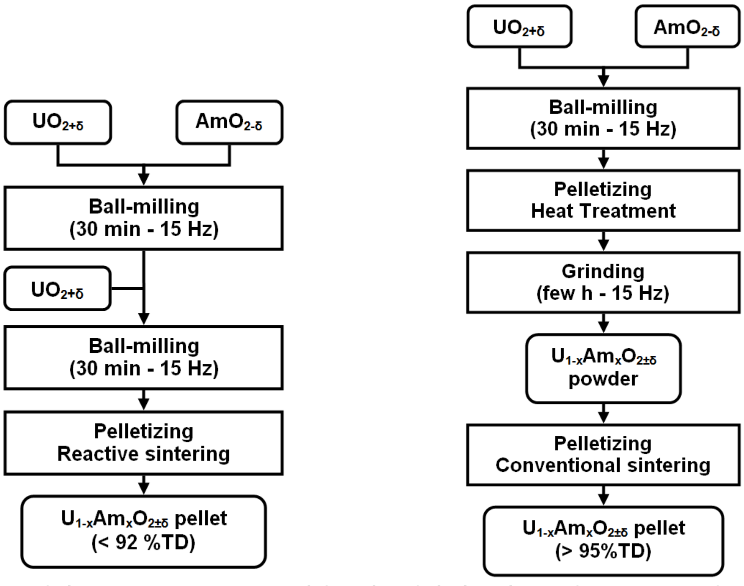

Fig 1. Flow charts of the processes used for the fabrication of *MARIOS* fuels: “*MIMAS*-like” (left), and *DIAMINO* fuels: *UMACS* (right).

To avoid the same limitations for *DIAMINO*, a new process, called *UMACS* (uranium-minor actinide conventional sintering), allowing the dissociation of the solid solution formation and the actual sintering, was developed. As seen in Fig 1 (right), it is composed of two successive thermal treatments separated by a grinding step. The first is used to synthesise the $U_{1-x}Am_xO_2$ solid solution via a solid-state reaction between UO_2 and AmO_2, the second is fully dedicated to the densification. Using this process, fuels with densities close to 95%TD were obtained, with open porosity ratios under the limit of detection (around 1 vol.%) [5]. In this case, a more homogeneous microstructure was obtained, as seen in Fig 2 (right).

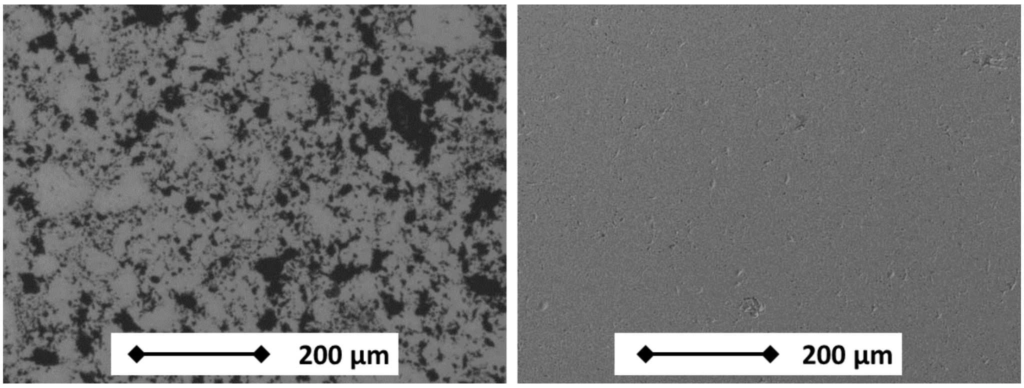

Fig 2. Micrographs of dense $U_{1-x}Am_{x}O2$ fuels for (left) *MARIOS* and (right) *DIAMINO*.

The discrepancies observed in sintered fuels suggest a different sintering behaviour for the two processes, which would be linked to the occurrence of the solid solution formation before (as in *UMACS*) or during (as in the *MIMAS*-like) the sintering. A comparison of dilatometric results obtained in both cases is used in the next sections to emphasize on this subject.

3. Experimental conditions

The UO_2 and AmO_2 powders are precursors already used for previous studies [5]. The two powders have similar morphologies, spherical agglomerates of submicronic particles, but the AmO_2 particles are around an order of magnitude larger. Thus, if the UO_2 powder seems suitable for sintering, with regards to its relatively high reactivity (5.6 $m^2.g^{-1}$), it is preferable to use at least one milling step for the AmO_2 powder, whose reactivity is assumed to be lower based on available data. Milling steps are thus included in both processes. The UO_2 powder also has a low level of impurities, whereas the AmO_2 has several per cent of impurities (mainly Ce, Na, Nd and Fe, as well as ^{237}Np from ^{241}Am α decay). The UO_2 powder is hyper-stoichiometric, whereas AmO_2 is expected to be hypo-stoichiometric.

For the *MIMAS*-like (*MARIOS*) process, two milling steps were used to homogenise the powder, and more particularly the distribution of AmO_2 particles in the mixture. These mixtures are ensured by milling performed in an oscillating ball-miller. For the first milling step, only half the UO_2 was inserted in the ball-miller. The remaining UO_2 was added before the second milling step. A pellet was then pressed from this mixture, up to around 60%TD.

For the *UMACS* process, a solid solution powder has to be synthesised from a powder mixture similar to that used for the *MIMAS*-like sample. The solid solution formation was performed for 4 h at around 2000 K under an Ar/H_2 (1%)/O_2 (75 ppm) atmosphere using pelletized samples. These conditions were chosen based on a HT-XRD (high temperature X-ray diffraction) study describing the $U_{1-x}Am_{x}O_{2\pm\delta}$ solid solution formation [6]. The monophasic pellets obtained were ground for a few hours in a ball-miller with two stainless steel 12-mm-diameter balls. A pellet was then prepared from this batch with a green density close to 70%TD.

The dilatometric measurements were performed using a horizontal *Netzsch* dilatometer. Its sample chamber is made of graphite, except for all parts in contact with the samples, which are tungsten. Measurements were performed in dynamic mode up to 2173 K, with a heating rate of 3 $K.min^{-1}$, under a reducing Ar/H_2 (4%) atmosphere. For each experiment, the pellet samples were weighed and measured before and after sintering in order to calculate their geometrical densities. XRD (X-ray diffraction) analyses were performed on powdered samples after sintering to check the completion of the solid solution formation, which was achieved in both cases.

4. Results and discussion

Fig 3 presents the relative shrinkage (dL/L_0, L_0 being the initial sample length) obtained for each pellet as a function of temperature, as well as their respective shrinkage rates, i.e. the derivatives of dL/L_0 as a function of the temperature. It has to be noted that a quantitative comparison between the shrinkage rate curves cannot be performed, as the two pellets exhibit different green densities, which has a “scale” influence on the shrinkage rate; a qualitative comparison remains, however, relevant.

The results for the reactive sintering show that the shrinkage begins around 1000 K and is slowed between 1200 and 1400 K. It then accelerates up to 1700 K, temperature at which it slows again until 1850 K, and reaccelerates at higher temperature. The final density was measured at 84.5(5)%TD. In this particular experiment, the maximum temperature was limited to 1940 K for technical reasons, which means that low density obtained cannot be considered a representative result. In the case of the conventional sintering, the shrinkage begins around 1200 K and progressively accelerates until around 2000-2100 K. At higher temperature, the shrinkage rate drops off, indicating the end of the densification. A final density of 95.4(5)%TD is reached, corresponding to what was obtained for the *DIAMINO* fabrication.

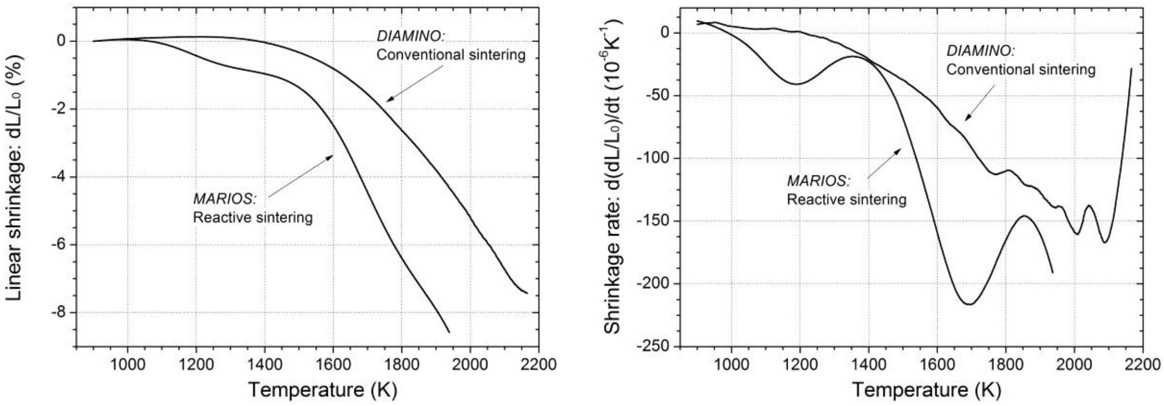

Fig 3. Dilatometric curves of *MIMAS*-like and *UMACS* process: (left) linear shrinkages and (right) shrinkage rates.

When the two sintering processes are compared, it can be seen that the reactive sintering begins around 200 K lower than in the case of the *UMACS* process. At such a temperature, however, interdiffusion between U and Am has not begun and thus sintering of only UO_2 (or only AmO_2) particles together is activated. Considering the low amount of AmO_2 in the powder mixture, only the self-sintering of UO_2 can be efficient and lead to a macroscopic shrinkage, which is confirmed by the comparison of the sintering of other similar systems [7]. In the case of the *UMACS* process, the increase in starting temperature is caused by the cation charge distribution in the solid solution: due to the presence of three different cations (U^{+IV}, U^{+V} and Am^{+III}) [8], the iono-covalent nature of bonds is greater, which reduces the cation mobility [9].

At higher temperatures, larger differences between the two processes appear. The main two are the two decreases of the shrinkage rate in the case of the reactive sintering, which are not present for the conventional sintering. Indeed, the latter exhibits a behaviour close to that found for standard sintering of monophasic powder, such as UO_2: the shrinkage rate progressively increases up to a maximum value after what it quickly decreases, indicating the end of the sintering. In the case of the reactive sintering, however, the observed decreases are the sign of a more complex behaviour. Notably, the first one is also found to occur in similar systems such as UO_2-CeO_2 [7], UO_2-Gd_2O_3 [10] or UO_2-Nd_2O_3 [11] and was clearly identified as a consequence of the solid solution formation: as long as U/Am interdiffusion has not started, shrinkage is precluded, as only UO_2 particles can sinter together. Even when the solid solution begins to form, a competition occurs between the solid solution formation and its densification, which delays the latter as long as the former is not finished. The second decrease of shrinkage rate observed only in the case of the reactive sintering confirms that the solid solution formation strongly impedes the densification. These results are thus consistent with the limitations in terms of density observed in the case of *MARIOS*, and the improvement of the fuel microstructure for *DIAMINO*. In general, the use of a monophasic powder (obtained by a solid-state reaction, or by another route, such as oxalic co-precipitation [12]) should thus be preferred, as it avoids the competition between the solid solution formation and the densification, as well as the emergence of an additional porosity by the Kirkendall effect (caused by differences in diffusion coefficients between U and Am) [5].

For the *UMACS* sample, the optimal temperature of sintering (i.e. the temperature at which the shrinkage rate is the highest) is found to be between 2000 and 2100 K. In the case of the *MIMAS*-like sample, considering that the formation of the solid solution is well-advanced, a similar temperature would presumably have been found if no technical reasons had limited the temperature to 1940 K. The plateau-temperature used for the sample fabrication for *MARIOS* and *DIAMINO*, 2023 K, was thus appropriate and did not limit the densification.

5. Conclusion

The processes used for the fabrication of dense $U_{1-x}Am_xO_2$ fuels for *MARIOS* and *DIAMINO* experimental irradiations were compared using dilatometric results. Their main difference is the use of a reactive sintering in the case of *MARIOS*, while a conventional sintering is used for *DIAMINO*, where the solid solution is formed via a solid-state reaction during a dedicated thermal treatment (*UMACS* process). Dilatometric studies show that the occurrence of the solid solution formation and the densification during the same thermal treatment slows the shrinkage and delays the densification. Thus, this explains why only limited densities (up to around 92%TD) were obtained for *MARIOS*, whereas higher densities (up to 95%TD) were reached for *DIAMINO*.

6. References

[1] M. Salvatores, *Nucl. Eng. Des.* **235** (2005) 805-16.
[2] F. Lebreton, D. Prieur, A. Jankowiak, M. Tribet, C. Leorier, T. Delahaye, L. Donnet, P. Dehaudt, *J. Nucl. Mater.* **420** (2012) 213-217.
[3] D. Prieur, A. Jankowiak, T. Delahaye, N. Herlet, P. Dehaudt, P. Blanchart, *J. Nucl. Mater.* **414** (2011) 503-7.
[4] E. D'Agata, P.R. Hania, S. Bejaoui, C. Sciolla, T. Wyatt, M.H.C. Hannink, N. Herlet, A. Jankowiak, F.C. Klaassen, J.-M. Bonnerot, *Nucl. Eng. Des.* **242** (2012) 413-419. .
[5] T. Delahaye, F. Lebreton, D. Horlait, P. Dehaudt, *J. Nucl. Mater.* **432** (2013) 305-12.
[6] F. Lebreton, R.C. Belin, D. Prieur, T. Delahaye, P. Blanchart, *Inorg. Chem.* **51** (2012) 9369-75.
[7] D. Horlait, A. Feledziak, F. Lebreton, N. Clavier, D. Prieur, N. Dacheux, T. Delahaye, submitted to *J. Eur. Ceram. Soc.* (2012).
[8] D. Prieur, P. M. Martin, A. Jankowiak, E. Gavilan, A. C. Scheinost, N. Herlet, P. Dehaudt, P. Blanchart, *Inorg. Chem.* **50** (2011) 12437-45.
[9] D. Horlait, F. Lebreton, T. Delahaye, P. Blanchart, P. Dehaudt, submitted to *J. Eur. Ceram. Soc.* (2012).
[10] M. Durazzo, F.B.V. Oliveira, E.F. Urano de Carvalho, H.G. Riella, *J. Nucl. Mater.* **400** (2010) 183-8.
[11] M. El-Sayed, R. Lorenzelli, *J. Nucl. Mater.* **87** (1979) 90-6.
[12] B. Arab-Chapelet, S. Grandjean, G. Nowogrocki, F. Abraham, *J. Nucl. Mater.* **373** (2008) 259-68.

ENC 2012

EUROPEAN NUCLEAR CONFERENCE

POSTER:

FUEL CYCLE

THE EFFECT OF TEMPERATURE AND STRESS ON HYDRIDE REORIENTATIONS OF HIGH BURNUP CLADDINGS UNDER INTERIM DRY CONDITIONS

KYU-TAE KIM, MYEONG-SU KIM, SU-JEONG MIN
Nuclear and Energy Engineering Department, Dongguk University
123, Dongdae-Ro, Gyeongju, Republic Of Korea, 780-714

ABSTRACT

Interim dry storage of spent nuclear fuel has been considered as an option for increasing spent fuel storage capacity in Korea. It is generally known that hydride reorientation from the circumferential to radial direction may reduce the critical stress intensity that accelerates radial crack propagation. In this work, the integrity of high burnup spent fuel during the interim dry storage was investigated, simulating interim dry storage and high burnup fuel conditions and using unirradiated Zr-Nb alloy claddings. First of all, mechanical property degradations of the as-received and hydrogen-charged Zr-Nb alloy claddings were generated at various temperature conditions. The effect of holding times at the solution temperature of 300°C under the tensile hoop stress of 300MPa on the mechanical properties of the hydrogen-charged Zr-Nb alloy claddings was also investigated. Then, the effects of cooling rate under the tensile hoop stress of 150MPa on hydride reorientation were investigated. It is found that the mechanical properties of the Zr-Nb claddings are strongly related to temperature, holding time and hydrogen content. In addition, the extent and morphology of radial hydride formed during the cooling process depends on cooling rate from the solution temperature of 400°C.

1. Introduction

The Korea Institute of Nuclear Safety (KINS) is focusing on the transportation and interim dry storage of high burnup fuel because high burnup fuel is known to have degraded mechanical properties, as compared to lower burnup fuel. It has been reported that the spent fuel cladding is the primary structural component during the transportation and interim dry storage, indicating that intact fuel claddings are being considered as a key barrier to retard radionuclide migration.

The mechanical properties of the Zirconium alloy claddings can be adversely affected by the presence of radial hydrides in the claddings [1-6]. The radial hydrides may be generated by a reorientation process when a specimen is cooled down under a tensile stress larger than a threshold value, which is a function of solution temperature and specimen hydrogen content, from the solution temperature at which some hydrides or all hydrides are dissolved.

In general, the Zirconium alloy claddings are subjected to ever-increasing internal pressure, oxide layer thickness and hydrogen content as the fuel burnup increases. However, the higher tensile hoop stress will make hydrides in the cladding more susceptible to tensile stress-induced hydride reorientation in the radial direction when the cladding experiences a temperature variation during the reactor operations or under the interim dry storage conditions [7-10]. In detail, the radial hydride formation in the Zirconium claddings requires the dissolution of circumferential hydrides when the claddings are heated up to a solution temperature and then tensile hoop stresses larger than a threshold value is acting on the cladding during the cooling process. It has been reported that the radial hydride formation during the cooling process is a complicated function of hydrogen solubility, hydrogen content, stress state, temperature, cooling rate and thermal cycling.

Therefore, the factors governing the radial hydride precipitation during the cool-down and the effect of the radial hydride on the cladding material degradation need to be investigated extensively. In this work, the as-received Zr-Nb alloy claddings and those charged with hydrogen up to 300 and 600ppm, respectively, were employed to examine the amount and morphology of the radial hydride formed under a constant tensile hoop stress with various cooling rates from the solution temperature of 400^{o}C as well as to measure the cladding mechanical property degradations. In addition, the effect of various holding times at 400^{o}C on the mechanical property degradation was also investigated.

2. Experimental

2.1 Materials and hydriding process

Stress-relief annealed Zr-Nb alloy claddings with an outside diameter of 9.5mm and a wall thickness of 0.58mm were employed. Its chemical composition is given in Table 1. Two cladding tubes, cut into 100mm length, were first uniformly hydrogen-charged by a mixed gas of 150torr H_2 and 200torr He at 400^{o}C. Then, the hydrogen-charged tubes were heat-treated for 24hrs at 400^{o}C in a vacuum to homogenize hydrogen distribution in the cladding tubes. The target hydrogen levels ranged from 300 and 600 ppm. Hydrogen concentrations of the cladding tubes were determined by an inert-gas fusion method using a LECO RH-600 hydrogen determinator. Typically hydrides were oriented in the circumferential direction and homogeneously distributed across the cross-section of the cladding specimens.

Table 1. Chemical composition of Zr-Nb alloy cladding (wt%)

Nb	Sn	Fe	Zr
1.0	1.0	0.1	Balance

2.2 Mechanical tests

As shown in Fig. 1, dog bone-shaped ring specimens with a width of 5mm, a gauge length of 2mm and a gauge width of 2mm were cut transversely from the as-received and hydrogen-charged cladding tubes.

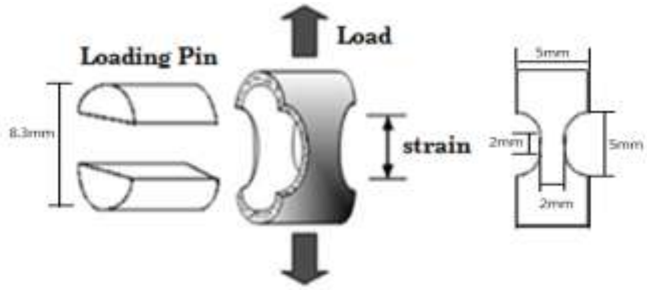

Fig. 1. Configurations of specimens and loading pins

Three kinds of mechanical tests were performed using the dog bone-shaped ring specimens and the Instron-3366. The first mechanical tests were carried out for the as-received and 600ppm hydrogen-charged Zr-Nb alloy cladding specimens at temperatures of 200, 300 and 400^{o}C at a strain rate of 0.12mm/min to examine the effect of temperature and hydrogen content on the cladding mechanical properties. The specimens were heated at a heating rate of 2.5^{o}C/min with no stress applied. The second mechanical tests were performed at 300^{o}C for the 600ppm hydrogen-charged Zr-Nb alloy cladding specimens after holding at 300^{o}C for 0, 4, 8 and 16hrs under a tensile hoop stress of 300MPa to investigate the effect of holding time on the mechanical property degradation. After the mechanical tests at 300^{o}C, fractured specimens were cooled in air to room temperature and then their microstructures were examined. The third mechanical tests, as shown in Fig. 2, were done for the hydrogen-charged specimens of 150, 300 and 600ppm at 200^{o}C after holding for 2hrs at 400^{o}C under a tensile hoop stress of 150MPa and then cooling to 200^{o}C at a cooling rate of 2.5^{o}C/min maintaining the same hoop stress to evaluate the effect of hydrogen content on the amount and morphology of radial hydride formed during the cooling from 400 to 200^{o}C and subsequently on the mechanical property degradation. After the mechanical tests at 200°C, fractured specimens were cooled in air to room temperature and then their microstructures were examined.

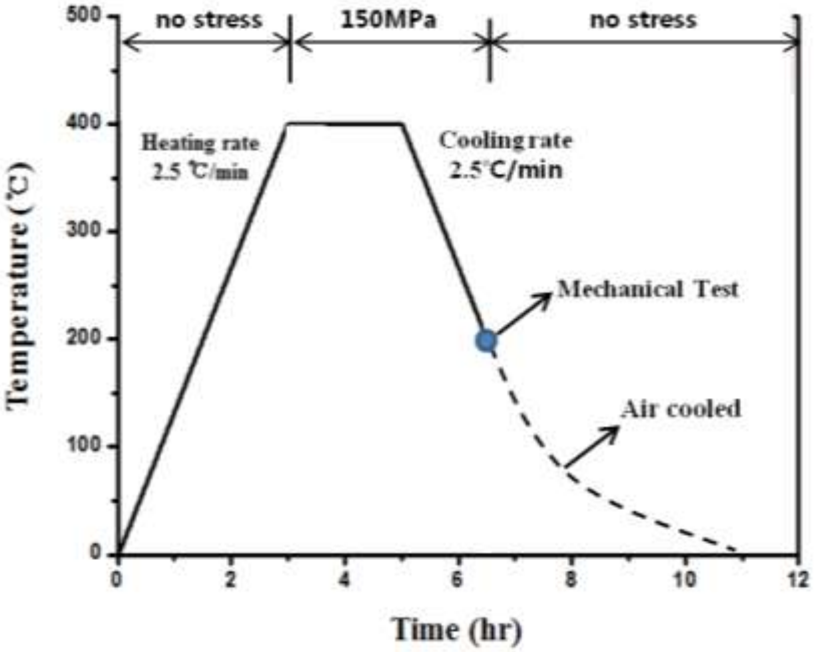

Fig. 2. Temperature and stress history for the mechanical tests at 200°C

2.3 Cooling rate-dependent radial hydride formation experiments

As shown in Fig. 3, the dog bone-shaped ring specimens containing 600ppm hydrogen concentration were employed to investigate the effect of cooling rate on the amount and morphology of radial hydride formed during the cooling to room temperature from 350°C. The Zr-Nb alloy cladding specimens were heated to 350°C at a heating rate of 3.5°C/min with non tensile hoop stress and then maintained for 4hrs at 350°C under a tensile hoop stress of 150MPa. After completing the holding, the specimens were cooled down to room temperatures at cooling rates of 2, 4 and 15°C/min, respectively, under a tensile hoop stress of 150MPa. And then the amount and morphology of the specimens were generated through microstructure examinations.

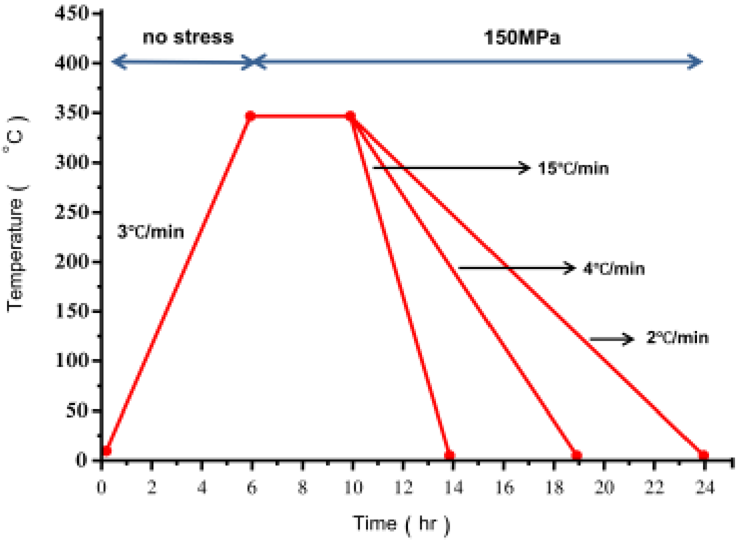

Fig. 3. Cooling rate history for the mechanical tests and hydride reorientation.

2.4 Microstructure examinations

Standard metallographic technique was followed to reveal the hydride morphology, its size and distribution using optical microscopy with the specimens etched in a solution of 10%HF-45%HNO_3-45%H_2O. The specimens were cut to generate faces parallel to the radial-circumferential plane of the cladding tube. In order to quantify the amount of the radial hydrides, the fraction of the radial hydrides was evaluated using Fn(40) [11], which is defined as follows;

$$\mathrm{Fn}(40) = \frac{\text{Sum of the number of hydrides in the radial direction } \pm 40^{\circ}}{\text{Sum of the number of all hydrides}}$$

3. Results and discussion

3.1 Effect of temperature and hydrogen content on mechanical properties

The first mechanical tests were carried out for the as-received and 600ppm hydrogen-charged Zr-Nb alloy cladding specimens at temperatures of 200, 300 and 400^{o}C. The test results are shown in Figs. 4 and 5. From these figures, the yield strengths and ultimate tensile strengths as well as elongations were calculated and summarized in Table 2.

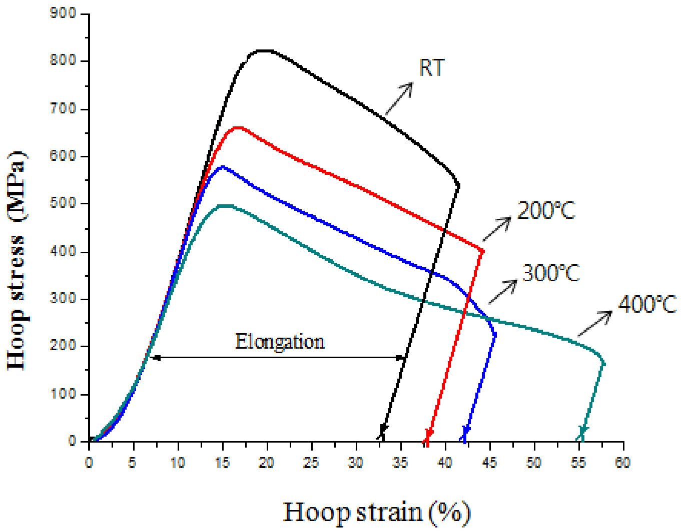

Fig. 4. Mechanical tests for as-received Zr-Nb alloy claddings at various temperatures.

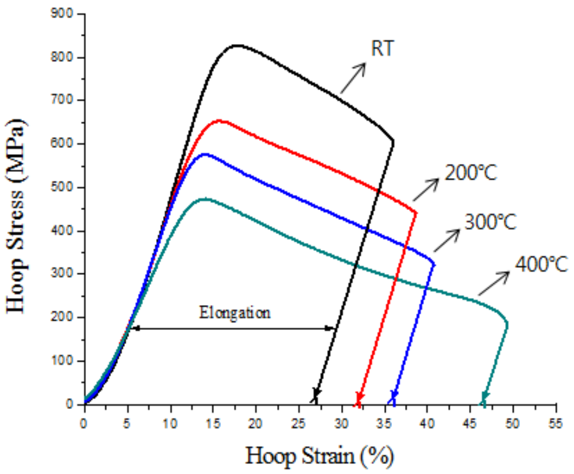

Fig. 5 Mechanical tests for 600ppm hydrogen-charged Zr-Nb alloy claddings at various temperatures.

Table 2. The effect of hydrogen content on mechanical property degradation

Hydrogen content (ppm)	Temperature (^oC)	Yield strength (MPa)	Ultimate tensile strength (MPa)	Elongation (%)
0	RT	760	822	29
	200	570	661	34
	300	525	575	39
	400	400	496	52
600	RT	780	825	24
	200	570	652	29
	300	497	575	33
	400	460	472	43

From Table 2, it can be said that the effect of hydrogen content on the yield strengths and ultimate tensile strengths of the Zr-Nb cladding is not considerable even though it was reported that yield strengths and tensile strengths will increase as hydrogen content in the cladding increases. However, the elongations of the 600ppm hydrogen-charged specimens are a little less than those of the as-received specimens, as expected.

3.2 Effect of holding time on mechanical properties

The second mechanical tests were performed at 300^oC for the 600ppm hydrogen-charged Zr-Nb alloy cladding specimens after holding at 300^oC for 0, 4, 8 and 16hrs under a tensile hoop stress of 300MPa to investigate the effect of holding time on the mechanical property degradation. The test results are shown in Fig. 6 and the yield strengths and tensile strengths are summarized in Table 3.

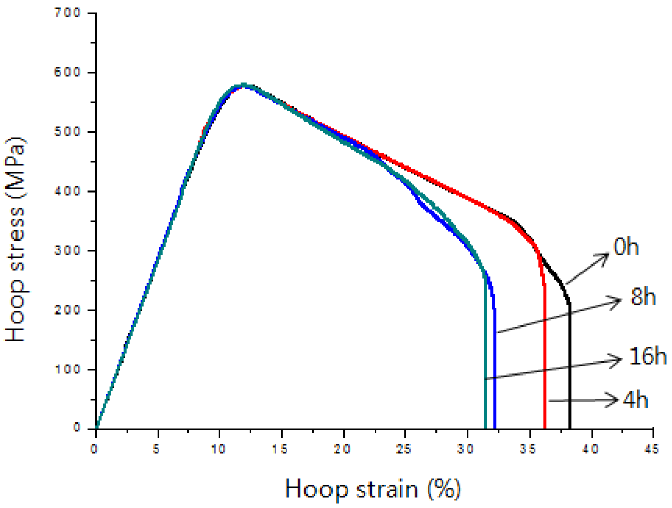

Fig. 6. Effect of holding time on the mechanical properties of 600ppm hydrogen-charged claddings.

Table 3. The effect of holding time on mechanical property degradations

Hydrogen content (ppm)	Temperature (^oC)	Holding time (hr)	Yield strength (MPa)	Ultimate tensile strength (MPa)	Elongation (%)
600	300	0	500	577	33
		4	498	575	29
		8	492	575	13
		16	535	578	11

From Table 3, it can be said that the effect of holding time on the yield strengths and ultimate tensile strengths is negligible except the yield strength for the 16hrs holding time, while the effect of holding time on the elongations are remarkable. The elongations for the 8 and 16hrs holding times were reduced considerably, compared to those for no holding time and 4hrs holding time. To investigate the reason for this behavior, the intact regions were cut from the fractured specimens and their microstructures were obtained, as shown in Fig. 7, which indicates that micro-cracks may initiate around the outer surfaces for up to the 4hrs holding time. Then, such micro-cracks might be growing into quite large cracks when the holding time increases to 8hrs and subsequently the crack growth might be retarded from the 8hrs to the 16hrs holding times. This may explain why there exists a large difference in the elongations between the 4hrs and 8hrs holding times.

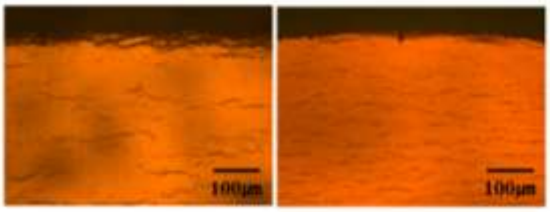

Zero holding time　　4hrs holding time

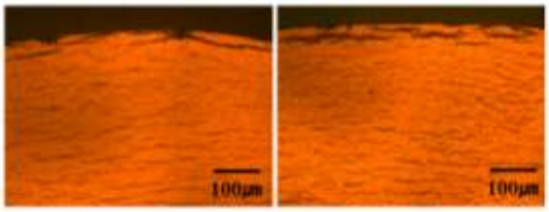

8hrs holding time　　16hrs holding time

Fig. 7. Holding time-dependent microstructure variation.

3.3 Effect of radial hydride morphology on mechanical properties

The third mechanical tests were done for the hydrogen-charged specimens of 150, 300 and 600ppm at 200°C after holding for 2hrs at 400°C under a tensile hoop stress of 150MPa and then cooling to 200°C at a cooling rate of 2.5°C/min maintaining the same hoop stress in order to evaluate the effect of hydrogen content on the amount and morphology of radial hydride formed during the cooling from 400 to 200°C and subsequently on the mechanical property degradation. The test results are shown in Fig. 8 and summarized in Table 4. From this figure, it can be seen that the 600ppm specimen is the most ductile, while the 150ppm specimen the most brittle.

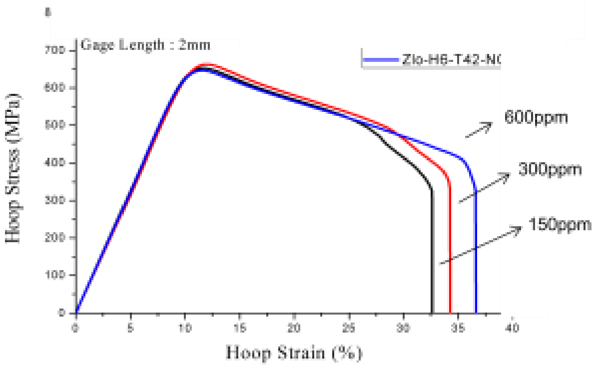

Fig. 8. Mechanical tests at 200 °C for hydrogen-charged Zr-Nb alloy claddings after cooling from 400 to 200 °C.

This can be explained by the morphologies of the specimens, as shown in Fig. 9. This figure indicates that the fraction of the radial hydrides is largest for the 150ppm specimen, while the fraction is about the same for the 300 and 600ppm specimens. In addition, the average lengths of the radial hydrides are 40, 36 and 26um for the 150, 300 and 600ppm specimens, respectively. It is noteworthy that the larger fraction and length of the radial hydrides may generate the more brittle cladding materials. Therefore, the 150ppm specimen generated the least elongation.

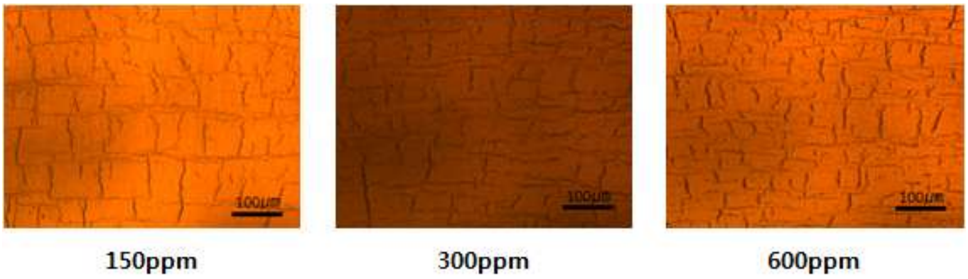

150ppm 300ppm 600ppm

Fig. 9. Hydrogen contents-dependent microstructure variation.

Table 4. The effect of radial hydride morphology on mechanical property degradations

Temperature (^oC)	Hydrogen content (ppm)	Yield strength (MPa)	Ultimate tensile strength (MPa)	Elongation (%)
200	150	610	653	27
	300	620	663	20
	600	600	647	18

3.4 Effect of cooling rate on the amount and morphology of radial hydrides

The specimens containing 600ppm hydrogen concentration were employed to investigate the effect of cooling rate on the amount and morphology of radial hydride formed during the cooling to room temperature from 350^{o}C. The optical micrographs are shown in Fig. 10. From this figure, it can be seen that the faster cooling rate generated the less amount and the shorter length of the radial hydrides.

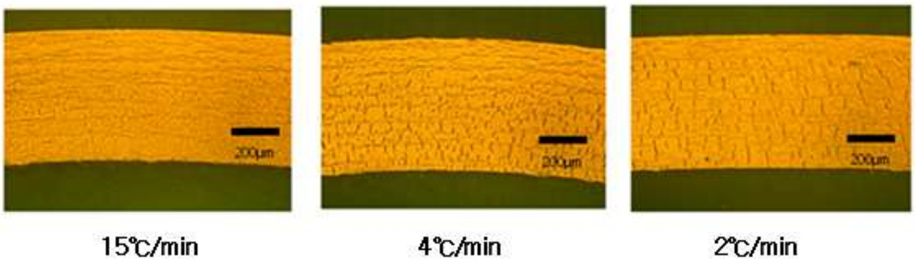

15℃/min 4℃/min 2℃/min

Fig. 10. Cooling rate-dependent microstructure variation.

4. Summary

- The effect of hydrogen content on the yield strengths and ultimate tensile strengths of the Zr-Nb cladding is not much large but the cladding ductility is reduced with a higher hydrogen content of 600ppm.
- The effect of holding time at 400^{o}C on the 600ppm hydrogen-charged cladding ductility is remarkable. The holding times of as much as 8hrs reduced the ductility drastically, which is may be related to micro-crack initiation and subsequent growth around the outer surfaces of the cladding specimens.
- The effect of initial hydrogen content in the cladding on the amount and morphology of radial hydrides are significant. The 150ppm hydrogen-charged cladding specimens generated larger fraction and shorter length of radial hydrides when cooling from 400 to 200oC under a tensile hoop stress of 150MPa, compared to the 300 and 600ppm

specimens.

- The faster cooling rate from 350°C to room temperature generated the less amount shorter length of radial hydrides for 600ppm specimens.
-

5. References

[1] R.P. Marshall, M.R. Louthan Jr., Trans ASM 56(1963)693.

[2] M.R. Louthan Jr., R.P. Marshall, J. Nucl. Mater. 9(2) (1963)170.

[3] R.N. Singh, R. Kishore, S.S. Smith, T.K. Sinha, B.P. Kashyap, J. Nucl. Mater. 325(2004)26

[4] S.I. Hong, K.W. Lee, J. Nucl. Mater., 340(2005)203.

[5] H.C. Chu, S.K., Wu, K.F. Chien, R.C. Kuo, J. Nucl. Mater. 362(2007)93

[6] H.C. Chu, S.K. Wu, R.C. Kuo, J. Nucl. Mater. 373(2008)319.

[7] R.P. Marshall, J. Nucl. Mater. 24(1967)34.

[8] R.P. Marshall, J. Nucl. Mater. 24(1967)49.

[9] J.J. Kearns, C.R. Woods, J. Nucl. Mater. 20(1966)241

[10] M. Leger, A. Donner, Can. Metall. Q. 24(3)(1985)235.

[11] T. Oohama, M.Okunishi, Y. Senda, K. Murakami, M. Sugano, the 6th International Conference on Nuclear Thermal Hydraulics, Operations and safety (NUTHOS-6), Nara, 2004.

ON-LINE QUANTITATIVE ANALYSES OF URANIUM IN MINING OPERATIONS

A. SOKOLOV, E. HASIKOVA, V. TITOV, A. ROZITE

Baltic Scientific Instruments, LV-1005, Riga, Latvia

ABSTRACT

At present article we present the results of uranium content determination in various ores and materials using on-line X-ray fluorescent analyzer Con-X. We demonstrate that on-line quantitative and semi-quantitative analysis on conveyor belt is possible from 100 ppm level up to 80% of uranium and more. When uranium is present in concentrations below about 1%, its detection limit in 5 minutes of measurement time is about 60-200 ppm even in the worst cases (presence of strong neighbouring Th XRF lines). Precision of its content determination in the same conditions is about 50-150 ppm. Relative precision of its content determination decreases when uranium concentration is higher. It becomes better than 1% (relative) in the concentrated product. The developed uranium measurement method provides simultaneous measurement of concentrations for more than 20 elements.

1. Introduction

The production of uranium is the basis of the entire nuclear fuel cycle [1]. Uranium (U) is characterized by considerable scattering in rocks, soils and sea water. Only rather small part is concentrated in fields where the content of uranium in hundreds times exceeds its average content in crust. Production of uranium ore is carried out in the basic either mine or career way – depending on a depth of ore layers. In 2011, 30% of the world's uranium production was the share of the underground mines, 17% were the share of open fields (pits), in-situ leaching accounted for 45%, and the remaining turned out as a by-product in the developing of other mineral resources [2].

At present, it is considered economically feasible to process ores with (0.05-0.07) % uranium oxide content. One thousand metric tons of uranium ore that contains 0.1% uranium has to be withdrawn from the depth of the earth to produce each 1 ton of uranium oxide, U_3O_8, without considering enormous amount of dead rock from the open and tunnel dredging.

It is reasonable to process and enrich such huge mass of ore in the close proximity to mines. The complex processing of uranium ore with the simultaneous extraction of the other valuable components (phosphorus, vanadium, sulphur, molybdenum, gold, copper and rare-earth elements) becomes an increasingly wide practice [2]. On-site processing requires prompt quantitative methods for the determination of the uranium and other valuable elements in the ore. X-Ray fluorescence (XRF) is the method that can be used for the analysis of uranium raw materials [3].

We present the results of determination of uranium content in various ores and materials using a Con-X on-line XRF analyser [4]. On-line analysis of material composition becomes possible only if the results are independent of variations in external parameters, such as temperature and humidity of the analysed material and in the analyser environment, variations in the material lump size and height, etc. The Con-X analyser has been designed to account for these variations [4]. Specifically designed software uses X-ray spectra to account for changes in the distance to the measured material, which provides the user with the correct results irrespective of the material flow rate. Variations in the humidity levels are also accounted for if they are found to affect the measurement results.

2. Analysis of uranium as trace element

The Con-X on-line XRF analyser is able to detect and estimate the uranium content in various materials in real time, even if the uranium is only moderately concentrated compared to the average crust composition. For example, after five minutes of measurement, Th and U spectral lines are clearly visible in a rutile sample (consisting of mostly TiO_2 sand), where the uranium concentration is on the order of 100 ppm (Fig.1). Con-X 02 and 03 analyzer modifications are equipped with SDD detector. Its excellent energy resolution and throughput significantly increases the signal-to-noise ratio at a fixed measurement time, which, in turn, enhances the instrument's sensitivity to trace elements measurement, including uranium. The detection limit in this case is approximately 60 ppm. Additionally, the detection limits are approximately the same for other sample types (e.g., in zircon, $ZrSiO_4$).

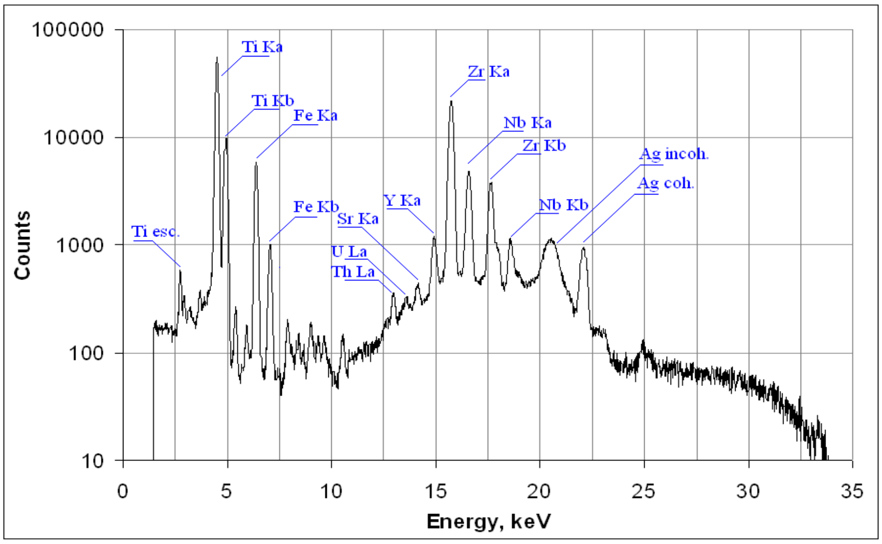

Fig.1. Spectrum of heavy mineral sand after separation from silica consisting from rutile as a major compound and zircon as a minor compound.
Parameters of measurements: X-ray tube voltage – 39 kV, current – 100 µA, 50µm thick Rh filter between x-ray tube and sample, measurement time – 300 seconds, distance between sample and detector 50 mm.

3. Analysis of uranium as a trace element in phosphate ores and products

Uranium is known to be one of the trace components of phosphate ores and thus of fertilisers produced from them. The world uranium resources in phosphate rock are estimated to be 9×10^6 metric tons of uranium. The average uranium content in phosphate rock, at 50-200 ppm or (0.005-0.020)%, is low. For comparison, some Canadian commercial uranium-rich ores contain as much as 15% or 150,000 ppm of this element [5].

In most situations, uranium is left in the produced fertiliser as a radioactive contaminant, which necessitates health physics and radiation protection measures to protect its handlers. For example, according to the International Atomic Energy Agency (IAEA) estimates, Morocco's uranium resources in phosphate deposits are approximately 6 million tons, which corresponds to twice the world's resources in uranium deposits [6].

Because the fuel cost is a small component of the total cost of nuclear electricity, countries that seek energy independence and secure energy supplies find it imperative to use their domestic uranium resources, even at the low uranium concentrations found in ore deposits.

With the appropriate extraction methods, uranium could be produced as a by-product of the phosphoric acid production process. Toward this end, the OCP (the Office Cherifien Des Phosphates, Moroccan state-owned agency) and the French Company AREVA plan to launch a joint study into the feasibility of an industrial site that produces uranium from phosphoric acid [6]. The uranium will be extracted from phosphate, converted to UF_6 and subsequently enriched.

Currently the feasibility of using a Con-X analyser to measure uranium concentration in phosphate ores (or phosphate products) on-line directly on the conveyor belt is highly prospective. In Fig. 2, five spectra of phosphate ores from two different deposits and phosphate fertilisers produced from these ores are shown. Differences between the intensities of the uranium line are clearly observed for different materials (Fig. 3): the intensity of the uranium line in the phosphate fertilisers derived from raw ores is higher than that in the phosphate ores. The uranium lines are identified in all of the products investigated using 5-minute measurements. This result indicates that the intensity of the XRF uranium line changes in proportion to the uranium content. Provided that the uranium content in Moroccan phosphate ore (light-blue line) is approximately 200 ppm (see previous discussion), the detection limit should be less than 50 ppm. This level of quantification allows sorting of the raw phosphate ore according to its uranium content or monitoring of the uranium concentration in commercial products (fertilisers) directly on the conveyor belt.

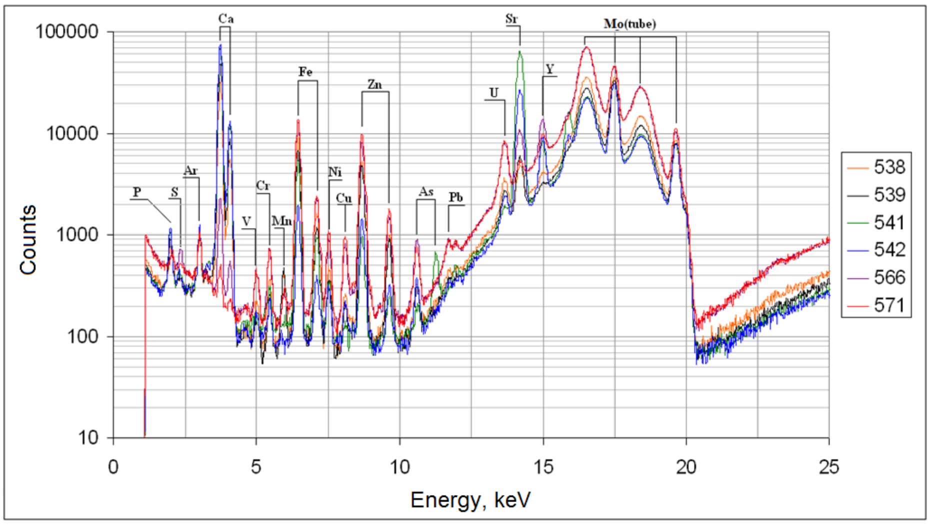

Fig.2. Comparison of spectra of various phosphate ores and products derived from them. Parameters of measurements: X-ray tube voltage – 39 kV, current – 100 µA, 100µm thick Mo filter between x-ray tube and sample, measurement time – 900 seconds, distance between sample and detector 40 mm.

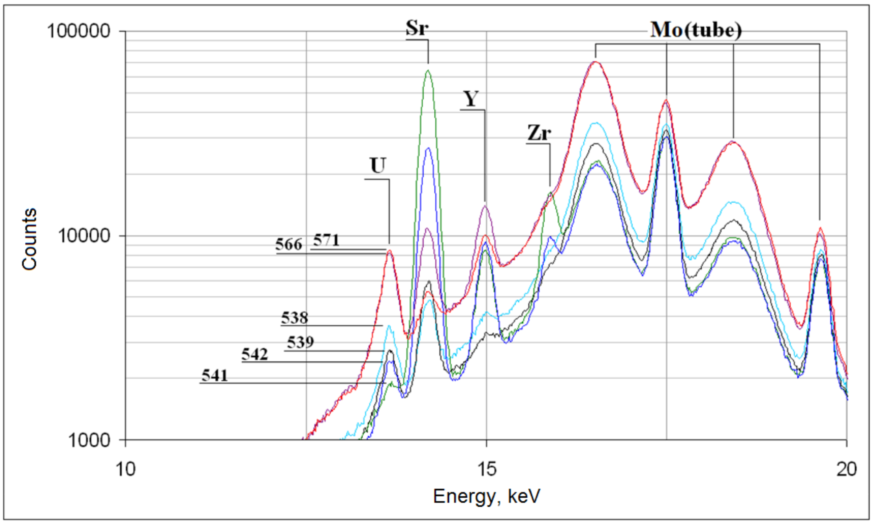

Fig.3. Zoom into U part of the spectra.

4. Analysis of uranium as a minor element

Normally, uranium ores, even before beneficiation, contain a significantly higher amount of U, typically at least 0.1%, or 1000 ppm. In this case with the help of Con-X analyzer, measurements of the U concentration become both more fast and accurate than measurements performed on samples with low U concentrations. For example, the uranium content in monazite ores is, on the average, approximately 0.2%; however, the amount of thorium may be as high as (4-7) %. An XRF spectrum of such monazite ore is shown in Fig. 4.

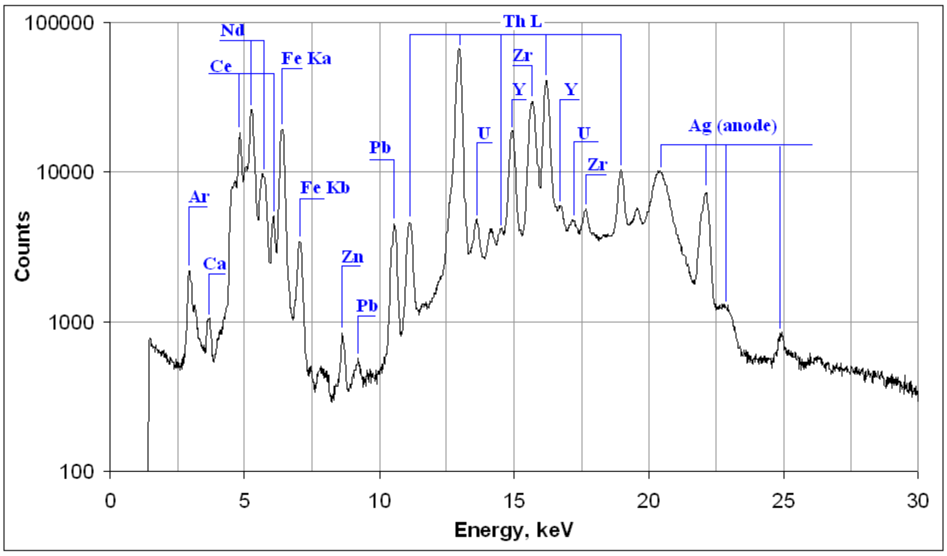

Fig.4. Spectrum of Monazite. Parameters of measurements: X-ray tube voltage – 39 kV, current – 400 µA, 40µm thick Rh filter between x-ray tube and sample, measurement time – 600 seconds, distance between sample and detector 45 mm.

In this measurement, a Si(Li) detector was used (Con-X 01 modification) to enhance the high-energy detection efficiency to the level needed for the analysis of rare-earth elements (La, Ce, Pr, Nd, etc.) using their K-series lines. Despite the inferior energy resolution of the Si(Li) detectors, the uranium XRF lines are clearly visible alongside the significantly more intense Th lines. Their partial overlap does not significantly affect the precision of the analysis because of the use of a spectral deconvolution algorithm in the software. Despite the presence of strong neighbouring Th lines, high-quality analysis is achieved. The U measurement precision is approximately 150 ppm (at the 2σ level), and the detection limit is approximately 200 ppm.

5. Analysis of uranium from associated minerals

Often, uranium content is correlated to the amount of other minerals that either occur in greater amounts or are easier to detect using the XRF method. In different ore bodies, these minerals may include Pb, Mo, Cu, Co, Ni, Bi, Sn and Ag, among other elements. In such cases, a faster analysis may be performed using X-ray signatures of these associated minerals. In some cases, time of semi-quantitative analysis may be as low as 10-100 ms, that allows implementing ore separation before leaching, secondary crushing or even before ore transportation from the mine. This separation process significantly reduces the costs associated with ore chemical treatment and transportation.
However, XRF is effective only as a surface technique since X-rays penetrate only to a depth of 1 mm inside the material. Therefore, mechanical separation of the material will be effective only if the ore lumps are more or less chemically homogeneous.

6. Analysis of uranium as the major element

The determination of uranium concentration in ores using the Con-X system is also possible in ores that contain high concentrations of uranium. In this case, the U concentration may be determined both from the intensity of its XRF spectral lines (Fig. 5) and from the intensities of spectral lines of the main admixture elements. The combination of the both methods can be implemented in the Con-X software and results in the best accuracy, which is typically less than 1% relative.

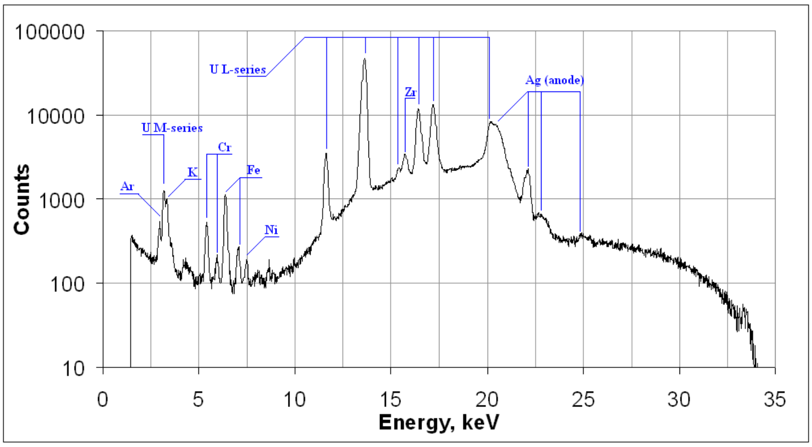

Fig.5. Spectrum of U_3O_8 on a Teflon substrate. Parameters of measurements: X-ray tube voltage – 39 kV, current – 100 µA, measurement time – 600 seconds, distance between sample and detector 50 mm.

7. Conclusion

The Con-X on-line XRF analyser is able to determine the uranium content in various ores and materials in real time. Quantitative and semi-quantitative analysis is possible from the 100 ppm level to uranium concentrations of 80% or more.

When uranium is present in concentrations less than approximately 1%, its detection limit for 5 minute measurements is approximately 50-200 ppm, even in the most adverse cases (i.e., the presence of strong neighbouring Th XRF lines). At this concentration level accuracy of U determination is approximately 50-150 ppm.

At higher uranium concentrations the relative accuracy of its measurement with Con-X analyzer improves and becomes better than 1% (relative) in the concentrated product.

The on-line determination of uranium content using the Con-X analyser provides fast and reliable results, which helps optimise the separation and concentration processes and reduce the costs of the end product.

References

[1]. D.Reilly, N.Ensslin, H.Smith, S.Kreiner. Passive Nondestructive Assay of Nuclear Materials. Los Alamos National Laboratory, US NRC, 1991.

[2]. World Nuclear Association, 22a St James's Square, London SW1Y 4JH, United Kingdom. World Uranium Mining 2011. http://www.world-nuclear.org/info/inf23.html

[3]. K.Tsuji, J.Injuk, R.van Grieken. X-ray Spectrometry: Recent Technological Advances. John Wiley & Sons Ltd, 2004.

[4]. http://www.bsi.lv/online_xrf_conveyor_analyzer_con_x_eng.html

[5]. M. Ceyhan, ed., “World Distribution of Uranium Deposits (UDEPO) with Uranium Deposit Classification,” IAEA-TECDOC-1629, Division of Nuclear Fuel Cycle, 2009.

[6]. https://netfiles.uiuc.edu/mragheb/www/NPRE%20402%20ME%20405%20Nuclear%20Power%20Engineering/Uranium%20Resources%20in%20Phosphate%20Rocks.pdf

NNL PRESTON LABORATORY TECHNOLOGIES/PROCESSES FOR THE TREATMENT OF ORGANIC WASTES

H. GREENWOOD, T.I. DOCRAT, S.J. ALLINSON, D.P. COPPERSTHWAITE
Waste Management and Decommissioning Directorate, National Nuclear Laboratory
Preston Laboratory, Springfields, PR4 0XJ - UK

ABSTRACT

Organic compounds of various kinds have been used in the nuclear industry for numerous duties in uranium chemical, metal and ceramic processing plants. In the course of the various operations undertaken, these organic compounds have become contaminated with uranic material, either accidentally or as an inevitable part of the process. Typically, the chemical/physical form and/or concentration of the uranic content of the organics has prevented off site disposal.

In order to address the issue of contaminated organics, the National Nuclear Laboratory (NNL) has developed a suite of treatments designed to recover uranium and to render the waste suitable for ultimate disposal off site. The developed processes are operated at considerable scale via the NNL Preston Laboratory Residue Treatment Plant.

The Oil Waste Leaching (OWL) Process is a fully industrialised process used for the treatment of contaminated oils with approximately 200 tonnes of uranium contaminated oil being treated to date. The process was originally developed for the treatment of contaminated tributyl phosphate and odourless kerosene which had been adsorbed onto sawdust. However, over the years, the OWL process has been refined for a range of oils including “water emulsifiable” cutting oils, lubricating oils, hydraulic oils/fluids and “Fomblin” (fully fluorinated) oils.

Chemically, the OWL process has proved capable of treating solvents as well as oils but the highly volatile/flammable nature of many solvents has required additional precautions compared with those required for oil treatment. These additional precautions led to the development of the Solvent Treatment Advanced Rig (STAR), a flameproofed installation operated under an inert atmosphere. STAR is a small “module” (100 dm^3 volume) which allows the treatment of both water miscible and immiscible solvents.

The NNL developed Springfields Washing Machine Process (SWAMP) to treat uranium contaminated “combustible wastes” such as ventilation filters, gloves, wipes, flexible plastics, filter cloths, lagging (e.g. Rockwool), mopheads, etc. The process employs slightly modified industrial washing machines and a range of chemical treatments with the resultant waste being targeted for disposal to landfill.

This paper discusses the challenges associated with the treatment of organic materials and the process developments which have allowed a wide range of materials to be successfully treated. New processes specifically developed for mixed resin/PVC residues, oily sludges and mixed Fomblin/hydrocarbon contaminated residues are also discussed.

1. Introduction

Organic compounds of various kinds have been used in the nuclear industry for numerous duties in uranium chemical, metal and ceramic processing plants. In the course of the various operations undertaken, these organic compounds have become contaminated with uranic material, either accidentally or as an inevitable part of the process. Typically, the chemical/physical form and/or concentration of the uranic content of the organics has prevented off site disposal.

In order to address the issue of contaminated organics, the National Nuclear Laboratory (NNL) has developed a suite of treatments designed to recover uranium and to render the waste suitable for ultimate disposal off site. The developed processes are operated at considerable scale via the Residues Treatment Plant in the NNL’s Preston Laboratory.

This paper describes the processes and equipment developed in NNL's Preston Laboratory to treat a range of organic materials.

2. OWL (Oil Waste Leaching)

OWL is a fully industrialised process used for the treatment of contaminated oils; approaching 200 te of uranium contaminated oil has been treated via various installations within the NNL Preston Laboratory Residue Treatment Plant.

The OWL process arose following the successful treatment of a residue comprising sawdust which contained considerable quantities of absorbed tributyl phosphate in odourless kerosene (TBP/OK), itself containing a significant amount of uranium. This residue was considered unsuitable for treatment via the available standard nitric acid leach routes (sawdust being incompatible with nitric acid on safety grounds) and was successfully treated by stirring with weak aqueous sulphuric acid. This operation physically displaced the solvent from the sawdust and chemically extracted uranium from the solvent to the aqueous phase. The solvent was easy to separate from the bulk for disposal via existing routes, whilst filtration of the sawdust/sulphuric acid, followed by washing the sawdust with water, yielded an aqueous solution of uranium which could be further processed for onward processing. The sawdust met the criteria for disposal to landfill.

Following successful application of the sulphuric acid wash to the sawdust residue, NNL investigated whether the same process could be used to treat oil contaminated with uranium. Laboratory testing showed that the process could be used to treat oil and full scale treatment was carried out using equipment already extant in the NNL Preston Laboratory Residue Treatment Plant. Cleaned oil achieved free release activity levels and recovered uranium was recycled to the fuel cycle.

In subsequent years, the OWL process has been refined and tested across a wide variety of oils contaminated with uranium with the majority of these being shown to be suitable for processing at full scale.

Processed oils included "water emulsifiable" cutting oils, lubricating oils, hydraulic oils/fluids and "Fomblin" (fully fluorinated) oils. For some oils, mainly cutting oils, direct treatment of the oil with aqueous sulphuric acid did not achieve free release levels and investigation showed this to be due to the presence of "sludges" at the base of the drums, these sludges comprising finely divided uranium metal/degraded metal (oxides)/carbonaceous material which was not dissolved nor sufficiently leached by the sulphuric acid treatment agent.

It was shown that removal of supernatant oil from the drums, followed by centrifugation of the oil rendered the material treatable by the standard OWL process. Solids recovered by centrifuge were re-combined with settled sludges for alternative treatment. It was also shown that the uranium removal process could often be enhanced by the addition of mild oxidants to the sulphuric acid.

The OWL process as currently configured requires that oil is tested via the laboratory (reasonably representative sampling is important, especially regarding any settled sludge) to determine the optimum process in terms of:

(a) whether bulk solids removal is required by sedimentation and/or centrifugation, and at what stage this is most advantageous (before any sulphuric acid contact or after a certain number of contacts),

(b) optimum agitation/mixing (a balance exists between uranium removal, which is enhanced by improved agitation, and phase separation after contact, which can be compromised by excessive emulsification at high degrees of agitation),

(c) optimum operating temperature, with higher temperatures aiding uranium extraction and phase separation but restricting sulphuric acid concentrations in some items of equipment,

(d) sulphuric acid concentration; again uranium extraction and phase separation are improved at higher sulphuric acid concentrations but not all available equipment can operate at the higher concentrations and some oils are chemically attacked at higher acid concentrations, complicating treatment,

(e) oil:aqueous sulphuric acid volumetric ratio,

(f) requirement to use additives which can aid uranium extraction for some oils but which can complicate uranium recovery downstream,

(g) required time per contact,

(h) number of contacts required (free release for uranium contaminated oil typically requires several contact cycles).

The process can be operated using various equipment within the NNL Preston Laboratory; a large industrial centrifuge is available together with tanks capable treating varying volumes of oils at a time (up to c. 2000 dm^3 oil has been treated per batch, though typically batch volumes are of the order of 200 dm^3). Approximately 1000 drums of oil have been treated via OWL and tens of tonnes of uranium contaminated TBP/OK solvent (including badly degraded solvent) have also been treated via a process and equipment more or less identical to OWL.

Recently, a specific rig has been constructed to operate OWL for the treatment of cutting oils contaminated with highly enriched uranium (namely HERO or “Highly Enriched Recovery, Oils”). The OWL process has also been tested in conjunctions with non-uranic alpha contaminated oils, yielding a very high decontamination factor even in the presence of a considerable amount of active solids. It would be expected that OWL could easily be applied to many other contaminated oils, though some alteration to the chemistry might be required or advantageous.

3. STAR (Solvent Treatment Advanced Rig)

Chemically, the OWL process has proved capable of treating solvents as well as oils but the highly volatile/flammable nature of many solvents has required additional precautions compared with those required for oil treatment.

STAR is a small treatment plant (100 dm^3 volume) which allows volatile and flammable solvents to be treated in aqueous sulphuric acid; the rig is flameproofed and operates inerted during operation. STAR has treated a few hundred litres of uranium contaminated solvents in recent years.

Part of the STAR rig can also be utilised in the treatment of water miscible solvents. This process involves the addition of caustic soda solution to precipitate uranium for recovery.

Solvents treated via STAR are targeted for free release. Again, STAR (which is largely constructed from off the shelf equipment) could likely be modified to treat solvents contaminated with species other than uranium.

4. Oily sludges

NNL have investigated the treatment of a wide variety of uranium contaminated “oily sludges”; most of the sludges tested have arisen from the same uranium metal machining operations that produced the contaminated oils treated by OWL and HERO and generally comprise settled sludges of metal fines/swarf, degraded metal/oxides, oil and degraded oil (including carbonaceous solids).

Techniques developed at the laboratory scale include, direct treatment in nitric, sulphuric and hydrochloric acids, pre-treatment with detergents, solvents or caustics (in advance of acid leaching); work in this area is ongoing and is being compared with alternatives such as vacuum distillation, low temperature pyrolysis and incineration.

5. SWAMP (Springfields Washing Machine Process)

The NNL developed SWAMP uses slightly modified industrial washing machines to treat uranium contaminated soft wastes such as ventilation filters, gloves, wipes, flexible plastics, filter cloths, lagging (e.g. Rockwool), mopheads and the like.

Some materials can be fed directly to the washing machines while others are shredded and loaded into permeable polypropylene bags before being loaded into the machine. Ventilation filters are dismantled and casings cleaned by jet washing with the medium being placed in permeable bags.

After residue loading the washing machine is put through a number of cycles using a nitric acid feed, the bulk nitric acid being removed during the empty/spin phase of the machine cycle. Upon completion of the nitric acid wash, a rinse cycle using water is carried out. The process typically targets material for disposal to landfill and can be easily modified to use a detergent wash (for oily materials) in advance of the nitric acid treatment stage. Some materials do not clean sufficiently well in nitric acid alone but a range of additives can be used to boost wash efficiency. Tens of tonnes of material have been cleaned using the SWAMP installation.

Again it would be expected that the SWAMP process could be modified to process material contaminated with non-uranium species.

6. SWORD (Springfields Waste Organic Residue Digester)

SWORD was developed to treat a specific residue comprising a resinous floor polish/PVC matrix contaminated with gross levels of uranium dioxide (UO_2). The residues arose during operation of a now long closed plant which produced enriched uranium dioxide powder for fuel manufacture and which also processed a wide variety of uranic residues.

In order to keep airborne contamination levels within the plant down to acceptable levels, floors (mainly concrete) were coated with an organic floor polish/sealant (“resin”) to prevent dust formation. As the polish itself became contaminated, additional polish layers were painted on top of the existing polish, forming a multi-layered “sandwich” of polish layers with dust between and within the polish layers. Eventually, as the thickness of the polish increased, the polish was removed from the floor either by “chipping” or by steam treatment which allowed the residue to be “rolled up” like a carpet. Polish layers up to 2 cm thick exist from the “chipping” operation, with the “rolled carpet” variant having been dropped “hot” into drums where the material has “set” into large masses. A significant fraction of the residue comprises variants in which the polish was laid down on either thin PVC floor tiles or thick PVC floor covering which were removed along with the adhered polish. Occasionally the residues contain layers of paint alternating with the polish.

Uranium at considerable concentrations has been found in the residue and almost all the uranium present is enriched. As such, the material represents a considerable criticality hazard, restricting the scale of any “non-safe geometry” process. As well as uranium, many metal oxides are present, as are minor concentrations of neptunium, plutonium and technetium.

Various methodologies for treating these residues were considered and many tested in the laboratory (e.g. incineration, low temperature pyrolysis, solvent treatment, treatment with caustic soda, direct treatment in aqueous mineral acids, etc.) but these methods proved inadequate; for example:

- incineration proved very problematic, with the production of large volumes of flammable gas and “vitrification” of the inorganic component rendering it unleachable in anything other than hydrofluoric acid,

- direct treatment with aqueous mineral acid, caustic soda and solvents was completely ineffectual and/or produced large volumes of intractable by-products.

NNL have developed the “wet oxidation” SWORD process to treat the target residues. A long development programme, spread over considerable time, settled on a sulphuric acid based wet oxidation system in which the residue is treated at high temperature in concentrated sulphuric acid. The process destroys the bulk structure of the residue and “carbonises” the solids, subsequently converting the carbon/organics to water vapour and carbon dioxide whilst dissolving uranium to solution as soluble sulphates.

The currently developed process involves chipping the residue into small pieces and feeding, at a controlled rate, to concentrated sulphuric acid held at temperature. The residue rapidly swells and carbonises with the production of considerable quantities of carbon dioxide and water vapour, before breaking down to form a carbonaceous slurry of fine particulate material. This stage is known as “matrix destruction” and is followed by a “carbon digestion” stage in which the reaction mixture is heated to reflux conditions. Once organic/carbon destruction is complete, an impure uranyl sulphate/sulphuric acid solution containing small amounts of undissolved/precipitated inorganics such as silica and/or calcium sulphate results. The reaction mixture is then cooled and diluted into water both to ease filtration and prevent subsequent crystallisation of dissolved solids.

The diluted liquor is filtered to remove residual undissolved inorganics which are subsequently treated by standard nitric acid leaching to further reduce their uranium content prior to disposal. The clarified liquor is treated with caustic soda to recover the uranium as sodium diuranate which is then suitable for onward processing via existing routes.

The process can be accelerated and operated at lower temperatures by the addition of concentrated nitric acid. In the “Nitric Boosted” SWORD process the matrix destruction stage is performed exactly as per the sulphuric only process, but at the end of the matrix destruction stage, the reaction mixture is cooled and concentrated nitric acid is bled to the reactor to speed up the carbon digestion phase. The “Nitric Boosted” process is currently at the laboratory development stage but results to date show that the process is much faster overall than the sulphuric only process, even when operated at much lower temperatures.

Plant design is currently underway for a “Nitric Boosted” SWORD facility to operate in NNL Preston Laboratory at a scale of up to 400 dm^3 liquor. Much of the plant will be constructed from “off the shelf” glass or glass lined equipment.

It is clear that the SWORD process will be applicable to a wide variety of organic wastes, most of which will be far less intractable than the floor cleaning residues. The sulphuric only process has been tested in conjunction with a “tritiated oil”; in this process (TOAST, or “Tritiated Oil Advanced Sulphuric Treatment”), the oil was initially treated in concentrated sulphuric acid at temperature selected to prevent oil boiling/evaporation, followed by the normal carbon digestion step. Tritium recovery to the acid was effectively quantitative with no measurable tritium escaping as off gas. It seems likely that the “Nitric Boosted” process would also be successful and that, destruction of oils in general could be accomplished by either of the tested SWORD processes.

7. SCIMITAR (Springfields Complex Intractable Material, Total Actinide Removal)

SCIMITAR has been developed for the treatment of uranium solvent extraction plant cruds. The cruds comprise a mixture of TBP/OK, aqueous liquor (impure uranyl nitrate/nitric acid), inorganic solids such as zirconium hydrogen phosphate and similar, magnesium fluoride and silica plus c. 20 % w/w organic solids; the residues are contaminated with uranium, and with very high levels of thorium and protactinium (as ^{231}Pa).

The process comprises an initial leach in aluminium nitrate/nitric acid at elevated temperature which releases some solvent encapsulated within the solids fraction of the residue and dissolves much of the uranium and thorium content of the residue. Residual solids from the first stage are then subjected to leaching in nitric acid/potassium fluoride, which dissolves zirconium hydrogen phosphate and silica, releasing more encapsulated solvent which is combined with solvent recovered at the first stage for treatment via OWL. A third stage leach in aqueous sulphuric acid solubilises protactinium.

Experience has shown that crud batches exhibit considerable variation and that SCIMITAR would operate most effectively if the process chemistry was optimised for a specific type of crud. Development work continues with respect to enhancing the performance of the SCIMITAR process.

8. ARTEMIS (Advanced Residue Treatment, Enrichment Materials Integrated System)

ARTEMIS is a suite of processes designed to treat a variety of uranic residues. Many of the residues are “oily”, the bulk comprising uranyl fluoride, uranium tetrafluoride, aluminium metal and various metal oxides/fluorides and other inorganics. A very significant fraction of the material is very heavily contaminated with hydrocarbon oils and greases, some of which has suffered considerable radiation damage resulting in the formation of both low molecular weight volatile species and heavy or waxy organics.

Prior to acid leaching, a pre-treatment stage, to remove any organic materials, is undertaken. A process has been developed in which the residues are treated with a proprietary “engineered fluid” (solvent) which has a high capacity for dissolving organics and a low surface tension, allowing it to access and dissolve organics present within inorganic matrices. Additionally, the solvent is readily available, is non-flammable and has low ozone depletion and global warming potential.

The selected fluid has a low boiling point which dictates that the pre-treatment of residues to remove oil must be carried out in specifically designed equipment to minimise solvent losses. Recovered solvent containing dissolved oil is distilled for re-use, recovered oil being sent for treatment via existing routes such as OWL.

The entire suite of ARTEMIS processes has been successfully tested at the laboratory scale and a 20 dm^3 scale ARTEMIS pre-treatment test rig is currently being designed. This is expected to be installed and tested in the near future. The test rig, and subsequent full scale plant are to be constructed from off the shelf heavy engineering glassware. Other parts of the ARTEMIS process are already operating at full scale.

9. Conclusions

NNL have wide experience in the treatment of a wide range of organic materials. The treatment techniques have primarily been developed for the recovery of uranium from organic matrices in order to facilitate disposal of the organic fraction of the residue. However, a number of the treatment techniques have been found to be similarly effective for residues containing other radioisotopes.

NOVEL INSPECTION DEVELOPMENTS REQUIRED TO UNDERPIN THE SAFE OPERATIONS OF SELLAFIELD NUCLEAR FUEL REPROCESSING PLANT

M. G. ARMSTRONG
Plant assessment and inspection equipment development
National Nuclear Laboratory
Central Laboratory, Sellafield, Cumbria, CA20 1PG, United Kingdom

DR. S. SHACKLEFORD
Asset Care
National Nuclear Laboratory
Central Laboratory, Sellafield, Cumbria, CA20 1PG, United Kingdom

Acknowledgement: *This work was funded by Sellafield Limited (SL) and the Nuclear Decommissioning Authority. We thank members of both SL and NNL technical teams who supported the various aspects of this work.*

ABSTRACT

The Sellafield Nuclear Fuel Reprocessing chemical plant contains plant items that are subjected to very corrosive environments and therefore have finite service life. These plant items are located in concrete biological shielded cells due to the very high gamma radiation levels and contamination environments and no man access is permitted. Periodic assessment of these plant items is required to ensure ongoing safe operations and planning for new build or replacement. In some cases this assessment can be achieved by desk top studies backed up by laboratory data. However some of the more corrosive species cannot be replicated using none active simulants. Also operational conditions within these plant items are also difficult to replicate within experimental rigs with sufficient level of assurance.

In reality the current robust safety cases for continued safe plant operations are underpinned by both quantitative and qualitative data taken from these plant items. This is achieved by invasive inspection even though the majority of the plant items and concrete cells have no or limited designed access for inspection This has been achieved by the design and application of novel inspection systems including deployment systems that can assure retrievability and the appropriate tool package to quantify/qualify the degradation of the plant item. These targeted inspection developments are specified using NNLs in-depth knowledge of corrosion mechanisms within the austenitic stainless steel plant.

This paper outlines the range of inspection equipment developments that has occurred of the last few years.

1. Introduction

The Sellafield Nuclear Fuel Reprocessing plants are similar to conventional chemical process plant in that degradation by corrosion or mechanical actions can occur both within the process vessels and pipework from operational conditions, and also externally due to environmental conditions. It is also the case that degradation can occur in locations where design allowance has not been made. The use of inspection in the condition monitoring of nuclear reprocessing plants to identify chronic issues is difficult due the vessels and pipework being housed within 1 m thick concrete biological shielded cells with very restricted remote access. Each Nuclear establishment has a Site Licence that governs their safe operations. Site Licence Condition 28 states that "the licensee shall make and implement regular and systematic Examination, Maintenance, Inspection and Testing (EMIT) of all plant which may affect safety". Compliance with this condition ensures that all plant that may affect safety remains capable of performing the function required by the safety case[1] assumptions to the required level of reliability.

It is not practicable to inspect all plant items in closed cells. Therefore a risk based assessment methodology is used to identify the critical plant items that require regular monitoring to underpin the robust safety case for continued safe plant operations. The core data for this process is provided from remote plant inspection, trending plant operational conditions, knowledge of construction materials, plant design, and corrosion assessment (where possible). A Gap Analyses process is then applied to identify where additional plant condition data is required. This paper provides an overview of the many inspection developments undertaken by National Nuclear Laboratory (NNL) to support the continued safe operation of Sellafield Nuclear reprocessing plants.

2. NNL support to the asset care of the Sellafield site

For many years the NNL Plant Assessment, Inspection and Equipment Development team has provided continuity to the asset care of plant in closed cells at Sellafield using a combination of corrosion/mechanical expertise and the development and application of remote plant inspections techniques.

The team has a core of highly motivated individuals with in-depth knowledge and experience of how the plants operate, plant assessment techniques and their application. They also possess specialist materials knowledge on degradation mechanism such as corrosion, erosion and mechanical failures. These skills have been used to identify the potentially vulnerable plant items and most appropriate inspection technique to provide the condition data required.

The inspection equipment developments throughout the years have occurred due to a variety of drivers. These include the quantification of previously unidentified degradation and the requirement to monitor this degradation, plant faults, new plant asset care, and safety and reliability of equipment.

The ability of NNL team to apply novel applications of existing technology to satisfy plant requirements is based on knowledge of plant design and access routes to the vulnerable components. The types of remote plant regularly inspected are vessels and process lines within HA and MA cells, waste storage facilities, pipe trenches, and other controlled areas. An experience 3-D CAD design team is part of the NNL support to these remote inspection equipment developments.

---

[1] Safety case: Is the totality of documented information and arguments developed by the licensee to substantiate the safety of a facility, activity, operation or modification.

Plant assessment techniques used in the remote inspection of Sellafield plant include CCTV, ultrasonic thickness techniques, potential drop, radiation measurement, infrared techniques, and of most importance the development of deployment systems. The design of this equipment also benefits from the inspection development team having worked in the controlled areas of site. These techniques provide either quantitative and/or qualitative data on plant condition. The nitric acid resistant austenitic stainless steels used in the construction of chemical plant within Sellafield unfortunately limits the NDT techniques that can be used due to their non-magnetic properties.

Restrictions to plant inspection are:
Closed cells: Access via a limited number of 150mm internal diameter roof or wall access holes.
Old plant: No engineered access so use of existing operational lines to deploy inspection equipment.
New plant: Dedicated inspection access lines designed into new plants.

NNL have provided input to the design of new plant or refurbished plant to improve condition monitoring provision. Often NNL have performed detailed case studies to develop the condition assessment of specific vulnerable plant item.

The following tables present examples of the many and varied inspection developments that have provided both qualitative and quantitative assessment of Sellafield plant components.

Range of NNL inspection systems developed to inspection closed cells and vessels.

Inspection system	**Equipment**
CCTV inspections of closed cells.	
Inspection deployment system for closed cells and vessels. Series of interconnecting poles with manual assisted deployment. Design aids decontamination operations. Fully CE marked system. Deployment length of 25m vertical and 3m horizontal into closed cells. Tool package, where possible, uses proprietary pan/tilt/zoom/in-built illumination CCTV system. Designed to pass through access holes of 150mm diameter. Radiation tolerant systems. Height controlled to ±1cm	 Deployment of CCTV system through roof of closed cell.
Horizontal deployment system manoeuvres the CCTV tool through 90° into a vertical orientation on a damped hinge to provide optimum views.	
Typical high quality of view within close cell.	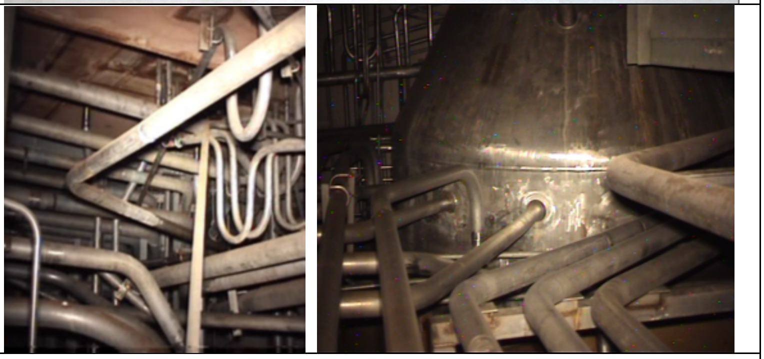
Horizontal to vertical adaptor to increase the closed cell inspection coverage. Again restricted to deployment through 150mm access holes.	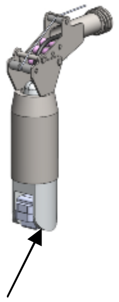 CCTV system lowered from housing

Inspection system	**Equipment**
CCTV inspections of closed cells (continued).	
Deployment and articulation of SLR type camera to gain very high quality images supporting the assessment of plant items. Designed by 3D CAD. See comparison of design and manufactured equipment.	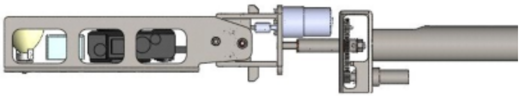 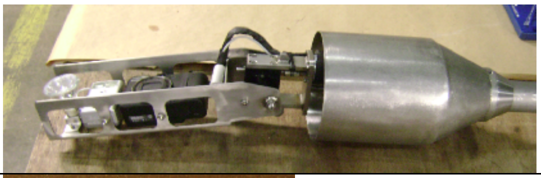
Example of image quality taken within a closed vessel after many years of operation.	

Use of 3D CAD modelling to identify potential for developments of inspection equipment.	
Requirement for a CCTV inspection system to enter closed cell and deploy away from obstructions in the line of access. 3D CAD models prove principle of design and provide theoretical views of plant items. Up to 4m deployment required within the closed cell. Followed up by actual manufacture of the inspection device. Rack and pinion controlled deployment system for horizontal movement. CCTV system with full pan/tilt/zoom/integrated illumination.	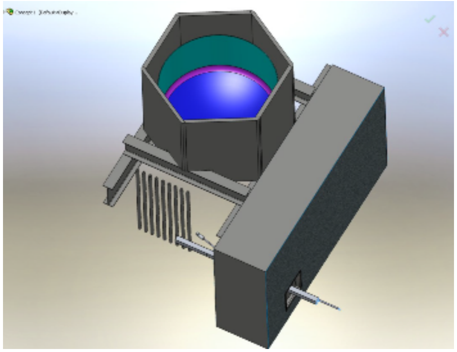 3D CAD model view from above and side of access hole 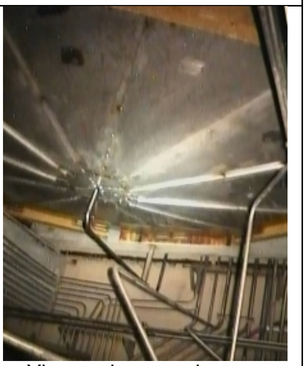 View under vessel
System manufactured at the NNL development location, Workington, Cumbria, UK.	

Thickness survey systems for closed vessels	**Equipment**
Tube boiler assessment	
Vertical tube boilers require periodic inspection. Access by standpipe with 150mm internal bore. Access 15m away from vessel upper tube sheet. Tubes 5m long with 49mm bore. All tubes requiring inspection. Up to x210 tubes per boiler. Deployment of a radially opening system that can be rotated > 360° to enable deployment of inspection tool into any tube. Inspection tools developed for internal inspection (process side) are: 1. CCTV to assess corrosion and deposits. 2. Wall thickness survey using ultrasonic thickness measurement system including in-built water retention for sound couple. 3. Deployment of tube washing system.	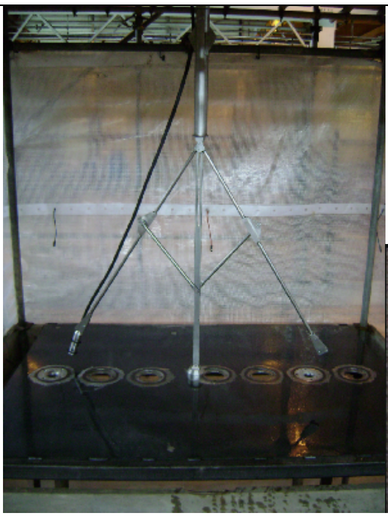 Mechanism used to remotely deploy tool into boiler tube. Mock-up rig at NNL Workington, Cumbria, UK. 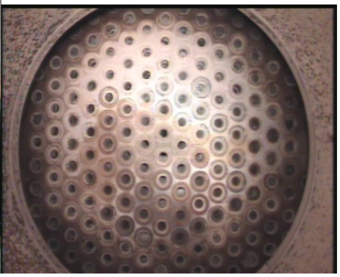 View of upper tube sheet Originally developed with Phoenix ISL, UK.

Use of both CCTV and ultrasonic technique in one system to assess degradation	**Equipment**
Inspection system to quantify the degradation of service pipework contained within process vessels. Vessel and pipework 4m high. Access via closed cell. Inspection system deployment via in-cell crane. All electrical and signal services linked to out-cell. The inspection head contained a high quality full pan/tilt/zoom/integrated illumination CCTV system for viewing corrosion of components. Ultrasonic transducers deployed using the pan/tilt functionality of the CCTV system. None contact thickness measurement system. Proven to measure thickness of the externally corroded pipework (20 and 50 mm NS pipes) at 0.7m away. Vessel wall thickness can be measure at much greater separation. Vessel filled with weak acid, acting as couple for the ultrasound. Measurement accuracy of ±0.03mm.	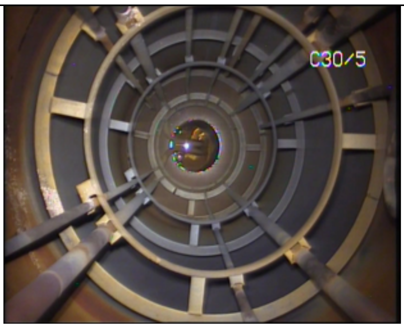 Example of vessel inspected. 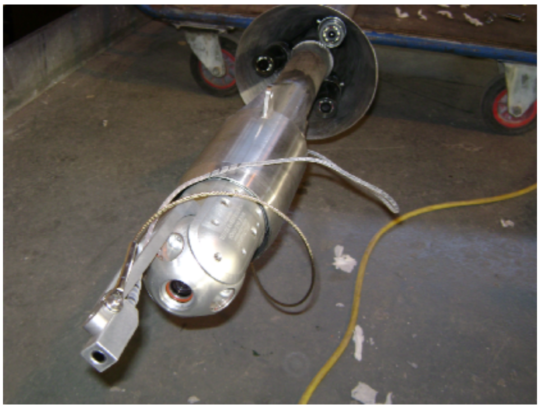 Inspection system tool package.

Long term condition monitoring using potential drop technique	**Equipment**
Specific locations on plant have unique operational conditions. The high radiation levels prevent easy access to these areas. NNL have developed potential drop systems that measure change in resistance and converts this to thickness change. These can be permanently installed via tack welding or via clamps. These either are installed on new build of plant or after washout of operational plant. Longevity proven at 103°C and high radiation fields for 8 years.	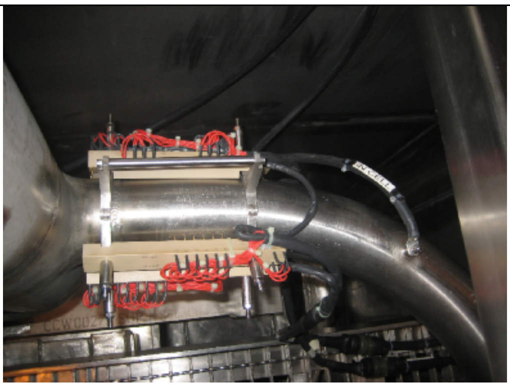 Potential drop system clamped on plant pipework.

Inspection systems for pipework or access via pipework to in vessel locations.	**Equipment**
Development of inspection "pig" type vehicles to measure the thickness within steam heated components within a kettle type evaporator. Two different heating components required to be measured. These are the steam heated helical coils, and the vessel base heated via a steam jacket. Each heating component is critical to the operational life of the evaporator and so any inspection vehicle development needed to prove to have minimal risk to retrieval. Full scale rig to simulate each inspection route was manufactured at the NNL facility, Workington, UK. Very robust inspection vehicles developed.	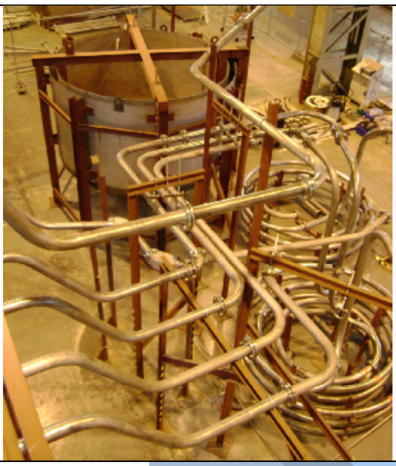 
Constraints for the development of the inspection systems. Each heating components was access from out-cell locations via through wall pipework. The helical coil inspection device needed to deploy up to 40m, through three changes in pipe bore, ranging from 74 – 90 mm. The tightest bend was x1.5OD elbow within an 80NS elbow. Thickness survey taken using none contact ultrasonic transducers, minimising risk to retrieval. Coil filled with water so inspection vehicle needed to be waterproof to 5m depth. Radiation level up to 1000 Gy/hr.	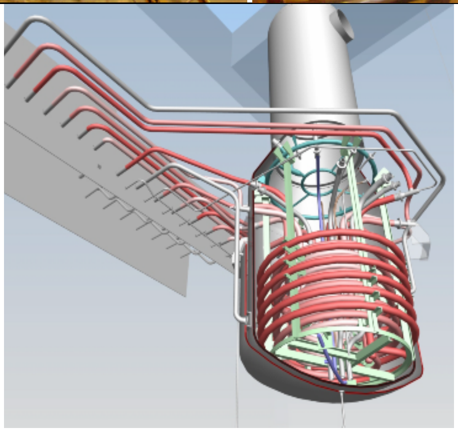 3-D CAD model of the coil and jacket access pipework
The access route into the steam jacket is more difficult than that for the coil inspection. This is via an 80NS x1.5 OD elbow and then over a knife edge into the steam jacket. The device then uses an ultrasonic transducer to measure the thickness of the evaporator base.	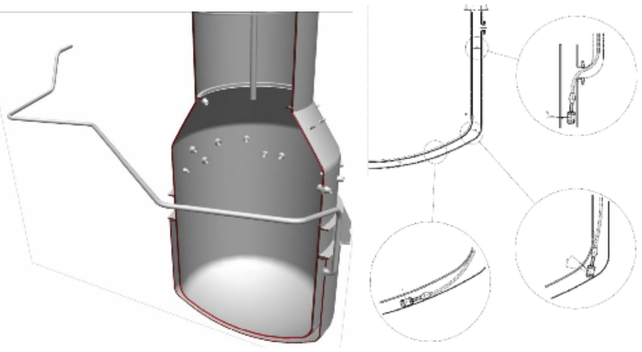
Inspection vehicles: Each has a CCTV inspection system to assess pipe route during deployment. Coil vehicle has x8 static ultrasonic transducers. The base vehicle transducer can rotate 360° and tilt ± 40° to facilitate base thickness measurements. Each use radiation tolerant CCTV systems.	 Coil inspection vehicle 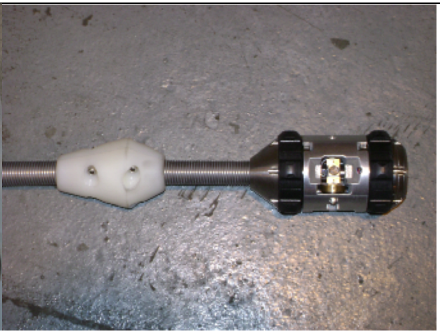 Base inspection vehicle

Vessel wall thickness survey.	**Equipment**
Collaboration with Strathclyde University. Bespoke CCTV and thickness measurements system developed to provide a thickness survey of a vessel. System deployed horizontally through cell wall and then lowered vertically within the cell on to a platform. A tractor is then used to manoeuvre the thickness measurements system to contact a vessel. Laser range finder fitted to aid future repeat thickness survey accuracy Developed initially using 3D CAD. Full scale mock-up manufactured at the NNL facility Workington, UK.	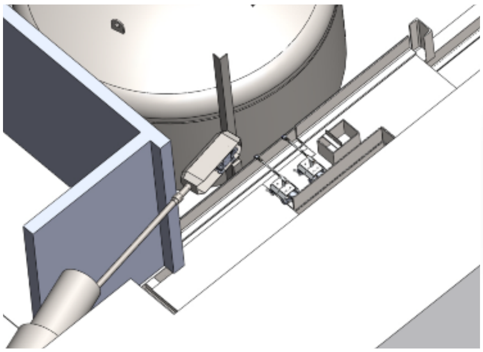 3 D CAD view of plant. 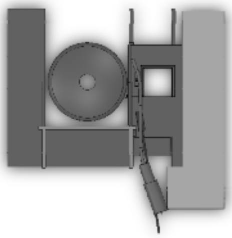 Plan view of plant
	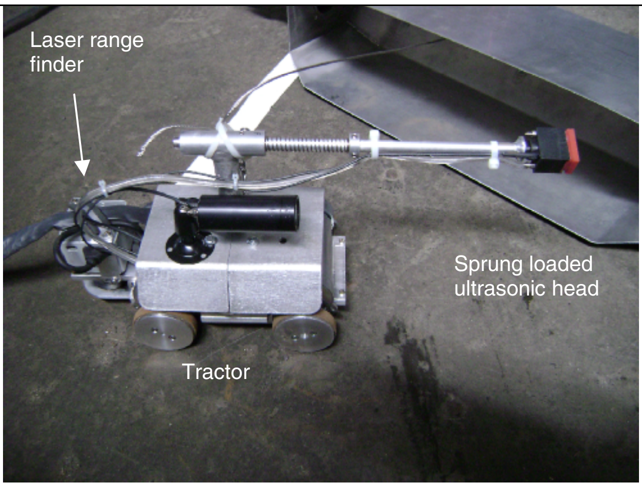 Inspection vehicle

Radiometric devices	**Equipment**
Bespoke radiation measurement devices have been developed to either measure static radiation fields or used during washout to determine when washout has been effective. Deployed down pipework of 20mm nominal bore. Radiation upper limit of 10,000 Gy/hr.	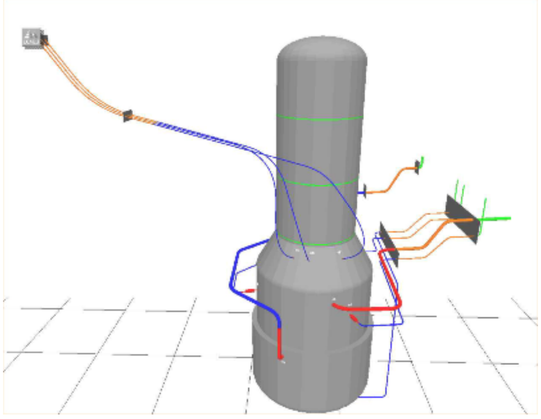 3D CAD model of the pipe route into vessel to monitor washout progress.

MODELLING OF PROCESSES IN RBMK-1500 FUEL RODS DURING THE OPERATION CYCLE AND SHORT AND INTERMEDIATE TERM STORAGE OF SPENT FUEL ASSEMBLIES

T KALIATKA, E. USPURAS
Laboratory of Nuclear Installation Safety, Lithuanian Energy Institute,
Breslaujos str. 3, LT-44403 Kaunas, Lithuania

ABSTRACT

Recently the reactors of both units of Ignalina NPP in Lithuania are shutdown for decommissioning (in 2004 and 2009). According to the design, the spent fuel should be returned for reprocessing to Russia. However, no fuel assemblies have been taken out from the territory of the Ignalina NPP: all assemblies of spent fuel are stored in the spent fuel pools and in the dry storage facility on-site of the Ignalina NPP. Thus, the safety justification for short and intermediate term spent fuel assemblies storage in Ignalina NPP is very important. The most important barrier, preventing release of radioactivity form fuel matrix to environment is the fuel rod cladding. The condition (integrity) of cladding at the end of intermediate storage of spent fuel assemblies may be evaluated by performing simulation of processes in fuel rods during whole “life time” of fuel assembly: beginning the first loading into reactor core and until the end of dry intermediate storage in special casks.

This paper presents the modelling of processes in fuel rod during normal operation of fuel assemblies in reactor, short term wet storage in spent fuel pool and intermediate storage in dry cask. The analysis was performed using FEMAXI–6 integral code for the analysis of processes in fuel rod. The behaviour of thermal (pressure inside fuel rod, temperatures of fuel pellets and cladding and etc.) and mechanical (change of the gap between pellets and cladding, stresses and plastic deformation in fuel pellets and cladding and etc.) parameters were calculated. The performed analysis demonstrates possibility to identify the state of fuel rods after normal operation and short and intermediate term fuel storage.

1. Introduction

Ignalina NPP is the only nuclear power plant in Lithuania which is comprised of two units, commissioned in 1983 and 1987. Both units are equipped wit channel-type graphite-moderated boiling water reactors RBMK-1500. Ignalina NPP Unit 1 was shutdown for decommissioning at the end of 2004 and Unit 2 was shutdown at the end of 2009. After final showdown of reactor the fuel assemblies from the reactor are transferred to the spent fuel pool where they will be kept at least for 5 years. Later – intermediate term storage in dry storage containers for the 50 year period. Thus the state of the fuel rods (intactness of cladding, residual stresses in the cladding and fuel pellets, gap between cladding and pellets and etc.) is very important because fuel rod cladding is one of the safety barriers. For this purpose the deterministic analysis of processes in fuel rods are performed.

In the beginning, Ignalina NPP operated with 2.0% U^{235} enrichment fuel. Before the final shutdown, the fuel of 2.4%, 2.6% and 2.8% U^{235} enrichment with burnable erbium absorber was used at Ignalina NPP. Nuclear fuel is compressed to pellets of 11.46 mm diameter and 15 mm height [1]. The 2 mm diameter hole through the axis of the pellet reduces the temperature at the centre of the pellet. In order to decrease the neutron escape from the reactor core in the axial direction, screen pellets of 0.7% U^{235} enrichment are included at the end close to the gag of the fuel rod.

The pellets are placed into a cladding with the outside diameter of 13.6 mm, wall thickness of 0.9 mm and active length of 3.41 m (Figure 1). The fuel cladding is made of a zirconium and niobium alloy (Zr+1%Nb). In RBMK reactor the fuel assembly is fit into a circular fuel channel with the inside diameter of 80 mm and core height of 7 m. In order to achieve the required height, the RBMK fuel assembly consists of two fuel bundles placed one above the other (Figure 1). Each fuel bundle includes 18 fuel rods placed in two circles around the carrying rod.

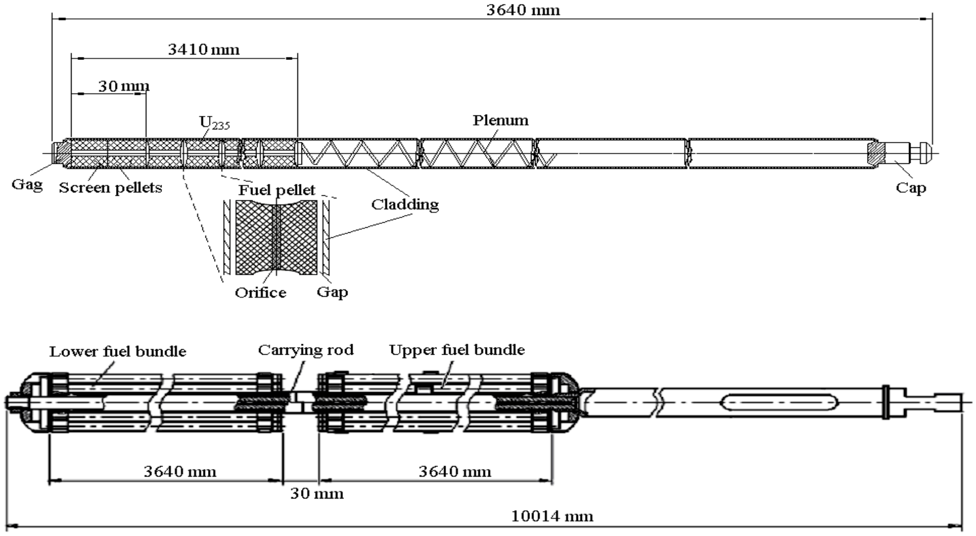

Fig. 1. Fuel assembly and fuel rod of RBMK-1500 [2]

This paper presents the information about the model development using FEMAXI-6 code and identification of fuel rods status after the normal operation short and intermediate term fuel storage.

2. Development of fuel rod model using FEMAXI-6 code

Lithuanian Energy Institute (LEI) uses FEMAXI-6 code for the modeling of the processes in the fuel rods of Ignalina NPP [3]. FEMAXI-6 code is designed for vessel type reactors. The materials of fuel and cladding and design of fuel rods in RBMK-1500 are different comparing to vessel type light water reactors. These differences are evaluated during the development of the model.

The FEMAXI-6 code was used because this code produces more detailed calculations and predicts the thermal and mechanical behaviour of a light water reactor fuel rod during normal operation and transient conditions. FEMAXI-6 code can analyze the integral behaviour of the whole fuel rod throughout its life as well as the localized behaviour of a small part of the fuel rod. FEMAXI-6 consists of two main parts: one for analysing the temperature distribution, thermally induced deformation, fission product gas release, etc., and the other for analysing the mechanical behaviour of the fuel rod. The present analysis conducts the entire fuel rod length analysis [4].

The model of RBMK-1500 fuel rod was developed using FEMAXI-6 code. For the analysis the fuel rod from the bottom fuel bundle was selected. The main parameters of fuel rod are presented in Table 1. In the developed fuel rod model, the length is divided into 12 segments and one of them describes the screen pellets (Figure 3). The top volume of the fuel rod was modelled as a separate segment. This volume contains the clamp, compressing column of pellets. A more detailed description of the model is presented in [5].

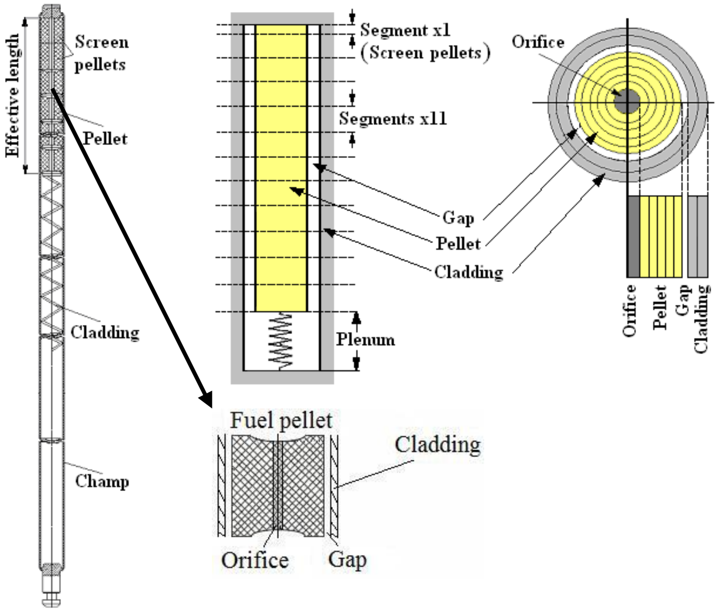

Fig. 2. Model of RBMK-1500 fuel rod (bottom bundle), developed using FEMAXI-6 code [5]

Parameter	**Value**
Length of the fuel rod	3640 mm
Active length of the fuel rod	3410 mm
Height of the screening pellets	30 mm
Length of the plenum	170 mm
Outside diameter of the fuel rod	13.45 mm
Inside cladding diameter	11.75 mm
Outside fuel pellet diameter	11.5 mm
Pellet central orifice diameter	2 mm
Fuel enrichment in U^{235}	2.6 %
Partition of erbium in fuel	0.5 %
Edge pellet enrichment	0.7 %
Fuel pellet density	10.55 g/cm^3
Mass of fuel within the fuel rod	3500 g
Initial pressure of gases in the fresh fuel rod at cold conditions	0.5 MPa

Table 1. Fuel rod parameters

The materials of fuel and cladding and design of fuel rods in RBMK have differences, comparing to vessel type light water rectors. So, the FEMAXI-6 code was adopted - the RBMK fuel rod characteristics (fuel pellets thermal conductivity and specific heat dependency from temperature; fuel rod's cladding thermal conductivity and specific heat dependency from temperature) were included into FEMAXI-6 code. The adaptation of this code was presented in the article [5].

The developed fuel rod model for Ignalina NPP and FEMAXI-6 code with included thermal properties for fuel pellets and cladding used in RBMK-1500 reactor were used for thermal hydraulic and structure analyses of fuel rod. These two possibilities of FEMAXI-6 code were validated. Thermal hydraulic part was validated using comparison of FEMAXI-6 calculation results and Kurchatov Institute calculation results. Structural – comparing FEMAXI-6 calculation results and received calculation from BRIGADE code. More about this validation process is presented in the paper [6]. The main conclusion of this validation was that FEMAXI-6 calculation results are in good agreement with received data from Kurchatov Institute and BRIGADE code. Thus, adapted FEMAXI-6 code version and developed model are suitable for future analysis of operational transients and accidents in fuel rods of RBMK-1500.

3. Analysis of processes in RBMK–1500 fuel rod during normal operation

In the RBMK type reactor, fuel assemblies operate for several years until they reach their limit of burnup. During this long–term operation, the reactor power changes several times due to an emergency shutdown or reduction of power. Moreover, the reactor is shutdown once a year for preventive maintenance.

For a detailed analysis, the specialists of the Ignalina NPP selected a fuel assembly which has the average power loaded with 2.6 % U^{235} enrichment with burnable erbium absorber fuel [7]. Parameters of the assembly were measured at intervals of about one week. For several typical cases of transient (reactor start–up, the increase/decrease in power, reactor shutdown), the parameters were recorded at the intervals of several minutes. The reactor power history of the second reactor unit of the Ignalina NPP during July 2003-January 2007 is presented in Fig. 3. During this period 50 changes in reactor power occurred and fuel burnup reached 24000 MWd/tUO_2 in the fuel channel with overage power. Within the time intervals when the reactor was shutdown, the burnup remained approximately constant [7].

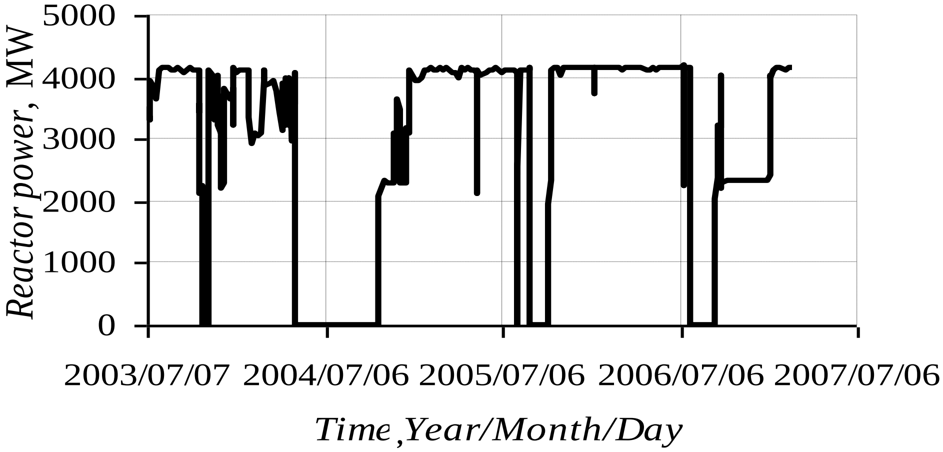

Fig. 3. Power history of the second unit of the Ignalina NPP [7]

As it is shown in Fig. 3, during the whole operation of fuel assembly, the full shutdown of the reactor occurred 5 times. Coolant velocity was reduced from ~3.5 m/s (normal operation) to 1.2 m/s when the reactor was shutdown. At the reactor shutdown stage the pressure in the fuel channels is decreasing down from ~7.5 MPa (normal operation) to the atmospheric pressure and the coolant temperature is reduced from 290 ^{o}C (normal operation) to 100 ^{o}C [7].

The analysis was performed for the fuel rod with average initial power (2.5 MW) from the bottom bundle. The initial fuel rod parameters were assumed as shown in Table 1; the linear power, coolant velocity, coolant pressure and coolant temperature dependencies on burnup were used as the initial input data for the FEMAXI–6 calculations. Axial power profile for the fuel bundle is shown in Fig. 4. The highest energy generation peak is into the middle of the fuel bundle (about 2 m from the core bottom – segment No. 7 in the FEMAXI–6 model). Thus, the calculations results of fuel rod parameters (Fig. 5 - Fig. 7) were presented only in segment No. 7.

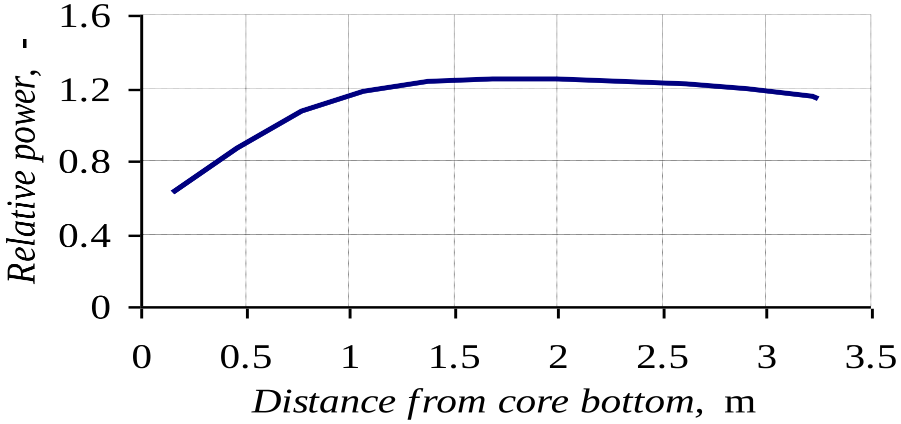

Fig. 4. Axial power profile of the bottom bundle [7]

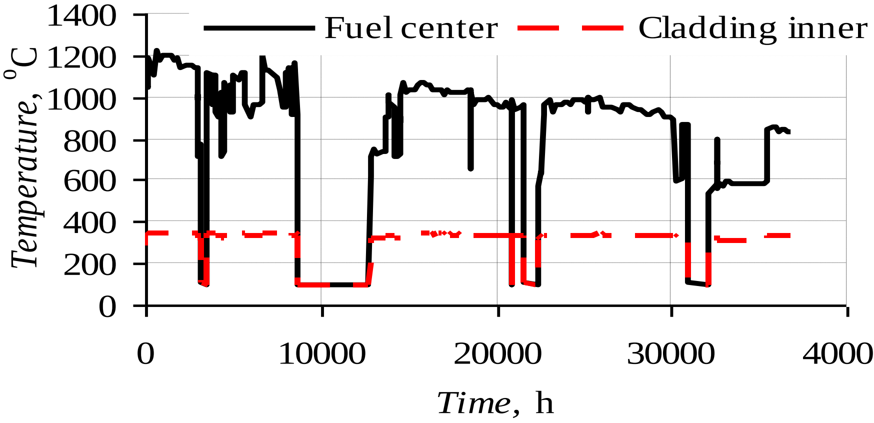

Fig. 5. Peak Temperatures in the fuel rod (about 2 m from the core bottom – segment No. 7 in the FEMAXI–6 model)

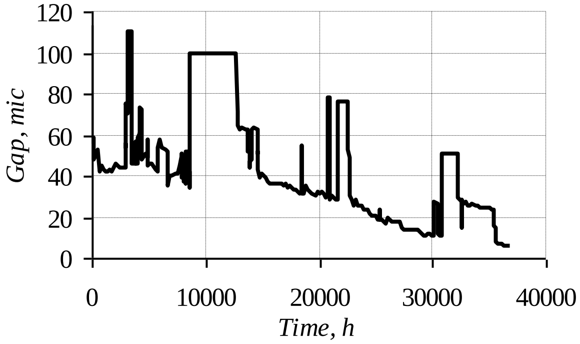

Fig. 6. Gap between the fuel pellet and cladding

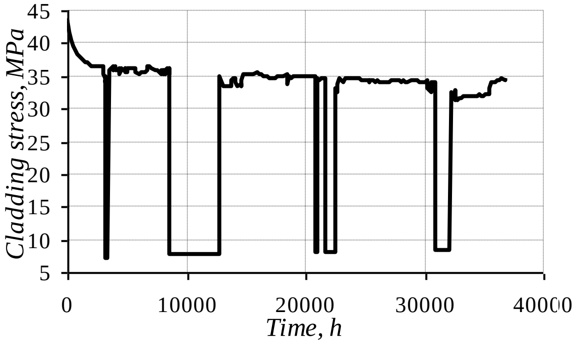

Fig. 7. Equivalent stress in fuel rod cladding

The main conclusions of calculation results are that: a) the peak temperatures of the fuel rod are decreasing due to the decrease of power during the reactor operation (Fig. 5). During the reactor shutdown, the temperatures of the cladding and fuel dropped down to 100 °C (such conditions are preserved during the reactor maintenance); b)the gap between the fuel pellet and cladding remains open during the whole normal operation period (Fig. 6); c) the maximal stresses of the fuel rod cladding is few times lower than the yield stresses (the highest stresses of the fuel cladding are in the range of 47 MPa, while the yield stress of Zr+1%Nb alloy is 180 – 220 MPa for 300 °C temperature [8] (Fig. 7). And all these results lead to the conclusion that the safety barrier is sustained - the fuel cladding remains intact during the whole life in the normal operation.

Detail analysis description with calculation results is presented in the article [9].

The results obtained from the analysis of the normal operation of the fuel rod was used as the initial conditions for the simulation of the processes in the fuel rods stored in the spent fuel pools.

4. Analysis of the processes in RBMK–1500 fuel rod during storage in spent fuel pool and dry storage

After defined burnup of fuel ~ 2400 MWd/tUO$_2$ is reached, the fuel bundle is removed from the reactor core to the spend fuel pool. The fuel bundle in the spent fuel pool is maintained not less then 5 years. After this 5-year period in the SFP the fuel bundle is transferred to the dry storage containers for the 50 year period. In this paragraph the processes in the fuel rods placed in the SFP and dry storage containers are analyzed concerning the fuel bundle history of normal operation in RBMK-1500 reactor.

Then the fuel bundle is taken out from the reactor core - the power of the bundle sharply decreases. However residual power still exists. The linear power of residual heat in the fuel bundle (2.6 % fuel enrichment) placed in the spent fuel pool is presented in Fig. 8.

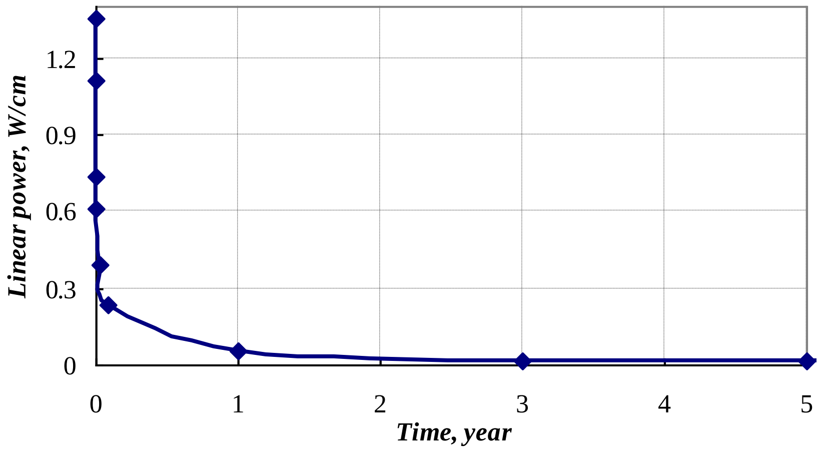

Fig. 8. Linear power of the fuel rod. [10]

Assumptions for the modelling of the fuel rod, placed in the spent fuel pool.

The coolant temperature in the spend fuel pool was assumed to be 50 ^{o}C. Coolant pressure – 0.2 MPa, coolant velocity 0.1 m/s (natural circulation of water). Fuel rod profile was assumed the same as during normal operation (Fig. 4).

Assumptions for the modelling of the fuel rod, placed in dry storage container.

After 5 years storage in the spent fuel pool, the fuel bundle is placed in the dry storage container. The residual linear power in the fuel rod must be ~ 0.01 W/cm (see Fig. 8). In order to have the conservative calculation results the linear power assumed constant during all 50 years of the storage in dry storage container. According to the IAEA requirements the temperature of fuel rod can not be higher then 300 ^{o}C [11]. Thus, in the FEMAXI-6 model the cladding outer temperature for the all nodes was assumed 300 ^{o}C and did not changed during all dry storage period.

Due to limitation of FEMAXI-6 code (only water or steam is assumed as the coolant) it is assumed, that the environment in the dry storage container is the water. Thus, it is assumed, that the fuel rod with constant temperature is placed inside the water (in reality should be in the helium ambience).

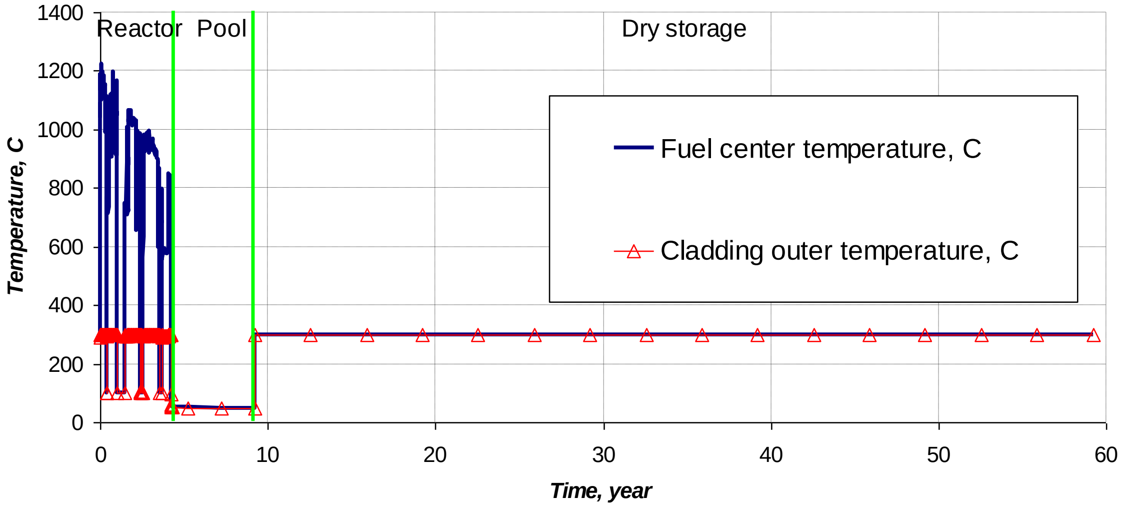

Fig. 9. Fuel center and cladding outer temperature.

The calculated fuel centre temperature and cladding outer temperatures are presented in Fig. 9. The linear power of the fuel rod is very low so the temperatures of the fuel and cladding are almost the same.

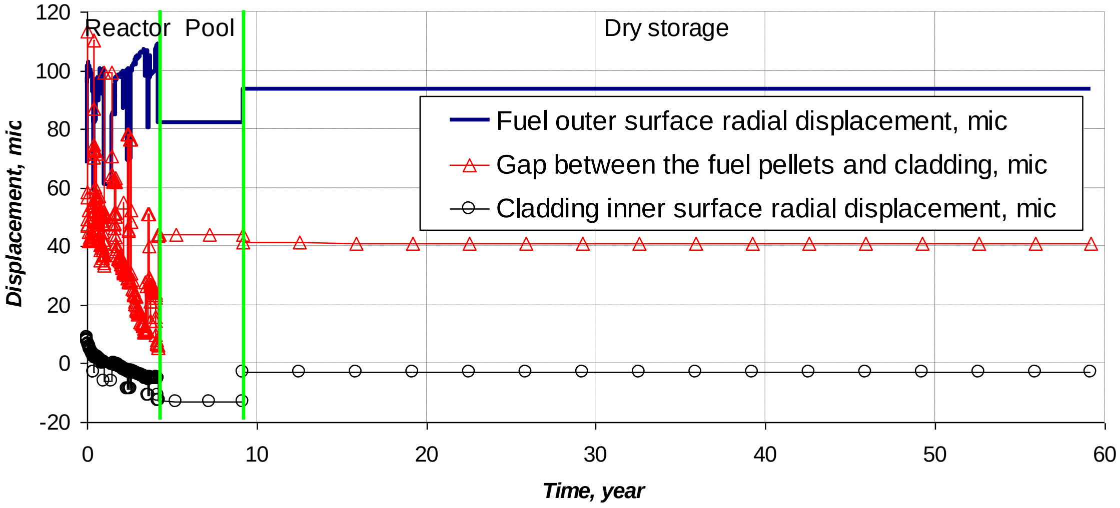

Fig. 10. Fuel outer, cladding inner surface radial displacement and gap between the fuel and cladding.

Then the fuel rod temperature decreases, the cladding and fuel is shrinking. The fuel and cladding radial displacement is presented in the Fig. 10. The shrinking of fuel rod components is bigger in the spent fuel pool then in the dry storage container, because of lower temperature. Similar behavior is also for the gap between the fuel pellets and cladding (Fig. 10). Then the fuel rod is placed in the spent fuel rod the gap form the 5 mic. increases to the ~45 mic. However in the dry storage container the gap decreases to ~40 mic.

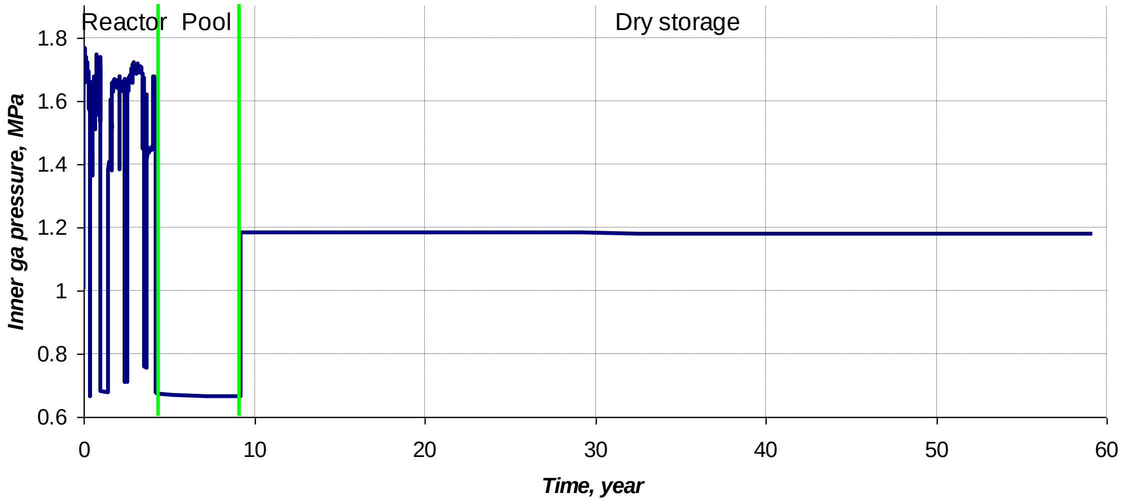

Fig. 11. Inner gas pressure.

Inner gas pressure mostly depends on the temperature in the fuel rod. Then the fuel rod is placed in the spent fuel pool the pressure decreases to the ~0.7 MPa and increases until 1.2 MPa in the case of storage in the dry storage containers.

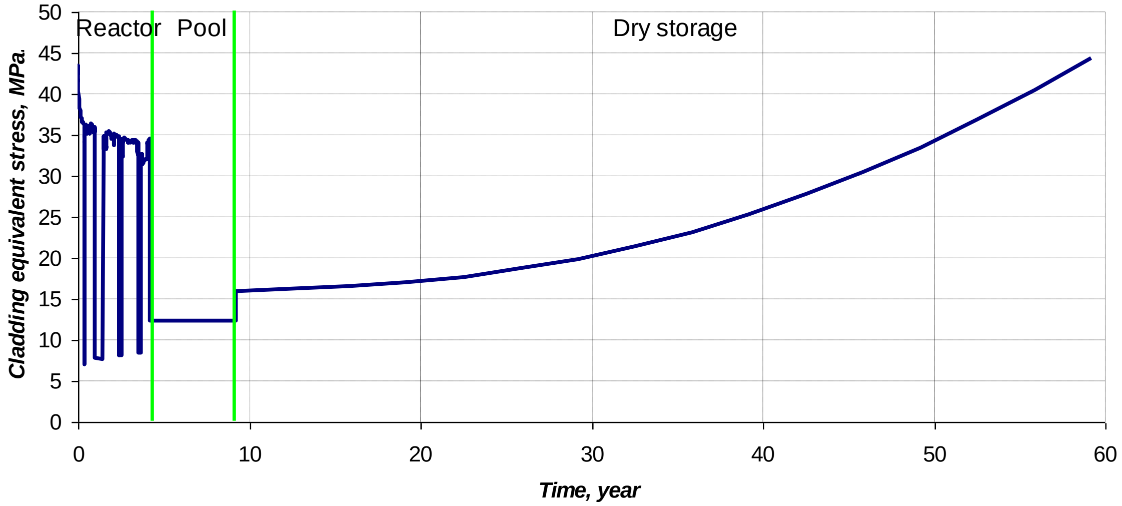

Fig. 12. Cladding equivalent stress

Cladding equivalent stress is presented in the Fig. 12. Then the fuel rod is in the spent fuel pool the cladding equivalent stress is very low. Then the fuel rod is paced in the dry storage container the equivalent stress is constantly increasing. It is also important to note that during normal operation of the fuel rod the biggest part to the cladding equivalent stress is circumferential stress, but in the dry storage container the biggest part is from the axial stress.

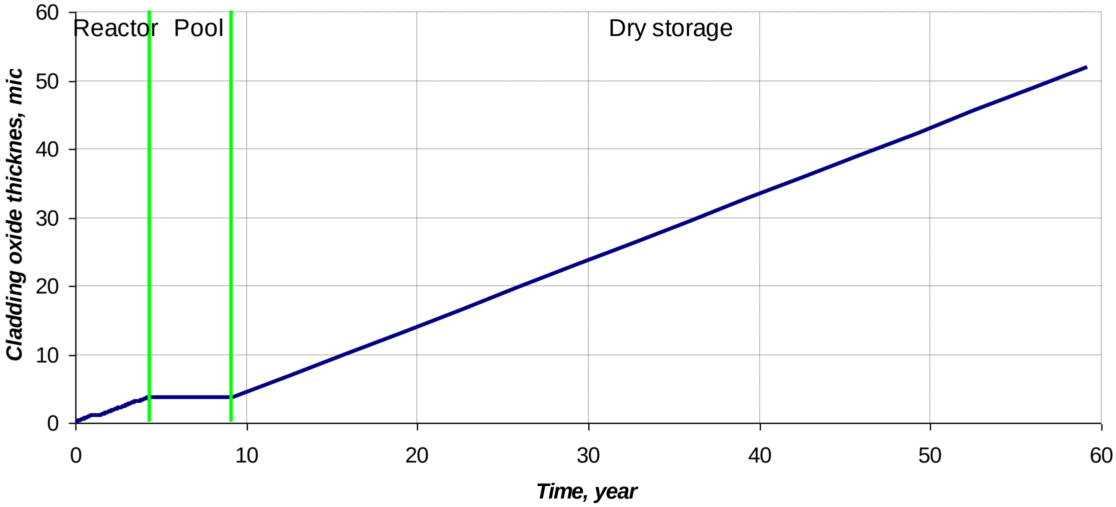

Fig. 13. Cladding oxide thickness

Cladding oxide thickness is the constant when the fuel rod is placed in the spent fuel pool. The oxide thickness is increasing them fuel rod is placed in the dry storage container. However it is need to remember that in the model it was made assumption that fuel rod is in the water. In reality, the environment inside the dry storage container should be helium, thus the oxidation process should be completely different.

5. Summary and conclusions

The analysis of the processes in RBMK-1500 fuel rod during the whole life of the fuel assembly in the reactor core was performed for the fuel rod of 2.6 % U^{235} enrichment with burnable erbium absorber from the fuel assembly with the average initial power (2.5 MW) from the bottom fuel bundle. The calculation results, showed that:

- the peak temperatures of the fuel rod are decreasing due to the decrease of power during the reactor operation. During the reactor shutdown, the temperatures of the cladding and fuel dropped down to 100 °C;
- the gap between the fuel pellet and cladding remains open during the whole normal operation period;
- the elastic deformation of the cladding is very small;
- the maximal stresses of the fuel rod cladding is few times lower than the yield stresses (the highest stresses of the fuel cladding are in the range of 47 MPa, while the yield stress of Zr+1%Nb alloy is 180 – 220 MPa for 300 °C temperature. And all these results lead to the conclusion that the safety barrier is sustained - the fuel cladding remains intact during the whole life in the normal operation.

The results obtained from the analysis of the normal operation of the fuel rod was used as the initial conditions for the simulation of the processes in the fuel rods stored in the spent fuel pools. The results of spent fuel storage inside spent fuel pool (5 years) and inside dry storage container (50 years) are presented also. To receive the conservative results, the maximal allowed temperatures were assumed in the calculation: 50 ^{o}C – the water temperature in the spent fuel pool and 300 ^{o}C of fuel rod claddings inside the dry storage container. The most parameters of fuel cladding during this intermediate term storage period remains similar as were during the normal operation.

References

1. **Almenas K., Kaliatka A., Uspuras E.** Ignalina RBMK-1500. A Source Book. Extended and Updated Version, Lithuanian Energy Institute, Kaunas, Lithuania, 1998.
2. Safety Analysis Report for INPP Unit 2. Task 5. Accident analysis, Ignalina NPP report, 2005.
3. **Jusevičiūtė A., Kaliatka A., Urbonavičius E., Duškesas G., Juodis L., Sonnenburg H.G.** Assessment of FEMAXI and TESPA-ROD codes for modelling of BDBA in RBMK-1500. Kerntechnik. ISSN 0932-3902. 2008. Vol. 73, No.4, p. 197-206.
4. **Suzuki M.** Light Water Reactor Fuel Analysis Code FEMAXI-6 (Ver. 1). Japan Atomic Energy Research Institute, 2005.
5. **Jusevičiūtė A., Kaliatka T., Kaliatka A., Ušpuras E.** Usage of FEMAXI–6 program code for RBMK-1500 nuclear fuel rods simulation. Energetika (in Lithuaniain). 2009, t. 55, no. 2, p 65-76.
6. **Kaliatka T., Marao A., Karalevičius R., Ušpuras E.** RBMK fuel rod modelling and investigation of process during operation cycle // Proceedings of the 18th international conference on nuclear engineering (ICONE 18,) Xian, China, May 17-21, 2010. USA: ASME, 2010, p. 1-7.
7. Ignalina NPP ICC data 2007.
8. **Antikain P. A.** Metals of equipment and pipe lines for Nuclear power plants, Moscow, 1984.
9. **Kaliatka T., Marao A., Karalevičius R., Ušpuras E., Kaliatka A.** Best estimate analysis of processes in RBMK fuel rods during the operation cycle // Mechanika. ISSN 1392-1207. 2011. Vol. 17. No. 4, p. 387-394.
10. Institute VNIPIET, Additional to Ignalina NPP design – safe storage of uranium-erbium fuel with enrichment of 2.8 %. No. 03-02499. TASpd-1299-70796 (2003) (in Russian).
11. **Bochvar A.A.** All Russia research institute of inorganic materials, clasification of fuel failures for WWER- and RBMK- fuel and its impact on long term storage, IAEA technical meeting/workshop on dry spent fuel management for WWER/RBMK reactors, 2002, Russia.

DYNAMIC ANALYSIS OF SYNERGISTIC DEEP BURN HIGH TEMPERATURE REACTOR SCENARIO WITH FAST REACTOR

C. J. JEONG, C.K. JO, J.M. NOH
Korea Atomic Energy Research Institute
989-111 Daedeok-daero, Yuseong, 305-353, Daejeon, Korea

ABSTRACT

A deep burn (DB) high temperature reactor (HTR) and sodium-cooled fast reactor (SFR) synergistic scenario has been analyzed using the DANESS system dynamic analysis code. First, the basic once-through fuel cycle was modeled, and the DB-HTR and SFR synergistic scenario was analyzed. In this study, the nuclear reactor deployment scenario, front-end cycle parameters, and back-end cycle parameters have been investigated compared with those of the once-through cycle. From the DB-HTR and SFR synergistic scenario analysis results, it is shown that the front-end fuel cycle parameters have been decreased more than 20% compared with those of the OT cycle. Also, it can be seen that the synergistic cycle can reduce spent fuel and trans uranic (TRU) element out-pile inventories. Therefore, a DB-HTR and SFR synergistic scenario is very efficient in reducing the SF and TRU inventories.

1. Introduction

The concept of a deep-burn (DB) of a trans uranic (TRU) element in a high temperature reactor (HTR) has been proposed and studied as an alternative TRU transmutation method [1,2]. In the DB, a graphite-moderated modular helium reactor (MHR) is used to obtain ultra high burnup. For the DB concept, ceramic-coated particle fuels (TRISO) are used along with deep-burning (typically 50~65%) of TRUs from light water reactors (LWRs). At first, the DB in a HTR is a single irradiation process without repeated reprocessing [3]. But there is still a significant amount of TRU after a single pass of irradiation. Therefore, it is necessary to burn the remaining TRU further by adopting a fast reactor (FR).

In this study, a synergistic fuel cycle of the DB-HTR and a sodium-cooled fast reactor (SFR) burner are considered for an efficient burning of TRUs from LWRs. In this HTR-SFR synergy, the fuel cycle is closed with an SFR burner: the spent fuel of DB-HTR is reprocessed and recycled into the SFR, providing a fuel cycle extension and true closure. Fig. 1 shows the concept of the LWR-HTR-SFR combined fuel cycle for the TRU transmutation. The recovered LWR TRUs are deep-burned in 600MWth HTRs, and the remaining TRUs are additionally incinerated in an SFR after reprocessing with pyro-technology, in which only the fission products are removed.

In this study, the fuel cycle characteristics are analysed for DB-HTR and SFR synergy scenarios. For the analysis, front-end and back-end parameters are compared with those of the OT cycle. The calculations were performed using DANESS (Dynamic Analysis of Nuclear Energy System Strategies) [4], which is an integrated system dynamic code for the analysis of current and future nuclear energy systems.

2. Fuel cycle model

The material flow is modelled through the process in Fig. 1. The LWR spent fuel is fed into the HTR through reprocessing. The HTR SF is then reprocessed and goes into the SFR. The spent SFR fuel is recycled in the SFR.

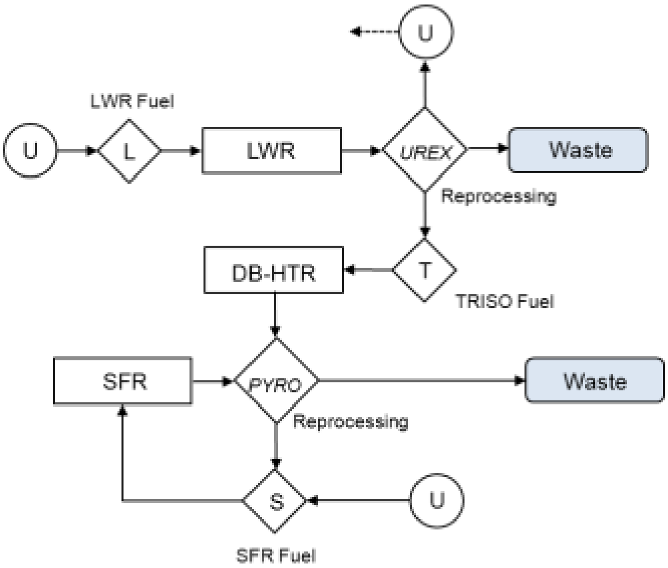

Fig 1. Fuel cycle concept of the DB-HTR and SFR synergy scenario

Fig. 2 shows schematic configurations of the DB-HTR-core. The DB-HTR core is an annular type with a small inner reflector for improving the neutron economy and higher fuel burnup. The active core consists of 5 fuel rings. The DB-HTR core is comprised of 9 axial layers, which results in 1296 fuel blocks in the core. The fuel block configurations are also shown in Fig. 2. The axial height of the block is 88.1cm including 2.9-cm graphite zones at the top and bottom. The detailed design parameters of the core and fuel are described in Ref. 5.

The 1500 MWt SFR core configuration [6] is shown in Fig. 3. As shown in Fig. 3, the core is a homogeneous annular type, and there is a large central non-fuel region. The central region is introduced to reduce the conversion ratio so as to achieve high transmutation capability and to reduce the sodium void reactivity. There are 300 fuel assemblies in the core.

The fuel is a metallic alloy of TRU-U-Zr including a small amount of rare earth (RE) elements. In this study, the Zr content is adjusted to achieve the targeted TRU consumption rate. The TRU compositions from LWR and HTR are presented in Table 4.

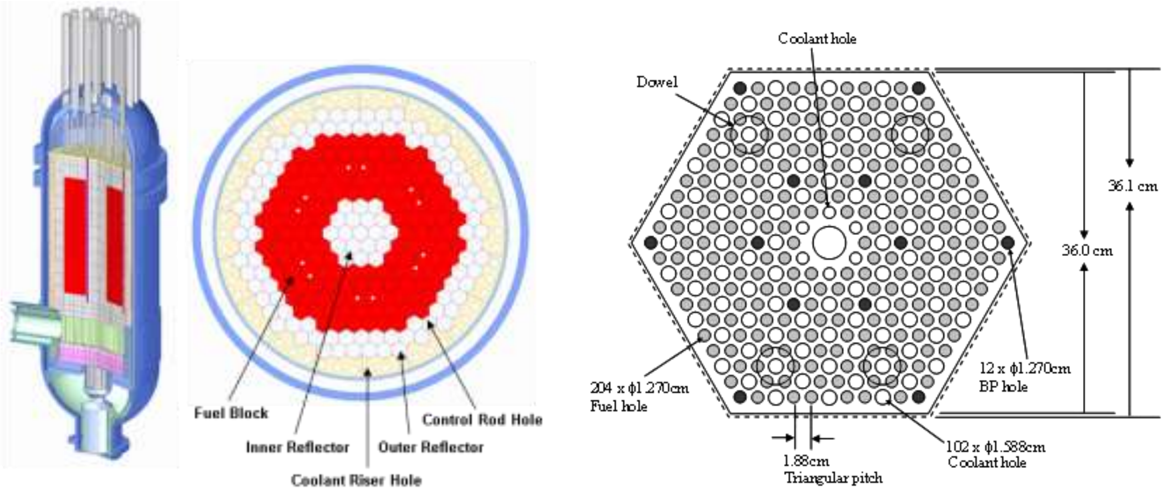

Fig 2. Core layout and fuel block configuration of DB-HTR

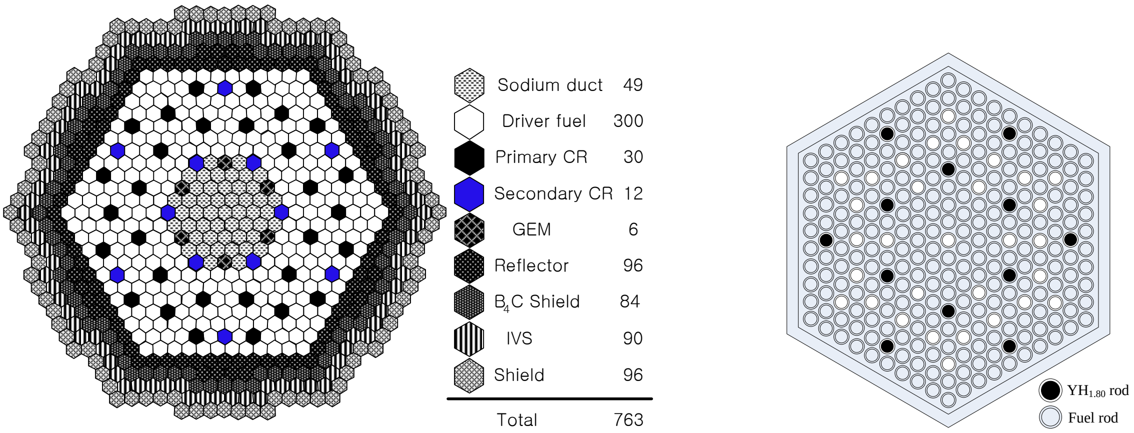

Fig 3. SFR core and fuel configurations

Nuclides	TRU from LWR (50 GWD/tU, 5-yr cooling)	TRU from DB-HTR, (58% burnup, 5-yr cooling)
^{234}U	-	1.080
^{235}U	-	0.057
^{236}U	-	0.027
^{237}Np	6.788	6.664
^{238}Pu	2.835	15.379
^{239}Pu	49.190	4.449
^{240}Pu	22.876	15.844
^{241}Pu	8.734	13.216
^{242}Pu	4.825	23.597
^{241}Am	2.779	6.565
^{242m}Am	0.019	0.114
^{243}Am	1.371	7.869
^{242}Cm	0.000	0.000
^{243}Cm	0.006	0.029
^{244}Cm	0.538	4.532
^{245}Cm	0.033	0.502
^{246}Cm	0.005	0.076

Table 1 Comparison of the feed TRU composition

3. Fuel cycle analysis results

3.1 Once-through cycle

In 2000, there are 4 operating CANDU reactors and 12 PWRs, and the total reactor capacity was 13.8 GWe. From the “National Energy Basic Plan” [7], the nuclear capacity in 2030 will increase to 27.3 GWe with 29 total operating reactors. Between 2018 and 2050, it is expected that the annual electricity demand growth rate will be 0.95%/yr, and the nuclear power capacity becomes 41.3 GWe, which occupies ~59% of the total electricity generation. After 2050, the nuclear growth rate decreases and gives a 70 GWe capacity in 2100.

With the above nuclear reactor operation, the total SF will be ~116600 t in 2100, which is shown in Figure 4. According to the SF inventory, shown in Figure 6, the out-pile inventories of Pu, MA, and TRU will be 1153 t, 95 t, and 1248 t, respectively, in 2100.

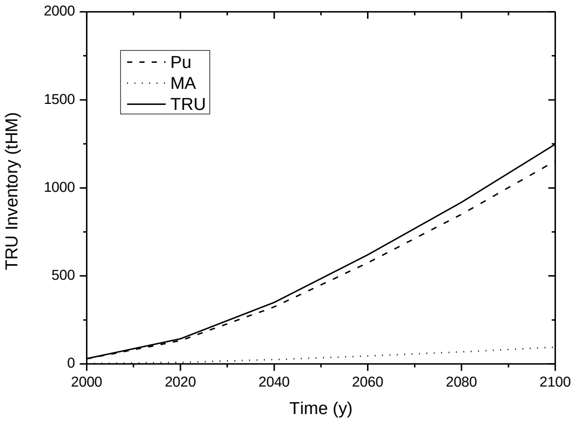

Fig 4. Out-of-pile TRU inventory in once-through cycle

3.2 DB-HTR and SFR scenario

The capacity deployments of DB-HTR and SFR are adjusted to minimize the TRU stockpile. In this study, the SFR deployment starts 10 years after the DB-MHR deployment. The power share of each reactor in 2100 is 12 and 23%, respectively.

For the HTR-SFR cycle, the uranium consumption decreases because a part of the uranium oxide (UOX) fuel is substituted by MHR and SFR fuel. The total uranium usage decreases by ~23% in 2100 compared with the OT case. In addition, the amount of fuel enrichment in 2100 decreases by ~24% compared with the OT cycle. The UOX fuel fabrication decreases by ~22% compared with the OT cycle. The HTR and SFR fuel fabrications become ~860 t and ~4130 t, respectively, in 2100.

The total amount of SF of the DB-HTR and SFR cycle reduces by ~80%. This is because most of the PWR fuel is reprocessed to feed the HTR. From a storage point of view, however, the long-term storing of SF or TRU may more meaningful. Fig. 6 compares the long-term stored SF. It is shown that the long-term stored SF is reduced by ~80%, which similar to that of the total SF.

In 2100, the total plutonium out-pile inventory becomes ~450 t, which is reduced by 61% compared with that of the OT cycle. If the long-term stored Pu inventory is considered, however, the reducing effect is more significant as 93%. As a result, the long-term stored TRU inventory decreases by ~92% compared with that of the OT cycle (Fig. 7).

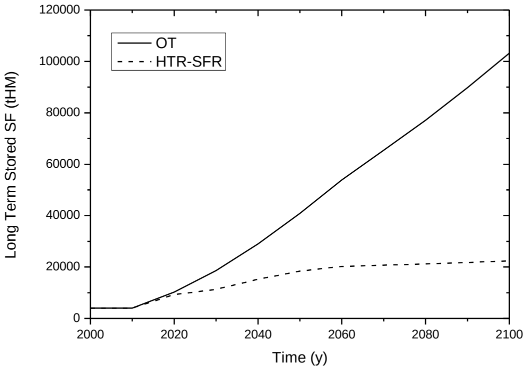

Fig 5. Comparison of long-term stored spent fuel inventory

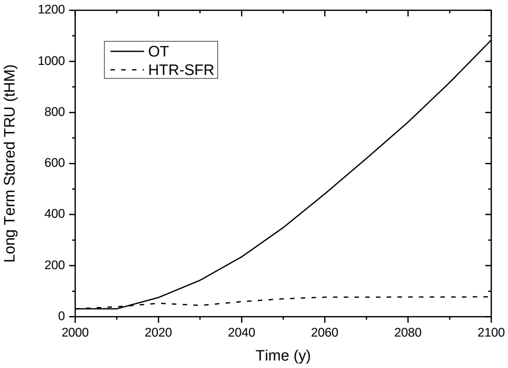

Fig 6. Comparison of long-term stored TRU inventory

4. Summary and conclusions

The Korean nuclear fuel cycles with the DB-HTR system were investigated for a period of 100 yrs from 2000. The results of the HTR cycle with different fuels were compared with those of the once-through cycle. The comparison results for the front-end and back-end fuel cycle parameters are as follows:

- The total natural uranium consumption and total enrichment in 2100 decrease by 23% and 24%, respectively. The UOX fuel fabrication decreases by 22%.
- The amount of total SF is reduced by ~80%. But if the long-term stored SF is considered, the reduction is more significant by 93%.
- The amount of total out-pile TRU can be reduced by 53% in 2100. Again, the long-term stored TRU is decreased by 92%.

From the above results, it is known that the DB-HTR FR synergistic scenario can effectively reduce the SF and out-pile TRU inventories. In particular, the reduction effects are significant for long-term stored heavy metals.

References

1. A. Baxter, C. Rodriguez, and F. Venneri, “The Application of Gas-Cooled Reactor Technologies to the Transmutation of Nuclear Waste,” Progress in Nuclear Energy, **38**, 81 (2001).
2. C. Rodriguez et al., “Deep-Burn: making nuclear waste transmutation practical,” Nuclear Engineering and Design, **222**, 299 (2003).
3. Y. Kim and F. Venneri, “Optimization of One-Pass Transuranic Deep Burn in a Modular Helium Reactor,” Nuclear Science and Engineering, **160**, 59 (2008).
4. L. V. D. Durpel, A. Yacout, D. Wade, and H. Khalil, “DANESS-Dynamic Analysis of Nuclear Energy System Strategies,” Global 2003, New Orleans, November 16-20 (2003).
5. C. K. Jo et al., “Core Performance Analysis of a DB-HTR with SiC Kernel Getter TRU Fuel,” Proceeding of HTR 2010, Prague, Czech Republic, Oct. 18-20 (2010).
6. S. G. Hong, Y. Kim, and F. Venneri, “Neutronic Characterization of Sodium-cooled Fast Reactor in an MHR-SFR Synergy for TRU Transmutation,” ICAAP 2007, Nice, France (2007).
7. “National Energy Basic,” Ministry of Knowledge and Economy, (2008).

FUEL ANALYSIS IN LBLOCA WITH CODE TRACE/FRAPTRAN

WEI CHEN, CHUNKUAN SHIH
Institute of Nuclear Engineering and Science
National Tsing-Hua University, Taiwan
No.101, Section 2, Kuang-Fu Road, Hsinchu 30013, Taiwan

JUNGHUA YANG
Department of Engineering and System Science
National Tsing-Hua University, Taiwan
No.101, Section 2, Kuang-Fu Road, Hsinchu 30013, Taiwan

HAO-TZU LIN, JONG-RONG WANG
Institute of Nuclear Energy Research, Taiwan
No. 1000, Wenhua Rd., Longtan Township, Taoyuan County 32546, Taiwan

ABSTRACT

FRAPTRAN 1.4 is the computer code which has been developed by PNNL to analyze and predict the fuel performances during power and/or cooling transients. The thermal hydraulic code, TRACE, was used to offer essential information, such as power profiles, coolant conditions, and reflooding situations, for FRAPTRAN 1.4 as required input information. In this paper, we studied about the transient fuel performance during a postulated Large Break Loss of Coolant Accident (LBLOCA) in Maanshan nuclear power plant. The results from plenum gas pressure shows the cladding failed at node 12 for heat option and coolant option at 480s and 510s respectively, and the hoop stress at rupture is 45.7MPa and 49.5MPa respectively. In order to protect the integrity of the fuel the reflooding rate should be at least increased from 0.225 in/s to 0.7 in/s in this case.

1. Introduction

Normally, evaluating the nuclear power plant (NPP) safety involves several disciplines, like thermal hydraulic, thermal mechanics, reactor physics. The previous studies usually focus on only one of the disciplines which sometimes neglect the other conditions which should also be taken into account for the whole assessment. Thus, it is a trend to survey the safety of the nuclear power plant in the perspective of multidisciplinary assessments [1] [2]. We had accomplished the study of LBLOCA (large break loss of coolant accident) analysis for the Maanshan NPP with TRACE code [3]. In this paper, we tried to use the previous results of NPP large break loss of coolant accident study with TRACE to offer input information for FRAPTRAN. By this method, we can understand more about the fuel behaviors during this transient accident in Maanshan NPP.

1.1 FRAPTRAN

FRAPTRAN [4] is a FORTRAN language computer code, and it is developed by Pacific Northwest National Laboratory, PNNL. The main propose of this code is to calculate the response to single fuel transient performance in light water reactor (LWR) during operational transients or hypothetical accidents, such as reactivity initiated accidents (RIA) or loss of coolant accidents (LOCA), up to the burnup level of 62 GWd/MTU. FRAPTRAN is also a companion code to the FRAPCON-3 which was developed to calculate steady-state high burnup level response of a single fuel rod. FRAPTRAN calculates the variation with time, power and coolant conditions of fuel rods such as fuel and cladding temperature, cladding strain and stress, and plenum gas pressure. FRACAS-I model is used in FRAPTRAN for calculating the mechanical response of the fuel rod and cladding. The failure model in FRAPTRAN apply to LOCA events where deformation is due to gas overpressure and the temperature of the cladding is relatively high (>700 K). After the cladding effective plastic strain is calculated by FRACAS-I, this value will compare with the instability strain given by MATPRO. If the cladding effective plastic strain is greater than the instability strain, the ballooning model, BALON2, is used to calculate the localized, non-uniform strain of cladding. The BALON2 model has two methods to predict failure in the ballooning node. One is when the cladding true hoop stress exceeds an empirical limit, and the other is when predicted cladding permanent hoop strain exceeds the FRAPTRAN strain limit. The verification assessment of FRAPTRAN code is provided by PNNL [5]. These cases contain two major types: RIA test programs and LOCA test programs. The LOCA assessment cases consist of 10 LOCA test case rods which were refabricated from different fuel rods that had been irradiated to burnup levels between 0 and 83 GWd/MTU. And the refabricated rods with Zircaloy-2, Zircaloy-4 and E-110 cladding had been tested in the NRU, PBF, TREAT, and Halden reactors under different LOCA scenarios which represent a large range of rod designs and reactor conditions. These assessments show that FRAPTRAN has great confidence in LOCA analysis.

1.2 TRACE

TRACE is an advanced and best estimate reactor systems code for analyzing thermal hydraulic behaviors in light water reactors [6]. TRACE consolidates the capabilities of the four codes, TRAC-P, TRAC-B, RELAP 5 and RAMONA, into one modernized code. One of the features of TRACE is its capability to model the reactor vessel with 3-D geometry. It can support a more accurate and detailed safety analysis of nuclear power plants. TRACE has a greater simulation capability for loss of coolant accident. Models in TRACE code for multidimensional two-phase flow, non-equilibrium thermo-dynamics, heat transfer, reflood, level tracking, and reactor kinetics are included.

1.3 LBLOCA and Maanshan NPP

The LBLOCA is one of the most important Design Basis Accidents (DBAs) in light water reactors and the double ended guillotine break of the largest primary piping system is limiting condition for the Emergency Core Cooling System (ECCS) requirements. LBLOCA is considered the worst case scenario. Although a LBLOCA is considered very unlikely to happen, the safety systems must be designed to secure adequate cooling of the reactor core. The Maanshan NPP operated by Taiwan Power Company has two Westinghouse PWR units. The rated core thermal power is 2775 MW. The reactor coolant system has three loops, each of which includes a reactor coolant pump and a steam generator. The pressurizer is connected to the hot-leg piping in loop 2. In the previous study, a LBLOCA is defined as a rupture in Maanshan NPP cold-leg with a total cross sectional area. The break was located in loop 1, which is one of the two loops that don’t have a pressurizer.

2. Establishment of FRAPTRAN input file with TRACE

Before we execute FRAPTRAN, we have to produce an input file for FRAPTAN, including fuel rod size, power history and coolant condition. We need mainly three categories to define our transient problem: Fuel rod geometry, Power history and Coolant boundary condition. The flowchart of combining FRAPTRAN and TRACE is shown in Figures 1.

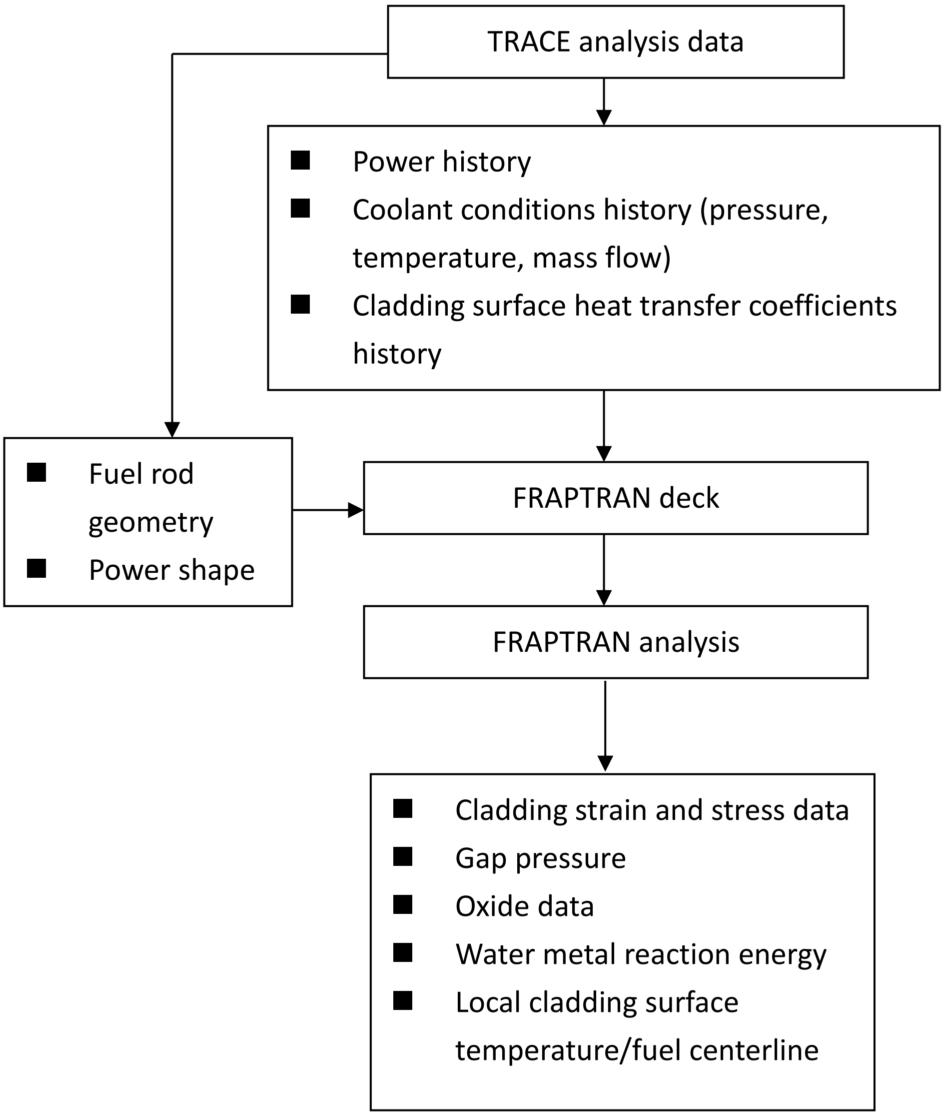

Fig 1. The flowchart of combining FRAPTRAN and TRACE

2.1 Fuel rod geometry

The fuel rod size was written according to the fuel rod that Maanshen NPP used nowadays. We assumed the rod was new one, zero burnup, and the rod data are reported in Tab 1. The axial fuel length from bottom to top was divided into 12 nodes and the fuel radial direction was divided into 17 nodes. By doing so, we can obtain detail temperature distributions inside the fuel rod during any transients.

Fuel stake length	12 ft
Cladding OD/ thickness	0.36/ 0.0225 in
Cladding type	ZIRLO
Cladding thickness	0.001875 ft
Filling gas	He, 225 psia
Burnup	0 GWd/MTU

Tab 1: Fuel rod design parameters

2.2 Boundary condition description

There are two suboptions in coolant data block to describe boundary condition, one is ‘coolant’ option, and the other one is ‘heat’ option, but only one option can be used. If the ‘coolant’ option is used, the ‘coolant’ option should not be used, and vice versa. The results from the previous study with TRACE were used as boundary condition and power history during transient for FRAPTRAN. First of all, in the coolant option, average core pressure, coolant mass flux history and coolant enthalpy history should be written into input file. Some can be directly read from TRACE outcomes and some have to assess through transforming relative results. Secondly, in the heat option, we divided the axial space of fuel rod into 4 zones, and described coolant pressure history, heat transfer coefficient history and coolant temperate history for each zone. All these essential information came from TRACE.

2.2.1 Mass flux setting in coolant option

Mass fluxes at fuel channel inlets were obtained from averaging values of the mass flow rates from TRACE and divided by the flow area. Normally, mass flow rates oscillate dramatically around zero in all system codes so that great care should be taken in order to provide a meaningful averaging mass flux for FRAPTRAN. Fortunately, the mass flux becomes relatively insensitive after the initiation of adiabatic heatup which corresponds to the time when the water level drops below the bottom of the core in the blowdown phase.

2.2.2 Reflooding description

In boundary data block, there is another suboption, ‘reflood’, which describes the coolant flow condition after adiabatic heatup beginning. The water level variation from TRACE is shown in Figure 2. This is helpful to determine the start time of adiabatic heatup and reflooding. The initiation of adiabatic heatup corresponds to the time when the water level drops below the bottom of the core in the blowdown phase. Next, the time when the water level rises up to the fuel again defines the initiation of reflooding phase. Based on the overall behaviors of water level change, one can estimates the corresponding reflooding rates from the slope of water level positions, 0.225806 in/s in the beginning and 0.07645 in/s in the end.

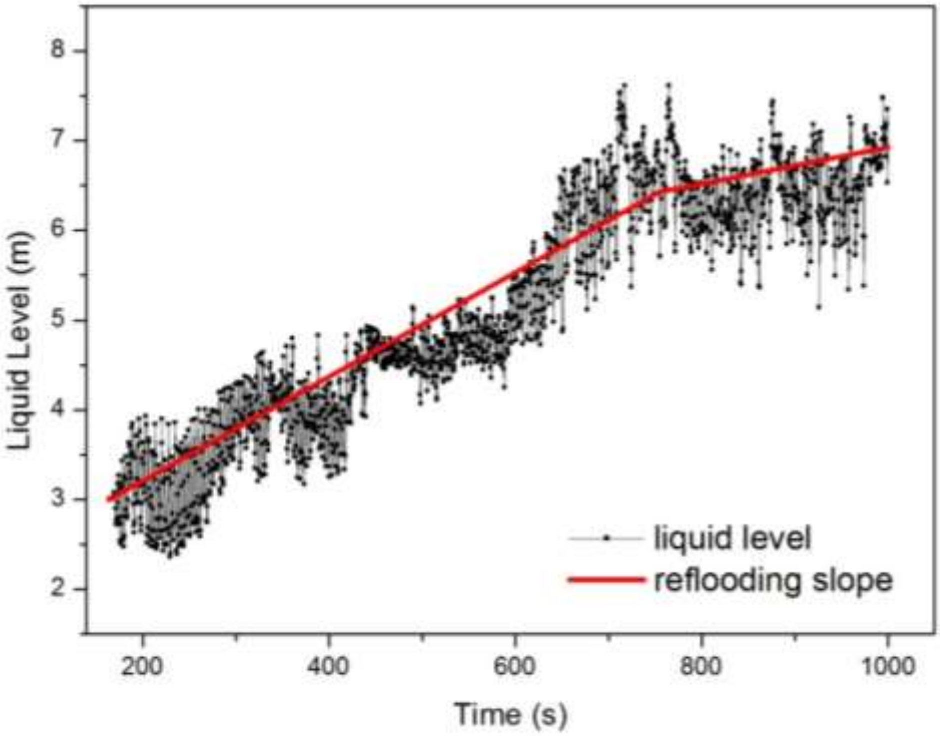

Fig 2. The method to approach reflooding rate

3. Result and Discussion

In this case BALON2 model in FRAPTRAN predicts that the cladding failure happened. The plenum gas pressure results came from two different boundary condition inputs, coolant option and heat option, are shown in Figure 3. The cladding ballooning happened at node 12 at 420 s and 450 s for heat option and coolant option respectively. Also, this phenomenon happened earlier for using heat option. After the cladding failure happened, there must be a balance between the plenum gas pressure and the environment (core) pressure. At the beginning of the rupture, the difference of the pressure value between the core and the cladding plenum is large. Thus, the phenomenon of the pressure drop can be seen while the cladding failed. Both options indicate the cladding failure, and the failure time is at 480 s for heat option and at 510 s for coolant option. In Figure 4, the hoop stress history at node 12 shows the rupture of the cladding as well. The hoop stress at burst of two options is 45.7MPa and 49.5MPa respectively. The Figure 5 shows the cladding temperature at node 2, 7, 11, 12 (from bottom to top) before 550s, the cladding temperature for heat option and coolant option are 1184.3K and 1173.1 K respectively. Therefore, the outcome of the high cladding temperature at ballooning location is not only reducing the strength of the cladding but also enhancing the oxidation reaction with water, eventually result in cladding failure.

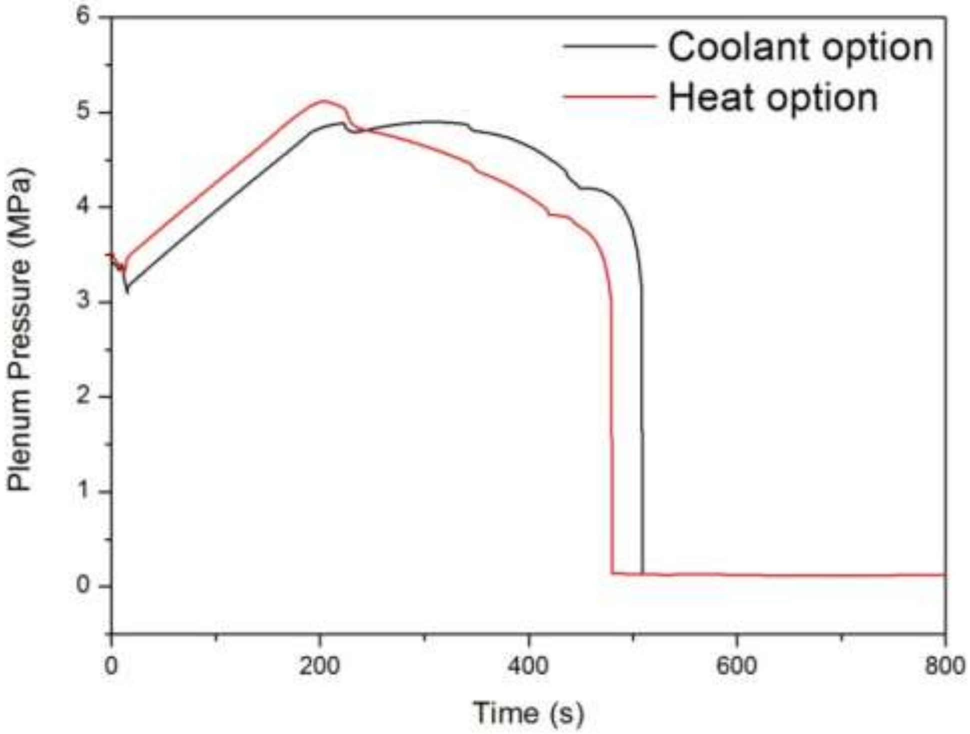

Fig 3. Plenum Pressure for coolant option and heat option

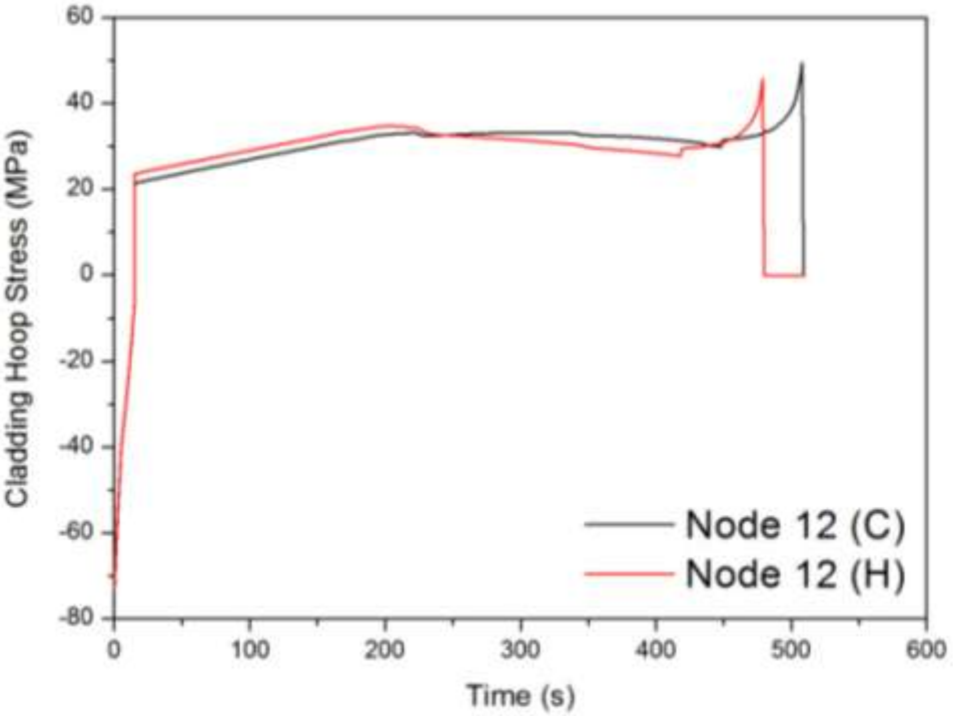

Fig4. Cladding Hoop Stress at node 12 before 515s. (C): coolant option; (H): heat option

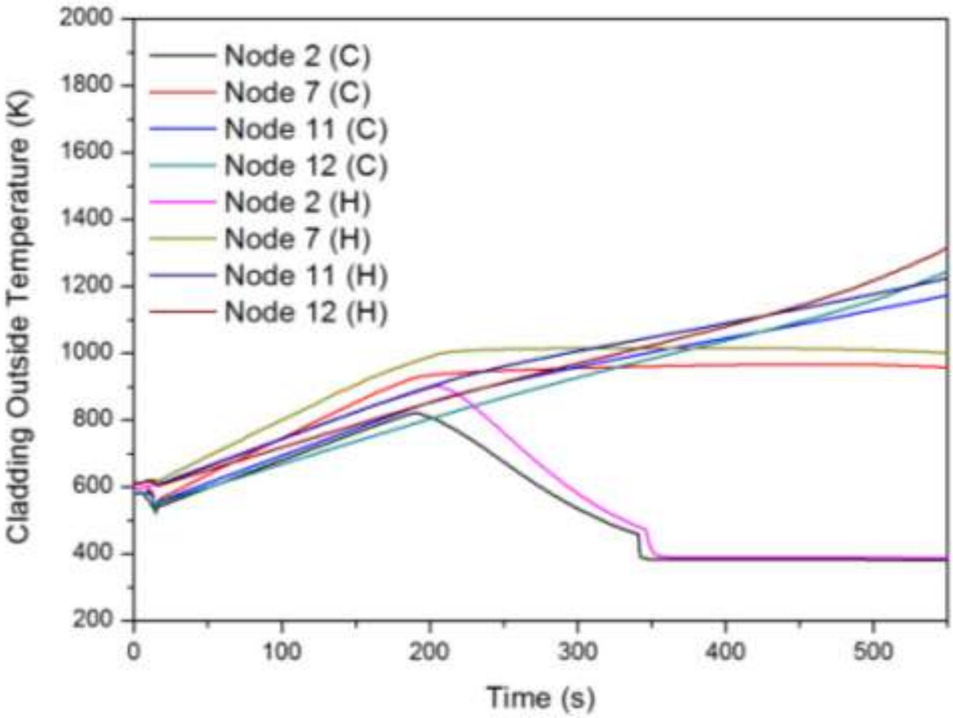

Fig 5. Cladding Outside Temperature before 550s. (C): coolant option; (H): heat option

According to LOCA licensing criteria, 10 CFR50.46, the limit peak cladding temperature is 2200°F (about 1480 K), and the maximum Equivalent Cladding Reacted (ECR) is 17%, this is important especially during high temperature oxidation. Figure 6 reveals the ECR fraction at node 11 and 12 increase with the trend of the cladding temperature after 300 s. Both ECR value at node 12 are less than 2% at the failure. Although 2% of ECR value is under the licensing criterion, which means the cladding embrittlement caused by oxidation is not the main reason for cladding failure, we can't deny the certain degreed of contribution of oxidation to weak the strength of the cladding.

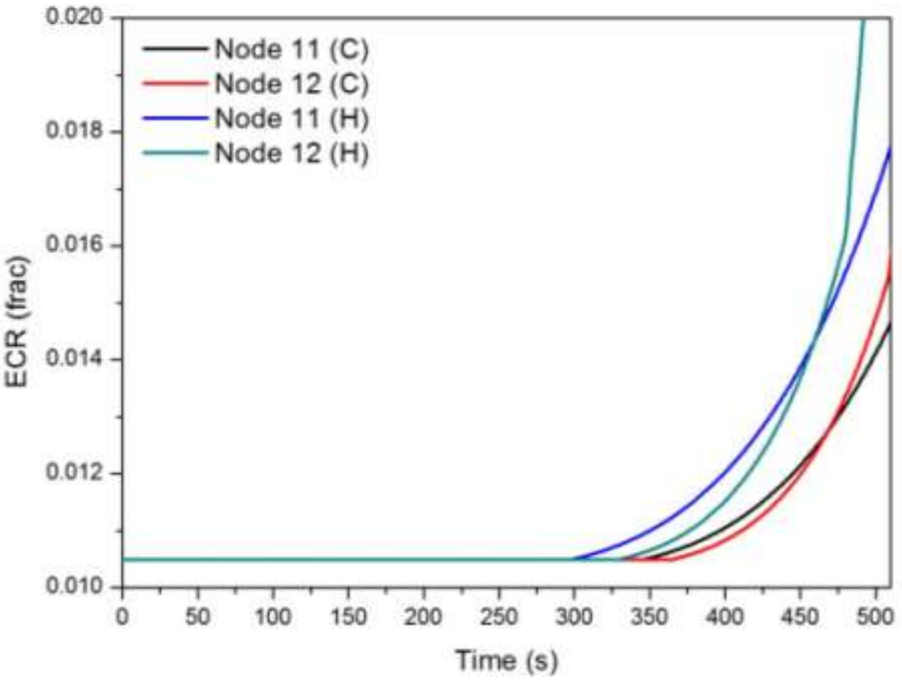

Fig 6. ECR at node 11,12 for two option before 510s. (C): coolant option; (H): heat option

Combining the outcomes above, we persumed that the slow reflooding rate should take the responsibility to prevent the cladding failure in this case. Thus, the minimun reflooding rate required in this case becomes the other issue that we are interested. Firstly, when reflooding rates were adjusted to 0.6 in/s, 0.65 in/s and 0.7 in/s, the gas pressure results in coolant option and heat option all indicate no failure happened, as shown in Figure 7.

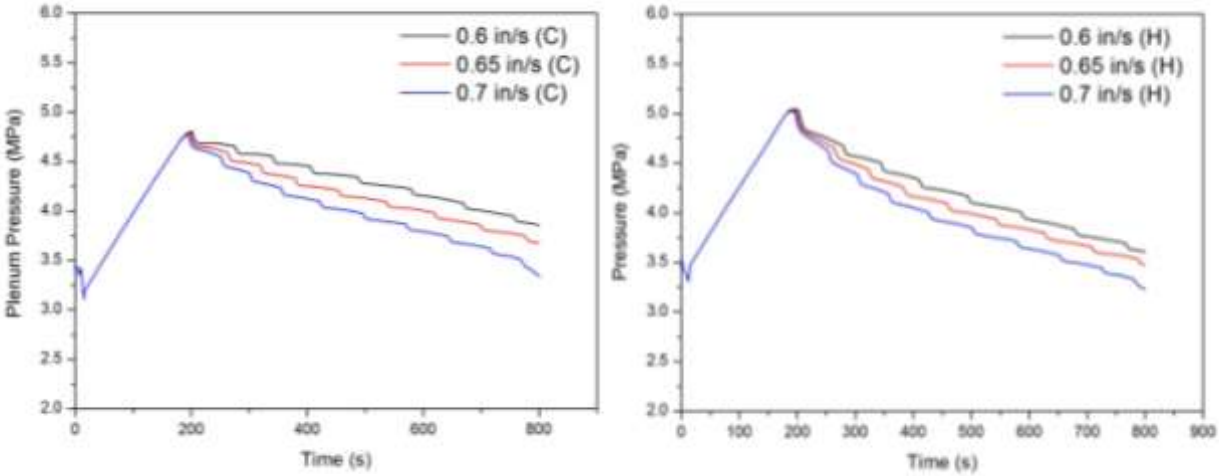

Fig 7. The Plenum Pressure for coolant option (left) and heat option (right) when reflooding rate is 0.6 in/s, 0.65 in/s and 0.7 in/s.

The Figure 8 shows the fuel centerline temperature and the cladding outside temperature when reflooding rate were 0.6 in/s, 0.65 in/s and 0.7 in/s. However, when reflooding rate is 0.6 in/s, it is obviously that the temperature at 12 node is still increasing. Next, the temperature at node 12 is stable in the end of the problem time while the reflooding rate is 0.65 in/s. Although the node 12 is stable, the output result informs the warning signal, the strains are too large, which we should notice in this assumption. Thus, to be sure conservatively the integrity of the fuel rod, the minium reflooding rate should be obtain 0.7 in/s in this case.

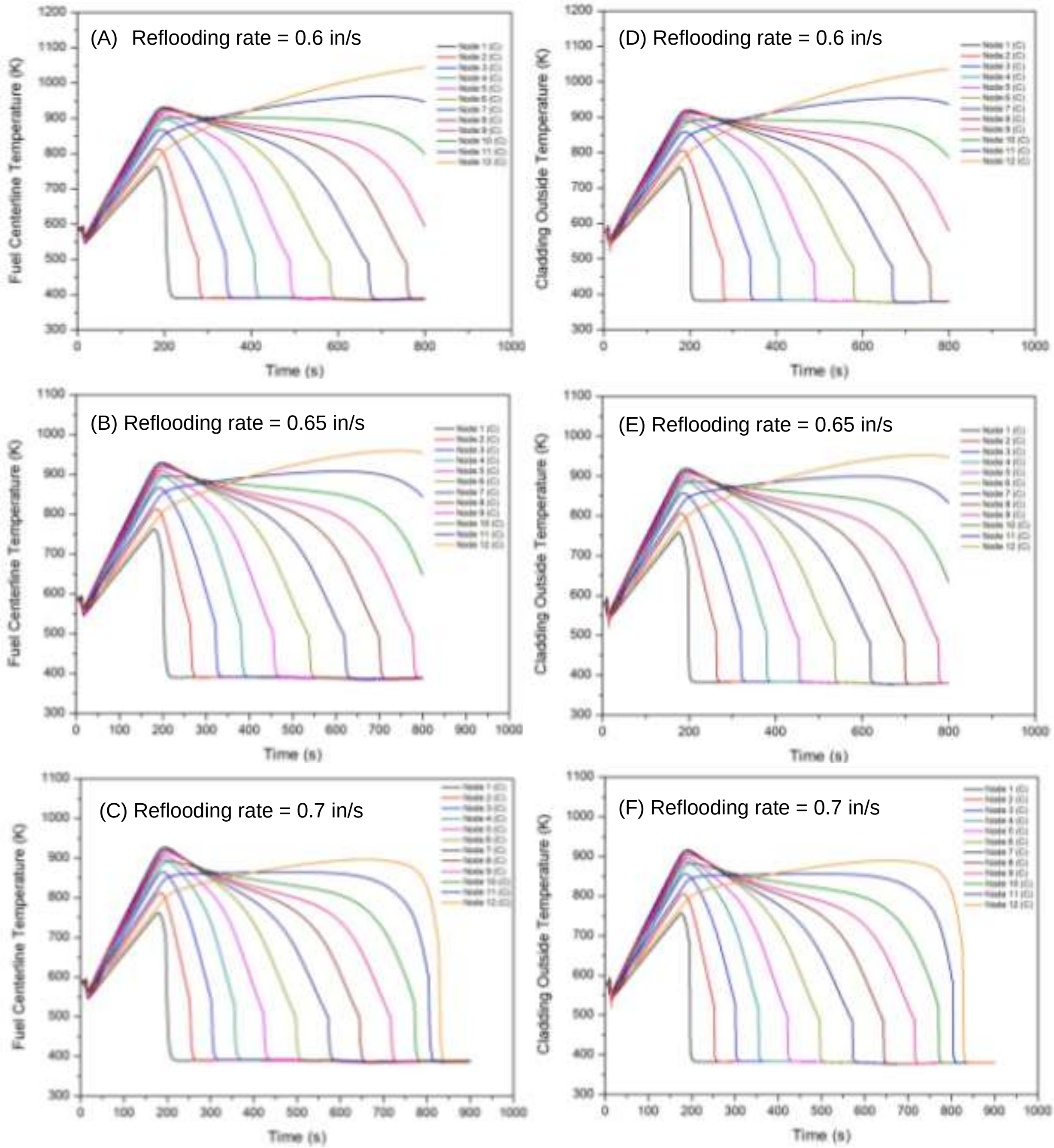

Fig 8. The Fuel Centerline Temperature (A,B,C) and the Cladding Outside Temperature (D,E,F) at 0.6 in/s, 0.65 in/s and 0.7 in/s for coolant option.

4. Conclusion

In this paper, we have combined TRACE and FRAPTRAN to calculate the fuel performance during LBLOCA transient successfully. According to FRAPTRAN results, the fuel cladding failed at node 12 for heat option and coolant option at 480s and 510s respectively, and the hoop stress at rupture is 45.7MPa and 49.5MPa. And the cladding temperature would be greater than the criterion after rupture because of the slow reflooding rate. Thus, to obtain the fuel rod integrity, the reflooding rate should be at least increased to 0.7 in/s.

Reference

1. K.J. Geelhood, W.G. Luscher, C.E. Beyer, J.M. Cuta, “FRAPTRAN 1.4: A Computer Code for the Transient Analysis of Oxide Fuel Rods” NUREG/CR-7023, Vol. 1, PNNL-19400, Vol. 1, March 2011
2. Antti Daavittila, Anitta Hämäläinen, Hanna Räty, “TRANSIENT AND FUEL PERFORMANCE ANALYSIS WITH VTT’S COUPLED CODE SYSTEM”, *Mathematics and Computation, Supercomputing, Reactor Physics and Nuclear and Biological Applications,* 2005
3. Jung-Hua Yang, Jong-Rong Wang, Hao-Tzu Lin, Chunkuan shih,“LBLOCA analysis for the Maanshan PWR nuclear power plant using TRACE”, *2011 2nd International Conference on Advances in Energy Engineering (ICAEE)* Volume 14, 2012, Pages 292–297
4. Ken Geelhood, “Modeling High Burnup RIA Tests with FRAPTRAN”, *Proceedings of 2010 LWR Fuel Performance*, 2010
5. K.J. Geelhood, W.G. Luscher, C.E. Beyer, J.M. Cuta, “FRAPTRAN 1.4: Integral Assessment” NUREG/CR-7023, Vol. 2, PNNL-19400, Vol. 2, March 2011
6. *US Nuclear Regulatory Commission (USNRC)*: TRACE V5.0p2 User Manual, 2010.

THE APPROACH OF USED FUEL INTEGRITY EVALUATION DURING TRANSPORTATION AND STORAGE

S.Y. KIM, S.K. LEE, B.S. CHOI, K.S. CHOI, C.J. LIM
R&D Center, KEPCO Nuclear Fuel Co.
989 beon-gil 242, Daedeok-daero, Yuseong-gu, Daejeon, Korea

ABSTRACT

One of the top tier requirements of UF during its transportation and storage is that the UF must maintain the integrity during its carrying and storage. The UF integrity relies on temperature, creep, stress, inner pressure etc. of fuel under this circumstance. Those items directly or indirectly impact on the UF integrity behavior, which is quite intricate and intractable since this is connected with its previous in-reactor operation and cooling time in pool. (The performance of fuel rod after burn-up is initial condition of UF.) From the view point of evaluation, two fields can be classified as one is related to the static mode and the other is dynamic one, similar to the scheme of in-reactor evaluation as upper mentioned. The former case mainly handles the integrity of UF clad during long-term storage. The latter is to evaluate UF structural integrity under handling and transportation or even storage which forms a load path from outside of cask to fuel clad through fuel structural components like spacer grids during normal operation(normal drop event) or accident(higher drop accident, seismic events, severe win storm etc.) conditions. Mostly UF becomes degraded during the long-term storage in some degree and sometimes these phenomena get worse to be failure. And also to carry and retrieve this UF in the degraded status, the integrity margin can be lowered. Thus, it is very important to understand the prediction of a degradation mechanism of fuel clad during the above campaign. Therefore, the existing fuel evaluation tools are extensively employed to evaluate fuel clad integrity using the code for the analysis of fuel rod performance. In this case, some improvement is necessary for it to apply to the evaluation by reflecting the in-reactor behavior data and some extra evaluation items. The other clad integrity evaluation under the dynamic impact is also performed by setting up DB for failure criteria such as strain energy density function, UF physical information such as geometry and material characteristics etc. and UF-cask load path system. This paper suggests a pictorial system of this UF integrity evaluation by analyzing current R&D activity and restructuring them.

1. Introduction

Long-term dry storage of used fuel (UF) is one of the promising countermeasures to handle it in Korea. To implement this process, UF integrity evaluation is an essential item. Especially, to avoid the release of radioactivity from an irradiated assembly, one of the top tier requirements of UF during its transportation and storage is that the UF must maintain the integrity during its carrying and storage under postulated normal or accident events.[1,2]

This evaluation is required to use various kinds of the in-reactor performance data such as oxidation, hydrogen re-orientation, creep, irradiation etc. and the structural mechanical characteristics. This information is to be used to evaluate and model of UF behavior under dry storage environment. And those items directly or indirectly impact on the UF behavior. (The initial condition of UF is the state of a standard fuel at end-of-life, generally.) That’s the reason why in-reactor data and response behavior are necessary to perform it. This primary information can be employed.

From the view point of evaluation, two fields can be classified as one is related to the static mode and the other is dynamic one, similar to the scheme of in-reactor evaluation as upper mentioned. The former case mainly handles the integrity of UF clad during long-term storage. The latter is to evaluate UF structural integrity under handling and transportation or even storage.

In Korea, however, when it comes to UF, the related R&D activities have been inactive compared to other nuclear ones because of Korean specific situation. Around ten thousand tons of UFs has been stored in each plant, and the year of storage capability limit is coming soon. Considering this time pressure, one of the related key technologies is to evaluate UF integrity. Currently, roadmap has been setup and the related study has been performed since a couple of years ago. To prevent something inattentive and to proceed with the further developed tasks, in this paper suggests a pictorial system of this UF integrity evaluation by analyzing current R&D activity and restructuring them. And hydrogen content of cladding is benchmarked with reference to EPRI report.

2. Fuel Behavior

2.1 Nuclear Fuel Behavior in Reactor

The characteristics of unloaded fuel rod (UF) depend on in-reactor history such as power uprating, longer-cycle or high burn-up operation, fuel design features (material, geometry etc.). Also, the basic phenomena of fuel in reactor include thermal and mechanical behavior, fission gas behavior radiation effect. Consequentially the fuel experiences several physical and chemical changes due to this changing reactor condition. Fig. 1 shows the typical mutation of these fuel clad characteristics and various parameter that affects fuel rod behavior.

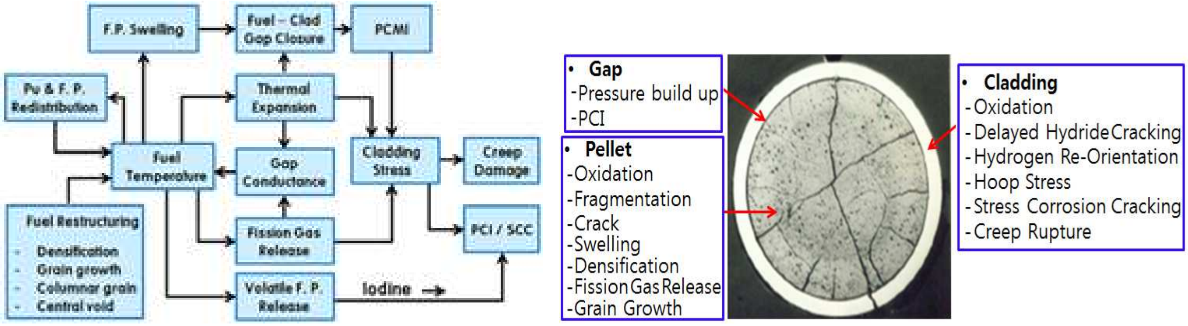

Fig 1. Fuel Characteristic Changes in reactor (left) and various parameter that affects fuel rod behavior (right)

Regarding the evaluation of fuel assembly, all of the conditions are considered and evaluated under normal or accident conditions such as exposure of high speed coolant, handling, earthquake etc. Fig. 2 shows the general fuel assembly structural behavior and its responses. As shown the figure, these responses are a cause of physical property changes. Thus, the property changes of fuel in reactor are inevitable during irradiation under a rigorous environment. As of now, there have been various kinds of fuels supplied to NPPs in Korea. This fact would give us some difficulties in performing the related projects such as object, methodology, scope etc. of evaluation. Since an analytical approach is so limited due to the aforementioned obstacles, almost all the evaluation approach must strongly depend on the practical data by using the related computer codes. This information is normally available from Poolside Examination (PSE) and Post-irradiated Examination (PIE). KEPCO NF has regularly established the related infra, acquired these necessary PSE and also generated PIE data with aid of KAERI. All the data is owned by KEPCO NF proprietary and could be used for diverse purpose such as UF evaluation and licensing acquisition activities of dry storage and transportation system [3,4].

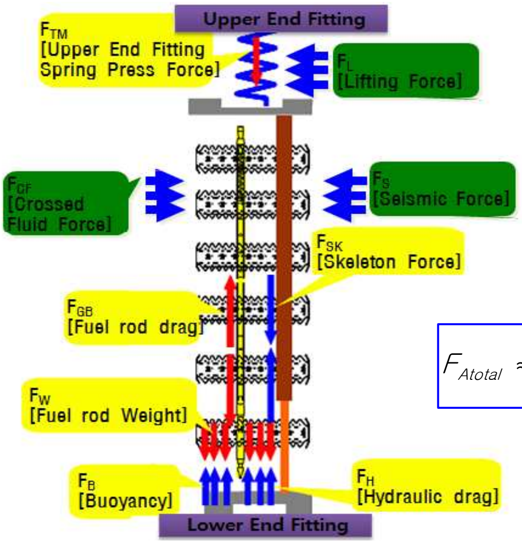

$$\boxed{F_{Atotal} \approx \sum_{Loading}^{Unloading} f(F_{TN}, F_{GB}, F_{SK}, F_{W}, F_{CF}, F_{B}, F_{H}, F_{L}, F_{S} \cdots)}$$

Fig 2. Free Body Diagram of Fuel Assembly

2.2 Used Fuel Behavior under Dry Storage and Transportation Condition

When discharged at the end of its burnup cycle the UF contain U, Pu, fission products and other actinides mostly in the form of oxide, but the exact composition depends upon various parameters (e.g. initial enrichment, initial composition, burnup, etc.) which differ considerably for the different types of reactors and even for the reactors within one type.[5] Also, The UF is affected by temperature, creep, hydride, stress, etc.. Those items directly or indirectly impact on the UF integrity behavior, which is quite intricate and intractable since this is connected with its previous in-reactor operation and cooling time in pool. So the behavior of fuel in reactor is important for UF integrity evaluation. (In general, the initial condition of UF is status of the very-after irradiation. The initial UF is very weak from the external force due to degradation of cladding.)

The view point of UF integrity evaluation is categorized typically in two groups. One is static mode and the other is dynamic mode. The static mode mostly is to evaluation UF integrity during dry storage. The dynamic mode is used to evaluation UF integrity under handling and transportation or even storage which forms a load path from outside of cask to fuel clad through fuel structural components like spacer grids during normal operation(normal drop event) or accident(higher drop accident, seismic events, severe win storm etc.) conditions. The UF integrity margin is relatively low due to degradation of fuel during the storage. As a result, to carry and retrieve this UF in the degraded status, the UF will probably have more failure probability. Thus, it is very important to understand the prediction of a degradation mechanism of UF during the above campaign.

To evaluate the UF integrity under the various situations, the information as described in previous section is necessary and based on DB as shown in Fig. 3, further evaluation is to be executed more clearly. Therefore, the existing fuel evaluation tools (ex. FATES, COROSN etc.) are extensively employed to evaluate UF integrity using the code for the analysis of fuel rod performance. In this case, some improvement is necessary for it to apply to the evaluation by reflecting the in-reactor behavior data and some extra evaluation items. The other clad integrity evaluation under the dynamic impact is also performed by setting up DB for failure criteria.

The performance system and procedure of integrity evaluation of UF can be summarized as shown in Fig 4. This approach is drawn in the frame of big picture in performing future R&D scheme and directivity.

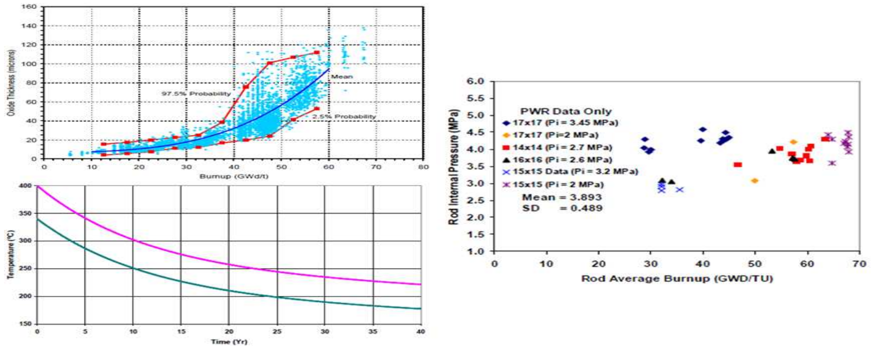

Fig 3. UF performance information [6]

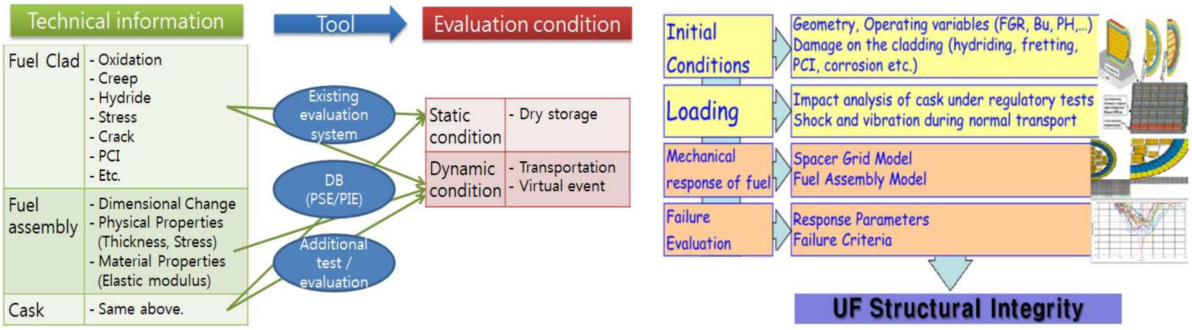

Fig 4. Approach of system (Left) and procedure (Right) for UF integrity evaluation

3. Evaluation of Used Fuel Integrity _ Calculation of Hydrogen Content

One of the phenomena that will affect UF integrity during storage and transportation is the pickup of hydrogen in cladding. If there is a hydrogen pickup in cladding at irradiation, hydrogen will be precipitated as hydride. Therefore, the hydrogen content of cladding is one of the essential factors to determine failure criteria of UF. In this chapter, the first step is to be deployed to simulate the EPRI's retrieving methodology of hydrogen content through the probabilistic treatments since we can only access the outlined information.

The hydrogen is created by corrosion reaction (1). About 20% of created hydrogen is absorbed into cladding. Therefore, the hydrogen content is increased as the corrosion reaction progressed. The cladding absorbed hydrogen become zirconium hydrides (ZrH_x, ceramic). These hydrides decrease the ductility of the zircaloy and make it more susceptible to fracture. So, in UF integrity evaluation, hydrogen content is important.

$$Zr + 2H_2O\ (\text{coolant}) \rightarrow ZrO_2 + 2H_2(g) \tag{1}$$

$$Zr + (x/2)H_2(g) \rightarrow ZrH_x \tag{2}$$

The average hydrogen content (H) is calculated from the oxide thickness of cladding (t_{ox}) and hydrogen pickup fraction (f_{pu}). The hydrogen pickup fraction is defined as the ratio of the hydrogen absorbed over the total hydrogen generation due to corrosion reaction. The data of oxide thickness of cladding is a function of burnup and the data of hydrogen pick-up fraction is a function of oxide thickness [2]. The probabilistic analysis is used to determine hydrogen content as a function of burnup. As a result of a series of probabilistic simulation mentioned in Fig. 5 is obtained. At this point, data of the oxide thickness and hydrogen pickup fraction is roughly selected from data to show just a tendency of EPRI result.

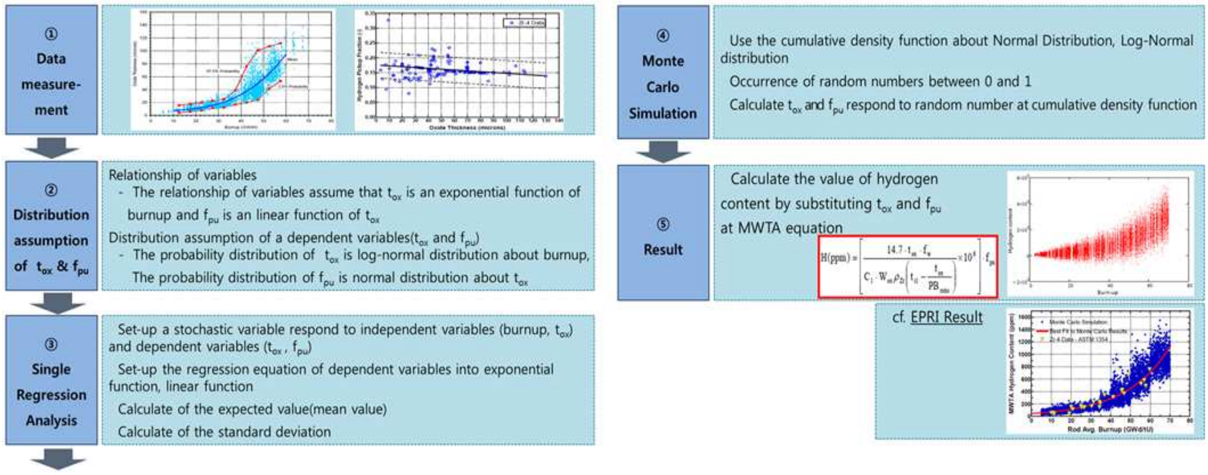

Relationship of variables
- The relationship of variables assume that t_{ox} is an exponential function of burnup and f_{pu} is an linear function of t_{ox}

Distribution assumption of a dependent variables(t_{ox} and f_{pu})
- The probability distribution of t_{ox} is log-normal distribution about burnup, The probability distribution of f_{pu} is normal distribution about t_{ox}

Set-up a stochastic variable respond to independent variables (burnup, t_{ox}) and dependent variables (t_{ox} , f_{pu})

Set-up the regression equation of dependent variables into exponential function, linear function

Calculate of the expected value(mean value)

Calculate of the standard deviation

Use the cumulative density function about Normal Distribution, Log-Normal distribution

Occurrence of random numbers between 0 and 1

Calculate t_{ox} and f_{pu} respond to random number at cumulative density function

Calculate the value of hydrogen content by substituting t_{ox} and f_{pu} at MWTA equation

$$H(ppm) = \left[\frac{14.7 \cdot t_{ox} \cdot f_w}{C_1 \cdot W_m \rho_{Zr}\left(t_{cl} - \frac{t_{ox}}{PB_{ratio}}\right)} \times 10^6\right] \cdot f_{pu}$$

cf. EPRI Result

Fig 5. Retrieving process and result of hydrogen contests

4. Conclusion

To avoid the release of radioactivity from an irradiated assembly, it is very important to understand the prediction of a degradation mechanism of UF clad during the normal operation or accident condition at storage and transportation (handling). Thus, the evaluation of UF integrity during storage and transportation is the key technology, and it is necessary to strengthen and reinforce it.

This paper suggests a pictorial system of this UF integrity evaluation and process by analyzing current R&D activity and restructuring them.

And, in the key item for UF integrity evaluation, hydrogen content of cladding is one of the essential factors to determine failure criteria of UF. So the benchmarking calculation referring to EPRI report was performed in this study. The simulation result shows similar trends to that of EPRI's using probabilistic approaches. Later, the hydrogen content will be calculated using the actual t_{ox} and f_{pu} data of UFs in Korea. By comparing this calculation result and hydrogen content value by PIE of UF, this methodology will be verified about suitability.

All the data (PIE and PSE data) to be utilized UF integrity evaluation is owned by KEPCO NF and will be researched later for UF evaluation and licensing acquisition activities for dry storage and transportation (handling) system.

5. References

[1] O. Ozer et al, Fuel-Assembly Behavior Under Dynamic Impact Loads Due to Dry-Storage Cask Mishandling, EPRI, 2008.

[2] J. Rashid et al, UF Transportation Applications: Longitudinal Tearing Resulting from Transportation Accidents-A Probabilistic Treatment, EPRI, 2006.

[3] S. K. Lee, Y. S. Nam, Y. H. Kim, S. Y. Jeon, C. S. Cho, Structural Deformation Evaluation of Spent Nuclear Fuel, KAERI/KNF, 2011

[4] S. K. Lee, O. H. Kwon, K. S. Choi, J. I. Kim, C. S. Cho, J. H. Kim, Spent fuel Integrity Evaluation Approach Considering Statistical Treatment and Succeeding Activities, Transactions of the Korean Nuclear Society Autumn Meeting, 2011.

[5] T Auf der Heyde et al, evaluation of spent nuclear fuel management options for south Africa, University of Johannesburg, 2007.

[6] Aachiels et al, Used fuel Transportation Applications - Assessment of Cladding Performance, EPRI, 2007.

HOW RECYCLING CAN HELP RESPOND TO FUKUSHIMA-DRIVEN REQUIREMENTS FOR USED FUEL MANAGEMENT

M. Chiguer
AREVA
1, Place Jean Millier, 92084 Paris-La-Défense – France
mustapha.chiguer@areva.com

ABSTRACT

Used fuel management is ever increasingly one of the major topics that countries and utilities operating or envisaging deployment of a nuclear power park have to face. “What will be done with the used fuel?” is a key question that raises several issues.
In addition, since the natural disaster of March 2011 in Japan, followed by the nuclear accident at the Fukushima Daiichi NPP, it has become clear that the reactor pools -the starting point of used fuel management- were an aggravating factor in the very difficult emergency situation faced by the nuclear operator; and that these reactor pools turned out to be far more vulnerable than initially assumed.
This paper lists and briefly describes challenges and issues at stake that used Fuel Management will be facing at existing Spent Fuel Pool (SFP) at reactor in operation or permanently shutdown in the light of the accident of Fukushima Daiichi.
Proven solutions going along risk reduction strategies that are of value to adequate protection and appropriately balances defence-in-depth and risk considerations as far as Used Fuel Management are considered and presented from the unloading of used fuel at SFP, up to the disposal of final waste.
Based on this and to come back to a more orthodox Used Fuel Management, utilities as well as stakeholders should rethink Used Fuel Management Strategy and Options going along with, starting at its very first stage, namely the storage configuration and requirements at SFP. This is one of the pre-requisite needed today to help provide more confidence for existing NPPs and for new builds to proceed.

1. Introduction

The Fukushima accident draws attention to a broader nuclear industry issue concerning used fuel management options and strategies, namely that used fuel was, and is still perceived as one of the crucial unresolved issues when referring to nuclear energy.
After being something of an afterthought in many national fuel cycle policies, Used Fuel Management Options are likely to be reconsidered in the aftermath of Fukushima Accident.
Whatever the changes that will be required by Safety Regulators across nuclear countries as well as new comers, oversight of Nuclear Power Plant safety performance will be strengthened by focusing more attention on defence-in-depth philosophy including deactivation or Spent Fuel Pool (SFP) at reactor [Ref. 1, 2 and 3], the very starting point of Used Fuel Management at Nuclear Power Plant.

These growing concerns about used fuel safety are providing a trigger for nuclear countries and stakeholders to look back on the excellent track record of three decades of recycling used nuclear fuel and its intrinsic contribution to safe and optimised used fuel management starting at the reactor pool. This safe and optimised management based on the transfer of used fuel into more optimised storage conditions and by separating the used fuel in various product and waste streams each with an optimised management approach

As concluded on December 2010, by the Waste Technical Board of the NRC [26], “the technical information available, together with the experience gained to date in the dry storage of spent fuel, demonstrates that used fuel can be safely stored in the short term and then transported for additional storage, processing, or repository disposal without concern.”

Moreover, the analysis concludes further that [26] to further extend dry storage and transportation of used fuel, “However, additional information is required to demonstrate with similarly high confidence that used fuel can be stored in dry-storage facilities for extended periods without the fuel degrading to the extent that it may not perform satisfactorily during continued storage and subsequent transportation.”

Indeed, in choosing to reprocess used nuclear fuel at the earliest and recycle valuable materials (namely plutonium and uranium recovered through used nuclear fuel reprocessing), one avoids accumulating used fuel inventories as well as drastically reduces waste volume, residual heat and radio-toxicity and, ultimately, manages waste more responsibly and optimally. This is in line with one of the nine principles set forth in [27] is that “Radioactive waste shall be managed in such a way that will not impose undue burdens on future generations” and were subsequently used to provide the technical basis for the Joint Convention on the Safety of Spent Fuel Management and the Safety of Radioactive Waste Management which entered into force in June 2001.

Recycling has prepared the future of civil nuclear power since and proven its maturity since its inception, notably to meet the challenges of the 21st century: challenges that are systemic, such as safety, non-accumulation of used fuel, non-proliferation, competitiveness, natural resources savings and security of supply, as well as unfortunate and surely unexpected challenges such as those resulting from the catastrophe at Fukushima.

In order to accommodate anticipated used fuel inventories while responding to current and upcoming Fukushima-driven requirements for used fuel safety, AREVA, over the past decades, has continuously concentrated its efforts on enhancing used fuel recycling performances and developing innovative solutions to respond to plant, utility or country related constraints. This were and still are illustrated through business cases that best describe the various proven solutions and implemented contractual schemes for the safe and optimized management of used fuel today.

2. Background and issues at stake…

….Before Fukushima and during decades, used fuel was perceived as one of the crucial unresolved issues when referring to nuclear energy. This conclusion, largely shared, was based on the results of several opinion surveys launched by governments, national and international institutions [Ref. 4, 5 and 6] and the nuclear industry across all nuclear countries.

Moreover, it was shown that Public Opinion main cause for reluctance to nuclear energy production during the Nuclear Renaissance is the large accumulation of waste and used nuclear fuel (Fig. 1) which remains, and by far, a very sensitive subject that crystallizes many fears and a worrisome issue in every country, regardless of their position on nuclear energy.
Up to Fukushima events, the above mentioned concerns have been nurtured and guided solely by the visible part of the used fuel inventories, while the hidden part of the iceberg, the majority of the inventories (more than 80%, Fig.1), were stored in SFPs pending decision on comprehensive used fuel management national policy.

Advanced opinion survey among “well informed” group of individuals familiar with the subject and “expert” group made up of local and national government representatives as well as journalists across the US and six nuclear countries in Europe (Ref. 6) showed in 2010 that they are in favor of current and proven recycling technology that brings down used fuel inventories or stockpile figures instead of waiting for a “leap-frog” technology, for example Gen

IV reactor and advanced recycling technology going along with, that might ultimately resolve all burden in the future!

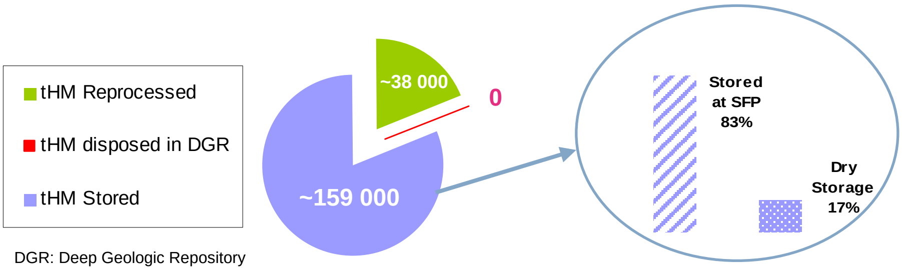

Figure 1. Worldwide Inventories of LWR's discharged used fuel at the end of 2011, in tons of Heavy Metal (tHM)

Paradoxically and despite this clear feedback from public opinion and opinion leaders, a cornerstone in the development of nuclear energy, Used Fuel Management was something of an afterthought in many national fuel cycle policies, leading to a large spread of "wait & see" strategy across nuclear countries and "new comers", the so called nations developing or aspiring to have civilian nuclear energy programs.

The interim solution to SFP increased inventories has then been a modification of spent fuel storage racks to further increase the ultimate discharge capacities of deactivation or reactor fuel pools at most reactor. This interim solution has since turned into a long term solution in most cases, if not a permanently solution in the case of shutdown reactors. This resulting in increasingly large inventories of used fuel and radionuclide being stored in reactor SFPs.

… After Fukushima, the natural disaster of March 2011, in Japan, followed by the accident at the Fukushima Daiichi NPP, it has become clear that SFPs were an aggravating factor in the difficult emergency situation faced by the operator and SFPs turned out to be far more vulnerable than initially assumed and have led to concerns of radioactive release [Ref.7 & 8]. Although the radiological consequences from Fukushima due to airborne releases have eventually far been predominately released from reactor cores, SFPs at Fukushima definitely presented a considerable potential threat given that there was no containment to prevent potential releases coupled with the large radionuclide inventories in SFPs [Ref.1 & 8].

Actually, while cooling down reactor core has been the first priority, the Operator quickly understood that keeping SFPs filled with water and adequately cooling used fuel were the other priorities at Fukushima following the earthquake and tsunami. Priorities needed to help:

- Maintain hall temperature below 80°C, threshold for human access in SFP hall needed for survey and control
- Maintain shielding to avoid release and dose intakes
- Protect the fuel structural integrity to avoid releases and re-criticality
- Prevent hydrogen formation due to the oxidation of the Zirconium cladding exposed to air, resulting in hydrogen generation, important only at elevated temperatures (>650°C), and possible risk of explosion. Though, clad structural failure could occur at temperatures as low as 650°C should thermal loading sustained fro several hours [Ref.13]
- Avoid fuel fires due to zirconium fire: the cladding ignition is about 850°C compared to the fuel melting point over 2800°C.

Five months later, the operator was still facing a difficult situation to restore normal condition in the SFPs, notably in unit 4, despite the 10-month cooling time of the latest discharged used fuel batch. This explains the shock and surprise among the public, and broadly among stakeholders, fed further by the apparent inadequacy of contingency plan and preparedness at the plant during the Fukushima accident relayed heavily by the new information and communication media. Even to date, and after prompt reinforcement to existing SFP structures, Fukushima operator knows that he has not turned the corner yet and removing all used fuel assemblies off SFP is still the pre-requisite to enhance safety of Fukushima shutdown accident-damaged NPP, notably to face risk of new earthquake [Ref 3 & 9] when structures and equipments have already been heavily impacted during March, 2011 accident.

This served as a grim reminder that used fuel at most reactor site might become today one of the biggest risk at some plant as concluded by the Japanese Atomic Energy Commission (JAEC) and presented by its president to Japanese Prime on March 25th, 2011 [Ref.8]. This confirms that earlier conclusions stating that *“the risks associated with spent fuel storage [at reactor pool] were extremely small in comparison with accidents associated with the reactor core*” is today no more intrinsically valid and could be significantly attributed to used fuel management at SFP along with other earlier plant related design parameters, instrumentation and layout.

Consequently all pre-Fukushima used fuel management related critics and weakness underlined by stakeholders are rushing back and regaining stakeholders’ confidence, and in particular public opinion, will be a long road and the Achilles heel of the civilian nuclear development.

3. Originally, a shared view, “no used fuel accumulation in deactivation pool”

Yet, as soon as the civil nuclear power age got underway, it became unthinkable to imagine generating nuclear electricity without reprocessing used nuclear fuel. In every country where this form of energy was being developed, construction programs involved not only Nuclear Power Plants, but also fuel cycle facilities, notably reprocessing spent fuel facilities [Ref.10]. This view has been extensively shared across European countries and overseas in the Fuel Cycle facilities development and implementation early 70s and 80s. We have been since witnessing the genuine join development of expertise and facility not only in the front-end of the fuel cycle (Enrichment), but also in the back-end of the fuel cycle with “Eurochemic” and “United Reprocessors Ltd” or other multi-lateral agreements [Ref. 10].

Unfortunately, the postponement of Back-end strategy implementation or the spread of the Wait & See strategy have meanwhile both led to the unavailability of off-site routes for used fuel discharged in the deactivation pool (SFP).

Consequently, more and more NPP has been challenged by limited storage space in SFPs at reactor, absolutely necessary for NPP operations (planned outages for loading/unloading batch operation, or for preventive maintenance and curative maintenance with a mandatory space for a Full Core Reserve, FCR). In order to accommodate this unanticipated upcoming larger used fuel inventories and to help Nuclear Power Plants across the world to continue their operations, high density racking in pools has been designed and ultimately licensed allowing maximizing SFP storage capacity.

This led storage rack design in SFPs to evolve from open and widely spaced structures, and consequently neutron flux “trap” design, to a closed and tightly packed frame steel containers relying heavily on permanently installed neutron absorbers to maintain criticality requirements (Fig.2).

This new rack design has been further spread and widely shared among NPPs with its corollaries, a fundamental design change in rack design and configuration as well as used fuel management option and storage requirements in SFP going along with. Both impacted the existing conservative margins in SFP safety analysis and, ultimately, accident risk analysis, in particular by decreasing drastically available grace period in case of loss of water inventory or cooling.

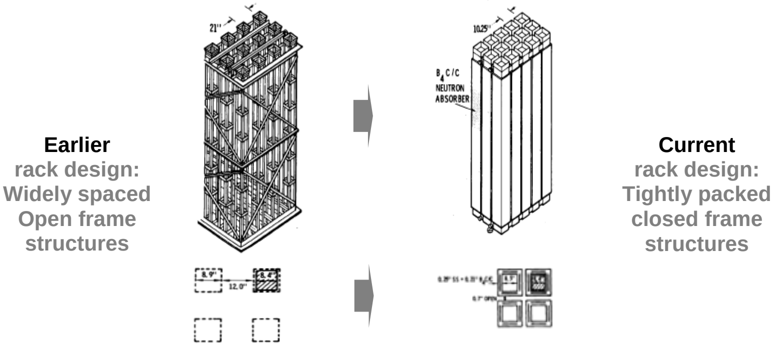

Figure 2 – Higher density racking to accommodate the larger used fuel inventory at SFP [11], PWR type case

Accident risk analysis associated with SFP was impacted further with refuelling outage duration reduction, reactor lifespan extension and increase in discharged fuel burnup.
In addition, fuel assemblies (FAs) themselves have become more reactive with increased ^{235}U enrichment an obvious example along with other more subtle changes: increased fuel pellet diameter and density, increased rod number per FA, increased use of fixed and integral burnable absorbers, and even changes to core operating parameters due to power uprates result in more reactive FAs to be stored in the SFP [Ref. 13].
Confluence of the various factors above mentioned coupled with the first lessons learned from the Fukushima Daiichi nuclear accident as well as from post-accident management will cause SFP safety margin assessments, accident risk analysis and storage requirements to definitely become far more complex with regard of today's and complete changes will take time before being defined and implemented.

4. Safe and Optimized Used Fuel Management

Whatever the changes that will be required by Safety Regulators, oversight of safety performance will be strengthened by focusing more attention on defence-in-depth philosophy including SFPs, the very starting point of used fuel Management. The effectiveness of the response of existing as well as upcoming SFPs, as part of the new build, and the effectiveness of the preventive safety strategy are related to the enhancement of safety margins and prevention of environmental damage, notably in extreme situations. In the following a three-pillar approach for a safe and optimized used fuel management is described.

4.1 The starting point, SFP hardening, with its corollary, the instrumentation upgrades, namely providing SFP with safety related instrumentations able to withstand design-basis natural phenomena to remotely monitor basics, though key parameters, such as area radiation, temperature and water levels. In most cases, those upgrades have been determined that should be started without unnecessary delay.
Hardening the pools, strictly speaking, consists mainly, in reinforcement of the robustness of cooling functions notably against some potential effect of severe natural events (i.e. loss of ultimate heat sink, loss of power supply and prolonged SBO conditions) and, if needed, reinforcement of structural integrity of the SFP to withstand a new safety requirements.
These upgrades are mainly consequences of stress-tests, complementary safety assessments or prioritized recommendations and are plant related.

4.2 The second and obvious measure, Used Fuel Inventory Reduction and Segregation, is under assessment in many nuclear countries following stress tests and prior to potential prioritization along with other measures of risk reduction [Ref. 23 & 24].
Should the decision be taken, this will definitely lower the inventory, and therefore the residual heat in the pool, enlarging the time to reach the boiling point and the time to boil

down to the top of the fuel and consequently enlarging the grace period. As Fukushima lessons learned clearly showed is that a simple action as SFP water refilling could be very difficult in extreme conditions and in that situation, comfortable grace period is essential to succeed.

Additionally, reducing used fuel at SFP introduces a clear segregation between various used fuel inventories at NPP and issues going along with, notably during refuelling outages. Both reduction and segregation enhance key parameters that govern likelihood and consequences of various SFP or plant accidents radionuclide inventories releases (see section 2). And again this is in line with the closing remarks of the1st International Experts' Meeting on "reactor and spent fuel safety in the light of the accident of Fukushima Daiichi" organized by the IAEA on March 2012 [Ref.16 & 25], where emphasis have been put by nuclear experts from more than 40 country members and 5 International Organizations on efforts to place priority not only on preventing accidents, but also mitigating them.

With four decades of excellent track records in Reprocessing and Recycling used nuclear fuel transferred from SFPs, utilities as well as stakeholders should take benefits of this proven solution that helps reduce drastically used fuel inventory in SFP [Ref. 17 & 19], including those recently discharged as early as one year after its off-load from reactor core [Fig.3] when re-assessing and re-thinking their used fuel management strategy. This duration figure could be adapted depending on core management, fuel type and performance and capacity of logistics means.

In addition to reducing accident prevention and mitigation, recycling used fuel currently stored in SFP and using current proven technology also alleviates the need for fresh natural uranium to be mined thanks to the recovery of 96% of valuable materials still encased in used fuel, namely uranium and plutonium and transforming them into ERU fuel (Enriched Reprocessed Uranium fuel) and MOX fuel (Mixed Oxide fuel) respectively. The remaining 4% is actual high level waste (HLW) which contains practically no remaining fissile material, consequently IAEA safeguards constraints free, and no energy value for the current and mid-term generation of reactors and fuel cycle facilities.

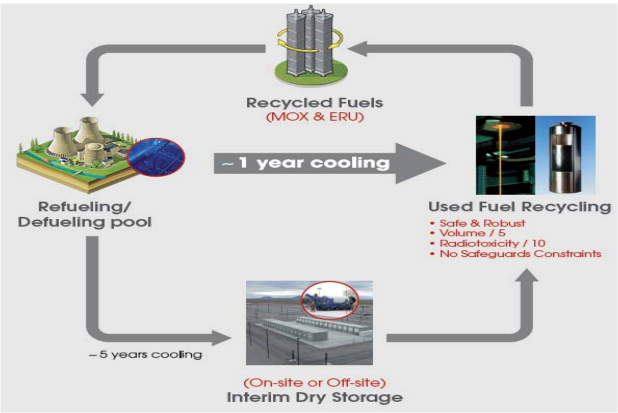

Figure 3 – Safe and Optimized Used Fuel Management Strategy
Recycling or interim storage flow diagram [Ref. 15]

Thus, recycling makes a positive contribution to the security of supply and market predictability [Ref.17] by saving up to 25 % of natural uranium reactor requirements that are subject to volatility of uranium market.

In conjunction with final disposal and for a long time now, recycling of used nuclear fuel has been used also to reduce drastically disposed waste volume (by a factor of 10) and radiotoxicity (by a factor of 5) as well as heat residual heat, a cornerstone in long term safe storage as well as of design and construction of the Deep Geological Repository.

Finally, and should recycling implementation not foreseen in the near term, the existing and proven dry storage solutions present an interim off-site route (Fig.3) for older used fuel, for example with 5 years of cooling time, that will help utilities to early transferring used fuel from reactor pools to dry storage [Ref. 21, 22 and 23] and Nuclear Waste National Agencies to choose an interim outcome to the accumulation of the used fuels stored or discharged currently in reactor pools awaiting for more broader strategic decisions to be taken [Ref 20] and, if so, to be timely and genuinely implemented. This latest time figure, namely 5 years of cooling time prior to dry storage is an average figure that depends on several parameters such as initial enrichment, burn-up, cask design, safety cases and licensing limits or economics considerations.
As concluded on December 2010, by the Waste Technical Board of the US-NRC [26], “the technical information available, together with the experience gained to date in the dry storage of spent fuel, demonstrates that used fuel can be safely stored in the short term and then transported for additional storage, reprocessing [28], or repository disposal without concern.”
However, the analysis concludes further that [26] to extend dry storage and transportation of used fuel further, “… additional information is required to demonstrate with similarly high confidence that used fuel can be stored in dry-storage facilities for extended periods without the fuel degrading to the extent that it may not perform satisfactorily during continued storage and subsequent transportation.”
There is a need to recall that proven technical solutions, namely used fuel reprocessing and recycling services, do exist and could be implemented in a decade or so if required and definitely quicker than safety demonstration and mastering financial uncertainties going along extension, or worse, indefinite used fuel storage solutions.

4.3 The ultimate measure, SFP’s racking configurations enhancement

After removing older used fuel currently stored at SFP as described above, utilities will be in position to enhance further the intrinsic safety of used fuel management at SFP by reviewing Fuel Assembly holder/basket configurations and promoting further the design of storage racks that enhance heat transfer for a drained SFP and large fuel spacing for criticality control giving more robustness to face beyond design basis accident and additional grace period.

5. Conclusion

To come back to a more orthodox Used Fuel Management, utilities, Safety regulators and stakeholders should rethink Used Fuel Management Strategy and Options going along with, starting at its very first stage, namely the storage configuration and requirements at SFP, including maximum cooling time of used fuel after its discharge SFP, through off-site routes up to disposal of final high level waste. This is one of the pre-requisite needed today to help provide more confidence for existing NPPs and for new builds to proceed.

By removing discharged used fuel and reducing their inventory, and consequently radionuclide inventory, in reactor pools at the earliest, used fuel reprocessing and recycling will help countries and utilities that have previously postponed used fuel management strategy to get back rapidly to a safer and optimized used fuel management.

In choosing to recycle used fuel and consequently reduce radionuclide inventories in reactor pools since its inception as well as managing ultimate waste responsibly [27] and optimally, civil nuclear power in Europe has prepared its renaissance and proven its maturity, notably to meet the challenges of the 21st century.

REFERENCES

[1] US NRC, Recommendations for enhancing reactor safety in the 21st century July, 2011
[2] WENRA Task Force “Stress tests specifications” April, 2011
[3] Report of Japanese Government to the IAEA, June 2011 at www.iaea.org
[4] EU country members’ survey, Eurombarometer 2005 & 2008 at http://ec.europa.eu/public_opinion
[5] US DOE/NEI nationwide Opinion Survey conducted by Bisconti Research Inc at www.nei.org
[6] Nuclear Energy and Recycling opportunities: the perceptions in Europe & the US at www.tns-sofres.com
[7] UK-ONR Report on implications of Fukushima for the UK nuclear industry Interim report, p.27/106-May 2011
[8] JAEC, “Contingency scenario outline of Fukushima Daiichi NPP” JAEC’s report to Prime Minister of Japan on March 25th 2011.
[9] TEPCO, “General Plan of the cover for fuel removal of Unit 4 in Fukushima Daiichi NPP” Attachment to Tepco release on April 16, 2012 at www.tepco.co.jp
[10] WNA annual symposium “recycling, back to the future”; M. Chiguer and al Sep. 2008
[11] US NRC-NUREG/CR-0649 “Spent Fuel Heatup Following Loss of Water during Storage”
[12] US-NUREG WASH- 1400 Reactor Safety Study- An assessment of accident in US Commercial Nuclear Power Plants, October 1975
[13] US NUREG - Severe accidents in SFP in support of Generic Safety issue 2- August 1987
[14] US NRR action Plan “On Site Spent Fuel Criticality Analyses, TAC- n° ME0372, May 2010
[15] IAEA International experts’ meeting on reactor and spent fuel safety in the light of the accident at the Fukushima Daiichi Accident, M. Chiguer March 2012
[16] IAEA International experts’ meeting on reactor and spent fuel safety in the light of the accident at the Fukushima Daiichi Accident, Chairman’s summary R. A. Meserve, March 2012
[17] Recycling as an option of used fuel Management strategy, Nuclear Engineering & Design V.241 p.1238-1242, T. Zagar, M. Chiguer and al. 2011
[18] UK-ONR, Japanese earthquake and tsunami: Implications for the UK nuclear industry, Final report, pp. 60/288 Sep. 2011
[19] ENC 2010, Recycling as an option of used fuel management strategy for Europe, M. Chiguer and al. June 2010
[20] US-NRC Prioritization of Recommended actions to be taken in response to Fukushima Lessons Learned, Policy Issue, Oct. 2011
[21] “Tennessee Valley Authority, TVA, considering moving additional spent fuel to dry storage” as reported by Spent Fuel Vol.19 n° 908 May 2012
[22] US NRC Fukushima Lessons Learned Actions » presentation by W. Borchardt at the International Experts’ Meeting organized by the IAEA on March 19-22, 2012
[23] US NRC on “NTTF identified the early transfer of spent fuel from pools to dry storage as an aea to examine » as reported by Spent Fuel Vol.19 n° 909, May 2012
[24] CSN, the Spanish Nuclear Safety Regulator, Acto del pleno del CSN n°1-208, Madrid October 13, 2011. In addition to Stress tests that could be viewed at www.ensreg.eu
[25] IAEA International Experts’ Meeting- Fukushima Daiichi Accident Spent Fuel Pools – Facts, actions and issues, H. Abe and all, Japan Nuclear Energy Safety Organization, March 2012
[26] US-NRC, Evaluation of the Technical Basis for Extended Dry Storage and Transportation of used nuclear Fuel, US-Nuclear Waste Technical Review Board, Dec. 2010
[27] IAEA, The principles of Radioactive Waste Management, Safety Series N° 111-F, Vienna 1995
[28] US-NRC, Environmental Topical Report for Potential Commercial Spent Nuclear Fuel Reprocessing Facilities in the United States, Final Report, Sep. 2012.

MECHANICAL AND THERMAL CARACTERIZATIONS OF U-Mo AND U-Nb-Zr ALLOYS

D.A. LOPES, T.A.G. RESTIVO[2], R.G. GOMIDE
LABMAT, Centro Tecnológico da Marinha em São Paulo, 18560-000 Iperó SP, Brazil.
[2] UNISO, Universidade de Sorocaba, 18023-000 Sorocaba SP, Brazil

Nuclear fuels composed by uranium alloys in monolithic and dispersed forms have been considered for research and power reactors due to their density properties (greater than 8 g-U/cm^3) and fast heat transfer. The U-Nb-Zr and U-Mo alloys are the most promised systems for plate type fuel elements owing to its broad γ-phase stability field, which shows higher ductility and isotropic behaviour, allowing extensive fabrication capability. In the present work, γ-phase stabilized U-7.5Nb-2.5Zr and U-10Mo alloys were characterized by mechanical and thermal analyses for comparison of their behaviour under deformation and heat treating. The results demonstrate the alloys have substantial different properties regarding deformations, kinetic phase transformation and recovery/recrystallization profiles.

Key works: Uranium alloys, U-Mo, U-Nb-Zr, cold rolling.

Introduction

Uranium alloys are presently the main options for advanced nuclear fuels to power and research reactors once they achieve superior combined features like high density fissile material and high thermal conductivity, besides low cost manufacturing. There has been a considerable amount of work aiming to develop uranium alloys [1, 2]. The first alloys systems considered were binary ones having high degree of solubility with gamma phase. Thereafter ternary alloys were developed in order to improve some desirable properties like gamma phase retention, high ductility and low cross section for capture of thermal neutrons. U-Nb-Zr and U-Mo alloys were selected based on screening among the potential candidates over gamma stability and what was known about irradiation behavior [3] .

Nowadays the Navy Technological Center at São Paulo CTMSP is carrying out experimental investigations on such materials as fuel candidates for power and research reactors. This has led to a new search for developing high uranium density monolithic plates holding the maximum uranium density as possible in the fuel region. However, in order to effectively achieve the objective, new developments in processing and fabrication of fuel elements have been initiated to provide a better understanding of material behavior. In this scenery, two alloys systems for monolithic fuel have been considered: U-Mo and U-Nb-Zr. Once each system shows both advantages and disadvantages the present study aims to compare some metallurgical properties of alloys U-10Mo and U-7.5Nb-2.5Zr (weight %). The work's prime objectives are to determine the processing characteristics of both alloys and their forming feasibility. The study also allows inferring over the expected behavior during service based on kinetic transformation observed.

Experimental Procedures

The U-7.5Nb-2.5Zr (Mulberry alloy) and U-10Mo alloys were melted in plasma and induction furnaces with purified argon. Alloys compositions were analyzed by ICP spectrometer: U-7.4Nb-2.3Zr and U-9.5Mo. The main impurities detected are Al, Fe and Cu rated to 1200 ppm total. The uranium alloys were heat treated at 1000 °C for 5 hours in argon followed by water-quenching to obtain a solid solution γ-phase stabilized structure. Some homogenized alloy samples were also annealed at 300 °C and 500 °C for 6 hours at argon to form γ decomposition phases.

Stabilized γ-phase samples employed on recovery and recrystallization studies were cold rolled on several passes followed by 1 hour isochrones treatment from 200 to 700°C into 100°C intervals. Dilatometry, DSC (into two modes: drop and scanning), X-ray diffraction and hardness were used to characterize the alloys. Transformation kinetic diagrams were built for both alloys by means of drop calorimetry analyses on up-quenching mode: γ-phase treated alloys samples (3x4x5mm) were dropped from ambient up to 200-700°C range, while the heat flow signal was continuously recorded during 6 to 8 hours. Drop calorimetry method can also access the heating enthalpy curves of the samples by cell calibration with previous sapphire standards. The ∆H curve shape gives some clues on reaction taking place at shorter times regarding the dropping peaks. Dilatometry was performed up to 800°C at a heating rate from 5 up to 40 °C/min. All allied techniques were employed to trace the kinetic diagram.

Results

For γ-quenched alloys the measured reflection angles match a typical body-centered cubic structure, with a space group Im-3m, where the lattice parameter was estimated as 3.481 Å for U-7.5Nb-2.5Zr alloy and 3.421 Å for U-10Mo according to Rietveld refinement (Figure 1). As treated U-10Mo and U-7.5Nb-2.5Zr alloys into γ-phase show uneven hardness values as shown in Table 1. U-10Mo alloy hardness is rather higher which, in general, is related to lower ductility and higher loads during the forming process.

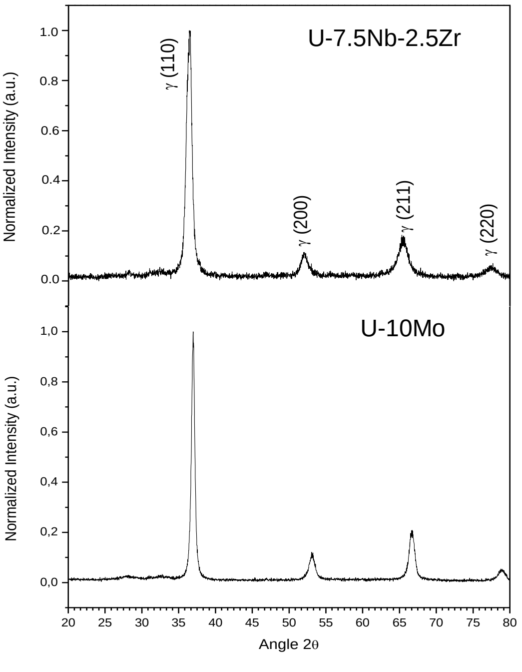

Fig 1: X-ray diffraction patterns of the U-7.5Nb-2.5Zr and U-10Mo alloys in the γ-quenched condition.

Tab 1. Average Vickers hardness of the alloys in the γ-phase conditions.

Alloy	Vicker hardness [Kgf/mm^2]		
	Present work	Waldron et al. [4]	Vandermeer [5]
U-7.5Nb-2.5Zr	173.93 HV$_{0.5}$ (±4.82)	--	181
U-10Mo	300.99 HV$_{0.5}$ (±7.44)	312	--

For a more accurate approach to the design of the rolling passes for uranium alloys (U-Mo and U-Nb-Zr) the normal pressure on the roll were measured. The actual rolling measured pressure demonstrate that U-10Mo alloy demands higher load along similar reduction pass of 10%, also compared to pure U, as shown in Table 2. This fact is a consequence of the solid solution hardening.

The pressure rise along the pass measured by a dynamics load cell is displayed against time in Figure 2.

Tab 2. Maximum Normal pressure (MPa) in the cold rolling process (pass 10%) for U, U-10Mo and U-7.5Nb-2.5Zr.

U	**U-10Mo**	**U-7.5Nb-2.5Zr**
1749	2691	2284

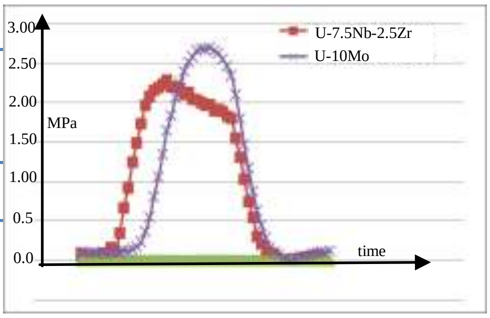

Fig 2: Measured normal pressure distributions in the cold rolling process (pass 10%) of U-10Mo and U-7.5Nb-2.5Zr alloys.

Exploratory cold rolling scanning showed the process can be sustained up to 60% thickness reduction without breakdown for the U-7.5Nb-2.5Zr alloy in agreement with Peterson and Vandervoot results [6]. On the other hand, the deformation limit of U-10Mo alloy has been determined to be farther small, between 10% and 15% reduction.

Figure 3 shows the low work-hardening characteristic of the gamma-annealed and quenched alloys in contrast to the strong hardening of pure uranium, as a consequence of its orthorhombic structure.

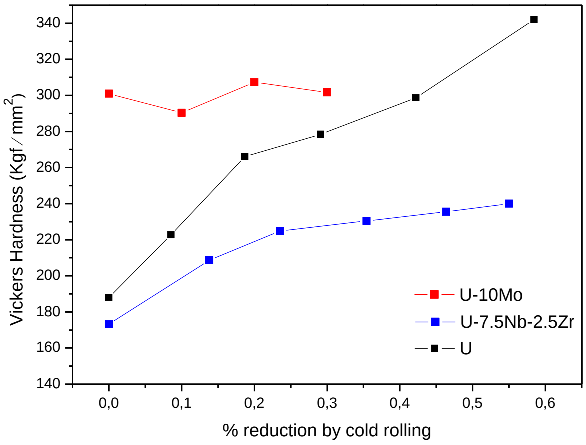

Fig 3. Hardness of U-10Mo and U-7.5Nb-2.5Zr alloys as a function of percent reduction by cold rolling compare to the pure uranium.

The X-ray profiles for isothermal-annealed samples of U-7.5Nb-2.5Zr and U-10Mo at 300 °C and 500 °C are shown in Figure 4. For Mulberry alloy, the 300 °C annealed sample display diffraction profile identified as α'' characterized by a doublet at about 2θ = 40° [7]. Two phases were identified at 500 °C annealed sample (Fig. 4b) where well defined peaks of α-phase coexist with γ_3 cubic structure reflections shifted toward higher angles regarding γ-phase. U-10Mo alloy X-ray profile is unchanged after 300 °C treatment (Fig. 4c) while the 500 °C annealed sample profile (Fig.4d) still shows a large amount of γ-phase besides noticeable reflections of α and δ (MoU_2) phases.

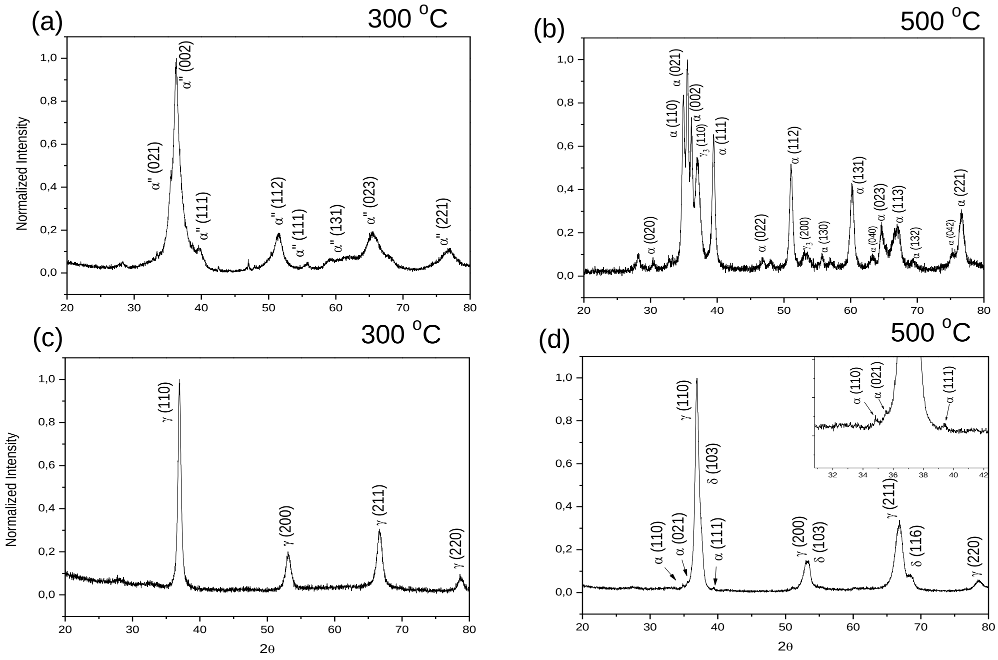

Fig 4. X-ray profiles for 6 hours heat treated U-7.5Nb-2.5Zr (a,b) and U-10Mo (c,d).

Figure 5 shows examples of drop calorimetry analysis, used to build the kinetic transformation diagrams for the alloys (Figure 7). There should be some fast transformations taking place inside the dropping peaks which were evaluated through the ΔH curves shown at Figure 5 (down). Some points of U-7.5Nb-2.5Zr dropped alloys show larger mismatch from the general trend of ΔH rising curve, indicating there are overlapping reactions at short times. The last is not the case for U-Mo alloy. Dilatometry can also determine the transformation points during heating samples (Figure 6).

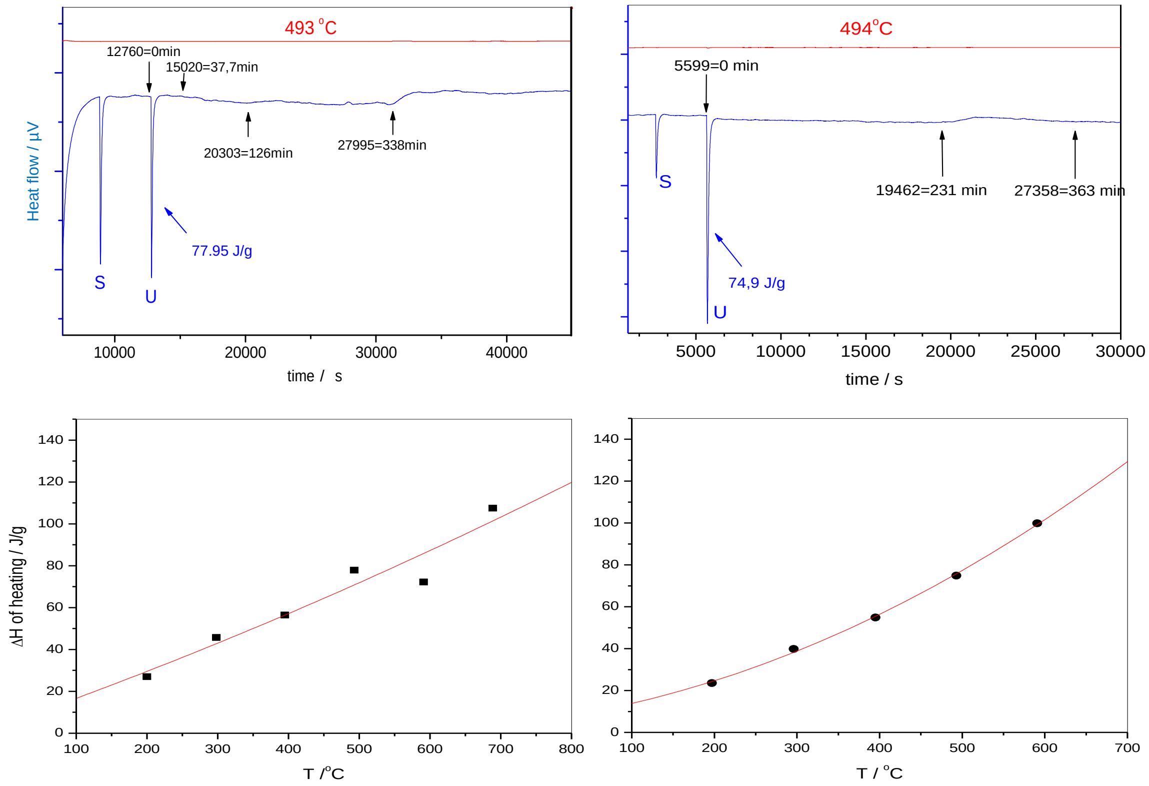

Fig 5. Drop calorimetry analyses (top) and respective Cp curves for (down) U-7.5Nb-2.5Zr (left) and U-10Mo (right).

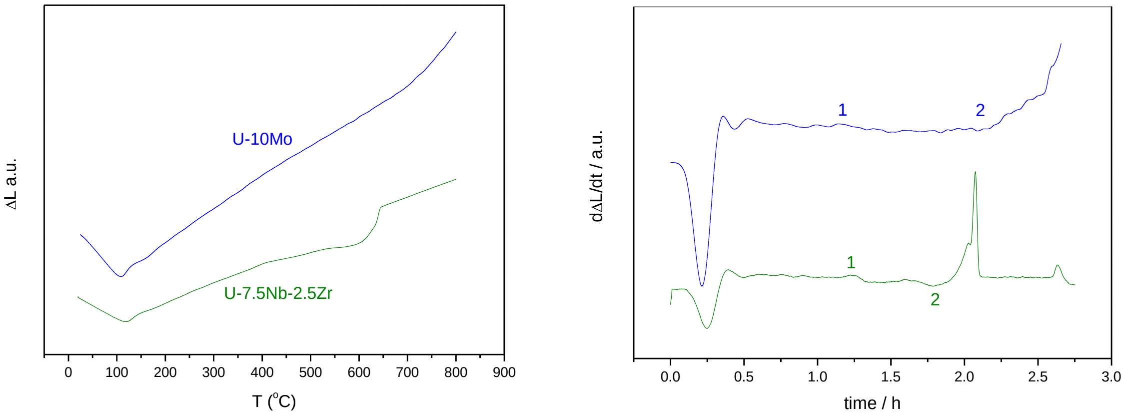

Fig 6. Dilatometric analysis of U-7.5Nb-2.5Zr and U-10Mo alloy: ΔL curves (left) and the respective dΔL/dt derivatives for heating rate 5°C/min.

Kinetic transformation diagrams were drawn for both alloys based on thermal analysis methods starting from stabilized γ-phase. Drop calorimeter, scanning DSC and dilatometry were employed under up-quenching mode, as compiled in Figure 7.

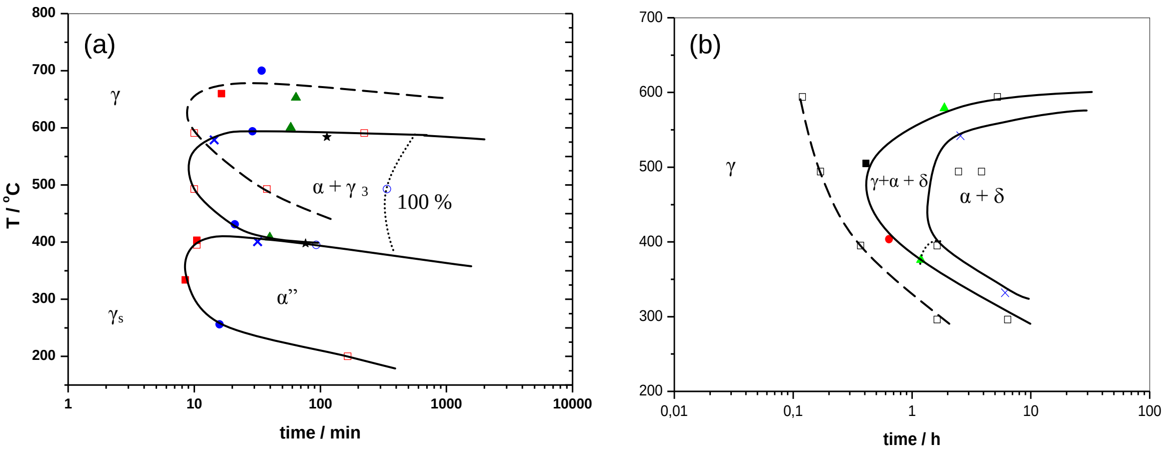

Fig 7. Diagram drawings for U-7.5Nb-2.5Zr (a) and U-10Mo (b); calorimetry (hollow) and dilatometry (filled); × points refers to scanning calorimeter sensor.

The disclosed diagrams are important in order to plan the alloys forming processes since they closely resemble the initial γ-phase condition after stabilization heat treatment.

The recovery and recrystallization heat treatment for the U-7.5Nb-2.5Zr alloy as monitored by annealing curve is shown in Figure 8, for a 60% thickness reduced cold-rolled sample plate. The recrystallization onset point in this case is found between 500 and 600 °C as indicated by the curve.

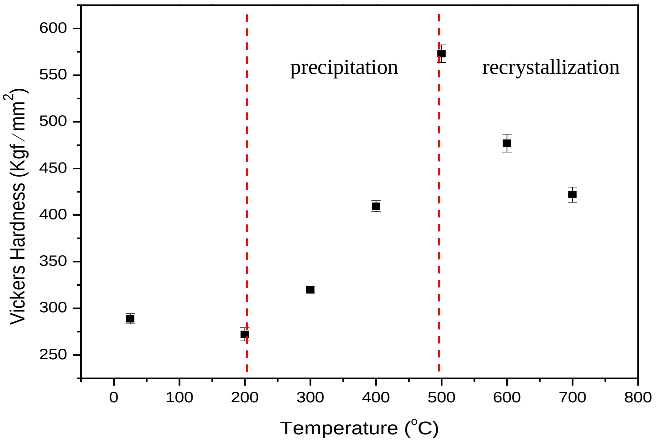

Fig 8. hardness x annealing temperature for 60% thickness reduced U-7.5Nb-2.5Zr alloy; 1-hour isochrone annealing.

The 60% reduced U-7.5Nb-2.5Zr alloy hardness firstly decreases slightly from 289 HV until 271 HV at 200 ºC, which can be assigned to the recovery phenomena. The softening is limited to 6% in this temperature level. Starting from 200 ºC up to 500 ºC, the hardness increases promptly, such behaviour typically indicates coherent precipitation to be dominant over recovery events. Afterwards the hardness quite decreases from 500 ºC which suggests the recrystallization overcome the competing processes. However, it should be noted the hardness did not restore the original γ-phase values or even the as-deformed one. This fact leads to consider the precipitation is still taking place for these temperature and time annealing conditions or the recrystallization has not yet finished. For this results we can conclude that, for this alloy in a deformed and supersaturated state, particles of second phase precipitate in the same temperature range over which recrystallization proceeds. Transformation of the perlite structure over 400 ^{o}C and towards α'' at low temperature will provide different mechanical behavior. Therefore, during mechanical forming process on this alloy, one must consider the solid phase precipitation onset.

Conclusions

The decomposition of the γ-phase in uranium U-10Mo and U-7.5Nb-2.5Zr alloys was studied by X-ray diffraction, dilatometry and DSC.

The incorporation of niobium and zirconium with uranium in the proportions U-7.5Nb-2.5Zr has resulted in an alloy which may have wide range properties by careful control of heat treatment. A soft, ductile alloy, suitable for extended fabrication operations, is produced by gamma-annealing and quenching for U-7.5Nb-2.5Zr alloy. However, during the subsequent heat treatments, decomposition of formed U-7.5Nb-2.5Zr alloy gamma phase was extremely fast. Otherwise the U-10Mo alloy shows slow phase decomposition kinetics but lower ductility closely above 10% therefore not suitable for extensive fabrication.

It is important to note that the monolithic fuel plate must be capable of surviving fabrication induced stresses, both thermally and mechanically, while also performing well during irradiation. Therefore, the data set evaluation leads to conclude the alloy U-7.5Nb-2.5Zr may be considered as an alternative to U-10Mo monolithic fuel.

References

[1] W. D. Wilkinson, Uranium metallurgy Vol. II. Interscience Publishers, 1st edition, New York, USA, 1962.

[2] C. A. W. Peterson, A Study of the Isothermal Transformations of Some Binary-Uranium-Base Alloys Between 400°C and 650°C. Lawrence Radiation Laboratory, University of California. Livermore, p. 28. 1965. (UCRL-7824).

[3] D. M. Wachs, RERTR Fuel Development and Qualification Plan. Idaho National Laboratory, 2007.

[4] M. B. Waldron, Burnett, R. C., Pugh, S. F., The Mechanical Properties of Uranium-Molibdenum Alloys, AERE-M/B-2554, 1958.

[5], R. A. Vandermeer, Recent Observation of Phase Transformation in a U-Nb-Zr Alloy. Oak Ridge National Laboratory, Oak Ridge, Tennessee, 1974.

[6] C. A. W. Peterson and R. R. Vandervoot, The Properties of a Metastable Gamma-Phase Uranium Based Alloy: U-7.5Nb-2.5Zr. Lawrence Radiation Laboratory, University of California. Livemore, 1964. (UCRL-7869).

[7] W. Lehmann, R. F. Hills. J. of Nucl. Mater. v. 2 , p. 261, 1960.

DEVELOPMENT OF QUANTITATIVE ANALYTICAL METHOD OF U, PU AND FISSION PRODUCTS IN SPENT FUELS BY COMBINED-CHROMATOGRAPHIC-MASS-SPECTROMETRIC-ISOTOPIC-DILUTION TECHNOLOGY

G. UCHIYAMA, H. FUKAYA, K. SUYAMA, M. ITO, T. UENO, S. MIYATA, T. SONODA,
H. USAMI, Y. KAWASAKI, Y. SAKADUME, T. KUROSAWA, K. TONOIKE,
J. INAGAWA, M. UMEDA, M. MAGARA, K. WATANABE, N. SHINOHARA
Japan Atomic Energy Agency (JAEA),
Tokai-mura, naka-gun, Ibaraki-ken, 319—1195, Japan

T. YAMAMOTO, M. SUZUKI
Japan Nuclear Energy Safety Organization (JNES)
Toranomon, Minato-ku, 105-0001, Tokyo

ABSTRACT

A quantitative analytical method of uranium, plutonium and fission products of spent fuels has been studied to develop improved safety design methods of nuclear reactor core. A combined method of chromatographic separation of uranium, plutonium and fission products from spent fuels and isotopic analysis by a high resolution inductively coupled plasma mass spectrometry (HR-ICP-MS) with isotopic dilution method (IDM) was developed to analyze fission products, especially lanthanide nuclides with high accuracy. The tentative analytical results obtained by the developed method were compared with those obtained by conventional analytical methods. The analytical results were also compared with the calculation results by using burn-up calculation code SWAT3.1. Relatively large differences between the analytical and calculation results were obtained in the analysis of several fission products such as ^{155}Gd, ^{99}Tc and ^{109}Ag. However, the analytical results of other fission products agreed with the calculation results within 5% difference.

1. Introduction

A quantitative analytical method of uranium, plutonium and fission products of spent fuels has been studied to develop improved safety design methods of nuclear reactor core with MOX fuels[1),2)]. A combined method of chromatographic separation of uranium, plutonium and fission products from irradiated nuclear fuels and isotopic analysis by a mass spectrometry with isotopic dilution method (IDM) has been developed to analyze fission products, especially lanthanide nuclides which are key nuclides for MOX reactor core design with high accuracy in the study. The combined method was applied to the analysis of spent fuels. The obtained analytical results were compared with conventional analytical methods. The results were also compared with burn-up calculation results by using SWAT3.1[3)].

2. Analytical procedure

The developed analytical procedure for chemical separation of elements in spent fuels is shown in the Fig. 1.Five samples (ZN2c2, ZN2c3, ZN3c2, ZN3c3, ZN3a9) of spent fuels with cladding of Unit 1 of Fukushima Daiinii nuclear power plant were dissolved in 3 M nitric acid solution at about 110 °C. The dissolution solutions of spent fuels were filtrated with filter papers of teflon. The filtrates were analyzed by gamma ray spectrometric measurement. The filtrate solution was fed to anion exchange resin of UTEVA (Eichrom tec. Co. USA) to separate U, Pu and Nd individually. The isotopic ratios of U, Pu and Nd in the eluate solution were analyzed by a conventional analytical method of thermal ionization mass spectrometer (TIMS) with isotope dilution method (IDM).

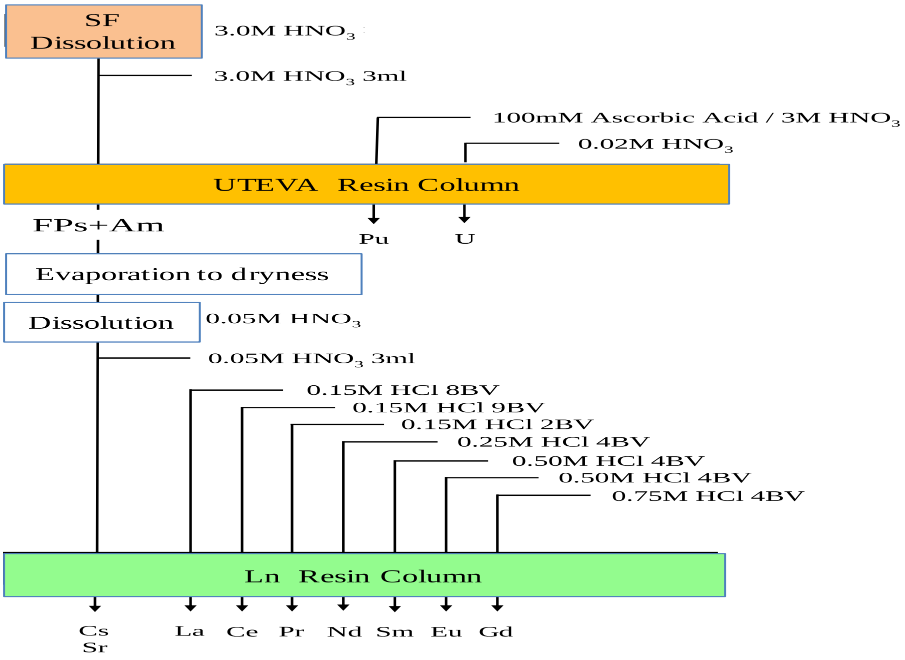

Fig. 1 Analytical procedure

The eluate solution from the UTEVA resin column was fed to the Ln resin column. Lanthanides elements were separated with hydrochloric acid solutions in the Ln resin column. In Fig. 2, the yields of lanthanide in each fraction eluted from the Ln resin column in the separation experiment using a simulated dissolution solution of spent fuel. More than 95% of U and Pu in the solution were separated. Each fraction solution eluted from the Ln resin column was analyzed by a high resolution inductively coupled plasma mass spectrometry (HR-ICP-MS) with IDM. The isotopic ratios of ^{142}Nd/^{143}Nd/^{144}Nd/^{145}Nd/^{146}Nd/^{148}Nd/^{150}Nd,

^{147}Sm/^{148}Sm/^{149}Sm/^{150}Sm/^{151}Sm/^{152}Sm/^{154}Sm, ^{151}Eu/^{153}Eu and ^{152}Gd/^{154}Gd/^{155}Gd/^{156}Gd/^{157}Gd/^{158}Gd/^{160}Gd in spent fuels were determined.

Also The dissolution residue was dissolved in mixed solutions of nitric, hydrochloric and sulfuric acids at 180 °C. The concentrations of ^{97}Mo, ^{99}Tc, ^{101}Ru, ^{103}Ru, ^{109}Ag and ^{133}Cs in the residue solution were analyzed by HR-ICP-MS.

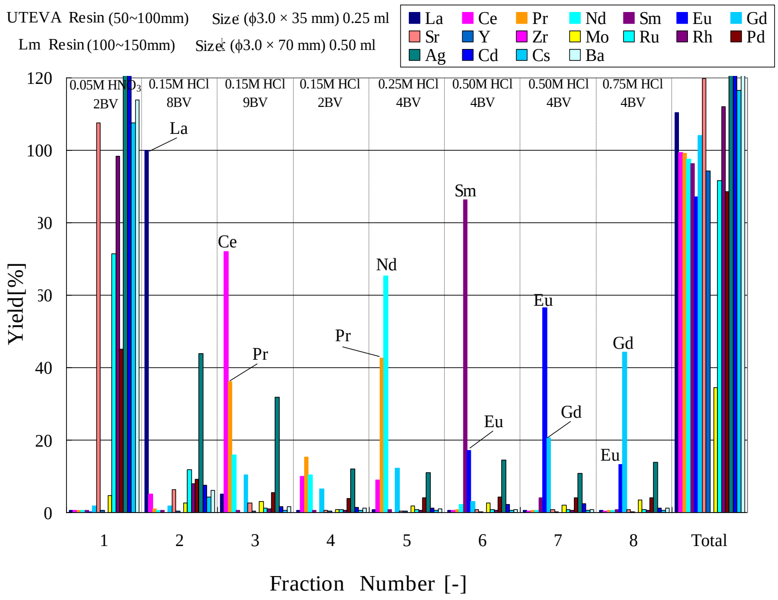

Fig.2 Separation behavior of lanthanides in the Ln resin column.

3. Results and discussion

The analytical results of 3 samples of ZN2c2, ZN3c2 and ZN3c3 are listed in Table 1 by using the developed quantitative analytical method by the combined chromatographic mass spectrometric-isotopic dilution technology. The burn-up of the samples of ZN2c2, ZN3c2 and ZN3c3 were evaluated as 27.8, 57.3, and 68.3 GWD/tU, respectively. The analytical result of ^{148}Nd was compared with a conventional analytical method of anion exchange–TMS-with isotopic dilution. The difference between the analytical results of ^{148}Nd by two methods was within 3% in the case of ZN3c2 sample. The analytical results of fission products in spent fuels were evaluated by the calculation results with SWAT3.1. The good agreement between the analytical and calculation results was obtained in the case of ^{137}Cs. In the case of ^{155}Eu, the difference was 27% for ZN3c2 sample and 16% for ZN3c3 sample. As for ^{137}Sm and ^{155}Gd, about 10% of difference was found. Concerning ^{99}Tc and ^{109}Ag, the difference between the analytical and calculation results was about 50%. It is considered that the large difference is due to the complicated chemical behavior of ^{99}Tc in the dissolution, separation and evaporation steps in the analytical procedures. The analytical results of other fission products of ^{95}Mo, ^{101}Ru and ^{103}Rh agreed with the calculation results within 5% difference.

4. Conclusion

The quantitative analytical method by the combined chromatographic mass spectrometric-isotopic dilution technology has been developed for of U, Pu and fission products in spent fuels. The analytical method was applied to post irradiation analysis of spent fuels from a nuclear power plant. The tentative analytical data of U, Pu and fission products including ^{133}Cs, ^{95}Mo, ^{99}Tc, ^{101}Ru, ^{103}Rh and ^{109}Ag which are hard to analyze with conventional analytical methods were obtained. The analytical results obtained by the developed method were compared with those obtained by the conventional analytical methods. The analytical results were also compared with the calculation results by using the burn-up calculation code SWAT3.1.

Relatively large differences between the analytical and calculation results were obtained in the analysis of several fission products such as ^{155}Gd, ^{99}Tc, ^{109}Ag. However, the analytical results of other fission products agreed with calculation results within 5% difference. The developed analytical method is considered to be applicable to isotopic analysis of spent fuels. As a further study, the improvement of separation conditions in the Ln resin column step is required to increase the accuracy of analytical data.

References

1). M. Ito, Y. Fukaya, T Ueno, S. Miyata, A. Sonoda, H. Usami, Y. Kawasaki, K. Sakatsume, T. Kurosawa, K. Suyama、K. Tonoike, G. Uchiyama, J. Inagawa, M. Umeda, M. Magara, K. Watanabe, T. Yamamoto, “Isotopic composition measurement of FP nuclides in spent LWR UO2 fuel and nucleonics analysis-[2] Measurements of FP nuclides-“, Proc. of 2011 Annual Meeting of the Atomic Energy Society of Japan, 2011.

2). M. Suzuki, T. Yamamoto, T. Nakajima, H. Fukaya. K. Suyama, G. Uchiyama, ”Isotopic composition measurement of FP nuclides in spent LWR UO_2 fuel and nucleonics analysis-[4] Nucleonic Analysis of Metallic FP isotopes- “, Proc. of 2012 Fall Meeting of the Atomic Energy Society of Japan, 2012.

3). K. Suyama, H. Mochizuki, T. Takada, S. Ryufuku, H. Okuno, M. Murazaki, K. Okubo, ”SWAT3.1; The Integrated burnup code system driving continuous energy Monte Carlo codes MVP and MCNP”, JAEA-Data/Code 2009-002, 2009.

Table 1 Analytical results by using developed quantitative analytical method by combined chromatographic mass spectrometric-isotopic dilution technology (atom/Total U).（Tentative）

Sample	ZN2c2	ZN3c2	ZN3c3	Sample	ZN2c2	ZN3c2	ZN3c3
Fuel	UO_2-Gd_2O_3	UO_2-Gd_2O_3	UO_2	Fuel Type	UO_2-Gd_2O_3	UO_2-Gd_2O_3	UO_2
Estimated Burnup (GWd/t)	27.8	57.3	68.3	Estimated Burnup (GWd/t)	27.8	57.3	68.3
U-234	1.70E-04	1.28E-04	2.34E-04	Eu-153	1.55E-04	3.09E-04	9.97E-01
U-235	1.12E-02	2.24E-03	3.69E-03	Eu-154	1.50E-05	3.41E-05	1.00E+00
U-236	3.80E-03	4.81E-03	7.89E-03	Eu-155	2.58E-06	8.71E-06	4.00E-04
U-238	9.85E-01	9.93E-01	9.88E-01	Pm-147	1.68E-05	3.30E-05	4.06E-03
U total	1.00E+00	1.00E+00	1.00E+00	Sm-147	4.01E-04	5.43E-04	3.28E-03
Pu-238	1.29E-04	4.05E-04	5.76E-04	Sm-148	1.86E-04	5.47E-04	1.01E-03
Pu-239	5.83E-03	4.67E-03	4.68E-03	Sm-149	5.10E-06	3.45E-06	2.34E-03
Pu-240	2.33E-03	3.52E-03	3.58E-03	Sm-150	3.78E-04	7.55E-04	1.11E-02
Pu-241	7.41E-04	1.11E-03	1.12E-03	Sm-151	1.79E-05	1.76E-05	1.93E-04
Pu-242	3.52E-04	1.47E-03	1.48E-03	Sm-152	1.45E-04	2.48E-04	1.14E-03
Pu total	9.37E-03	1.12E-02	1.15E-02	Sm-154	6.61E-05	1.30E-04	5.31E-03
Nd-142	3.15E-05	1.14E-04	1.50E-04	Gd-152	4.96E-05	9.55E-06	1.76E-03
Nd-143	1.23E-03	1.59E-03	1.95E-03	Gd-154	1.40E-03	1.07E-03	2.58E-03
Nd-144	1.78E-03	4.41E-03	5.71E-03	Gd-155	2.03E-05	2.33E-05	1.23E-03
Nd-145	9.67E-04	1.76E-03	2.19E-03	Gd-156	2.68E-02	2.68E-02	6.50E-04
Nd-146	9.61E-04	2.18E-03	2.76E-03	Gd-157	1.07E-05	5.87E-06	1.29E-02
Nd-148	5.15E-04	1.08E-03	1.32E-03	Gd-158	3.24E-02	3.36E-02	7.21E-05
Nd-150	2.50E-04	5.46E-04	6.37E-04	Gd-160	1.70E-02	1.72E-02	4.50E-06
Nd total	5.73E-03	1.17E-02	1.47E-02	Mo-95	1.69E-03	2.81E-03	4.05E-03
Cs-133	1.78E-03	2.92E-03	3.93E-03	Tc-99	1.19E-03	1.98E-03	2.74E-03
Cs-134	6.20E-06	3.77E-05	6.87E-05	Ru-101	1.59E-03	2.98E-03	3.98E-03
Cs-137	1.48E-03	3.14E-03	2.30E-04	Rh-103	1.00E-03	1.49E-03	1.83E-03
Eu-151	2.31E-06	2.04E-06	2.92E-03	Ag-109	9.76E-05	2.09E-04	2.45E-04

EUROPEAN NUCLEAR SOCIETY

European Nuclear Society
Rue Belliard 65
1040 Brussels, Belgium
Telephone: +32 2 505 30 50 - FAX: +32 2 502 39 02
enc2012@euronuclear.org
www.enc-2012.org